WHOI-2014-04

A Crossroads of the Atlantic Meridional Overturning Circulation: The Charlie-Gibbs Fracture Zone Data Report August 2010 – June 2012

by

H. Furey, L. Trafford, and A. Bower
August 2014

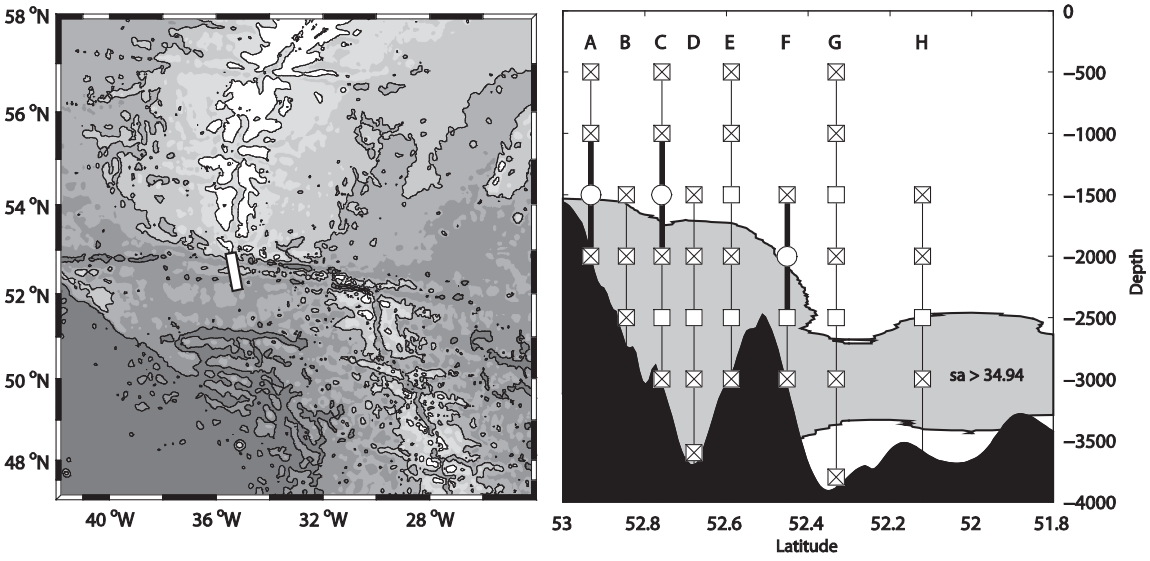

Technical Report

Funding was provided by the National Science Foundation
Grant OCE-0826656.

WHOI-2014-04

A Crossroads of the Atlantic Meridional Overturning Circulation: The Charlie-Gibbs Fracture Zone Data Report August 2010 – June 2012

by

H. Furey, L. Trafford, and A. Bower

August 2014

Technical Report

Funding was provided by the National Science Foundation
Grant OCE-0826656.

Approved for Distribution:

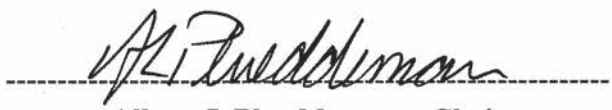

Albert J. Plueddemann, Chair
Department of Physical Oceanography

Abstract

This is the final data report of all mooring data collected by the Woods Hole Oceanographic Institution in 2010-2012 during the experiment *A Crossroads of the Atlantic Meridional Overturning Circulation: The Charlie-Gibbs Fracture Zone*. The objectives of this experiment were (1) to obtain an improved direct estimate of the mean and low-frequency variability of the deep westward transport of the Iceland-Scotland Overflow Water through the Charlie-Gibbs Fracture Zone (CGFZ), and (2) to gain a better understanding of the causes of the low-frequency variability in the transport of overflow waters through the CGFZ, especially of the role of the North Atlantic Current in generating this variability. The mooring deployment and recovery cruises were on German research vessels, courtesy of Drs. Monika Rhein and Dagmar Kieke: the R/V Meteor cruise M82/2 in August 2010 and R/V Maria S. Merian cruise MSM 21/2 in June 2012, respectively. The CGFZ moored array complemented other moored arrays being maintained by German scientists just west of the CGFZ (Pressure Inverted Echo Sounders, or PIES) and the Faraday Fracture Zone (current meter and microcat moorings).

A set of eight moorings were set up across the CGFZ to measure the intermediate and deep water variability for a two-year period, from a depth of 500 m to the ocean floor. The moorings held a total of three McClane Moored Profilers (MMPs), 10 Nortek and 18 Aanderaa current meters, and 36 Seabird MicroCATs, deployed from 18-20 August 2010 through 28-30 June 2012. This yielded a nearly two-year record of velocity, temperature, salinity and pressure. The MMPs profiled every five days, and resulted in a high-resolution time series of temperature, salinity, pressure and velocity data across the interface between the generally eastward flowing Labrador Sea Water carried underneath the North Atlantic Current, and the westward flowing deep Iceland-Scotland Overflow Water.

Front Cover Figure Caption:

The location (left) and vertical composition (right) of this report's mooring array across the Charlie-Gibbs Fracture Zone. On the left, array location is marked with a black-outlined white box, bathymetry is shaded every 500 meters, and contoured every 1000 meters. On the right, the vertical section shows the moorings, lettered 'A' through 'H', against the 34.94 isohaline, which is drawn from 1994 CTD data taken along a station track that generally follows the ridgeline. This isohaline approximately defines the interface between the lower westward-flowing Iceland-Scotland Overflow Water and upper eastward-flowing North Atlantic Current. See text for further details.

Table of Contents

List of Figures

List of Tables

1. Introduction

The oceanic Meridional Overturning Circulation (MOC) is a global circulation pattern that redistributes heat and freshwater over the largest spatial scales. The importance of the MOC was recently recognized in the U.S. Ocean Research Priorities Plan, which includes as a priority the need for an "improved understanding of the mechanisms behind fluctuations of the MOC, which will lead to new capabilities for monitoring and making predictions of the MOC changes" (National Science and Technology Council Joint Subcommittee on Ocean Science and Technology, 2007). Some have argued that a significant change in the strength and/or pathways of the MOC could accompany an abrupt change in Earth's climate, especially over the continents surrounding the North Atlantic.

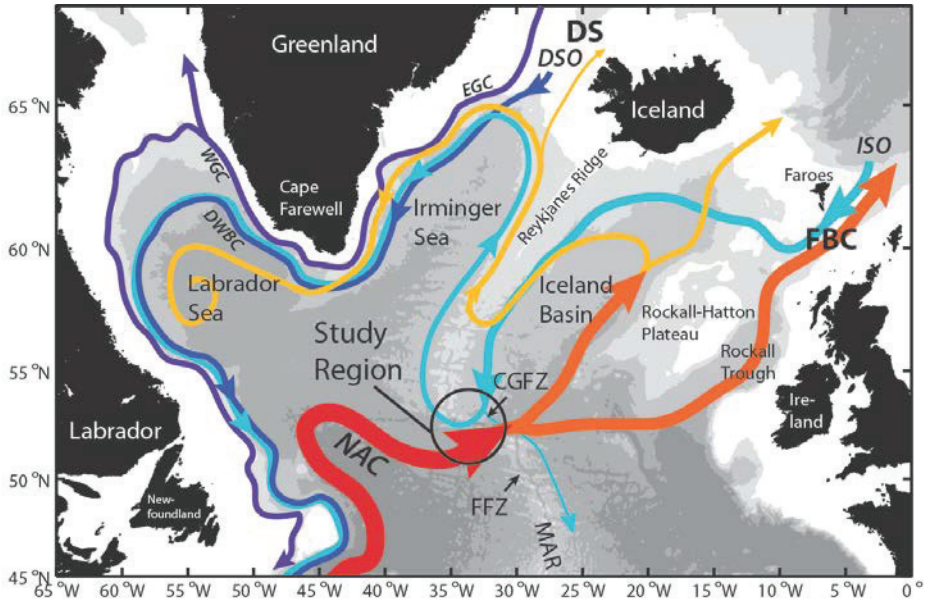

Figure 1. Chart showing the location of the study region at the Charlie-Gibbs Fracture Zone (CGFZ). Bathymetry is shaded every 1000 m. Acronyms: DS, Denmark Strait; FBC, Faroe Bank Channel; DSO, Denmark Strait Overflow; ISO, Iceland-Scotland Overflow; EGC, East Greenland Current; WGC, West Greenland Current; DWBC, Deep Western Boundary Current; NAC, North Atlantic Current; FFZ, Faraday Fracture Zone; MAR, Mid-Atlantic Ridge.

The Atlantic MOC (AMOC) is considered to be the strongest part of the global MOC. While considerable observational effort has been made to describe the basic structure (and in some cases, low frequency variability) of the AMOC at a selected number of locations, little attention has been paid over the past two decades to the Charlie-Gibbs Fracture Zone (CGFZ), where both the warm and cold limbs of the AMOC cross the Mid-Atlantic Ridge (Figure 1). Cold, dense Iceland-Scotland Overflow Water (ISOW) streams westward through the CGFZ into the western basin, where it eventually joins the

other components of North Atlantic Deep Water in the Deep Western Boundary Current. Warm subtropical water, recirculating Subpolar Mode Water and recently convected Labrador Sea Water are carried eastward over the CGFZ by the northernmost branch of the North Atlantic Current (NAC).

Many fundamental questions remain about the currents that flow through (and over) this major gateway between the eastern and western North Atlantic. The first and most basic question is what is the mean westward transport of overflow water through the deep CGFZ? The single direct measurement of 2.4 Sv (Saunders, 1994; see mooring locations in Figure 2) is a factor of 2 to 2.5 times smaller than all estimates derived from hydrography. Why? Second, what is the cause of the energetic, low-frequency variability in the deep currents in the CGFZ, which results in a range of instantaneous transport from 10 Sv westward to 7 Sv eastward? Third, what controls the latitude at which the NAC crosses the MAR, and thus the potential for interacting with the deep westward flow? Finally, are the eastward flowing NAC and the westward flowing ISOW dynamically linked? If so, this would have implications not only for the delivery of warm water to high latitudes in the eastern North Atlantic, but also for the delivery of cold waters to the western boundary current and low latitudes.

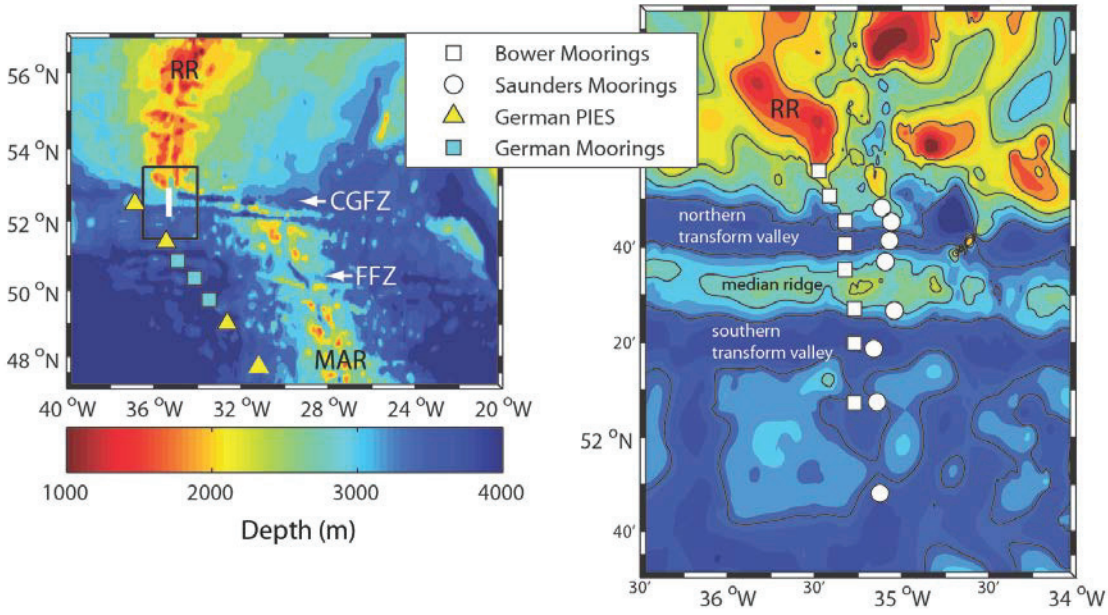

Figure 2. (left) Chart showing mooring array location (white line), along with the larger German Array placed and serviced on the same deployment and recovery cruises. (right) Enlargement of study area, including the Saunders mooring locations, which recorded current and CTD data from 1988-1989.

This research project includes both observational and process-oriented modeling components to study the AMOC at the CGFZ. The primary objectives are: (a) to obtain an improved direct estimate of the mean and low frequency variability of the deep

westward transport of Iceland-Scotland Overflow Water through the CGFZ, and (b) to gain a better understanding of the causes of the low-frequency variability in the transport of overflow waters through the CGFZ, especially of the role of the NAC in generating this variability. This report describes the observational component of the project.

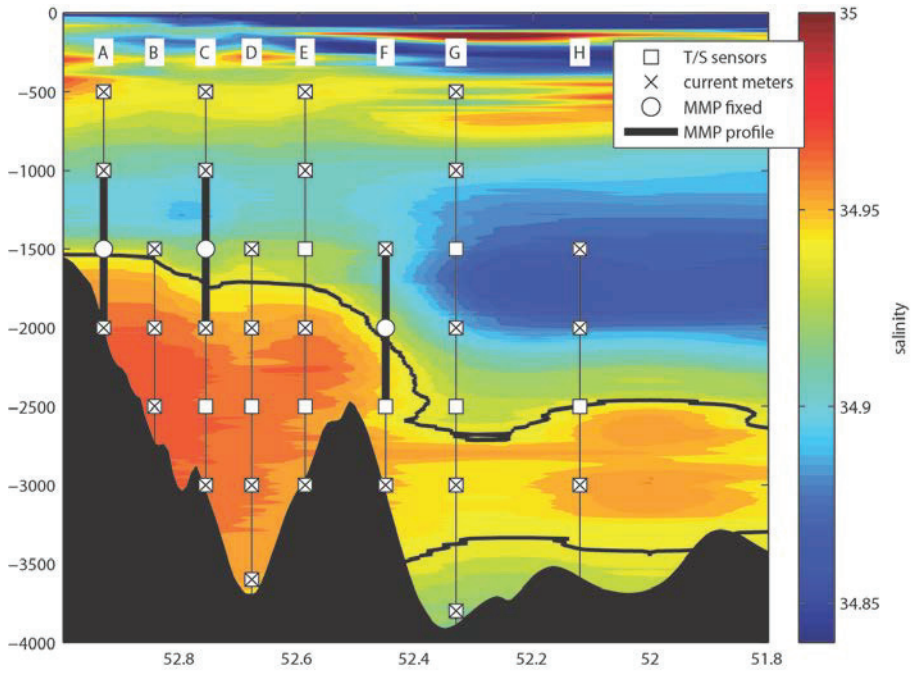

Figure 3. Mooring array comprised of current meters, MicroCATs (T/S or T/S/P sensors) and MMPs. The salinity field in the background is from 1994 CTD data taken along a station track that generally follows the pathway of the German mooring array and PIES shown in Figure 2. The 34.94 isohaline is contoured in bold, and approximately defines the interface between the lower westward-flowing ISOW and upper eastward-flowing NAC.

To meet the observational objectives, we installed an array of eight current meter and hydrographic moorings across the CGFZ that measured the currents and water properties between the bottom and 500 m from August 2010 through June 2012 (Figure 2, 3). This array provided the first long-term, simultaneous observations of both the westward and eastward flows through the CGFZ, as well as the first simultaneous measurement of both currents and water properties. The array included three McLane Moored Profilers (MMPs), which measured two up and down 1000-m profiles across the interface between the eastward flowing LSW (Labrador Sea Water) and deep westward flowing ISOW every five days for two years. A complementary array of Pressure-Inverted Echo Sounders (PIES) and current meter moorings installed by M. Rhein and colleagues of the University of Bremen monitored the path of the NAC as it approached the ridge (Figure 2, left; Rhein, 2010). The mooring array was designed to mimic the Saunders (1994) 1988-1989 array (Figure 2, right), while additionally capturing flow higher in the water column, and flow farther to the north in the CGFZ. The array was also shifted slightly

west by about 17 km because digital topography indicated a possible channel for deep westward flow west of the original Saunders array.

2. Mooring array setup and instrument performance

The array of eight moorings, A through H, included 18 Aanderaa RCM-11 and 10 Nortek AquaDopp 6000 DM current meter instruments, 36 Seabird SBE-37 MicroCATs, and three MMPs, which measured velocity as well as CTD data. The moorings were deployed 18-20 August 2010, and recovered 28-30 June 2012. Details of the deployment and recovery cruises may be found in Rhein (2010) and Kieke (2012), respectively.

All current meter and MicroCAT instruments returned ~100% of expected data, except for one current meter (s/n 6738 at 2000 m on Mooring G) which failed in September 2011, returning ~56% data, and one MicroCAT (s/n 7584, the bottom instrument at 2738 m on mooring B) which returned ~50% data. The MMPs were less successful: the northern MMP (Mooring A) returned about 80% of data, the central MMP (Mooring C) returned 100% of CTD data but only 65% of velocity data, and the southern MMP (mooring F) returned only about 25% useful data. See Table 1 for summary.

Table 1. Instrument Performance Summary.

Instrument type/property	Data return
Current meters (28): Aanderaa (18), Nortek (10)	
pressure (Nortek only)	96%
temperature	98%
velocity	98%
Microcats (36)	
pressure	100%
temperature	100%
conductivity	98%
MMPs (3)	
pressure	68% (80, 100, 25)*
temperature	68% (80, 100, 25)
conductivity	68% (80, 100, 25)
velocity	58% (80, 68, 25)

* MMP data return percentages broken down as follows: '68% (80, 100, 25)' indicated 68% total data return for three MMPs, with 80% data return at northern MMP, 100% data return at central MMP, and 25% data return for southern MMP.

Appendix A contains instrument metadata, mean statistics, mooring diagrams, and inter-instrument comparison plots. Table A1 lists all instruments by mooring, including serial number, depth, measured properties, and performance notes. Table A2 lists current meter, MicroCAT, and stationary MMP (the fixed-position time series data) instrument mean, minimum, maximum, and standard deviation. Table A3 describes output MATLAB data structure format and variable definitions. Table A4 lists instrument calibration corrections, and Table A5 data segments deleted. Table A6 contains a summary of instrument accuracy and resolution. Figures A1 through A8 show individual mooring diagrams. Figures A9 through A12 show comparison between MicroCAT, current meter, and bottle-calibrated CTD data from deployment and recovery cruises.

3. McLane Moored Profilers

Three MMPs were deployed from August 2010 to June 2012 in order to autonomously profile the water column at 2-dbar resolution at three locations across the CGFZ (Figure 3; Moorings A, C, and F). The MMP missions were set up to profile 1000-meter ranges, either from 1000 to 2000 m on Moorings A and C, or 1500 to 2500 m on Mooring F. This choice was made so that there would be high-resolution CTD and velocity data collected across the interface between the westward-flowing ISOW and the eastward-flowing LSW above. The MMPs profiled the 1000-m distance four times (two times up, two times down) every five days. A schematic of MMP mission is shown in Figure 4.

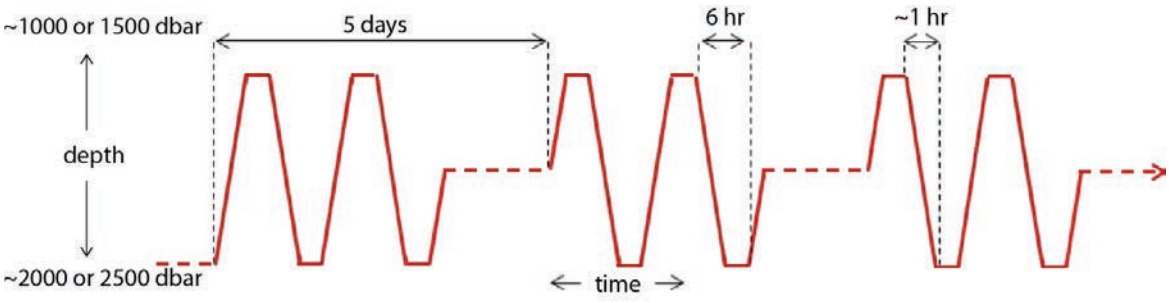

Figure 4. MMP mission details.

Throughout their deployments, the MMP units wrote CTD, acoustic current meter (ACM), and engineering files for each vertical profile completed. The MMP profile data were binned in 2-dbar bins, the MMP stationary data were binned in 2-hourly measurements. Original MMP CTD and ACM data were sampled at ~2 Hz for s/n 117 and s/n 118 and ~1 Hz for s/n 142, difference due to instrument performance, not pre-programmed mission. Processed MMP data are available in MAT-files per profile, and also as a time series, concatenated from the data recorded while the MMP was at its fixed mid-depth positions.

Appendix B details the conversions and calibrations performed to obtain pressure-gridded profiles of the data from the MMPs' CTD and current meter units, and methods to calibrate and edit the resulting gridded data. MMP clocks, in practice, do not require a correction for drift. Performance of each instrument is detailed and output MMP data format is described. Hövmoller plots of resultant MMP data along with diagnostic engineering plots are provided in Appendix C. Particular notice should be taken of MMP118 (the southernmost MMP) conductivity data, which was difficult to calibrate (see Figure B4, and Appendix B text).

4. Current meter quality control and calibration

All current meter instrument data were truncated to in-water time periods, which were mooring dependent, but generally from 18-20 August 2010 to 28-30 June 2012. The initial and final instrument clock offsets were applied as linear offsets to each mooring instrument. Initial clock offsets were all assumed to be 0, as instrument clock information was not recorded at deployment. Final clock offsets were recorded on deck at recovery, provided in a spreadsheet by Scott Worrilow (WHOI), and may be found in Table A4. Pressure data from pressure-recording current meters were not de-trended.

Quality control and calibration procedures specific to instrument sensor type are detailed below. After all quality control and calibration steps were performed, the mooring data were low-pass filtered to remove tides using a 40-hour 2^{nd} order Butterworth filter. The data were left at the original sampling rate of 30 minutes for the current meters. Raw, quality controlled and calibrated, and low-pass filtered data are available in each instrument's MATLAB structure file (see Table A3 for structure format).

4.1 Aanderaa Current Meters (RCM11s)

All Aanderaa RCM11 current meters performed full missions. Data were delivered by B. Hogue post cruise with manufacturer calibrations applied, including thermistor calibration. Eighteen instruments were further processed by applying clock drift, geomagnetic correction, sound velocity correction, additional thermistor calibration, and truncating the data records down to in-water segments. Table A4 details data processing information.

There was one unusual correction to the data: data was missing whenever a datum was recorded at 00:00. The time was not recorded to the file, and so those data lines were shorter than the others. The correction was to insert '00:00' at the start of all affected data lines.

Geomagnetic corrections were applied linearly over time using routines written by D. Torres (WHOI) and the IGRF11 data set. Speed data were modified by a scale factor of the ratio *in-situ* sound velocity/standard sound velocity (where standard sound velocity is 1500 m/sec), as recommended by AADI. Hogg and Frye (2007) suggest scaling all RCM11 speed data by a factor of 1.1. This correction was not applied based on information provided by D. Torres (WHOI) and I.Victoria (AADI). Both felt that since the Hogg and Frye study was based on a single instrument, the Hogg and Frye results were not necessarily applicable to all RCM instruments.

The current meter velocities were qualitatively checked against the independent information provided by the MMP current meters, and by cross referencing with current meters at similar depths at other moorings. We corrected the current meter temperature data to the companion MicroCAT temperature record (the MicroCAT at the same depth) in the following way: we took the 10-day mean of the calibrated, quality controlled, unfiltered MicroCAT temperature offsets at the deployment and recovery times and calculated a linear trend from those two points. We then added the trend to the Aanderaa current meter temperature data. Corrective offsets are saved in the 'aanderaa.setup' structure file, and listed in Table A4. No synthetic pressures were created for the RCM-11s (as in Furey et al., 2013), instead companion MicroCATs exist for each current meter, and these pressures may be used as a proxy.

Processed data are stored in MATLAB structure format, containing metadata. As an example, the contents of the Aanderaa current meter s/n 370 are shown in Table A3. Plots of calibrated and quality controlled data and raw engineering data plots are included in Appendix D, organized by Mooring letter and then depth.

4.2 Nortek AquaDopp 6000 DW Current Meters (NTK)

Of the ten Nortek AquaDopp 6000 DW current meters, all performed full missions except for s/n 6738, which quit in July 2011 due to battery failure, as shown in the return engineering data. Data were delivered by B. Hogue post cruise with manufacturer calibrations applied, but this did not include thermistor calibration.

Eight instruments were further processed by applying clock drift, geomagnetic correction, sound velocity correction, thermistor calibration, and truncating the data down to in-water segments. No pressure drift corrections were applied. Geomagnetic corrections were applied linearly over time using routines written by D. Torres (WHOI) and the IGRF11 data set. Sound velocity was calculated *in situ*, so no corrections were made post recovery. We corrected the current meter temperature data to the companion MicroCAT temperature record (the MicroCAT at the same depth) in the same way as we did for the Aanderaa current meters: we took the 10-day mean of the calibrated unfiltered

MicroCAT temperature at the deployment and recovery times and calculated a linear trend from those two points. We then added the trend to the Nortek current meter temperature data. Corrective offsets are saved in the 'nortek.setup' structure file, and listed in Table A4.

Processed data are stored in MATLAB structure format, containing metadata. As an example, the contents of the Nortek current meter s/n 6741 are shown in Table A3. Plots of calibrated and quality controlled data and raw engineering data plots are included in Appendix D, organized by Mooring letter and then depth.

5. Sea-Bird MicroCAT quality control and calibration

All MicroCAT instrument data were truncated to in-water time periods, which were mooring dependent, but generally from 18-20 August 2010 to 28-30 June 2012. The initial and final instrument clock offsets were applied as linear offsets to each mooring instrument. Initial clock offsets were all assumed to be 0, as we had no information to the contrary. MicroCAT final clock offsets, recorded on deck at recovery, were provided in a word document by Brian Hogue (WHOI), and may be found listed in Table A4. Pressure data from pressure-recording MicroCATs were not de-trended.

Quality control and calibration procedures specific to instrument sensor type are detailed below. After all quality control and calibration described in Sections 3.1 through 3.3, the mooring data were low-pass filtered to remove tides using a 40-hour Butterworth filter. The data were left at the original sampling rate of 15-minute interval for the MicroCAT data. Raw, quality controlled and calibrated, and low-pass filtered data are available in each instrument's MATLAB structure file (see Appendix A for structure format).

After the clock correction described above, the MicroCAT instruments were processed as follows: The pressure data were left alone, as it was thought that any variations were "real," and not from instrument drift. The temperature data required no editing, as there were no obviously erroneous spikes. The temperature was calibrated using the SeaBird, Inc. offsets measured in factory calibration post-cruise. The offset was applied to the temperature data linearly, as recommended by SeaBird, Inc.'s "appnote31Feb10.pdf." Temperature offsets are listed in Table A4.

The conductivity measured by the MicroCATs without pressure sensors assumes a constant reference pressure when converting frequency counts to conductivity. Seabird considers this a negligible error under normal circumstances (minimal pressure variability), and although there were minimal pressure variations in deep CGFZ moorings, we performed this correction. (Maximum pressure excursions were about 20 meters; usually excursions were about 5-10 meters.) Synthetic pressure was created by

taking the fractional average of the pressure excursions of the nearest above and below instruments and adding the instrument reference pressure recorded at deployment. Applying a linear fraction of pressure excursion (as opposed to fitting a spline offset) was considered sufficient after looking at the modeled blow-down curves from S. Worrilow, which were linear in shape for these deep moorings. Synthetic pressure data were saved in each MicroCAT structure output file.

The conductivity time series contained some obviously bad data that needed to be removed (instruments s/ns 2029 2030 7584 7589 7597) and replaced with NaNs; the gross adjustments are detailed in Table A4. All conductivity data points less than 3.2 conductivity units were deleted. There were no long-period segments that could be 'adjusted' in these data. Once these edits were made, all conductivity data were processed to remove outliers using a 12-hour (49-point) window with a 2.0 standard deviation cutoff, done twice. (This is similar to the procedure done by R. Curry for HydroBase, http://www.whoi.edu/hydrobase/.)

Finally, the conductivity data were calibrated using the post-recovery Seabird calibration coefficients (provided in Table A3), which were applied to the data according to the method outlined in SeaBird, Inc.'s "appnote31Feb10.pdf". The resultant MicroCAT conductivity values were *not* adjusted to the deployment and/or recovery CTD conductivity values, as they were within the envelope of the bottle-corrected deployment and recovery CTD data. See Figures A9 through A11 for *in situ* temperature and salinity versus pressure, Theta-S diagrams and theta-potential conductivity diagrams that compare MicroCAT to CTD data. Potential temperature versus potential conductivity plots of the raw conductivity, quality controlled and calibrated conductivity, and the deployment and recovery CTD profiles are shown in Appendix E.

6 Acknowledgements

We are deeply grateful for the generosity of Prof. Dr. Monika Rhein and Dr. Dagmar Kieke for allowing us to deploy and recover the CGFZ moorings on their research cruises, and the crews of the *R/V* Meteor and *R/V* Maria S. Merian for aide in this project. We are also sincerely grateful to B. Hogue at WHOI for deploying and recovering these moorings, the Worrilow Mooring Lab (WHOI) for instrument preparation and data recovery, and R. Trask and the Rigging Shop (WHOI) for mooring fabrication. Heather would also like to acknowledge F. de Jong's assistance in vetting the quality control and calibration procedures used on these data and J. Hildebrandt's help creating the appendix tables, editing, and putting together the final report. This work was funded by the National Science Foundation Grant OCE-0826656.

7 References

Furey, H. H., T. McKee, M. F. de Jong, P. E. Robbins, and A. S. Bower, 2013. Impact of Irminger Rings on Deep Convection in the Labrador Sea: Mooring Instrument, Cruise CTD, and APEX Data Report, September 2007 – September 2009. *WHOI Technical Report WHOI-2013-05,* 103 pp.

Kieke, D., 2012. Short Cruise Report, RV Maria S. Merian, cruise MSM-21, leg 2, Reykjavic-Nuuk, June 25th – July 24th, 2012. Institut für Umweltphysik, AG Ozeanographie, Universität Bremen, 12 pp.

Rhein, M., 2010. Cruise Report, RV Meteor: cruise M82/2, from St John's, Canada, to Ponta Delgada, Acores, Portugal, August 4th to September 1st, 2010. Institut für Umweltphysik, AG Ozeanographie, Universität Bremen, 38 pp.

Appendix A: Instrument metadata tables (Table A1), instrument statistics (Table A2), mooring data structure format (Table A3), calibration information (Table A4), quality control information (Table A5), and mooring instrument accuracy and resolution (Table A6). Final mooring diagrams are represented in Figures A1-A8. Note that some specific instruments plotted on mooring diagrams were swapped out with equivalent instruments (therefore different serial numbers) at sea; this will be noted in figure captions. The final depths for all moorings were recorded by B. Hogue in the deploy log sheets, and in each case, these depths matched the design depths. Note also that although the mooring revision versions are not marked 'F' for final, these diagrams were provides to H. Furey from S. Worrilow in March 2014 and are to be considered the final drawings. Mooring instrument and deployment and recovery CTD comparison plots are shown in Figures A9-A12.

Table A1. Mooring layout with nominal instrument depths (based on mooring design and target water depth) and properties for eight moorings A-H. The observed parameters are eastward velocity (u), northward velocity (v), temperature (T), conductivity (C), and pressure (P). Unless noted, data return is 100 per cent.

Mooring & Location	Nominal Depth (m)	Instrument Type & #s/n	Properties / Notes
A 52.9250N 35.4447W	500	RCM11 #157	u, v, T
	500	SBE37 #7595	P, C, T
	1000	RCM11 #367	u, v, T
	1000	SBE37 #7585	P, C, T
	1000-2000 profile; 1500 fixed	MMP #117	u, v, P, C, T 80% data return
	1963	NTK #6476	u, v, P, T
	1963	SBE37 #7583	P, C, T
B 52.8467N 35.3733W	1506	RCM11 #155	u, v, T
	1506	SBE37 #7594	P, C, T
	2006	NTK #6728	u, v, P, T
	2006	SBE37 #7593	P, C, T
	2738	RCM11 #368	u, v, T
	2738	SBE37 #7584	P, C, T 50% data return
C 52.7747N 35.324W	500	RCM11 #374	u, v, T
	500	SBE37 #7591	P, C, T
	1000	NTK #6756	u, v, P, T
	1000	SBE37 #7582	P, C, T
	1000-2000 profile; 1500 fixed	MMP #142	u, v, P, C, T 68% data return on current meter data
	2000	NTK #6733	u, v, P, T
	2000	SBE37 #7592	P, C, T
	2500	SBE37 #2034	C, T
	2963	RCM11 #150	u, v, T
	2963	SBE37 #7581	P, C, T
D 52.6803N 35.3308W	1506	RCM11 #158	u, v, T
	1506	SBE37 #7587	P, C, T
	2006	NTK #6730	u, v, P, T
	2006	SBE37 #7588	P, C, T
	2506	SBE37 #1649	C, T
	3006	RCM11 #371	u, v, T
	3006	SBE37 #7586	P, C, T
	3688	RCM11 #343	u, v, T
	3688	SBE37 #7598	P, C, T

Table A1. Mooring layout with nominal instrument depths and properties for eight moorings A-H. (continued)

E 52.5848N 35.3438W	505	RCM11 #366	u, v, T
	505	SBE37 #7589	P, C, T
	1005	NTK #6770	u, v, P, T
	1005	SBE37 #7590	P, C, T
	1505	SBE37 #2029	C, T
	2005	NTK #6741	u, v, P, T
	2005	SBE37 #7596	P, C, T
	2505	SBE37 #2032	C, T
	2938	RCM11 #160	u, v, T
	2938	SBE37 #7602	P, C, T
F 52.459N 35.268W	1511	RCM11 #370	u, v, T
	1511	SBE37 #7601	P, C, T
	1511-2514 profile; 2011 fixed	MMP #118	u, v, P, C, T 25% data return
	2514	SBE37 #2028	C, T
	2972	RCM11 #156	u, v, T
	2972	SBE37 #7604	P, C, T
G 52.3353N 35.2968W	491	RCM11 #339	u, v, T
	491	SBE37 #7597	P, C, T
	992	NTK #6731	u, v, P, T
	992	SBE37 #7576	P, C, T
	1492	SBE37 #2030	C, T
	1992	NTK #6738	u, v, P, T 56% data return
	1992	SBE37 #7577	P, C, T
	2492	SBE37 #2037	C, T
	2993	RCM11 #148	u, v, T
	2993	SBE37 #7579	P, C, T
	3826	RCM11 #369	u, v, T
	3826	SBE37 #7603	P, C, T
H 521182N 35.2725W	1489	RCM11 #147	u, v, T
	1489	SBE37 #7578	P, C, T
	1990	NTK #6744	u, v, P, T
	1990	SBE37 #7580	P, C, T
	2490	SBE37 #1640	C, T
	3161	RCM11 #162	u, v, T
	3161	SBE37 #7605	P, C, T

Table A2. Instrument property statistics, organized by property type, then mooring, then depth. These statistics are calculated from the quality controlled, calibrated raw data.

Property	Mooring	Instrument Type #s/n	Depth (m)	Mean	Minimum	Maximum	Standard Deviation
P (dbar)	A	SBE37 #7595	500	481	480	489	0
		SBE37 #7585	1000	988	987	995	0
		NTK #6476	1963	1975	1974	1976	0
		SBE37 #7583	1963	1966	1965	1967	0
	B	SBE37 #7594	1506	1502	1501	1503	0
		NTK #6728	2006	2020	2019	2021	0
		SBE37 #7593	2006	2008	2006	2009	0
		SBE37 #7584	2738	2755	2753	2755	0
	C	SBE37 #7591	500	485	484	509	2
		NTK #6756	1000	997	994	1020	2
		SBE37 #7582	1000	991	990	1014	2
		NTK #6733	2000	2018	2015	2031	1
		SBE37 #7592	2000	2009	2008	2022	1
		SBE#37 2034	2500	2519	2518	2525	1
		SBE#37 7581	2963	2992	2990	2992	0
	D	SBE37 #7587	1506	1523	1523	1532	1
		NTK #6730	2006	2038	2036	2045	1
		SBE37 #7588	2006	2027	2026	2034	1
		SBE37 #1649	2506	2540	2540	2546	0
		SBE37 #7586	3006	3055	3055	3059	0
		SBE37 #7598	3688	3753	3751	3754	0
	E	SBE37 #7589	505	528	527	537	1
		NTK #6770	1005	1049	1047	1056	1
		SBE37 #7590	1005	1035	1034	1043	1
		SBE37 #2029	1505	1544	1543	1550	1
		NTK #6741	2005	2063	2062	2068	1
		SBE37 #7596	2005	2054	2053	2058	0
		SBE37 #2032	2505	2565	2565	2567	0
		SBE37 #7602	2938	3009	3008	3010	0

Table A2. Instrument property statistics (continued)

Property	Mooring	Instrument Type #s/n	Depth (m)	Mean	Minimum	Maximum	Standard Deviation
P (dbar)	F	SBE37 #7601	1511	1516	1515	1520	0
		SBE37 #2028	2514	2539	2538	2541	0
		SBE37 #7604	2972	3010	3008	3011	0
	G	SBE37 #7597	491	509	507	527	2
		NTK #6731	992	1016	1014	1034	2
		SBE37 #7576	992	1011	1009	1029	2
		SBE37 #2030	1492	1519	1517	1534	2
		NTK #6738	1992	2040	2038	2053	2
		SBE37 #7577	1992	2028	2027	2041	1
		SBE37 #2037	2492	2540	2539	2549	1
		SBE37 #7579	2993	3054	3053	3060	1
		SBE37 #7603	3826	3913	3912	3914	0
	H	SBE37 #7578	1489	1513	1512	1518	0
		NTK#6744	1990	2013	2012	2016	0
		SBE37 #7580	1990	2021	2020	2025	0
		SBE37 #1640	2490	2532	2531	2535	0
		SBE37 #7605	3161	3219	3218	3220	0
T (°C)	A	RCM #157	500	4.68	4.03	6.18	0.25
		SBE37 #7595	500	4.71	4.10	6.18	0.24
		RCM #367	1000	3.78	3.62	4.03	0.06
		SBE37 #7585	1000	3.78	3.62	4.03	0.06
		NTK #6746	1963	3.22	3.05	3.41	0.06
		SBE37 #7583	1963	3.22	3.03	3.43	0.06
	B	RCM #155	1506	3.40	3.20	3.67	0.07
		SBE37 #7594	1506	3.40	3.20	3.67	0.07
		NTK #6728	2006	3.16	2.91	3.39	0.09
		SBE37 #7593	2006	3.16	2.91	3.39	0.09
		RCM #368	2738	3.06	2.87	3.21	0.04
		SBE37 #7584	2738	3.06	2.88	3.21	0.04

Table A2. Instrument property statistics (continued)

Property	Mooring	Instrument Type #s/n	Depth (m)	Mean	Minimum	Maximum	Standard Deviation
T (°C)	C	RCM #374	500	4.60	4.07	6.09	0.23
		SBE37 #7591	500	4.60	4.08	6.10	0.23
		NTK #6756	1000	3.77	3.60	4.07	0.07
		SBE37 #7582	1000	3.77	3.61	4.08	0.07
		NTK #6733	2000	3.15	2.90	3.40	0.09
		SBE37 #7592	2000	3.15	2.90	3.40	0.09
		SBE37 #2034	2500	3.06	2.86	3.23	0.06
		RCM #150	2963	3.01	2.83	3.19	0.05
		SBE37 #7581	2963	3.01	2.84	3.19	0.05
	D	RCM #158	1506	3.43	3.26	3.62	0.07
		SBE37 #7587	1506	3.43	3.25	3.62	0.07
		NTK #6730	2006	3.15	2.85	3.40	0.09
		SBE37 #7588	2006	3.15	2.85	3.40	0.09
		SBE37 #1649	2506	3.03	2.85	3.22	0.06
		RCM #371	3006	2.97	2.80	3.12	0.05
		SBE37 #7586	3006	2.97	2.80	3.13	0.05
		RCM #343	3688	2.65	2.34	3.01	0.16
		SBE37 #7598	3688	2.65	2.33	3.02	0.16
	E	RCM #366	505	4.41	4.03	5.01	0.17
		SBE37 #7589	505	4.42	4.03	5.02	0.17
		NTK #6770	1005	3.75	3.63	3.91	0.05
		SBE37 #7590	1005	3.74	3.62	3.91	0.05
		SBE37 #2029	1505	3.42	3.22	3.62	0.07
		NTK #6741	2005	3.12	2.85	3.36	0.09
		SBE37 #7596	2005	3.12	2.85	3.37	0.08
		SBE37 #2032	2505	2.99	2.78	3.18	0.05
		RCM #160	2938	2.92	2.61	3.06	0.05
		SBE37 #7602	2938	2.92	2.61	3.06	0.05

Table A2. Instrument property statistics (continued)

Property	Mooring	Instrument Type #s/n	Depth (m)	Mean	Minimum	Maximum	Standard Deviation
T (°C)	F	RCM #370	1511	3.46	3.28	3.67	0.07
		SBE37 #7601	1511	3.56	3.28	3.68	0.07
		SBE37 #2028	2514	2.96	2.77	3.20	0.07
		RCM #156	2972	2.87	2.62	3.06	0.08
		SBE37 #7604	2972	2.87	2.62	3.06	0.08
	G	RCM #339	491	4.44	4.05	4.88	0.15
		SBE37 #7597	491	4.44	4.06	4.89	0.15
		NTK #6731	992	3.76	3.63	4.01	0.06
		SBE37 #7576	992	3.77	3.63	4.02	0.06
		SBE37 #2030	1492	3.48	3.28	3.68	0.07
		NTK #6738	1992	3.18	3.00	3.42	0.08
		SBE37 #7577	1992	3.17	2.99	3.41	0.07
		SBE37 #2037	2492	2.97	2.84	3.19	0.05
		RCM #148	2993	2.81	2.59	3.07	0.08
		SBE37 #7579	2993	2.81	2.59	3.07	0.08
		RCM #369	3826	2.48	2.36	2.86	0.05
		SBE37 #7603	3826	2.48	2.36	2.86	0.05
	H	RCM #147	1489	3.52	3.31	3.70	0.08
		SBE37 #7578	1489	3.52	3.31	3.70	0.08
		NTK #6744	1990	3.19	3.01	3.39	0.07
		SBE37 #7580	1990	3.19	3.00	3.40	0.07
		SBE37 #1640	2490	2.97	2.85	3.18	0.05
		RCM #162	3161	2.71	2.52	2.96	0.07
		SBE37 #7605	3161	2.71	2.52	2.96	0.07
S (-)	A	SBE37 #7595	500	34.936	34.859	35.021	0.017
		SBE37 #7585	1000	34.916	34.874	34.952	0.009
		SBE37 #7583	1963	34.970	34.930	34.989	0.006
	B	SBE37 #7594	1506	34.930	34.894	34.965	0.012
		SBE37 #7593	2006	34.959	34.897	34.996	0.017
		SBE37 #7584	2738	34.974	34.954	34.985	0.003

Table A2. Instrument property statistics (continued)

Property	Mooring	Instrument Type #s/n	Depth (m)	Mean	Minimum	Maximum	Standard Deviation
S (-)	C	SBE37 #7591	500	34.932	34.856	35.022	0.015
		SBE37 #7582	1000	34.909	34.866	34.964	0.012
		SBE37 #7592	2000	34.949	34.883	34.998	0.020
		SBE37 #2034	2500	34.972	34.924	34.995	0.010
		SBE37 #7581	2963	34.975	34.950	34.991	0.005
	D	SBE37 #7587	1506	34.923	34.894	34.961	0.012
		SBE37 #7588	2006	34.942	34.889	35.000	0.020
		SBE37 #1649	2506	34.964	34.914	35.000	0.015
		SBE37 #7586	3006	34.965	34.929	34.988	0.008
		SBE37 #7598	3688	34.920	34.875	34.986	0.017
	E	SBE37 #7589	505	34.924	34.877	34.980	0.014
		SBE37 #7590	1005	34.907	34.870	34.950	0.011
		SBE37 #2029	1505	34.931	34.903	34.971	0.011
		SBE37 #7596	2005	34.933	34.890	34.994	0.018
		SBE37 #2032	2505	34.960	34.912	34.999	0.014
		SBE27 #7602	2938	34.960	34.913	34.984	0.008
	F	SBE37 #7601	1511	34.920	34.901	34.959	0.007
		SBE37 #2028	2514	34.958	34.913	35.013	0.015
		SBE37 #7604	2972	34.952	34.904	34.986	0.011
	G	SBE37 #7597	491	34.922	34.879	34.972	0.012
		SBE37 #7576	992	34.902	34.870	34.941	0.010
		SBE37 #2030	1492	34.923	34.909	34.964	0.007
		SBE37 #7577	1992	34.926	34.896	34.981	0.013
		SBE37 #2037	2492	34.942	34.912	34.988	0.011
		SBE37 #7579	2993	34.944	34.911	34.986	0.011
		SBE37 #7603	3826	34.904	34.889	34.938	0.004
	H	SBE37 #7578	1489	34.919	34.907	34.951	0.004
		SBE37 #7580	1990	34.992	34.902	34.971	0.008
		SBE37 #1640	2490	34.939	34.908	34.994	0.011
		SBE37 #7605	3161	34.930	34.903	34.970	0.009

Table A2. Instrument property statistics (continued)

Property	Mooring	Instrument Type #s/n	Depth (m)	Mean	Minimum	Maximum	Standard Deviation
U (cm/s)	A	RCM #157	500	-0.8	-33.8	17.3	5.6
		RCM #367	1000	-0.8	-20.3	19.8	5.1
		NTK #6746	1963	-8.0	-41.3	23.3	8.2
	B	RCM #155	1506	-0.9	-19.0	17.9	4.9
		NTK #6728	2006	-3.6	-22.2	12.7	4.6
		RCM #368	2738	-2.5	-24.7	22.2	4.7
	C	RCM #374	500	1.9	-23.7	31.1	6.1
		NTK #6756	1000	2.7	-23.6	31.9	8.1
		NTK #6733	2000	-2.8	-24.9	18.9	5.5
		RCM #150	2963	-7.9	-33.1	12.5	6.2
	D	RCM #158	1506	1.8	-19.3	23.9	5.5
		NTK #6730	2006	0.2	-20.9	20.2	5.9
		RCM #371	3006	-0.4	-27.5	15.1	5.2
		RCM #343	3688	2.1	-29.1	23.2	5.4
	E	RCM #505	505	1.9	-22.3	25.0	5.9
		NTK #6770	1005	2.1	-20.2	22.1	6.9
		NTK #6741	2005	0.3	-17.7	16.6	5.0
		RCM #160	2938	0.0	-24.7	23.9	5.9
	F	RCM #370	1511	0.0	-15.9	21.2	5.3
		RCM #156	2972	-8.0	-23.9	14.1	4.8
	G	RCM #339	491	2.0	-18.6	22.1	6.5
		NTK #6731	992	2.2	-27.4	27.4	8.2
		NTK #6738	1992	0.7	-19.8	19.1	5.9
		RCM #148	2993	-0.2	-22.0	17.8	3.7
		RCM #369	3826	1.0	-25.5	31.0	5.8
	H	RCM #147	1489	2.5	-18.3	19.8	5.0
		NTK #6744	1990	2.0	-17.1	19.9	4.8
		RCM #162	3161	-0.3	-13.4	14.6	2.8

Table A2. Instrument property statistics (continued)

Property	Mooring	Instrument Type #s/n	Depth (m)	Mean	Minimum	Maximum	Standard Deviation
V (cm/s)	A	RCM #157	500	-1.1	-30.7	17.7	4.7
		RCM #367	1000	-1.2	-19.6	17.1	3.9
		NTK #6746	1963	0.5	-15.0	20.7	4.7
	B	RCM #155	1506	-0.1	-17.2	15.4	4.0
		NTK #6728	2006	0.7	-15.6	20.4	4.3
		RCM #368	2738	0.0	-16.4	13.5	3.9
	C	RCM #374	500	-0.2	-18.9	17.1	4.9
		NTK #6756	1000	-0.1	-21.0	21.6	6.4
		NTK #6733	2000	2.2	-15.0	20.3	5.2
		RCM #150	2963	2.5	-18.8	18.2	3.6
	D	RCM #158	1506	0.2	-18.0	16.7	4.3
		NTK #6730	2006	0.6	-14.9	18.6	4.2
		RCM #371	3006	0.6	-13.0	18.0	3.2
		RCM #343	3688	0.3	-19.2	15.0	3.6
	E	RCM #366	505	0.2	-20.4	19.4	5.3
		NTK #6770	1005	0.3	-22.3	19.3	5.6
		NTK #6741	2005	0.1	-14.0	16.7	3.7
		RCM #160	2938	-0.5	-13.9	12.7	2.7
	F	RCM #370	1511	1.6	-14.1	19.5	4.7
		RCM #156	2972	3.5	-11.6	16.5	3.3
	G	RCM #339	491	0.9	-18.4	27.1	5.9
		NTK #6731	992	1.6	-19.8	29.5	6.9
		NTK #6738	1992	0.5	-13.5	19.6	4.8
		RCM #148	2993	0.4	-12.1	16.5	3.2
		RCM #369	3826	0.2	-23.3	24.3	4.7
	H	RCM #147	1489	-0.3	-20.7	22.1	5.6
		NTK #6744	1990	-0.4	-24.0	21.9	5.3
		RCM #162	3161	-0.4	-15.4	14.2	4.1

Table A3. MATLAB data structure variables and definitions for current meters and MicroCATs.

```
>> load nortek6741.mat

>> nortek =

               setup: Nortek AQD setup
            datenums: Matlab datenum
                date: Date (year,mon,day,hr,min,sec)
              rawdir: Direction before corrections applied (deg).
              magvar: Magnetic variation (0-360 degrees)
                 spd: speed (cm/s)
                 dir: direction (deg T North, corrected for mag. Var.)
                   u: East component of velocity (cm/s)
                   v: North component of velocity (cm/s)
                   w: vertical velocity (cm/s)
                  te: temperature (°C)
                  pr: pressure (dbars)
                *_lp: data after 40hr low pass Butterworth filter applied.
```

```
>> nortek.setup

              cruiseID: 'CGFZ'
             mooringID: 'E'
            instrument: 'Nortek s/n 6741'
              latitude: 52.5848°N
             longitude: 35.3438°W
             instdepth: 2005 meters
         in_water_time: '2010-Aug-19 16:00:00'
        out_water_time: '2012-Jun-29 08:30:00'
     init_clock_offset: '0 seconds'
    final_clock_offset: '-55 seconds'
            lp_per_hrs: 40
             processor: 'H. Furey, WHOI'
     geomag_correction: 'IGRF11'
               comment: 'No sound velocity correction applied.'
        processed_date: '13-Mar-2013 12:55:42'
         deploy_adj2mc: [datenum, temperature correction]
        recover_adj2mc: [datenum, temperature correction]
```

Table A3. MATLAB data structure, continued.

```
>> load aanderaa370.mat

>> aanderaa =

       setup: Aanderaa RCM-11 setup
    datenums: Matlab datenum
        date: Date (year,mon,day,hr,min,sec)
      rawspd: Speed before sound velocity correction applied (cm/s).
      rawdir: Direction before compass correction applied (deg).
      magvar: Magnetic variation (0-360 degrees)
         spd: speed (cm/s)
         dir: direction (deg T North, corrected for mag. Var.)
           u: East component of velocity (cm/s)
           v: North component of velocity (cm/s)
          te: temperature (°C)
        *_lp: data after 40hr low pass Butterworth filter applied.
```

```
>> aanderaa.setup

              cruiseID: 'CGFZ'
             mooringID: 'F'
            instrument: 'Aanderaa s/n 370'
              latitude: 52.4590°N
             longitude: 35.2680°W
             instdepth: 1511 meters
         in_water_time: '2010-Aug-19 19:59:00'
        out_water_time: '2012-Jun-29 09:20:00'
     init_clock_offset: '0 seconds'
    final_clock_offset: '-1289 seconds'
                 SSfac: 0.9929
             processor: 'H. Furey, WHOI'
     geomag_correction: 'IGRF11'
               comment: 'Sound velocity correction applied.'
        processed_date: '03-Jun-2013 11:19:16'
         deploy_adj2mc: [datenum, temperature correction]
        recover_adj2mc: [datenum, temperature correction]
```

Table A3. MATLAB data structure, continued.

```
>> load microcat2030.mat

>> microcat =

           setup: MicroCAT SBE37 setup
        datenums: Matlab datenum
            date: Date (year,mon,day,hr,min,sec)
          raw_te: temperature before processing
          raw_pr: pressure before processing
          raw_co: conductivity before processing
          co_cal: conductivity after post-cruise
                  calibration coefficients applied.
              pr: pressure (dbar)
              te: temperature (°C)
              sa: practical salinity
            *_lp: data after 40hr low pass Butterworth filter applied.
```

```
>> microcat.setup

              cruiseID: 'CGFZ'
             mooringID: 'G'
            instrument: 'microcat s/n 2030'
              latitude: 52.3353°N
             longitude: 35.2968°W
             instdepth: 1492 meters
          in_water_time: '2010-Aug-20 15:29:58'
         out_water_time: '2012-Jun-27 14:59:59'
      init_clock_offset: '0 seconds'
     final_clock_offset: '164 seconds'
         synthetic_pres: 'yes'*
             lp_per_hrs: low-pass filter window (hours)
              processor: 'H. Furey, WHOI'
       stddevmultiplier: standard deviation multiplier
              winlength: length of outlier filter
            data_format: 'TEOS-10 and ITS90'
         processed_date: '12-Mar-2014 12:42:35'

*Note: some MicroCATs have pressure sensors, some do not.  Pressure was fabricated for
MicroCATs without pressure, as described in Section 5, from a linear fit between
bounding instrument pressure data.
```

Table A4. Calibration corrections, separated by instrument type. Clock offset is of opposite sign. If negative clock correction, then final clock measurement was fast. (E.g., Aanderaa #157 has a +580 second final clock correction. This means at the end of mission, the instrument clock read a time 580 seconds earlier than the UTC time. Specifically, the instrument clock read 18:52:35 at the UTC time of 19:02:15.)

Aanderaa RCM11 current meter						
Inst #	Mooring ID	Start underwater date	End Underwater date	Final clock correction (s); init. clock offset assumed 0.	Adjustment to fit MicroCAT temperature (see individual structure files for dates corrections applied).	
		(YYYY MM DD HH Min SS)			deployment	recovery
157	A	2010 08 18 13 30 00	2012 06 28 08 30 00	+580	-0.087	-0.007
367	A	2010 08 18 13 30 00	2012 06 28 08 30 00	+1228	0.015	0.014
155	B	2010 08 18 17 00 00	2012 06 28 11 00 00	+1441	0.003	0.002
368	B	2010 08 18 17 00 00	2012 06 28 11 00 00	+4145	0.007	0.008
374	C	2010 08 18 22 00 00	2012 06 28 14 30 00	+470	0.008	0.006
150	C	2010 08 18 22 00 00	2012 06 28 14 30 00	+182	0.040	0.039
158	D	2010 08 19 12 30 00	2012 06 28 15 30 00	+1255	0.004	0.004
371	D	2010 08 21 12 30 00	2012 06 28 15 30 00	+1211	0.007	0.007
343	D	2010 08 19 12 30 00	2012 06 28 15 30 00	+1521	0.024	0.023
366	E	2010 08 19 16 00 00	2012 06 29 07 30 00	+1442	-0.012	-0.012
160	E	2010 08 19 16 00 00	2012 06 29 07 30 00	-990	0.004	0.003
370	F	2010 08 19 20 00 00	2012 06 29 09 30 00	+1289	0.001	0.001
156	F	2010 08 19 20 00 00	2012 06 29 12 30 00	+109	0.003	0.003
339	G	2010 08 20 15 30 00	2012 06 29 15 00 00	+1220	-0.017	-0.022
148	G	2010 08 20 15 30 00	2012 06 29 15 00 00	+1216	0.011	0.010
369	G	2010 08 20 15 30 00	2012 06 29 15 00 00	+1235	0.005	0.005
147	H	2010 08 20 18 30 00	2012 06 30 08 30 00	+964	-0.003	-0.004
162	H	2010 08 20 18 30 00	2012 06 30 03 30 00	+1668	0.005	0.003
Nortek current meter						
Inst #	Mooring ID	Start underwater date	End Underwater date	Final clock correction (s); init. clock offset assumed 0.	Adjustment to MicroCAT temperature (see individual structure files for dates corrections applied).	
		(YYYY MM DD HH Min SS)			deployment	recovery
6746	A	2010 08 18 13 30 00	2012 06 28 08 30 00	-25	0.003	0.005
6728	B	2010 08 18 17 00 00	2012 06 28 12 00 00	-38	-0.071	-0.069
6756	C	2010 08 18 21 00 00	2012 06 28 14 30 00	-71	0.041	0.043
6733	C	2010 08 18 21 00 00	2012 06 28 14 30 00	-47	0.003	0.006
6730	D	2010 08 19 11 30 00	2012 06 28 17 30 00	0	-0.068	-0.066
6770	E	2010 08 19 16 00 00	2012 06 29 08 30 00	-37	-0.035	-0.032
6741	E	2010 08 19 16 00 00	2012 06 29 08 30 00	+55	0.033	0.036
6731	G	2010 08 20 15 30 00	2012 06 29 15 00 00	-43	0.019	0.024
6738	G	2010 08 20 15 30 00	2011 09 04 17 44 01	-43	-0.056	-0.054
6744	H	2010 08 20 18 30 00	2012 06 30 09 30 00	-35	0.056	0.058

Table A4. Calibration corrections, separated by instrument type, continued.

SeaBird SBE37 MicroCAT

Inst #	Mooring ID	Start underwater date (YYYY MM DD HH Min SS)	End Underwater date (YYYY MM DD HH Min SS)	Final clock correction (s); init. clock offset assumed 0.	Sea-Bird factory calculated T and S drifts, approx. spring 2010 – fall 2012. T (mdegC)	S (psu per month) **
7595	A	2010-Aug-18 13:30:08	2012-Jun-28 08:30:07	-3	0.81	-0.0001
7585	A	2010-Aug-18 13:30:08	2012-Jun-28 08:30:07	-26	0.09	0
7583	A	2010-Aug-18 13:30:08	2012-Jun-28 08:30:07	17	-0.26	0.0001
7594	B	2010-Aug-18 17:00:08	2012-Jun-28 11:00:08	-3	0.90	0.0001
7593	B	2010-Aug-18 17:00:08	2012-Jun-28 11:00:08	39	0.86	0
7584	B	2010-Aug-18 17:00:08	2012-Jun-28 11:00:08	15	0.25	0
7591	C	2010-Aug-18 22:00:07	2012-Jun-28 11:30:07	11	0.68	-0.0004
7582	C	2010-Aug-18 22:00:07	2012-Jun-28 14:30:07	0	-0.25	-0.0001
7592	C	2010-Aug-18 22:00:07	2012-Jun-28 14:30:07	11	0.52	0
2034	C	2010-Aug-18 22:00:01	2012-Jun-28 14:30:01	150	0.01	-0.0002
7581	C	2010-Aug-18 22:00:07	2012-Jun-28 14:30:07	17	-0.08	0.0003
7587	D	2010-Aug-19 12:30:08	2012-Jun-28 15:30:08	19	-0.18	0
7588	D	2010-Aug-19 12:30:08	2012-Jun-28 15:30:08	3	0.17	0
1649	D	2010-Aug-19 12:29:59	2012-Jun-28 15:30:01	3	-0.44	0
7586	D	2010-Aug-19 12:30:08	2012-Jun-28 15:30:08	11	0.17	0
7598	D	2010-Aug-19 12:30:08	2012-Jun-28 15:30:08	2	-0.72	-0.0001
7589	E	2010-Aug-19 16:00:07	2012-Jun-29 07:30:08	-595	0.56	0
7590	E	2010-Aug-19 16:00:07	2012-Jun-29 07:30:08	37	-0.59	-0.0001
2029	E	2010-Aug-19 16:00:00	2012-Jun-29 07:30:01	161	-1.00	-0.0003
7596	E	2010-Aug-19 16:00:07	2012-Jun-29 07:30:08	-35	1.08	0
2032	E	2010-Aug-19 15:59:59	2012-Jun-29 07:30:00	272	-0.30	0
7602	E	2010-Aug-19 16:00:07	2012-Jun-29 07:30:08	8	-0.56	0.0001
7601	F	2010-Aug-19 20:00:08	2012-Jun-29 12:30:08	-29	-0.40	0
2028	F	2010-Aug-19 20:00:00	2012-Jun-29 12:29:59	192	-0.06	-0.0003
7604	F	2010-Aug-19 20:00:08	2012-Jun-29 12:30:08	-24	0.15	0
7597	G	2010-Aug-20 15:30:08	2012-Jun-29 15:00:08	-15	-0.09	-0.0002
7576	G	2010-Aug-20 15:30:08	2012-Jun-29 15:00:08	-17	0.13	0
2030	G	2010-Aug-20 15:29:58	2012-Jun-27 14:59:59	164	0.88	-0.0002
7577	G	2010-Aug-20 15:30:08	2012-Jun-29 15:00:08	21	0.32	0.0001
2037	G	2010-Aug-20 15:30:00	2012-Jun-29 15:00:01	44	-0.33	0
7579	G	2010-Aug-20 15:30:08	2012-Jun-29 15:00:08	13	-0.09	0
7603	G	2010-Aug-20 15:30:08	2012-Jun-29 15:00:08	-11	-0.08	0.0001
7578	H	2010-Aug-20 18:30:08	2012-Jun-30 03:30:08	2	-0.26	0.0001
7580	H	2010-Aug-20 18:30:08	2012-Jun-30 03:30:08	22	0.48	0
1640	H	2010-Aug-20 18:30:01	2012-Jun-30 03:30:02	174	-0.12	-0.0001
7605	H	2010-Aug-20 18:30:08	2012-Jun-30 03:30:08	17	-0.04	0

* Clock offset is of opposite sign. If negative clock correction, then final clock measurement was fast.

** Note that factory calibration coefficients for conductivity (not shown) were applied to conductivity using slope correction, and salinity calculated from corrected temperature and conductivity, according to Sea-Bird, Inc. release note "appnote31Feb10.pdf." Salinity drift provided here to give indication of drift in conductivity cell.

Table A5. MicroCAT conductivity quality control cuts.

Instrument s/n	Conductivity sections cut
mc7584	10-Sep-2010 05:16:48 to 02-Sep-2011 00:00:00
mc7597	25-Apr-2012 19:40:48 to 28-Jun-2012 19:40:48
mc7589	20-Aug-2011 20:52:48 to 03-Sep-2011 00:43:12
mc2029	27-Jan-2011 05:00:00 to 27-Jan-2011 17:00:00

Table A6. Instrument accuracy and resolution.

Instrument	Component	Initial accuracy	Typical drift	Resolution
Seabird MicroCAT SBE 37-SM*	conductivity	±0.0003 S/m (±0.003 mS/cm)	±0.0003 S/m (±0.003 mS/cm) per month	0.00001 S/m (0.0001 mS/cm)
	temperature	±0.002°C	±0.0002°C per month	0.0001°C
	pressure (Druck)	0.1% of full scale range	0.05% of full scale range per year	0.002% of full scale range
Current Meter Aanderaa RCM-11**	speed	±0.15 cm/s	Not specified.	0.3 cm/s
	direction	±2°	Not specified.	0.1°
	temperature (Fenwall GB32JM19)	±0.05°C	Not specified.	0.1% of full scale range Note: All RCM11s used the Low Range (–2.70 to 21.77°C) for temperature conversion, so resolution for this mooring is 0.02°C.
Current Meter Nortek AquaDopp 6000 DM***	speed	1% of measured value plus ±0.5 cm/s	Not specified.	0.5 – 1.0 cm/s (instrument uncertainty)
	direction	±5° for 0-15° tilt and ±7.5° for 15-35° tilt.	Not specified.	0.35°
	temperature	±0.01°C	Not specified.	0.01°C
	pressure	0.25%	Not specified.	Better than 0.005% of full scale per sample.

*http://www.seabird.com/products/spec_sheets/37smdata.htm @ 20 December 2011
**http://www.icm.csic.es/bio/projects/eflubio/RCM11.pdf @ 20 December 2011
***http://www.coastal-usa.com/aquadopp.pdf @ 16 April 2014

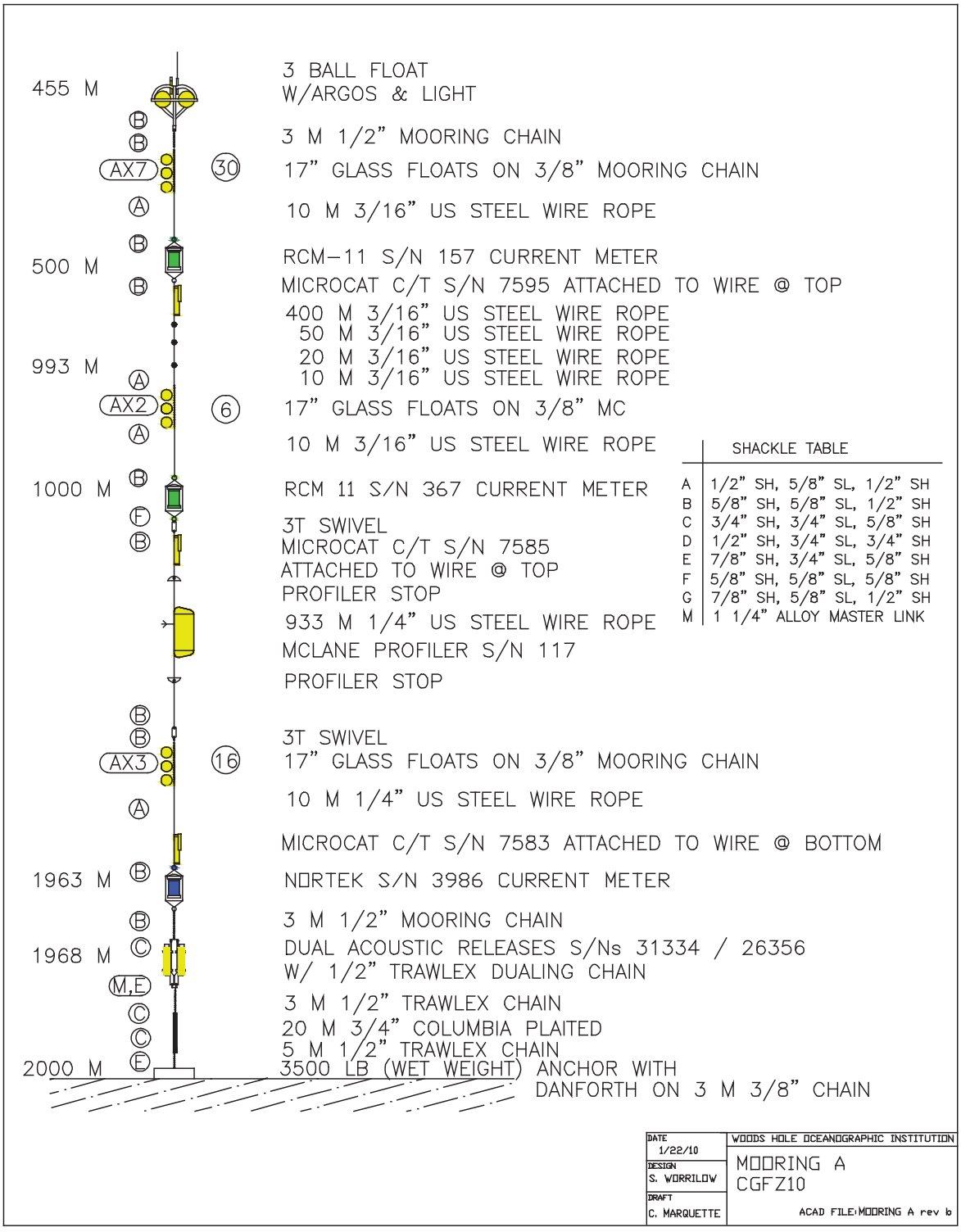

Figure A1. Diagram of Mooring A. Nortek s/n 3938 was replaced with Nortek s/n 6746.

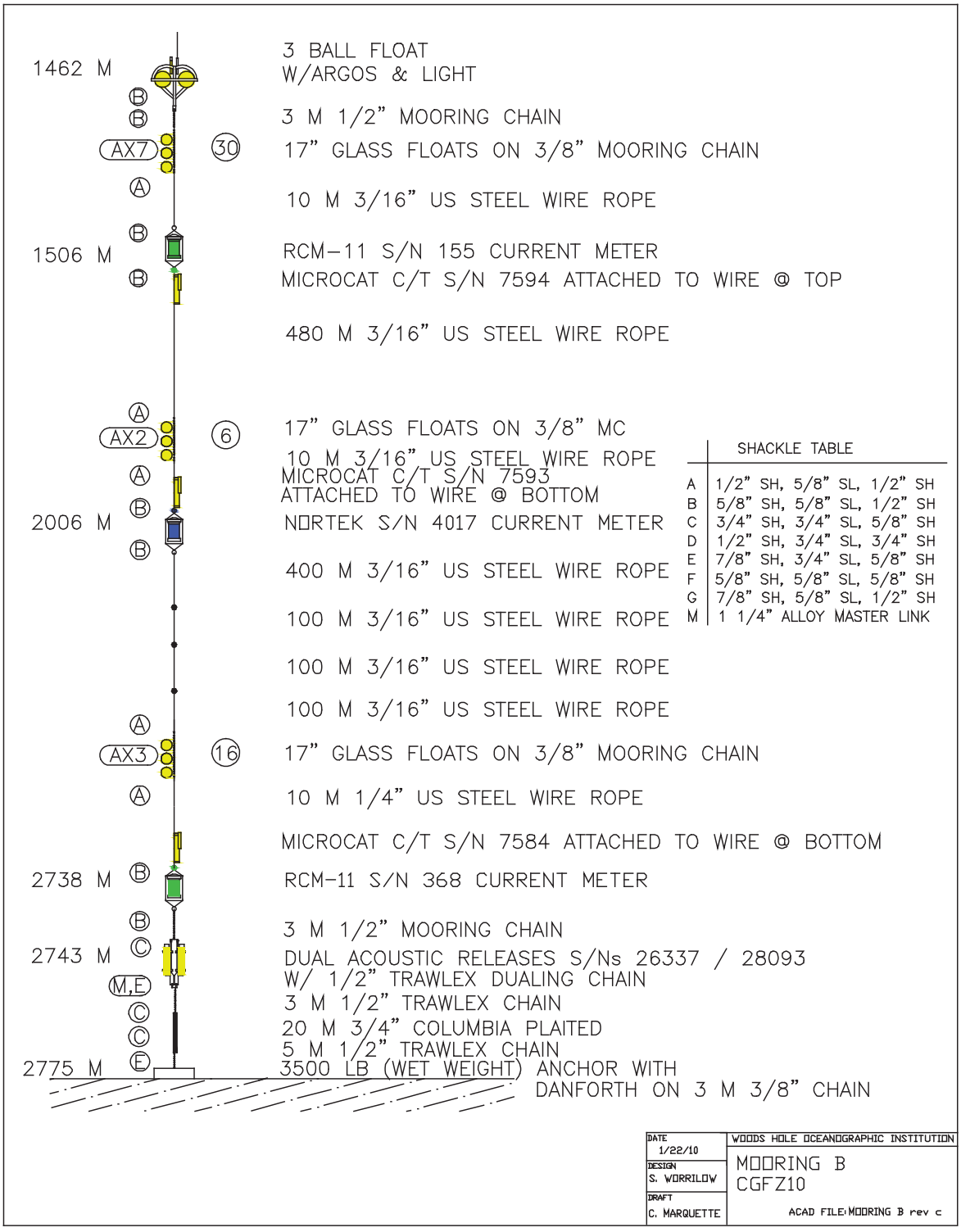

Figure A2. Diagram of Mooring B. Nortek s/n 4017 was replaced with Nortek s/n 6728.

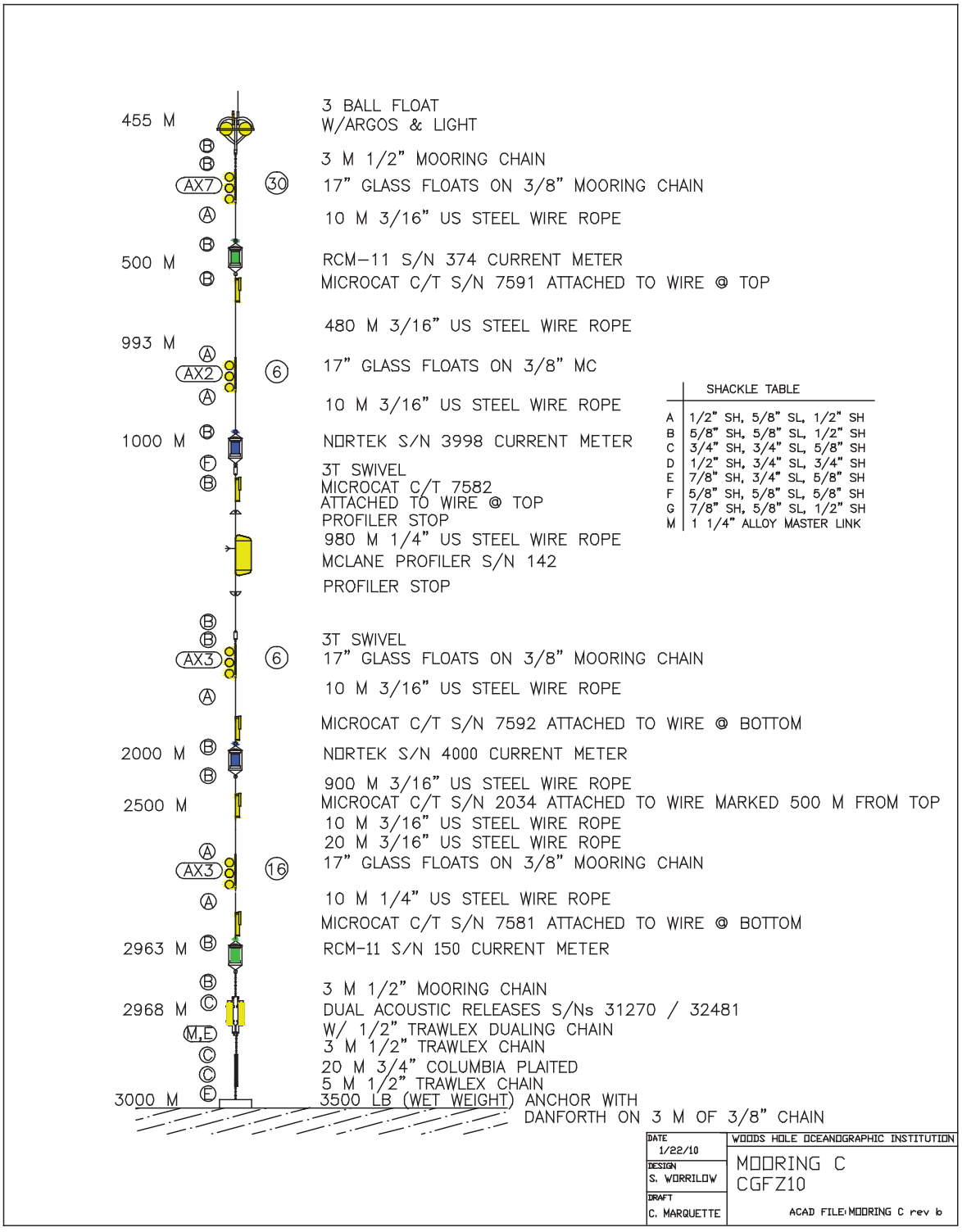

Figure A3. Diagram of Mooring C. Norteks s/n 3998 and 4000 were replaced with Norteks s/n 6756 and 6733, respectively.

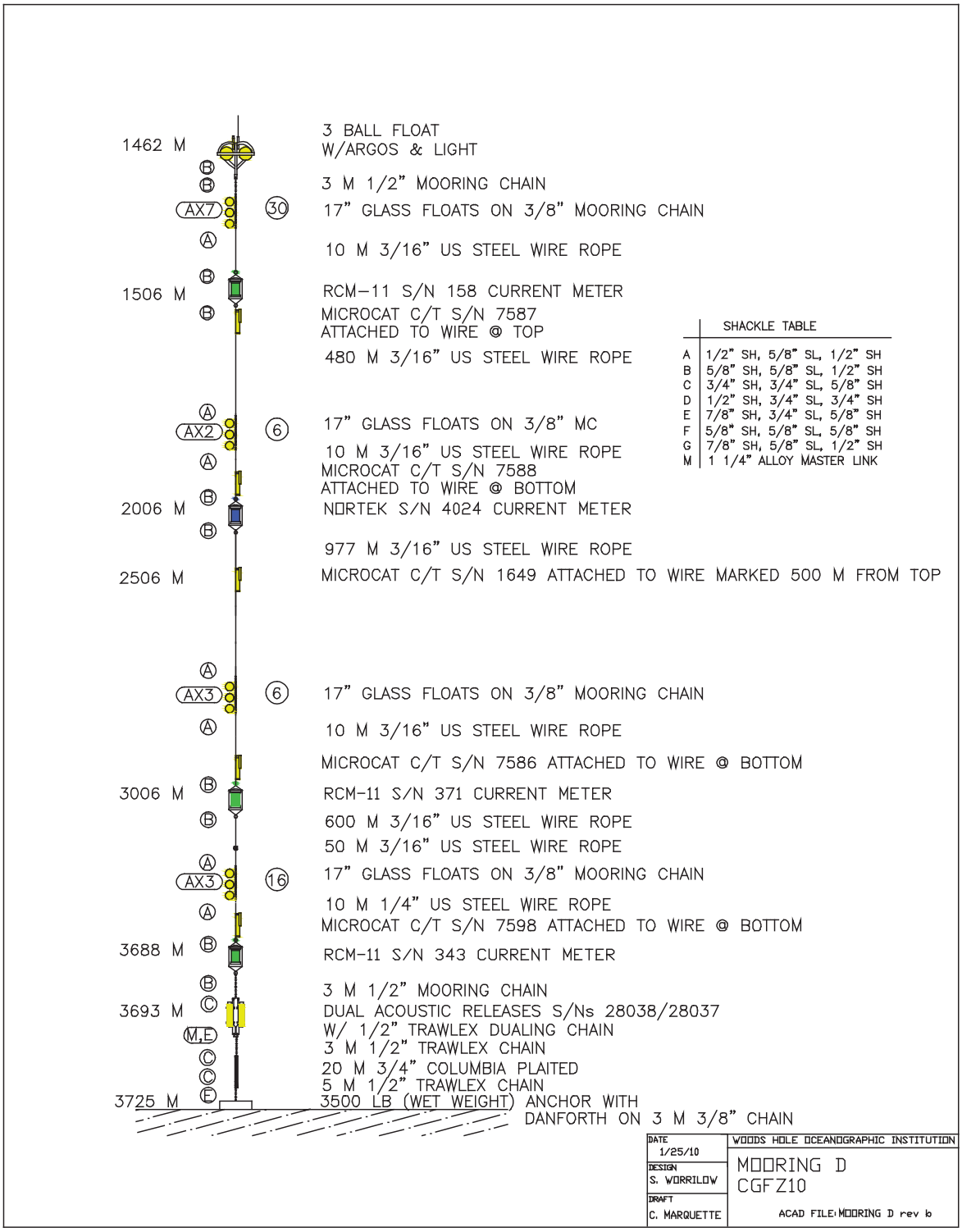

Figure A4. Diagram of Mooring D. Nortek s/n 4024 was replaced with Nortek s/n 6730.

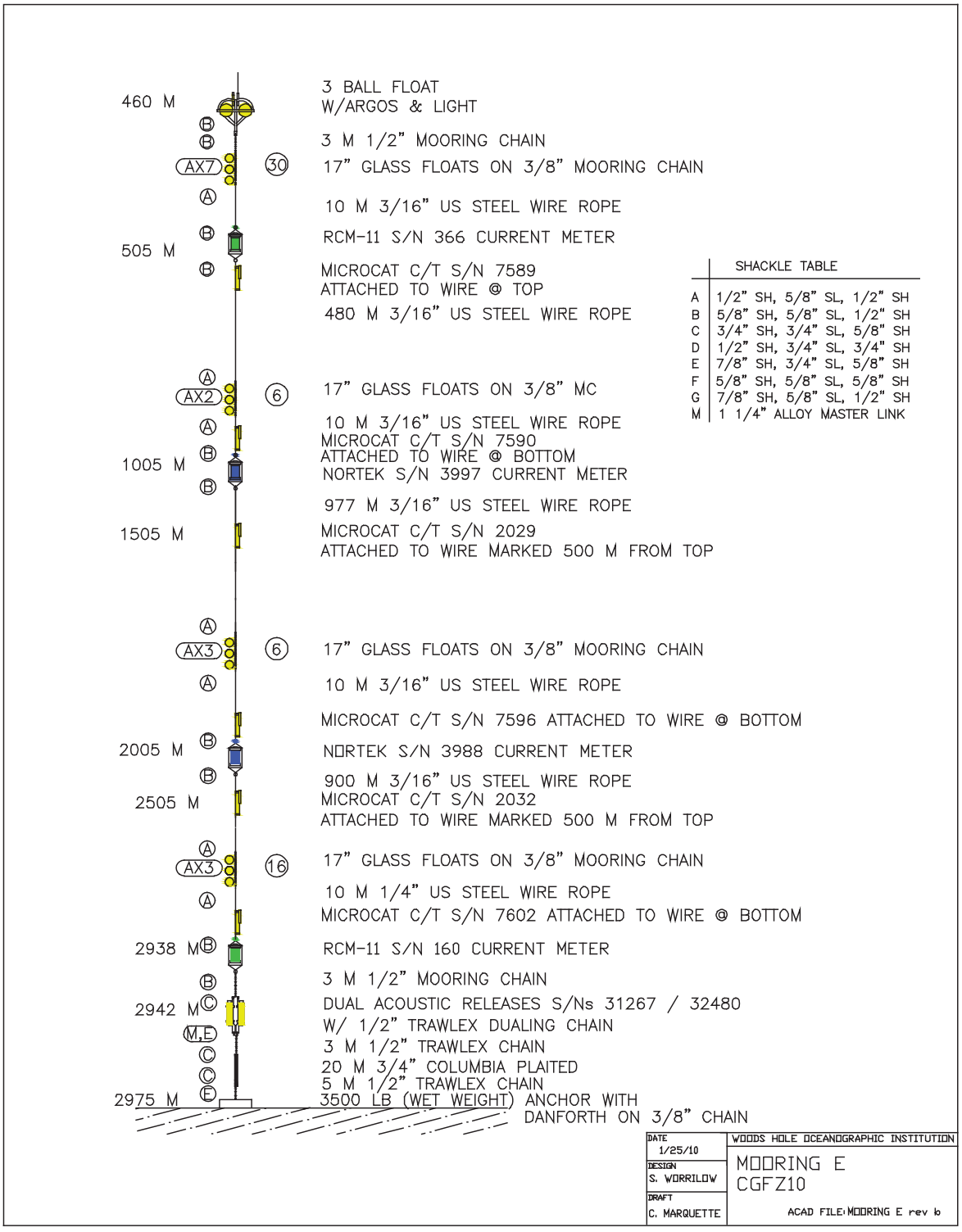

Figure A5. Diagram of Mooring E. Norteks s/n 3997 and 3988 were replaced with Norteks s/n 6770 and 6741, respectively.

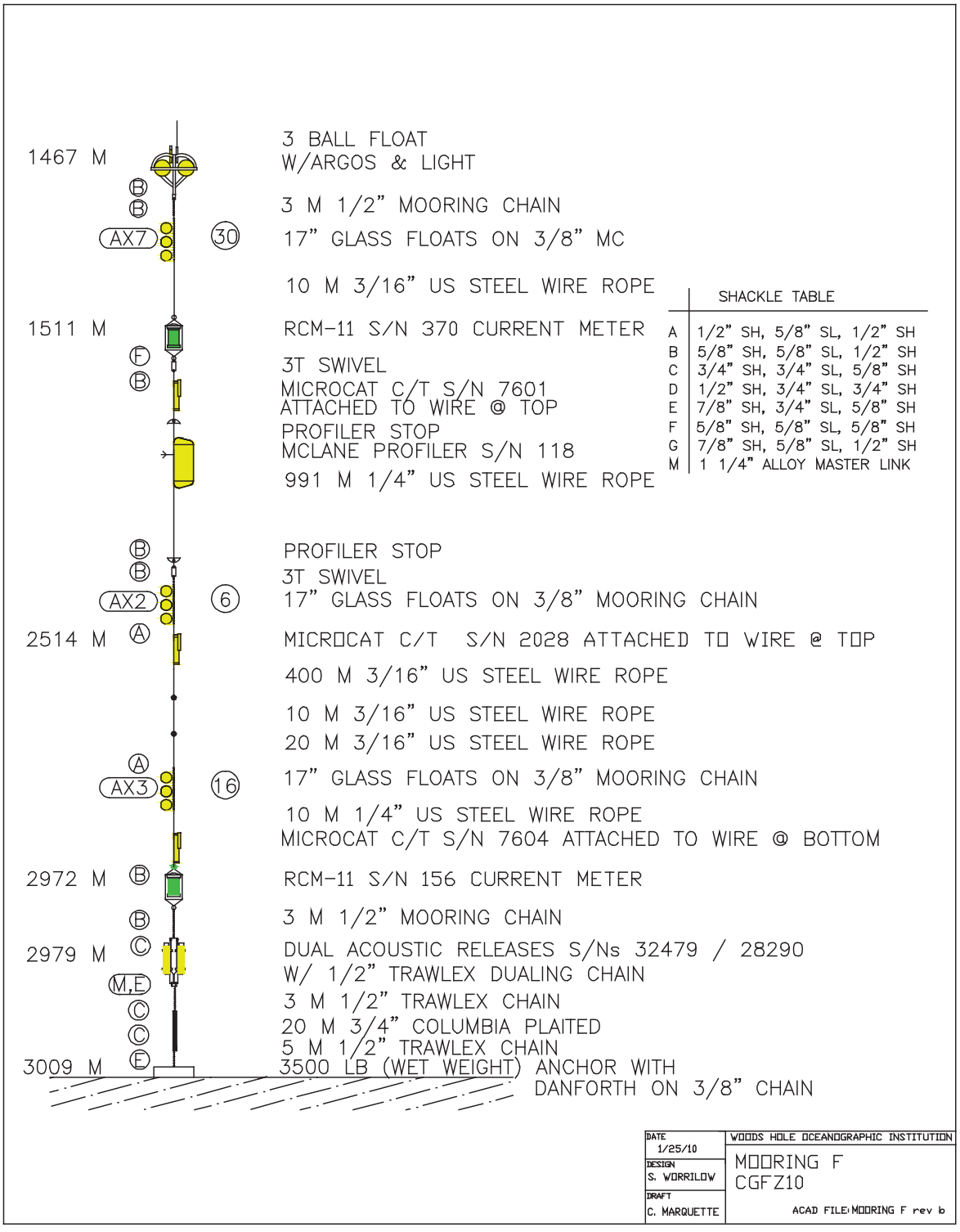

Figure A6. Diagram of Mooring F. No instrument replacements were made.

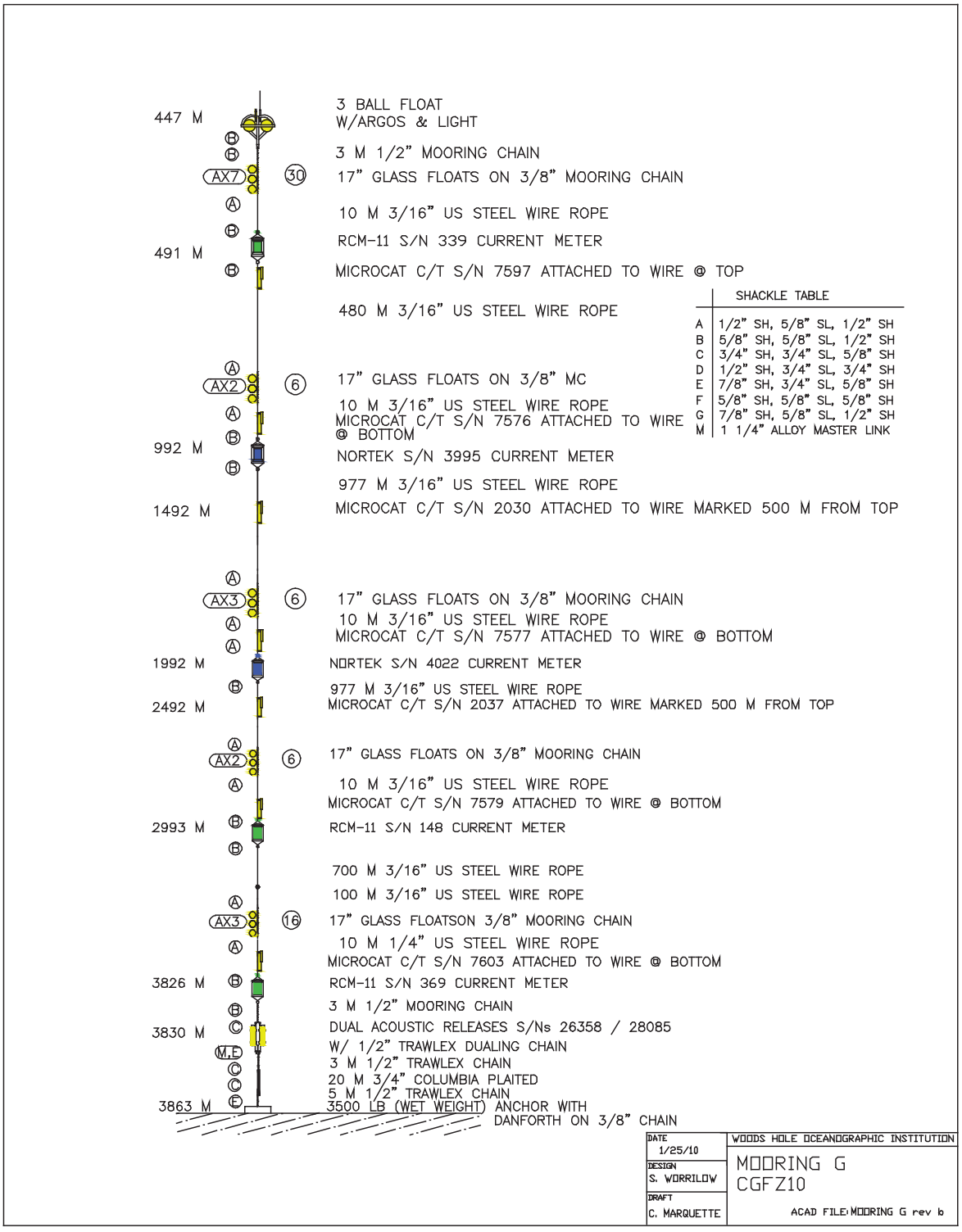

Figure A7. Diagram of Mooring G. Norteks s/n 3995 and 4022 were replaced with Norteks s/n 6731 and 6738, respectively.

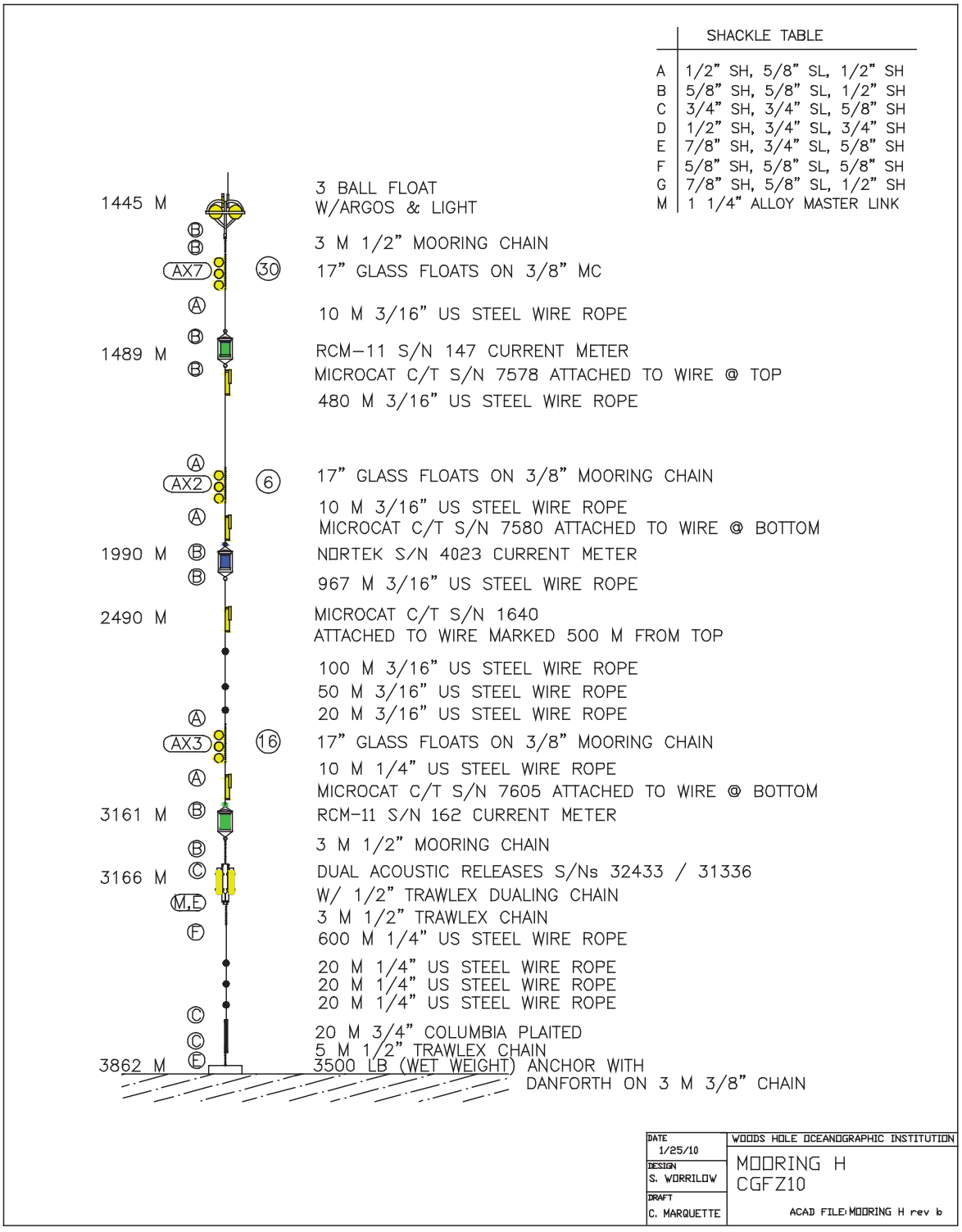

Figure A8. Diagram of Mooring H. Nortek s/n 4023 was replaced with Nortek s/n 6744.

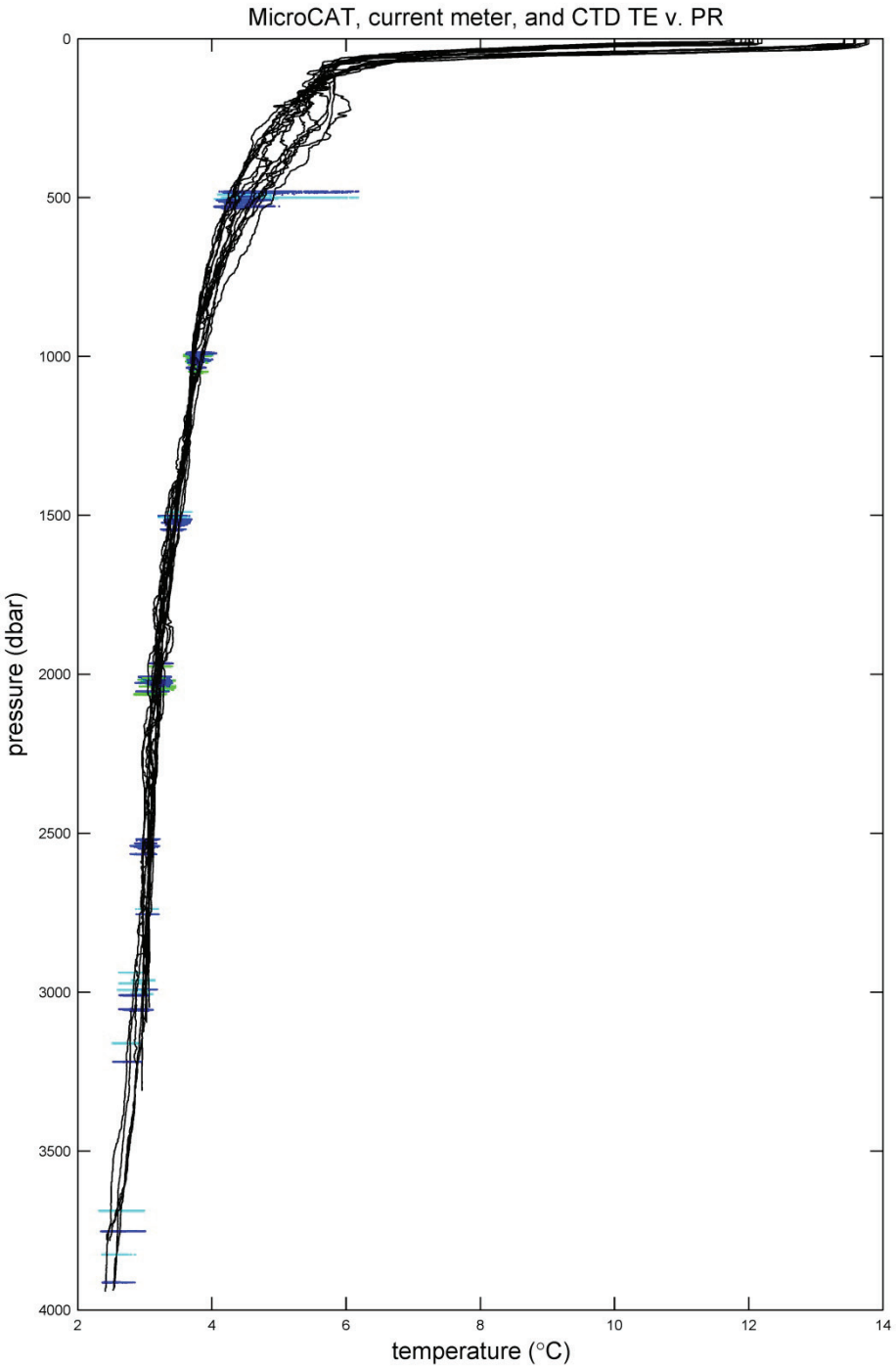

Figure A9. MicroCAT data (blue dots), Aanderaa (cyan dots) or Nortek (green dots) current meter data, and deployment and recovery CTD data (black lines) *in situ* temperature versus pressure. Every tenth data point is plotted for the mooring instruments. The unusually large scatter at 500 decibars of two MicroCATs (s/ns 7595 and 7591) and two current meters (Aanderaa s/ns 367 and 374) are from the shallowest instrument pairs on Moorings A and C. (Mooring B was a deep mooring, with shallowest instruments at 1500 meters depth.)

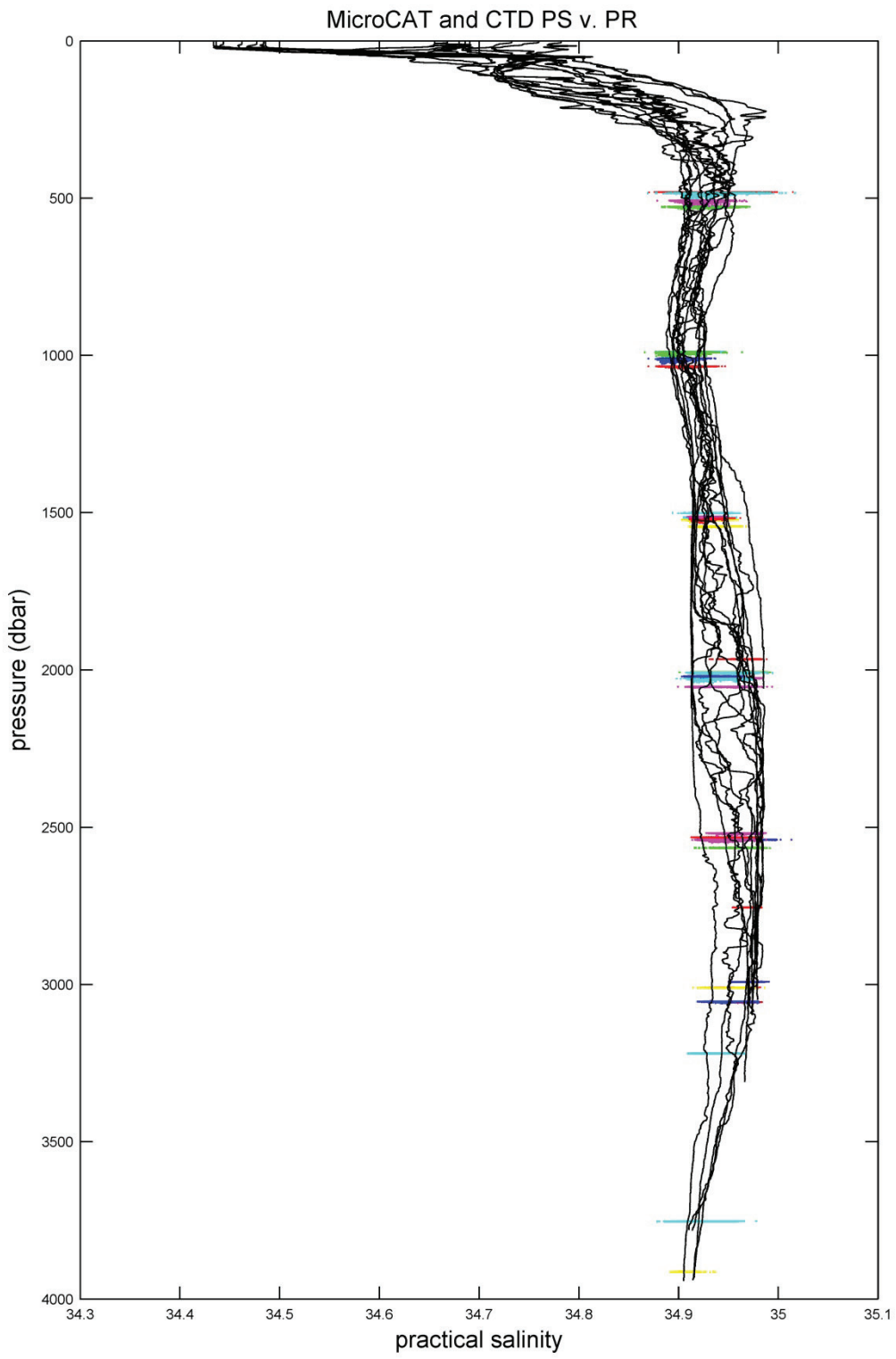

Figure A10. MicroCAT data (colored dots) and deployment and recovery CTD data (black lines) practical salinity versus pressure. Every tenth data point is plotted for the mooring instruments.

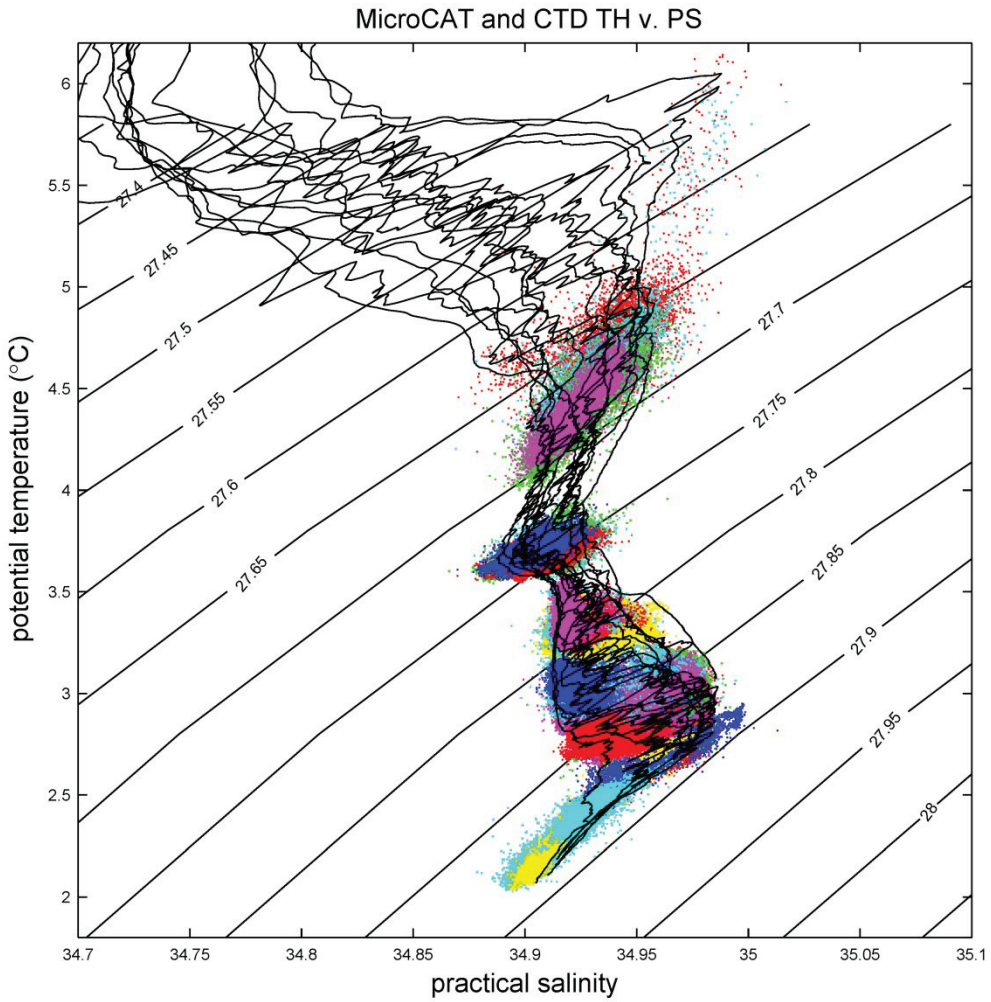

Figure A11. Theta-salinity diagram for all MicroCAT data (colored dots) and deployment and recovery CTD data (black lines). MicroCAT data are colored with one color per instrument, with some colors repeating. Every tenth data point is plotted for the mooring instruments. Mooring instrument data were not corrected to CTD cast data, as conductivity versus temperature of both CTD and MicroCAT data (next figure) show no offsets, CTD data were not contemporaneous, and CTD casts were not located at the same position.

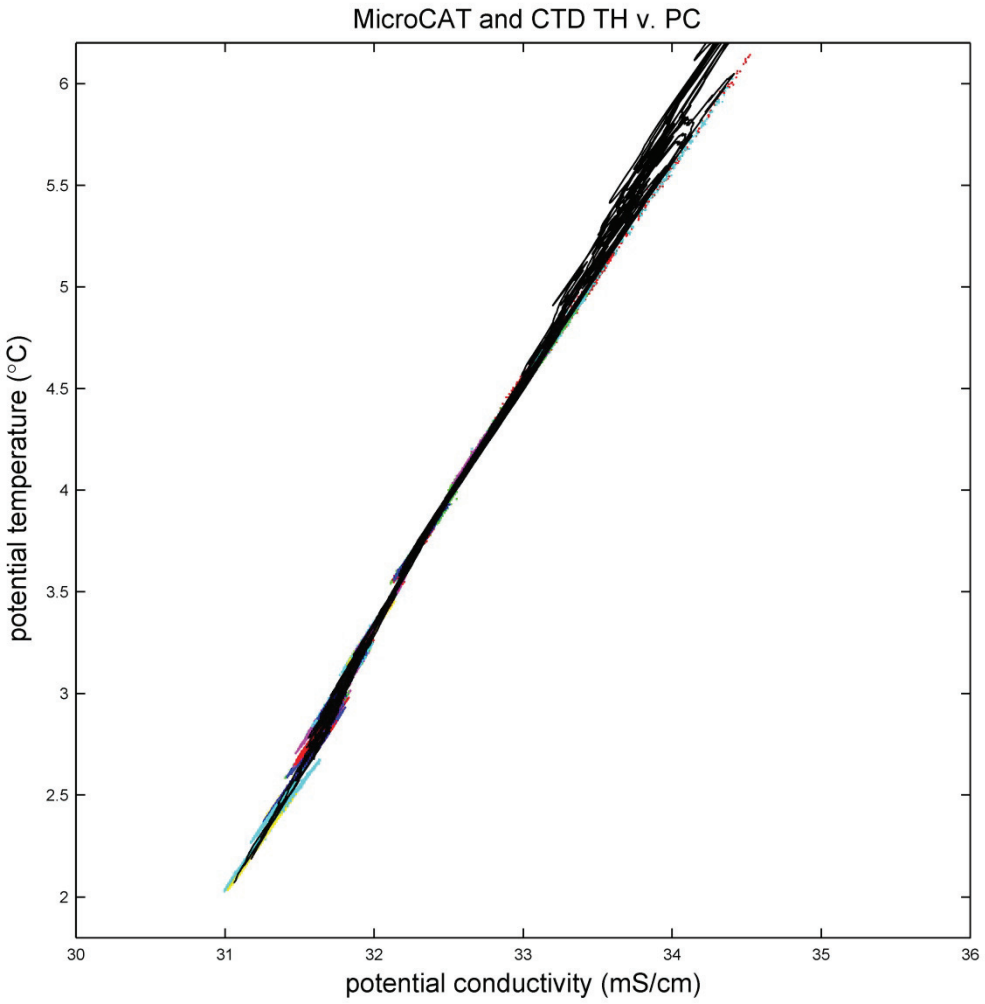

Figure A12. Potential conductivity versus potential temperature for MicroCAT data and deployment and recovery CTD data. Data is plotted as in Figure A11.

Appendix B: McLane Moored Profiler data calibration and quality control procedure, and output data formatting.

This Appendix describes the calibration and data reduction procedures performed at the Woods Hole Oceanographic Institution on observations collected by McLane Moored Profilers (MMPs). Specifically, the procedures applied to the three MMPs, s/n 117, 142 and 118, used in the Charlie-Gibbs Fracture Zone (CGFZ) experiment. The software for binary to ASCII data conversion is provided by McLane Research Laboratories, Inc. The data files were then processed (together with calibration information that characterizes the raw sensor data) into uniformly binned pressure series of ocean temperature, salinity, and velocity using a series of MATLAB scripts (L. Trafford and J. Toole, WHOI).

The appendix text is arranged as follows. Section B1 includes MMP configuration and programmed missions, section B2 details MMP data return and problems encountered, section B3 contains the outline of raw data and calibration, section B4 details merging raw data and pressure gridding, section B5 discusses velocity bias and scaling of FSI current meters, section B6 reviews the methods used for CTD conductivity calibration, and finally, section B7 reviews the final MMP data format.

B1. MMP Configuration and Programmed Missions

As currently configured, the McLane Moored Profiler (MMP) consists of three major units which acquire different types of data during each vertical profile:

- **Main Instrument Controller:** the unit that governs profile and sampling operations and creates the engineering file holding time, motor current, battery voltage, pressure, and optionally fluorescence or optical back scatter.
- **CTD unit:** a Falmouth Scientific Inc. (FSI) or Sea-Bird Electronics Inc. (SBE) sensor unit measuring conductivity, temperature, and pressure.
- **ACM unit:** a Falmouth Scientific Inc. (FSI) or a Nobska MAVS acoustic current meter with four channels of raw velocity data, three channels of compass readings and two axes of tilt.

The three MMPs were deployed with the Charlie Gibbs Fracture Zone moored instrument array as specified in Table B1.

Table B1. MMP mooring details and corresponding shipboard CTD information.

MMP Serial Number	Mooring ID	Deployment Latitude	Deployment Longitude	Deployment Date (UTC)	Recovery Date (UTC)	Closest 2010 M82/2 CTD Station / Profile #	Closest 2012 MSM-21/2 CTD Station / Profile #
MMP117	CGFZ-A	52°55.50'N	35°26.68'W	18.8.2010	28.06.2012	37 / 604	387 / 001
	Pressure range ~ 1000 dbar to 2000 dbar						
	Recorded from 26 August 2010 – 11 June 2012						
	654 moving profiles completed						
MMP142	CGFZ-C	52°46.48'N	35°19.44'W	18.8.2010	29.06.2012	35 / 601	389 / 003
	Pressure range ~ 1000 dbar to 2000 dbar						
	Recorded from 25 August 2010 – 27 June 2012						
	676 moving profiles completed						
MMP118	CGFZ-F	52°27.54'N	35°16.07'W	19.8.2010	29.06.2012	38 / 609	395 / 006
	Pressure range ~ 1500 dbar to 2500 dbar						
	Recorded from 26 August 2010 – 8 May 2012						
	353 moving profiles completed						

All MMPs were scheduled to complete a series of moving and stationary profiles throughout their deployments. The MMPs were programmed to begin a set of 5 moving profiles every 5 days, which spanned a given pressure range (see Table B1), and started and ended in the middle of the range. In contrast, the first burst of moving profiles completed by the MMPs began at the deeper pressure limit for deployment purposes. Within a burst, moving profiles had their start times separated by 6 hours. Moving profiles spanning the full pressure range took roughly one

hour to complete, while shorter profiles took about 30 min to complete. MMPs 117 and 118 spanned 1000 to 2000 dB and MMP 142 spanned 1500 to 2500 dB and have their relative sampling pattern depicted in Figure B1.

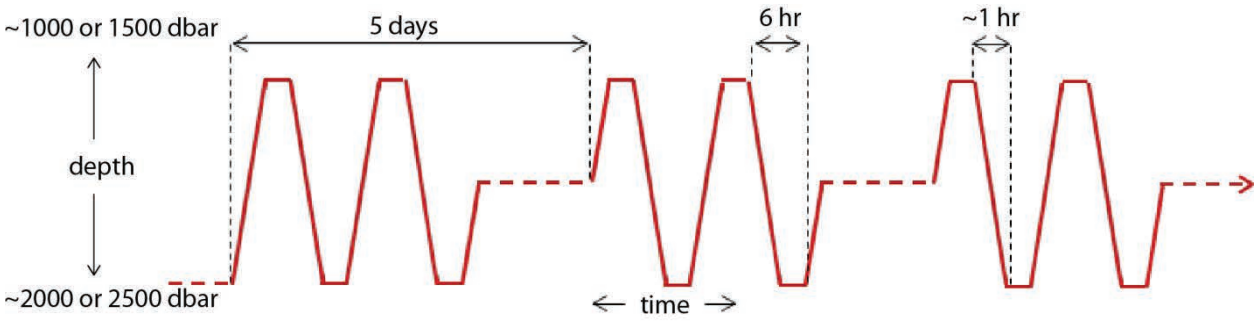

Figure B1. MMP mission details repeated from main text, Figure 4.

B2. MMP Data Return and Problems Encountered

While MMPs are programmed to complete specific missions, instrument failures resulting in poor data collection are always a possibility. Due to the MMP's complexity and motion along a mooring line, special care has been taken to assess any problems that may have occurred during a given deployment. Below summarizes MMP performance of instruments included in the CGFZ field array.

MMP 117 experienced relatively normal profiling with good data return until profile 4132, when the CTD pressure, temperature, and conductivity sensors began to malfunction and record unphysical data. Since data from both the CTD unit and the current meter unit are pressure gridded using the CTD pressure values, this became problematic when creating a gridded data product. As a solution, the MMP's pressure data from the engineering unit was interpolated to match the sampling rate of the MMP CTD unit and was used to replace segments of bad data. This proved to work very well with the pressure gridding steps mentioned below. There was still a loss of some temperature and conductivity data near the end of the record.

MMP 142 was very successful in completing the scheduled profiling pattern and full pressure range. All CTD data appear to be within good physical ranges throughout the whole deployment. The current meter on this unit, however, experienced severe malfunctions. Firstly, data return from the current meter unit was far below average as many profiles saved by the MMP did not contain any current meter data, while still containing data from the CTD unit. In addition, after assessing the data quality of the raw current meter sensor, one of the four raw

speed channels logged completely unphysical values for the whole deployment. This was amended due to the fact that the MAVS current meters measure redundant raw speed paths and velocity vectors were still able to be calculated as detailed in methods listed below.

While MMP 118 returned a considerable amount of data, it did experience difficulty moving along the mooring line for certain windows of its deployment. Profiles 1585- 3370 occurred while the instrument was stuck near 1500 dB, which resulted in the MMP recording mostly stationary profiles at 1500 dB rather than 2000 dB and recording very few moving profiles during this time. Near the end of the record, MMP 118 experienced difficulties moving into shallower waters. Due to this, profiles 4992- 6894 were on average only sampled between 2200 dB- 2500 dB.

The FSI EMCTD mounted on MMP 118 also experienced problems with its temperature and conductivity sensors. A large unphysical drift in conductivity calibration near the beginning of the record was characterized and removed using methods detailed in later sections. In addition, the CTD unit on this MMP stopped recording physical conductivity and temperature data after profile 4990. The conductivity, salinity, temperature and potential temperature data for profile 4990- 6894 have been set to NaN with appropriate quality flags changed.

B3. Raw Data and Calibration Outline

For each vertical profile, one binary file of each type is written to the flash memory card. The binary data on the MMP's flash card are accessed on a PC via the McLane Research Laboratories (MRL) unpacking routine, Unpacker.exe. The output of the unpacking program is a set of three ASCII data files for each profile saved: *C#######.TXT*, *A#######.TXT*, and *E#######.TXT*, where ####### is the profile number, padded with leading 0's.

Once data are converted to ASCII, four general processing steps are performed. More information on each is provided in the sections below.

1. *Merging Raw Data Files*
   Since each one-way profile performed by an MMP produces a set of three binary files, the output of the binary to ASCII software provided by McLane produces three ASCII files: the main controller unit file, the CTD unit file, and the ACM unit file. After the unpacking software has been used, a MATLAB script is used to merge the three ASCII files into one MATLAB format file per profile.

2. *Pressure Gridding Raw Files*
   Once raw MATLAB files are created, a corrected time vector is created for all variables in each profile MATLAB file allowing common binning of all data against pressure.

Pressure, temperature, and conductivity sensor values then have polynomials generated from laboratory calibrations applied to convert raw sensor values to calibrated values. A laboratory compass spin test is used to determine the physical alignment of the flux gate compass coordinate system relative to the MMP body and *in situ* data are used to calculate bias and scale factors for the flux gate compass data. ACM and CTD data are then averaged into 2 dbar pressure bins and pressure-gridded data files are written for each profile.

3. *Velocity Bias and Scaling*
   ACM transducer channel biases are determined using *in situ* data. Biases are removed and east, north, and vertical velocities are derived.

4. *CTD Conductivity Calibration*
   CTD conductivity data is calibrated using shipboard CTD measurements if available and spikes are edited out on a profile-by-profile basis.

B4. Merging Raw Data and Pressure Gridding

To facilitate processing and archiving the raw MMP data, the Engineering, CTD, and ACM data from each profile are merged into one MATLAB-format data file. The raw data from the CTD and ACM are checked to ensure that all variables are within physical ranges and bad data are interpolated.

Since time is only logged in the engineering files, which are logged at a much slower rate than the CTD and ACM units, the time vector is interpolated to the sampling rates of the CTD and ACM. This is done by aligning the pressure time series of the engineering unit and the CTD unit and interpolating to produce a time estimate for each CTD scan. Since the ACM unit does not measure time or pressure, there are no cross-referenced time marks between the CTD and ACM data apart from a manufacturer-stated sample rate and the recorded times when the units are instructed to turn on. To align the CTD and ACM data streams, the starting and ending transients at the beginning and end of each profile interval are located using the rate of change of pressure for the CTD unit and velocity for the ACM unit. The data records are aligned using the points where the time rate of change of pressure and vertical velocity are both 50% of their steady values during profiling, which corresponds to the middle of the speed-up and slow-down events of the MMP. A constant (but not necessarily same) sample rate for each sensor is then assumed so that after aligning a time for each ACM scan is determined, the CTD pressure time series is interpolated to get a pressure value for each ACM scan, allowing common binning of all data against pressure.

In the case of MMP 117, after which profile 4132 began to malfunction and record unphysical data from the CTD pressure, temperature, and conductivity sensors, this method was slightly altered. First, all unphysical CTD pressure data was identified within a moving profile. In most cases, a given profile's beginning portion of the CTD pressure data was well behaved and as the profile progressed the data would switch to being unphysical. Reasonably and unreasonably behaved pressure values were first located using a simple wild edit criterion. The point at which the bad data section began was then matched in time using the engineering pressure values in a similar fashion as described above. Using this time marker and the time difference between the CTD and ACM unit powering down after completing a profile, a time basis could be derived for interpolating the engineering pressure values to match the sample rate of the CTD unit.

CTD Lab Calibrations

Lab calibrations are carried out for the pressure, temperature, and conductivity (if available) sensor on the CTD before and/or after a deployment (Table B2). The standard laboratory values are fit as a function of the CTD sensor responses and the resulting polynomial fits are used to convert raw CTD sensor values to calibrated values. In the event that no laboratory conductivity calibrations are available, raw sensor values are carried forward instead. All conductivity data are then further calibrated using shipboard CTD data that is close in space and time (Table B1).

Table B2. Dates of EMCTD calibrations

MMP Serial Number	Mooring ID	EMCTD	Pre Deployment Calibration Dates	Post Deployment Calibration Dates
MMP117	CGFZ-A	FSI 1365	April 2008	Not available
MMP142	CGFZ-C	SBE 0060	May 2010	December 2010
MMP118	CGFZ-F	FSI 1316	April 2008	Not available

In the event that laboratory calibrations from before and after a deployment produce very different calibrations for a given sensor, both sets of calibrations are assessed. If there is reason to believe one set of calibrations should not be used, then the other set is used independently. There are several factors that can contribute to disagreements of before and after calibrations, for example, a large drift in sensor response throughout the course of a deployment.

In addition, a time lag parameter describing the number of scans the thermometer lags the conductivity cell is used to recursively filter both the conductivity and pressure data such that they match the time response characteristics of the temperature data as best as possible. Figure B2, taken from the Seabird Electronics CTD Processing Manual, demonstrates the importance of having temperature, conductivity, and pressure data properly related in time: unphysical salinity spikes and density inversions result from misaligned measurements.

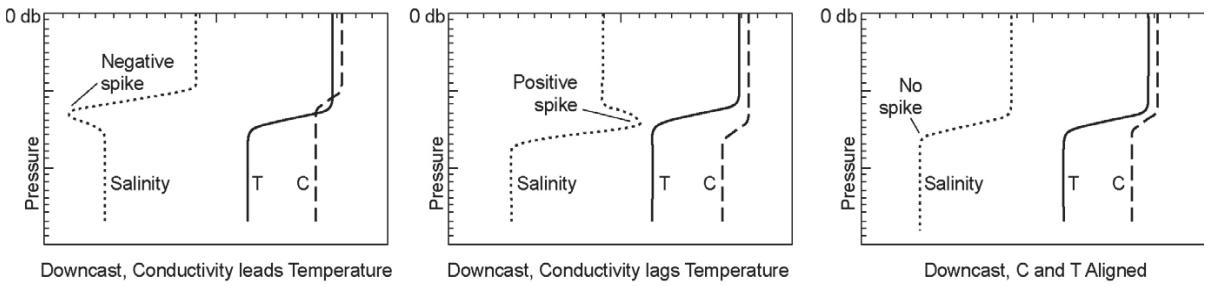

Figure B2. Alignment of C and T, from Seabird Electronics CTD Processing Manual.

After both steps, the CTD data are fully calibrated with the exception of the conductivity data, which are adjusted and edited in later stages.

ACM Compass Lab Calibrations

In situ data are used to work out the magnetometer bias and range terms that will scale the compass data to a unit circle. These can be estimated simply by over plotting the two raw signals from the compass, aHx versus aHy, from a subset of profiles and working out the offsets and range adjustments so that the data define a circle centered on the origin.

The magnetometer data are scaled to the unit circle as follows:

$$[(aHx - Hx\_bias) / Hx\_range]^2 + [(aHy - Hy\_bias) / Hy\_range]^2 = 1,$$

where aHx and aHy are the original vector components of the compass, Hx_bias and Hy_bias describe the offset of the traced out circle from the origin, and Hx_range and Hy_range describe the scaling factors required for the circle to have a radius of 1.

At WHOI, a compass calibration procedure is performed in which each assembled MMP is held vertically (in normal operating position) and rotated to fixed points every 45 degrees around a circle (beginning with local magnetic north) while the raw compass data are logged. After the raw magnetometer data have been adjusted to the unit circle as detailed above, the result of the compass calibration is used to relate the position of the ACM stings to the compass data.

The true compass direction towards which the ACM sensor sting points is derived as follows:

$$MMPdir = dir\_sign * \arctan(aHy,aHx) + compass\_bias + mag\_dev,$$

where mag_dev is the earth's magnetic deviation, aHx and aHy represent the magnetometer data after scaling to the unit circle. The term mag_dev is the earth's magnetic declination for the

deployment site. The laboratory spin test data are used to derive 'dirsign' (which is usually +1) and 'compass_bias'. Dates of the spin test calibrations are listed in Table B3.

Table B3. Dates of CGFZ current meter calibrations.

MMP Serial Number	Mooring ID	ACM	Pre Deployment Calibration Dates	Post Deployment Calibration Dates
MMP117	CGFZ-A	FSI 1713	April 2010	April 2013
MMP142	CGFZ-C	MAVS 10273	Not Available	Not Available
MMP118	CGFZ-F	FSI 1808	May 2009	April 2013

Pressure Gridding

Once the ACM alignment is set and the raw data have had laboratory calibrations applied, bin-averaging against pressure is carried out for each MATLAB file and the resulting data are written out to a new MATLAB file (one for each moving profile). The data are typically bin averaged on a 2-dbar pressure grid having a span slightly greater than the pressures sampled in the entire deployment. In addition to outputting calibrated pressure and temperature data, velocities are derived in east, north, and vertical coordinates, and other water properties are derived such as salinity, potential temperature, and potential density (however, at this point, these variables have been derived with an uncalibrated conductivity/salinity). Bins in which there are no data for a given profile are filled with NaNs.

B5. Velocity Bias and Scaling of FSI Current Meters

It has become evident that the raw path velocity data recorded by FSI ACMs on Moored Profilers can have a depth- and temperature-dependent bias, as well as require a significant scaling adjustment. The former errors appear to be due to a combination of electronic component sensitivities to temperature and impedance variations of the acoustic transducer ceramics and/or leads to the transducer with pressure or temperature. In the laboratory, the errors have the form of sinusoidal variations of the zero-current readings with temperature having amplitudes of up to several centimeters per second peak-to-peak and "wavelength" of around 5˚C. Each of the velocity paths appear to behave independently. While the manufacturer works to ameliorate these errors in their instrument, the users of MMPs need a procedure for correcting the errors in existing data sets. A procedure has been developed to quantify and remove a depth-varying but time-independent velocity bias profile from the raw ACM data that assumes (1) the bias errors are steady with time and (2) the biases may be defined as a function of pressure only. Note that if the ocean's temperature profile is relatively steady in time, defining bias as a function of pressure or temperature is equivalent.

The basic assumptions of the procedure are that during the course of a deployment: zero true velocity is sampled at each pressure bin at least once, the time-mean ocean vertical velocity is

zero, and the raw biases are steady in time. The bias in the two horizontal paths at each depth is taken as the minimum speed recorded by those paths during the entire deployment. This assumes that at each depth, at some time during the deployment, the real ocean current was zero. For situations where the amplitude of the velocity fluctuations exceeds that of the mean, this is a reasonable assumption. In practice, the 1^{st} –2.5^{th} percentile of the speed distribution at each depth is located, and the resulting bias estimates in depth are manually edited and low-pass filtered before removing the bias profile of raw ACM data for each profile. Bias profiles for the two vertically-angled paths are derived under the assumption that the time-mean ocean vertical velocity is zero. Biases are derived such that the ensemble-averaged inferred vertical ocean velocity (difference between relative vertical velocity and vertical velocity of the MP body deduced from the pressure data) is made zero. Because wakes affect these vertically-angled paths, the up-going and down-going ensembles are treated separately. On occasion, upward moving and downward moving horizontal raw velocity paths may also need to be treated differently, as is discussed below.

The bias correction procedure involves three steps:

Raw Velocity Gridding
Pressure-averaged raw path velocity profiles are created by merging and averaging the raw velocity data with the previously created pressure gridded data (normally this data file only includes the derived north, east, and vertical velocities, which were preliminarily derived with velocity biases of zero with no slope adjustment). The result is a MATLAB-format file per input profile holding pressure-bin-averaged raw path velocity data.

Raw Velocity Bias Trace
All files from the previous step are divided into their respective upward or downward moving profile groups. Upward and downward moving profiles are often traced separately in this step since horizontal transducers may not always be perfectly aligned with respect to the MMP body and one of the two vertical transducers is always affected by the wake of the traveling MMP. The profiles in each of these groups are used to create a deployment speed distribution as a function of pressure. The 1^{st} –2.5^{th} percentile of the speed distribution are traced out and compared. The goal here is to find the smallest percentile trace that properly outlines the “zero speed” curve for each velocity path affected by the wake of the traveling MMP. The profiles in each of these groups are used to create a deployment speed distribution as a function of pressure. The 1^{st} –2.5^{th} percentile of the speed distribution are traced out and compared. The goal here is to find the smallest percentile trace that properly outlines the “zero speed” curve for each velocity path. Normally small variations of percentile choices between 1 and 2.5 produce nearly identical distribution traces. The remaining set of profiles is also traced and bias curves for all transducers for both upward and downward profiles are saved.

Velocity Bias Removal

The bias curves produced in the previous steps are manually edited to remove any spikes or NaNs and filtered to eliminate high-frequency noise as seen fit. Bias curves are then subtracted from their respective ACM raw path speeds (again as a function of pressure) in the raw velocity files from step one. The north, east, and vertical velocity components are then re-derived for each profile and new versions of the calibrated pressure-gridded profiles are saved.

Additional Velocity Calibrations

In order to obtain a speed measurement, the ACM relates the difference in time sound travels from a transducer x to a transducer y as compared from y to x to the ocean current in the direction between x and y. The distance between transducers is known, as well as the speed of sound in water, so this time difference is used to calculate a relative ocean speed between the two transducers. There can be several issues regarding the scaling between the time of flight difference and measured velocity related to flow separation, wake effects, speed of sound corrections, and instrument electronics. For MMPs in the CGFZ experiment, a scaling factor of 1 was used for all speed channels since no evidence for needing scaling correction was found.

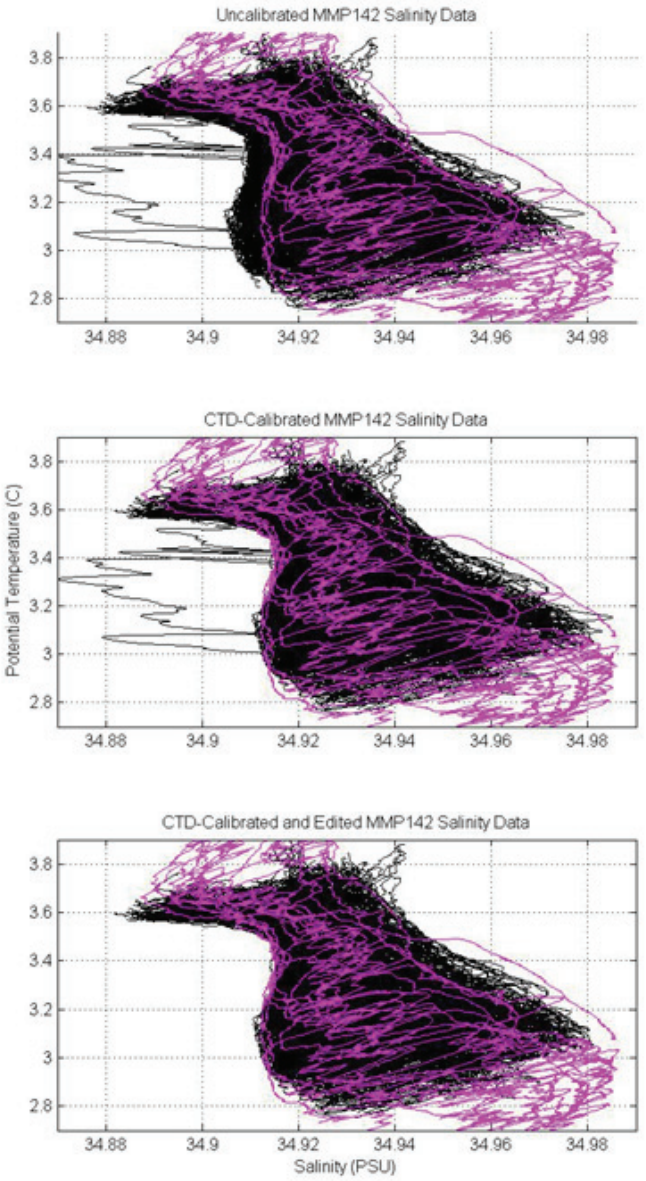

Figure B3: The two steps of MMP calibration are shown using MMP 142 from CGFZ mooring deployment. The black lines in the top plot show salinity calculated from the raw MMP conductivity data and the pink lines show the calibrated shipboard CTD salinity data. The middle plot shows the MMP salinity data derived from calibrated MMP conductivity data. The bottom plot shows the final data for MMP 142, which has been manually edited to remove spikes and offset conductivity sections.

B6. CTD Conductivity Calibration

Similar to a standard shipboard CTD instrument, conductivity data from MMPs CTD must be calibrated and edited (for example to remove spikes and larger offset segments when the cell is fouled by biological contamination). In the absence of reference conductivity data, procedures have been developed to derive conductivity and salinity adjustments based on available shipboard CTD and mooring data. All CTD data mentioned below were collected on the mooring deployment and recovery cruises, M82/2 and MSM-21/2 and have had their salinities calibrated with bottle samples as described in Rhein (2010) and Kieke (2012).

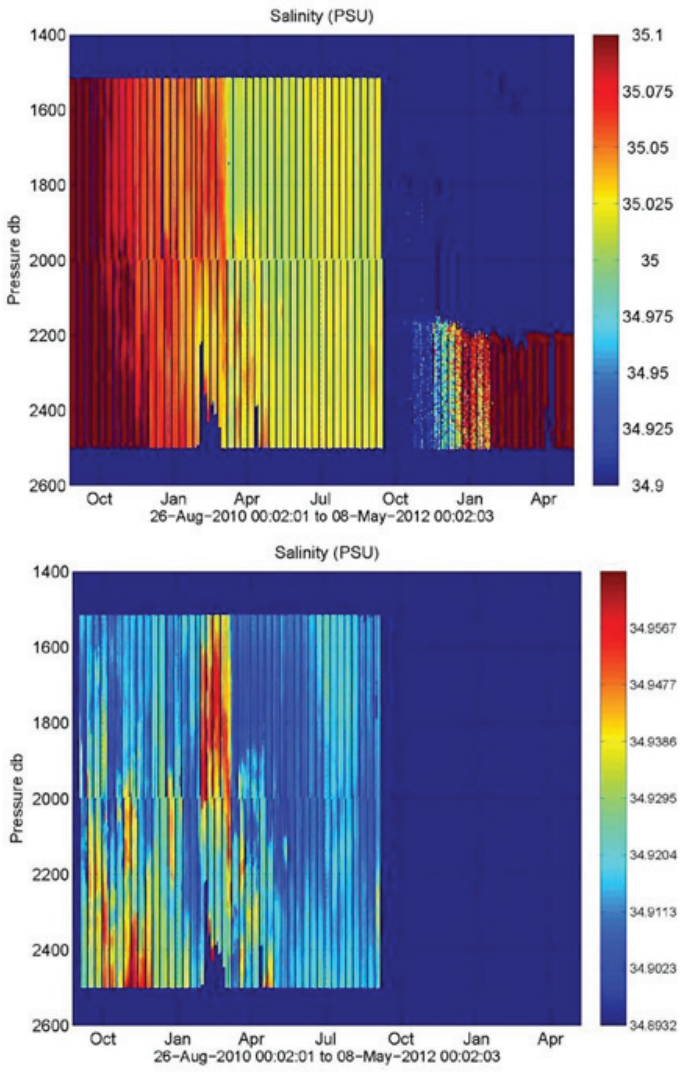

Figure B4: a) MMP 118's uncalibrated salinity data showing three periods in time: very sudden drift in calibration near beginning of record, gradual drift near middle of record, and unphysical data near the end of the record. b) MMP 118's final salinity data, which has been calibrated partially by the ratio method and partially by salt shifts.

Conductivity Calibration Methods for CGFZ

MMP 117 and 142 had very well behaved conductivity measurements throughout their deployments and no large sensor drifts were noticeable. Because of this, a constant salinity shift was applied to all profiles in order to have all data align with available shipboard CTD data in potential temperature-salinity space. Figure B3 a) and b) demonstrate this calibration method using data from MMP 142. The final salinity shift applied to MMP 142 is +0.00582 PSU and the final salinity shift applied to MMP 11 is +0.01246 PSU.

Different salinity calibration methods were used for MMP 118's salinity record as its sensor experienced dramatic calibration shifts throughout the deployment (Figure B4). Most striking on the record are the salinities recorded after October 2011, which were very unphysical. As a result those values were set to NaNs and flagged as bad data. The resulting record consisted of two parts, one

needing a profile-depending salinity shift, and another that could be broken into time windows for applying salinity shifts as detailed above.

Profiles 1 through 515 experienced such a large conductivity drift in time that special calibration methods were used. In the absence of reference conductivity data, a procedure has been developed to derive a profile-dependent conductivity adjustment that forces the salinity at a specified potential temperature to be stable in time. The approach uses the calculated potential conductivity: conductivity inverted from salinity, potential temperature and zero pressure – a quantity that, like potential temperature, should be independent of adiabatic vertical heaving of the water column.

Ratio Calibration

Shipboard CTD data and MicroCAT data are first used to determine a calibrated potential conductivity on a specified deep and stable isotherm. If enough calibrated data are available for the isotherm, a time series of calibrated conductivity will be interpolated for the time span of the MMP deployment. Given the dynamic nature of the CGFZ, it was difficult to find water masses that were stable in time. Because of this, a relatively large potential temperature range of 3.1-3.35˚C near a more defined density feature was used to provide a time-dependent potential conductivity with the addition of available MicroCAT data.

Once a calibrated potential conductivity value has been calculated, MMP conductivity profiles are also fit linearly in potential temperature-conductivity space at the same isotherm as the reference data. Using this set and the calibrated potential conductivity values, a conductivity ratio factor for each MMP profile is created:

Ratio = (calibrated potential temperature) / (raw MMP potential conductivity).

This ratio value, which is uniquely defined for each MMP profile, is then multiplied with its respective potential conductivity profile and salinity is re-derived. This step forces the potential temperature/salinity relationship to be stable on the chosen isotherm.

MMP 118's salinity calibrations are as follows: Profile 1:771 – ratio calibration using the 3.1-3.35 ˚C potential temperature isotherm, profile 772:1504 – salinity shift of -0.13300 PSU, profile 1505: 3492– salinity shift of -0.10900 PSU, profile 3493:6324 – salinity shift of -0.104500 PSU.

Manual Editing

Various editing routines for the pressure-gridded data have been developed to interpolate across salinity spikes or depth intervals where the conductivity sensor was fouled. Quality control editing for each individual CTD profile is the final step in the MMP processing and occurs after

all calibrations have been finalized. Small spikes are interpolated using the temperature-salinity relationship of the profile in question. Larger spike sections are interpolated using the potential temperature-conductivity relationship(s) from one or two user- specified reference profiles (with good conductivity data) to estimate the conductivity on a profile with fouled data. This approach yields reasonable interpolated data when the temperature-conductivity relationship is monotonic, but not when intrusions are present. Treatment of segments with intrusions can be better handled using density surfaces for interpolation rather than potential temperature. The middle and bottom plots in Figure B3 c) give examples of the result of the final conductivity/salinity editing stages.

B7. Final MMP Data

The final version of MMP data consists of a set of MATLAB-format files (one for each profile completed by the MMP). Within each file, all variables measured by the MMP:

1. have been 2-dbar-pressure gridded
    a) with a first difference quality edit on the data,
    b) with pre-deployment (and/or post-deployment) laboratory pressure calibrations applied,
    c) with pre-deployment (and/or post-deployment) laboratory temperature calibrations applied,
    d) with corrections applied such that the two compass channels define a unit circle,
    e) with ACM transducer speed biases corrected;
2. have had salinity data calibrated using associated calibrated shipboard CTD profiles that are available;
3. have had salinity and velocity data quality control edited for spikes, etc.

The final data files all contain the same variables as mentioned in the pressure gridding section with the addition of quality flag vectors. Every variable that has gone through a calibration procedure is assigned with a WOCE standard vector such that every data point of that variable is assigned a quality code as follows:

***WOCE quality flags used:**
1 = not calibrated
2 = calibrated acceptable measurement
6 = interpolated value

Each gridded file contains the following quality control variables: dpdtave_Q, pave_Q, s_ave_Q, tave_Q, uave_Q, vave_Q, wave_Q.

Profile Data Output Format

Each gridded file (one per profile) contains the following variables:

startdaytime: start day and time of the profile (serial date number)
stopdaytime: stop day and time of the profile (serial date number)
pgrid: the center values of the pressure grid used in the bin-average (dbar)
ctimave: day and time of values averaged in each pgrid bin (serial date number)
pave: average of the pressure values in each pgrid bin (dbar)
tave: average of the temperature values in each pgrid bin (˚C)
cave: average scaled conductivity in each pgrid bin (mmho)
s_ave: salinity computed using pave, tave and cave (PSU)
thetave: potential temperature computed from pave, tave, and s_ave (˚C)
sigthave: potential density computed from pave, tave, and s_ave relative to 0 dbar (kg/m^3)
uave: average east velocity in each pgrid bin, corrected for magnetic declination (cm/s)
vave: average north velocity in each pgrid bin, corrected for magnetic declination (cm/s)
wave: average relative vertical velocity in each pgrid bin, corrected for magnetic declination (cm/s)
dpdtave: average time rate of change of pressure (dbars/s)
cscan1, cscan2: indices of the CTD data averaged in each pgrid bin
ascan1, ascan2: indices of the ACM data averaged in each pgrid bin
dpdtave_Q, pave_Q, s_ave_Q, tave_Q, uave_Q, vave_Q, wave_Q: quality control flag vectors for each variable, as described above.

All serial date numbers are meant to be processed with MATLAB function *datenum.m.*

Fixed-Position Data Output Format

Fixed position MMP data, when the MMP records data at its mid-depth position (either 1500 m or 2000 m), has been quality controlled using the processes described above. The output for these data are in a single mat-file, 'tim_CGFZ.mat', one file per MMP. Each of these gridded data files contains the following variables:

files: file number for each data point, or stationary 'profile'
startdaytime: start day and time of each stationary profile (serial date number)
stopdaytime: stop day and time of each stationary profile (serial date number)
pave: average of the pressure values in each time bin (dbar)
tave: average of the temperature values in each time bin (˚C)
cave: average scaled conductivity in each time bin (mmho)
s_ave: salinity computed using pave, tave and cave (PSU)
thetave: potential temperature computed from pave, tave, and s_ave (˚C)
sigthave: potential density computed from pave, tave, and s_ave relative to 0 dbar (kg/m^3)
uave: average east velocity in each time bin, corrected for magnetic declination (cm/s)
vave: average north velocity in each time bin, corrected for magnetic declination (cm/s)
wave: average relative vertical velocity in each time bin, corrected for magnetic declination (cm/s)
pave_Q, s_ave_Q, tave_Q, uave_Q, vave_Q, wave_Q: quality control flag vectors for each variable, as described above.

All serial date numbers are meant to be processed with MATLAB function *datenum.m.*

This page left intentionally blank.

Appendix C: McLane Moored Profiler data.

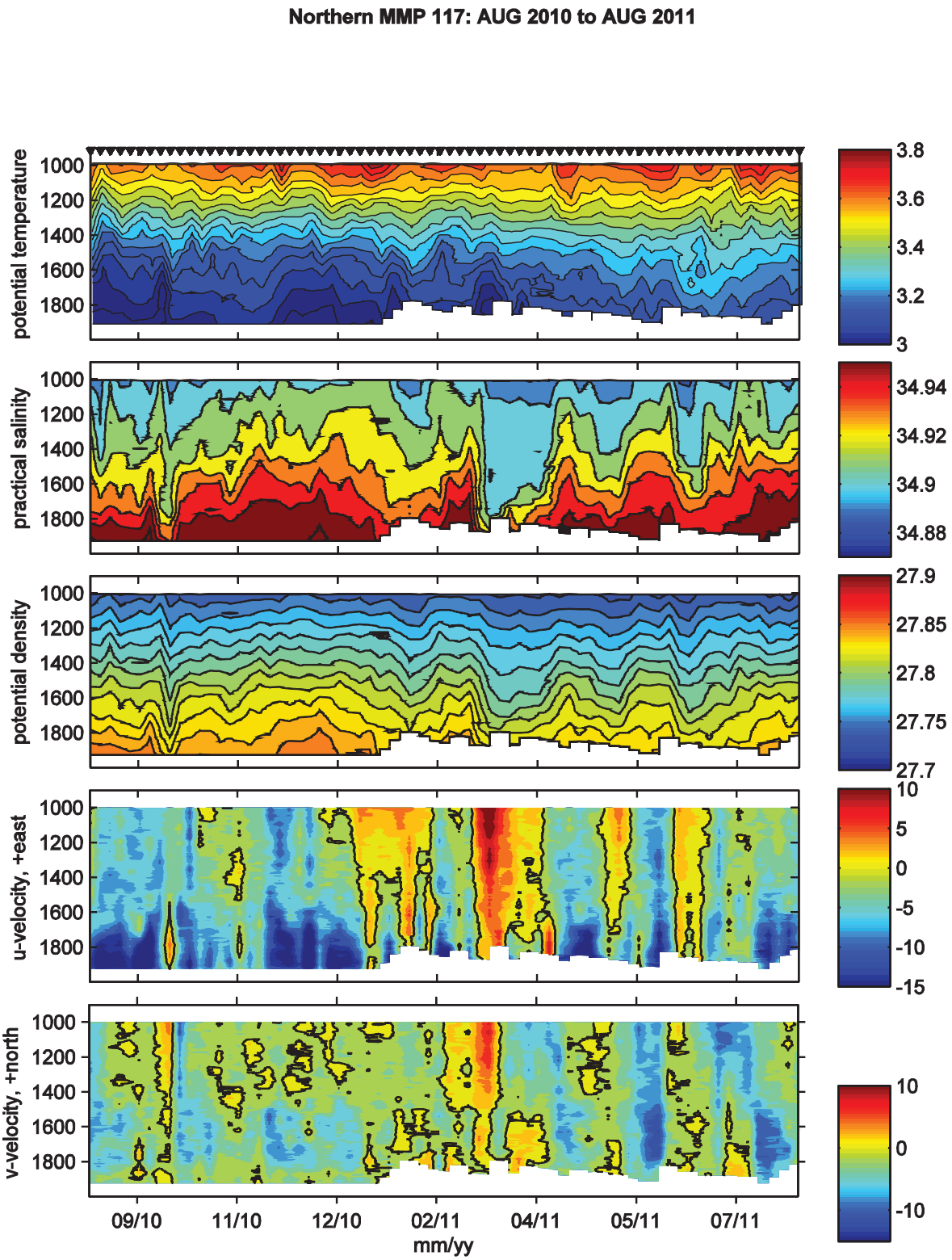

Figure C1. Northern MMP #117 on Mooring A, Year 1. Subplots are from top to bottom: potential temperature, practical salinity, potential density, u-velocity, and v-velocity.

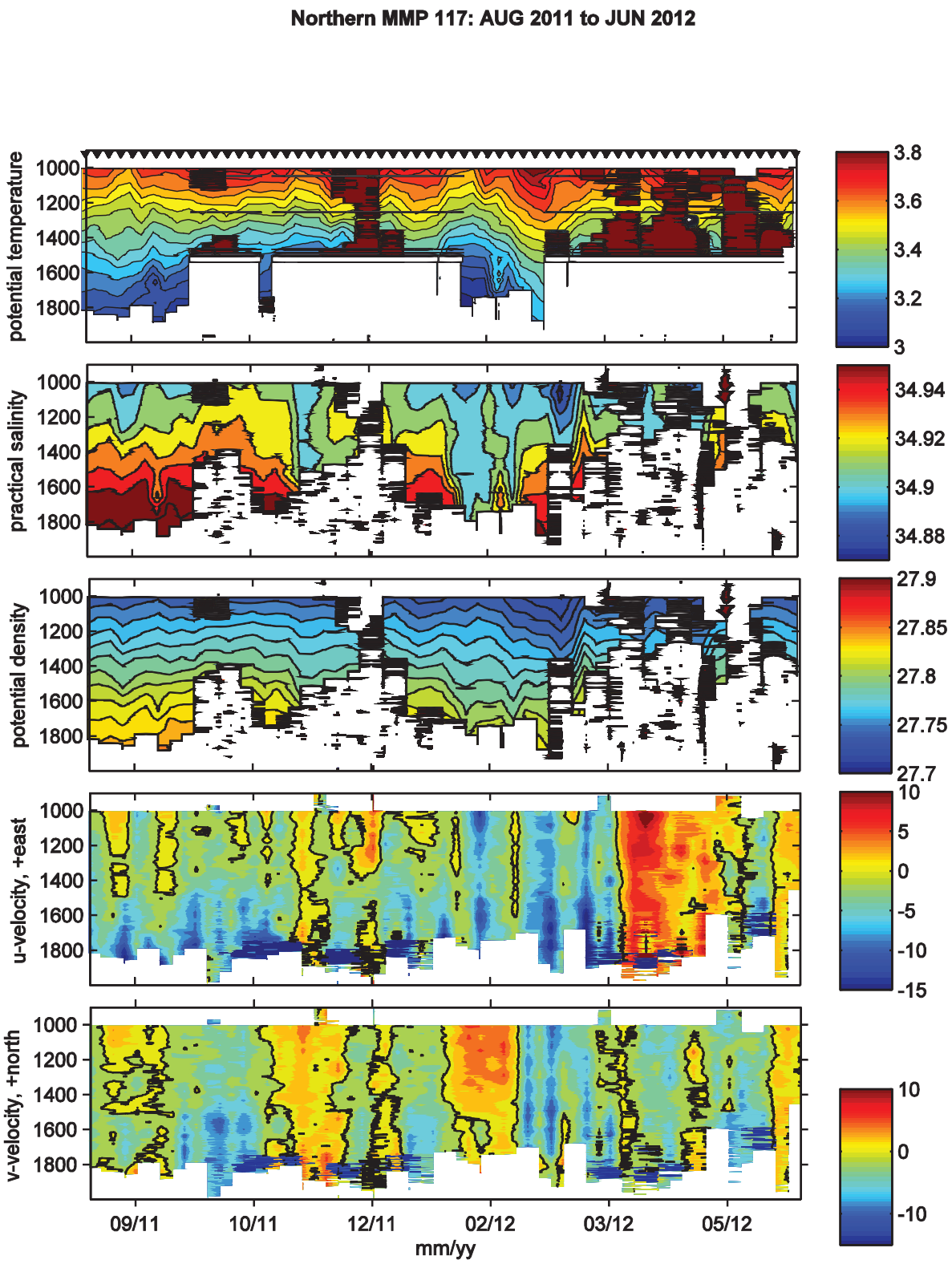

Figure C2. Northern MMP #117 on Mooring A, Year 2. Subplots are from top to bottom: potential temperature, practical salinity, potential density, u-velocity, and v-velocity.

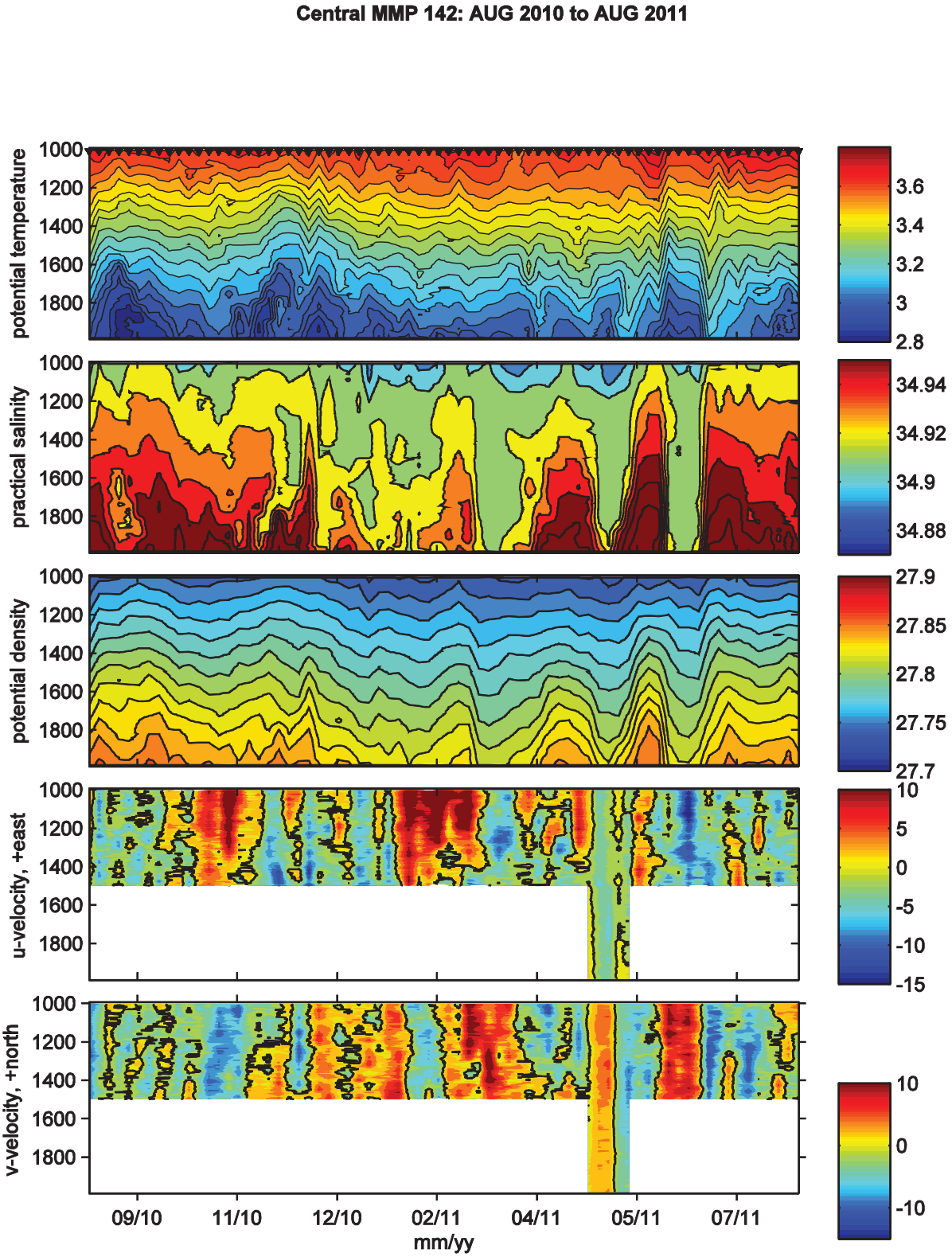

Figure C3. Central MMP #142 on Mooring C, Year 1. Subplots are from top to bottom: potential temperature, practical salinity, potential density, u-velocity, and v-velocity.

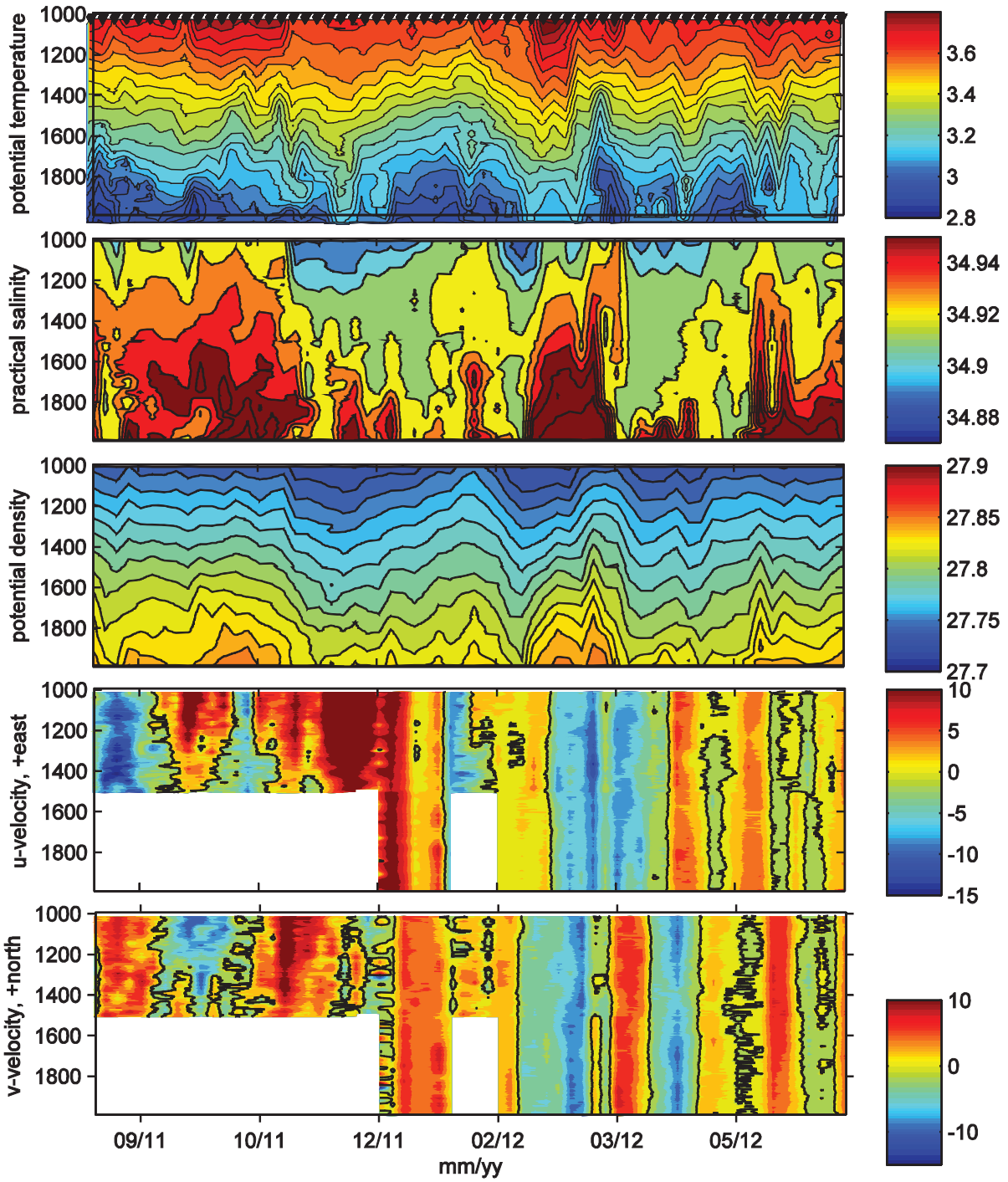

Figure C4. Central MMP #142 on Mooring C, Year 2. Subplots are from top to bottom: potential temperature, practical salinity, potential density, u-velocity, and v-velocity.

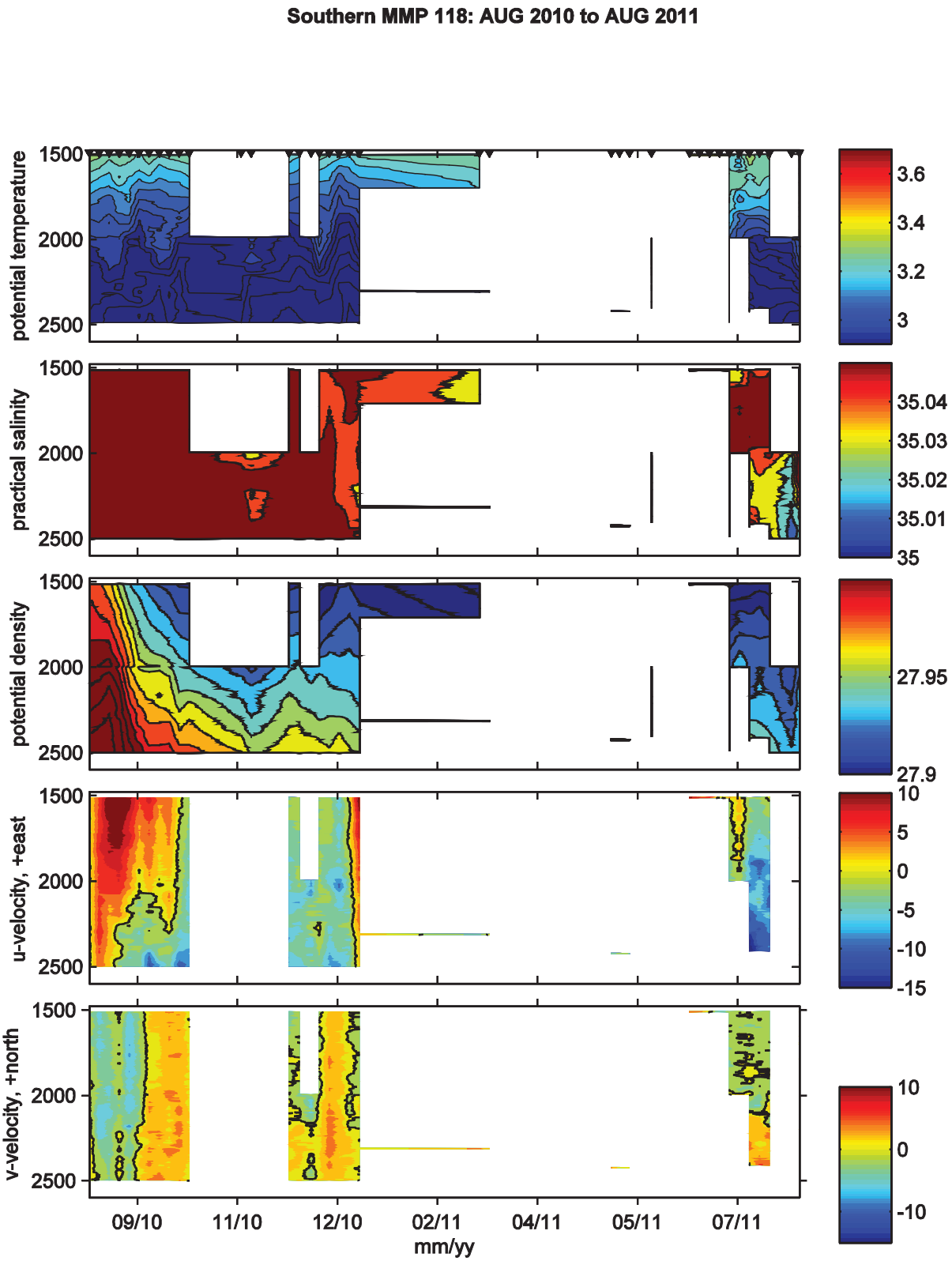

Figure C5. Southern MMP #118 on Mooring F, Year 1. Subplots are from top to bottom: potential temperature, practical salinity, potential density, u-velocity, and v-velocity.

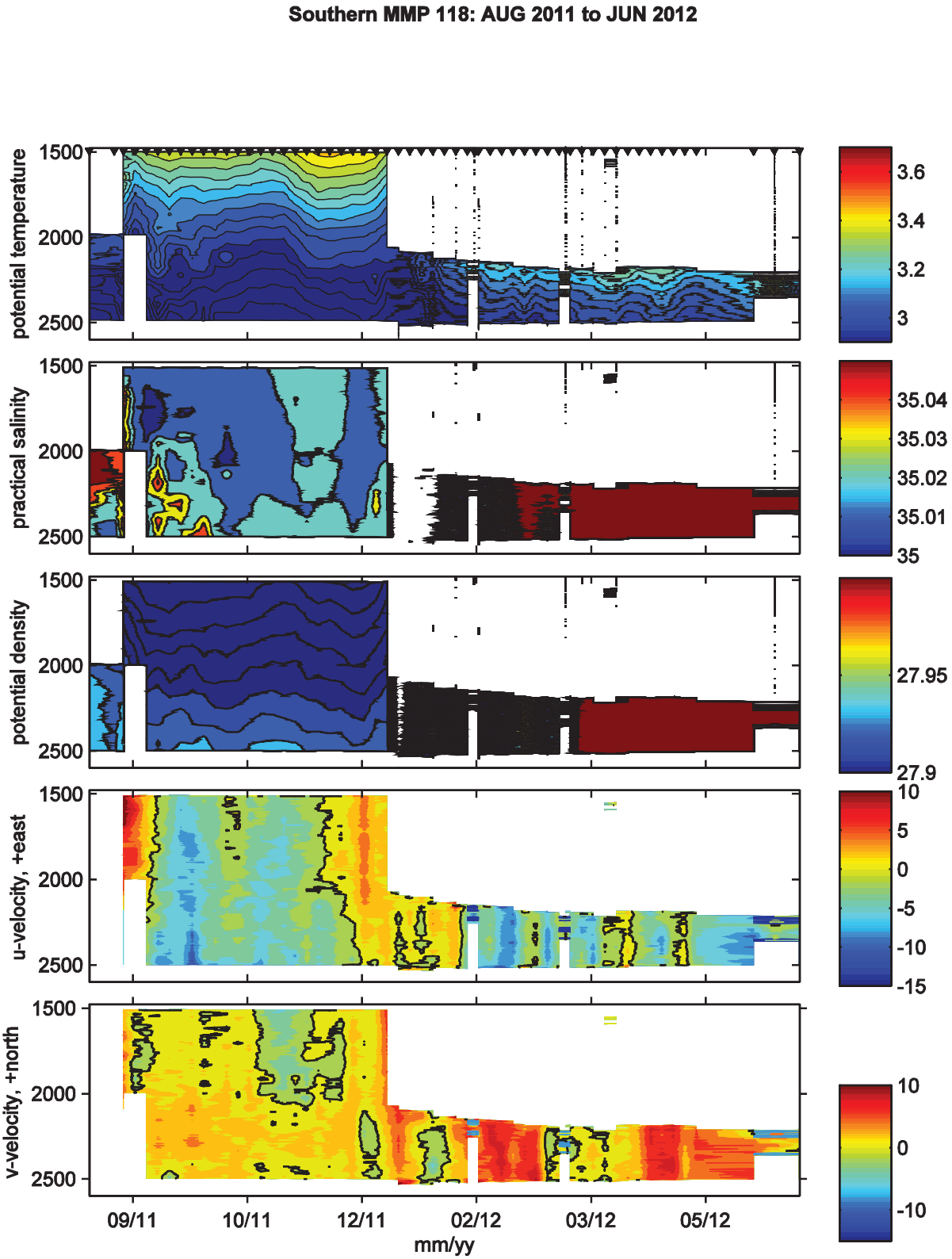

Figure C6. Southern MMP #118 on Mooring F, Year 2. Subplots are from top to bottom: potential temperature, practical salinity, potential density, u-velocity, and v-velocity.

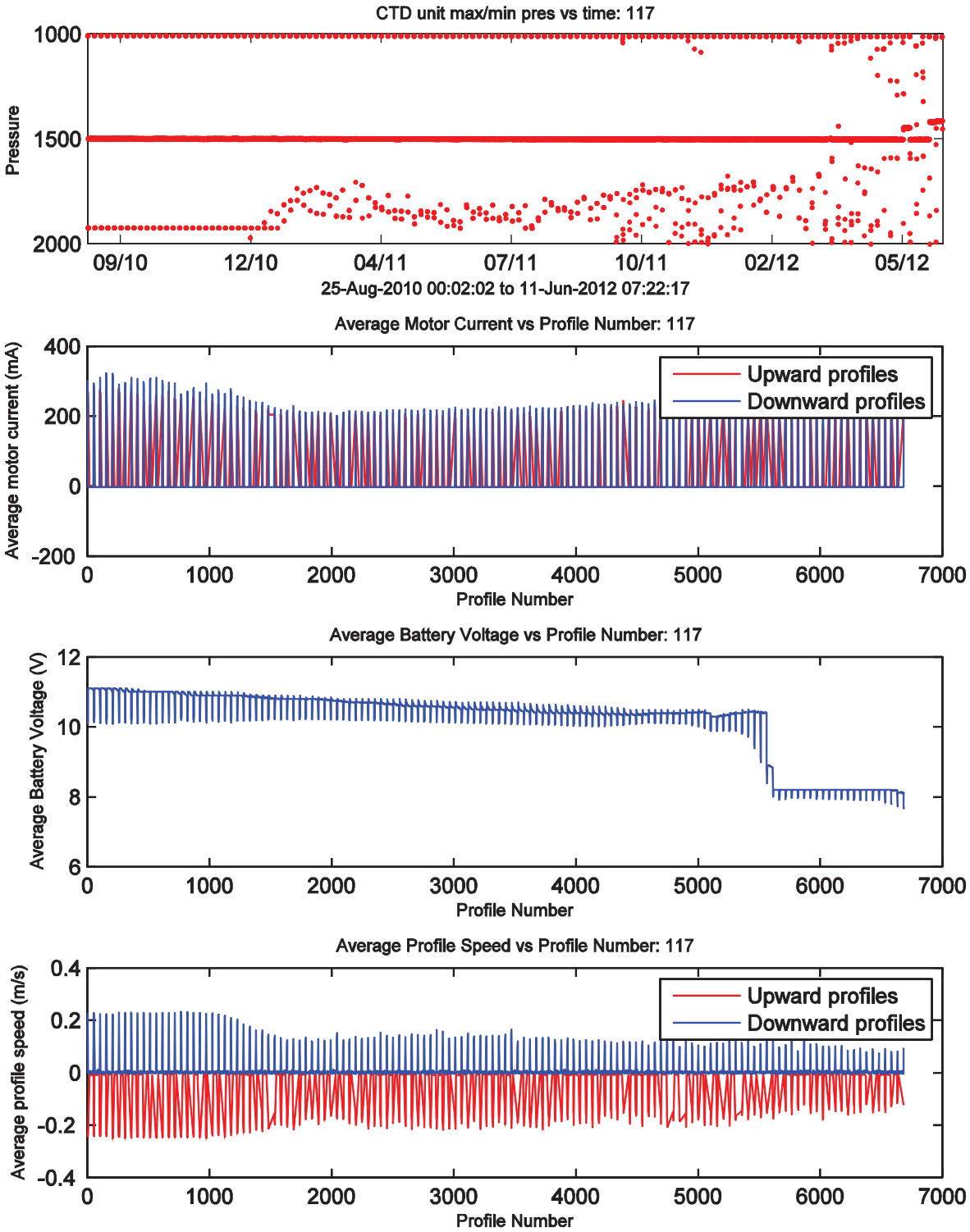

Figure C7. MMP#117 diagnostic plot: CTD min/max pressure, motor current, battery voltage, and speed per profile versus time.

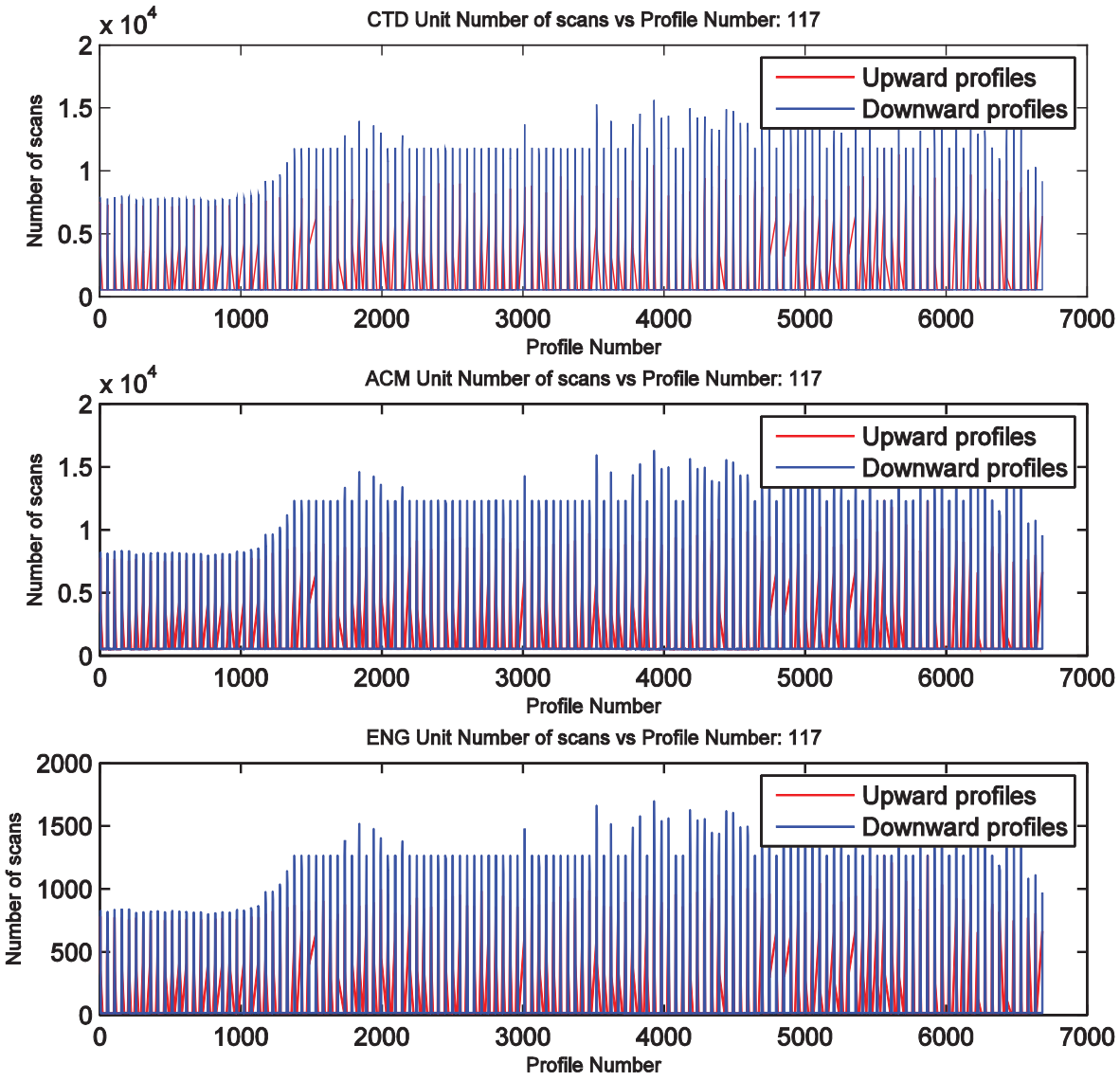

Figure C8. MMP#117 diagnostic plot: CTD ACM, and ENG Unit number of scans per profile for upward and downward profiles.

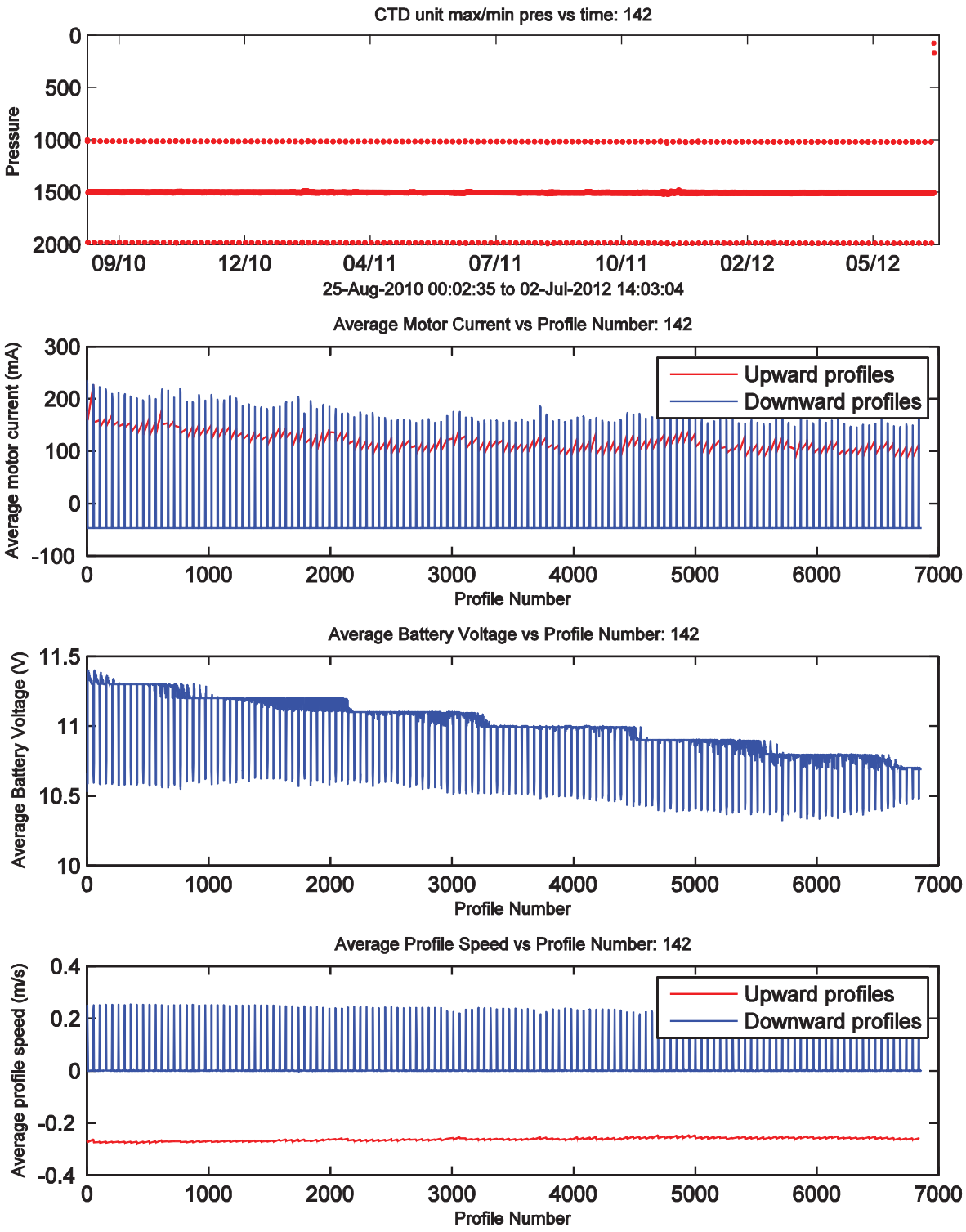

Figure C9. MMP#142 diagnostic plot: CTD min/max pressure, motor current, battery voltage, and speed per profile versus time.

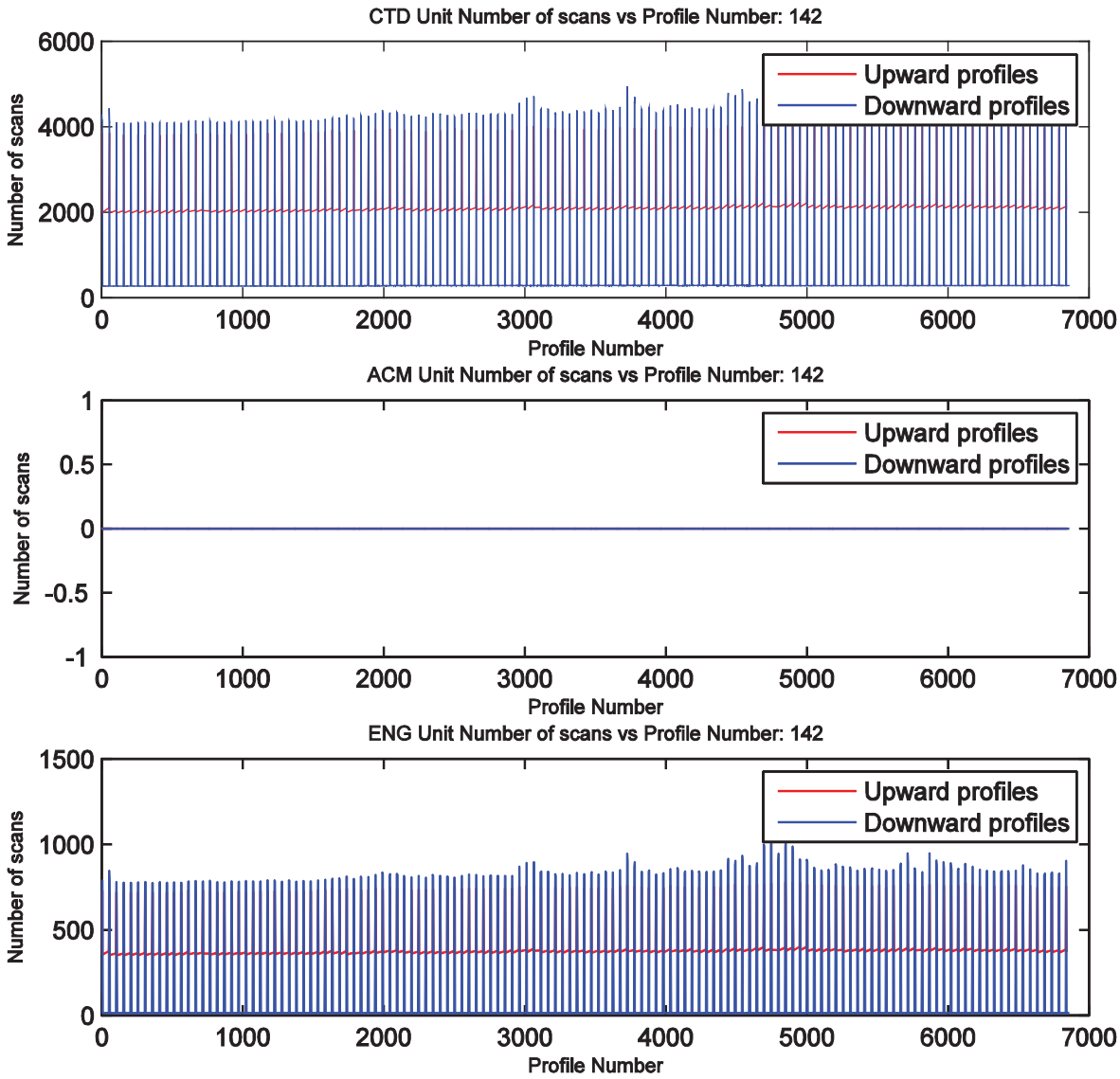

Figure C10. MMP#142 diagnostic plot: CTD ACM, and ENG Unit number of scans per profile for upward and downward profiles.

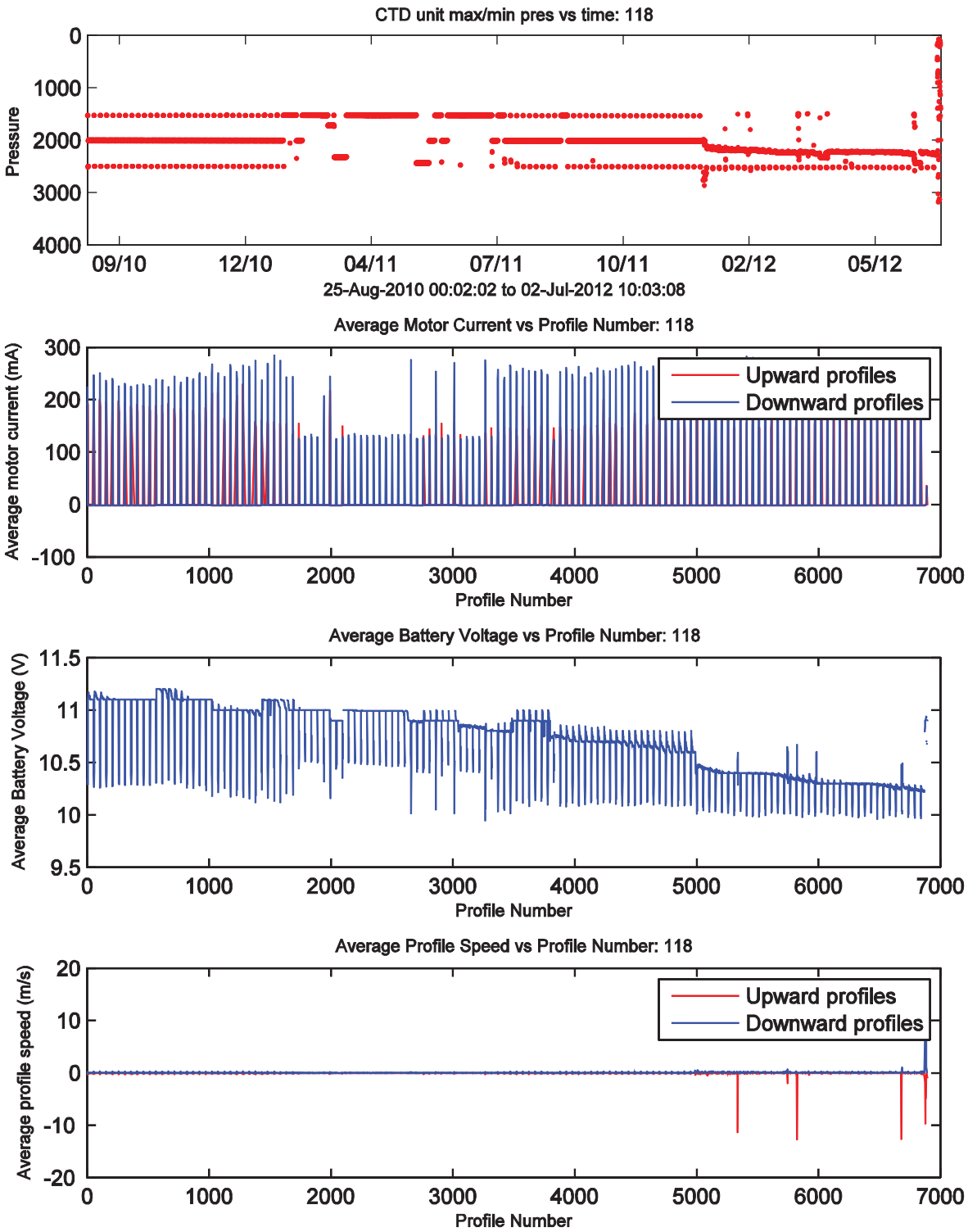

Figure C11. MMP#118 diagnostic plot: CTD min/max pressure, motor current, battery voltage, and speed per profile versus time.

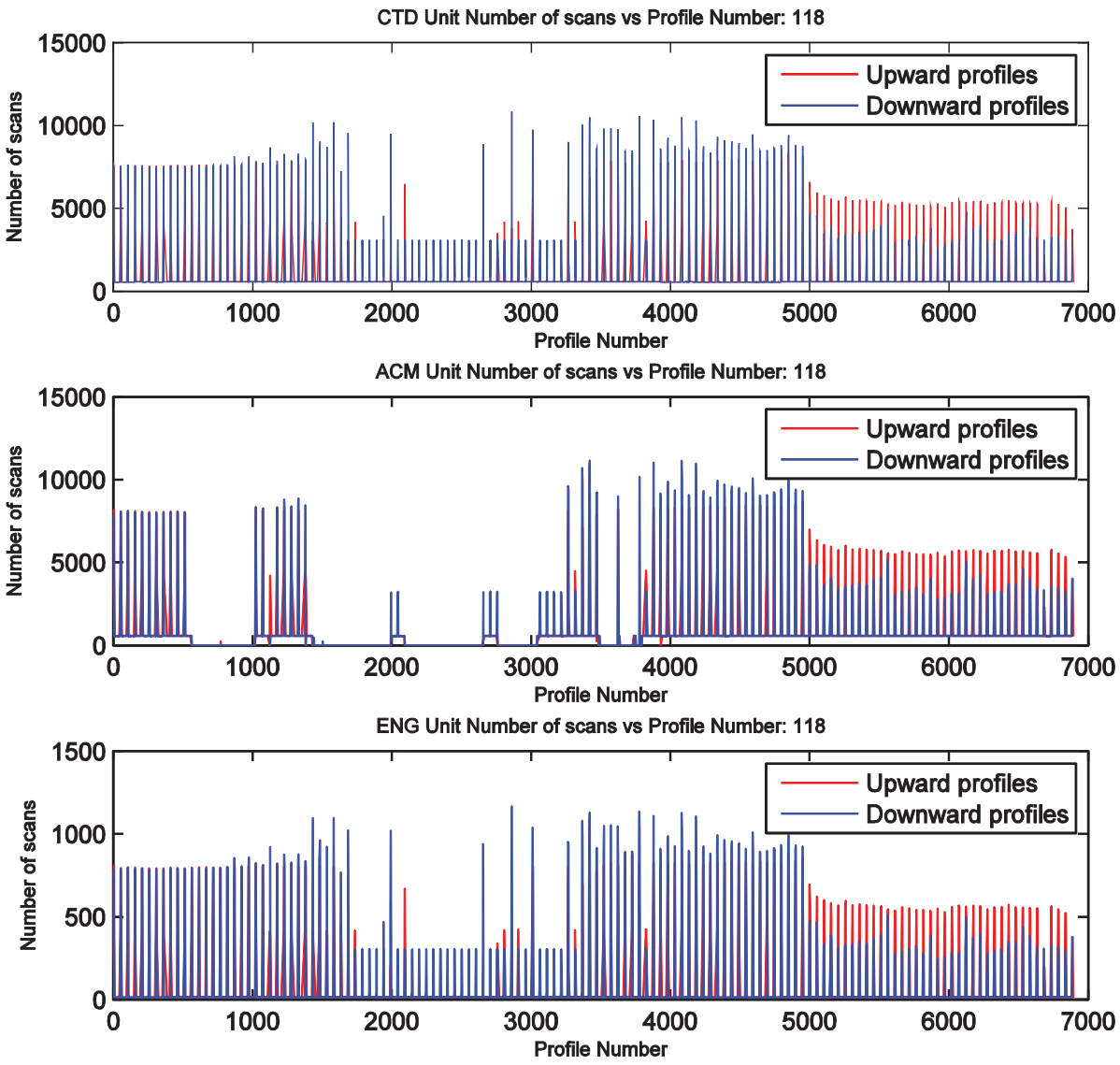

Figure C12. MMP#118 diagnostic plot: CTD ACM, and ENG Unit number of scans per profile for upward and downward profiles.

This page left intentionally blank.

Appendix D: Aanderaa RCM-11 and Nortek current meter data, presented by mooring letter, north to south (A to H), and then depth, shallow to deep. Y-axis scales on all plots are not uniform, so to show most variability possible. Aanderaa current meters are not equipped with pressure sensors, so variables w-velocity and pressure are only provided on Nortek plots. In the speed plot, red is before application of sound velocity correction, blue is calibrated data. Since sound velocity correction only needed for Aanderaa current meters, only Aanderaa plots have raw speed plotted. In the 'direction' subplot, red is raw direction data, and blue are the same data after the magnetic variation correction have been applied. In the bottom three (or four if instrument measured pressure) subplots, blue lines are quality controlled and calibrated data, and red lines are of the same data, but with 40-hour low pass 2nd order Butterworth filter applied.

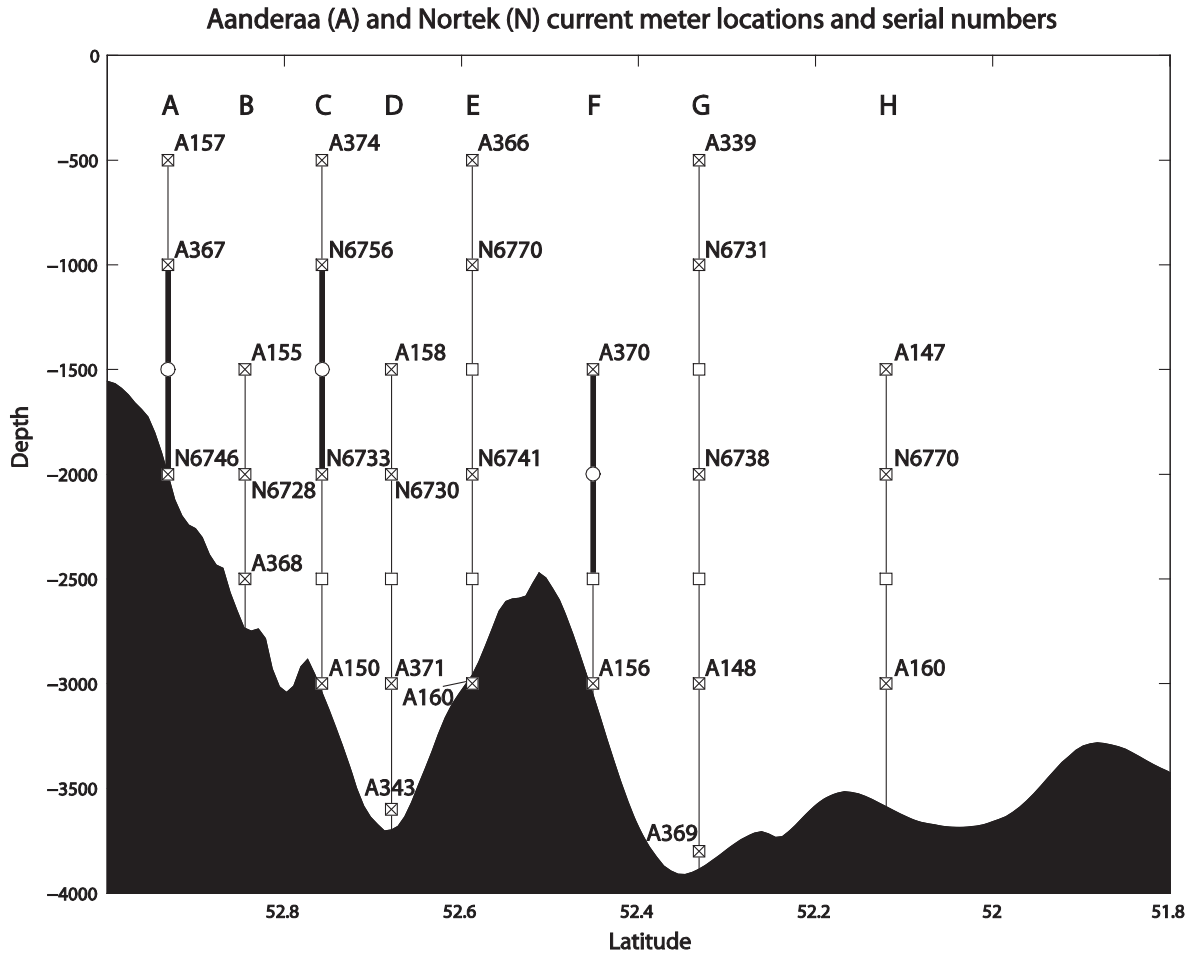

Figure D1. Locations of Aanderaa ('A') and Nortek ('N') instruments in array. Serial numbers identify specific instruments and may be used for reference for the upcoming appendix plots.

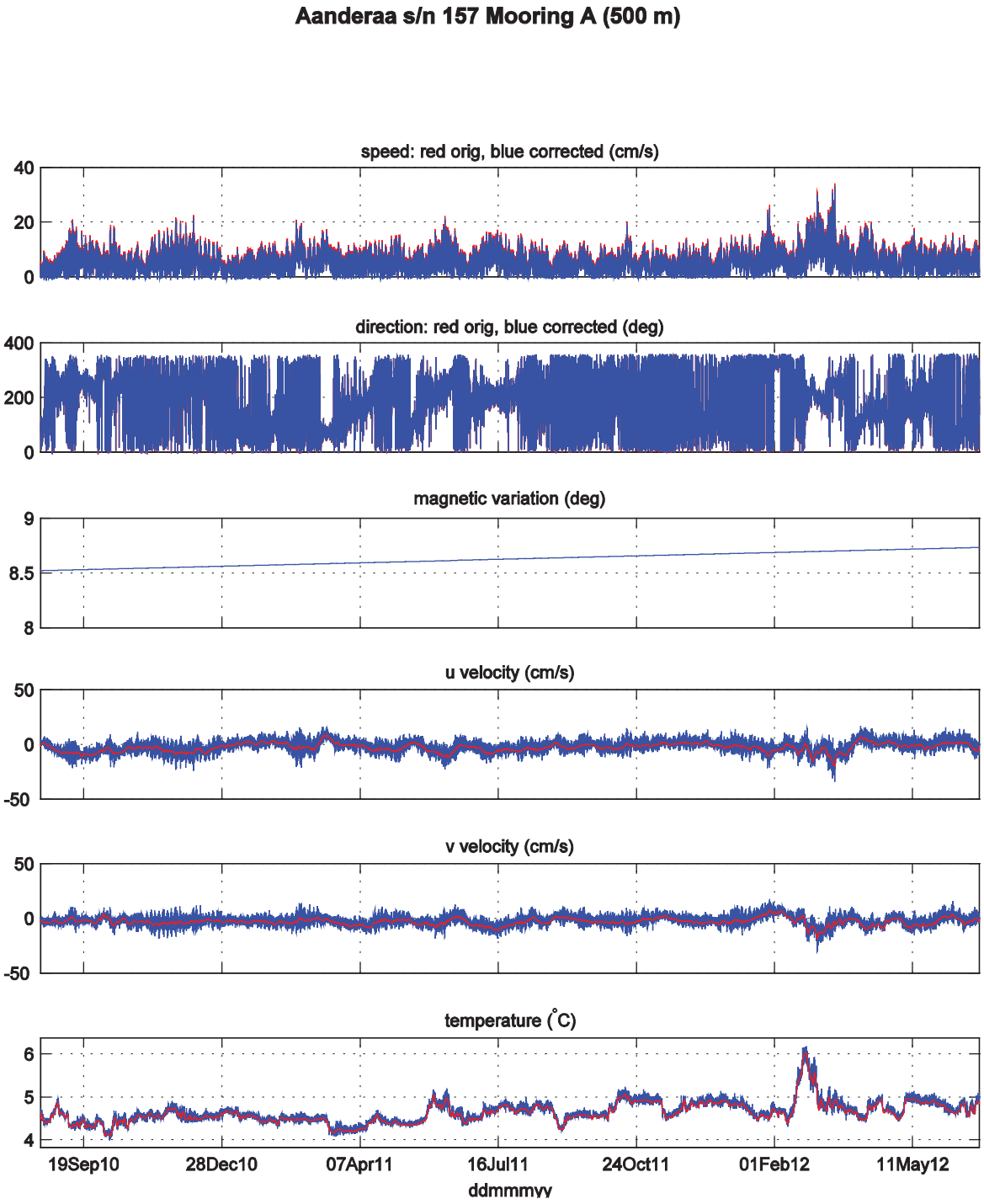

Figure D2. Aanderaa RCM-11 s/n 157, Mooring A, 500 m nominal depth. Subplots are from top to bottom: speed, direction, magnetic variation, u-velocity, v-velocity, and *in situ* temperature.

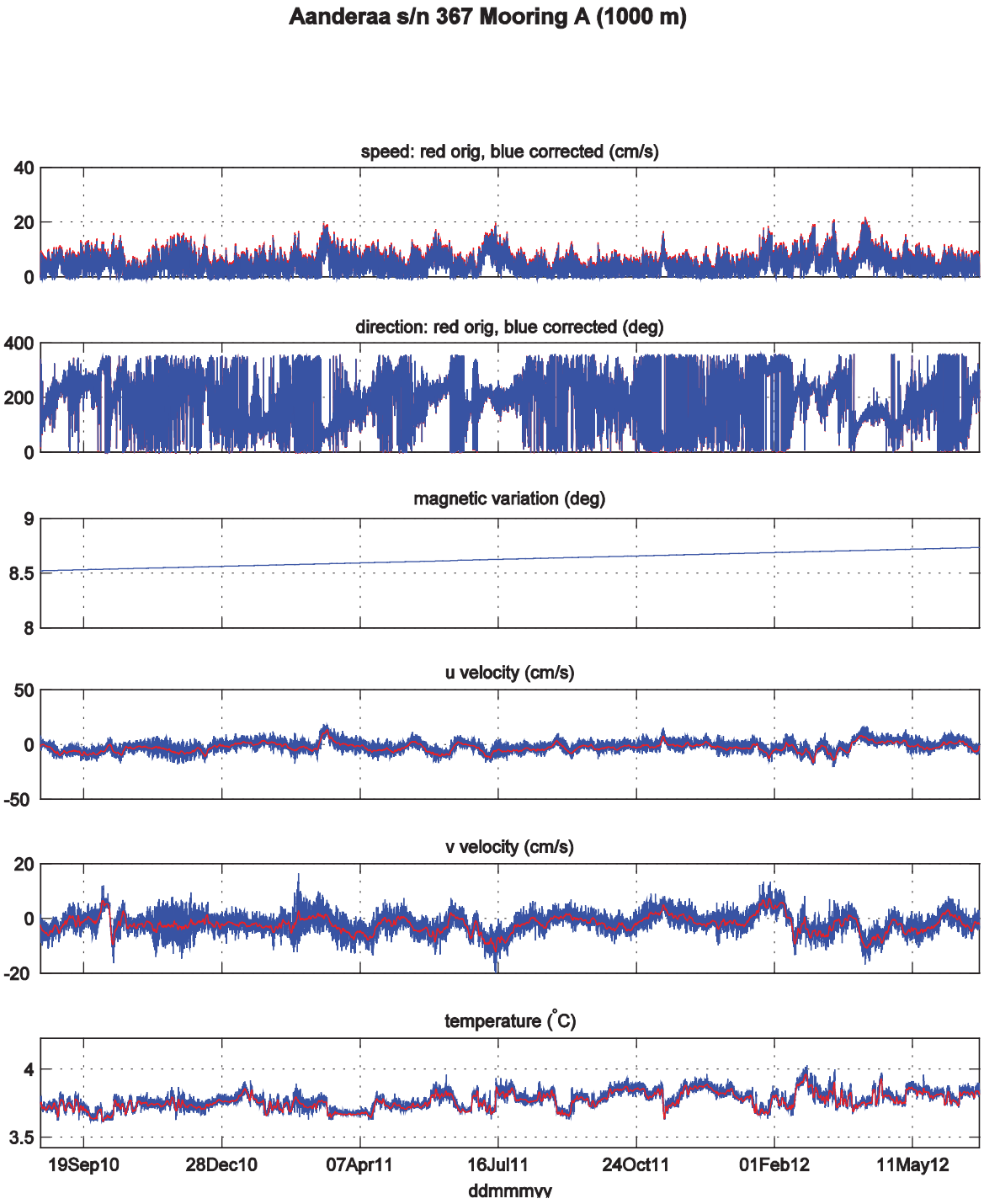

Figure D3. Aanderaa RCM-11 s/n 367, Mooring A, 1000 m nominal depth. Subplots are from top to bottom: speed, direction, magnetic variation, u-velocity, v-velocity, and *in situ* temperature.

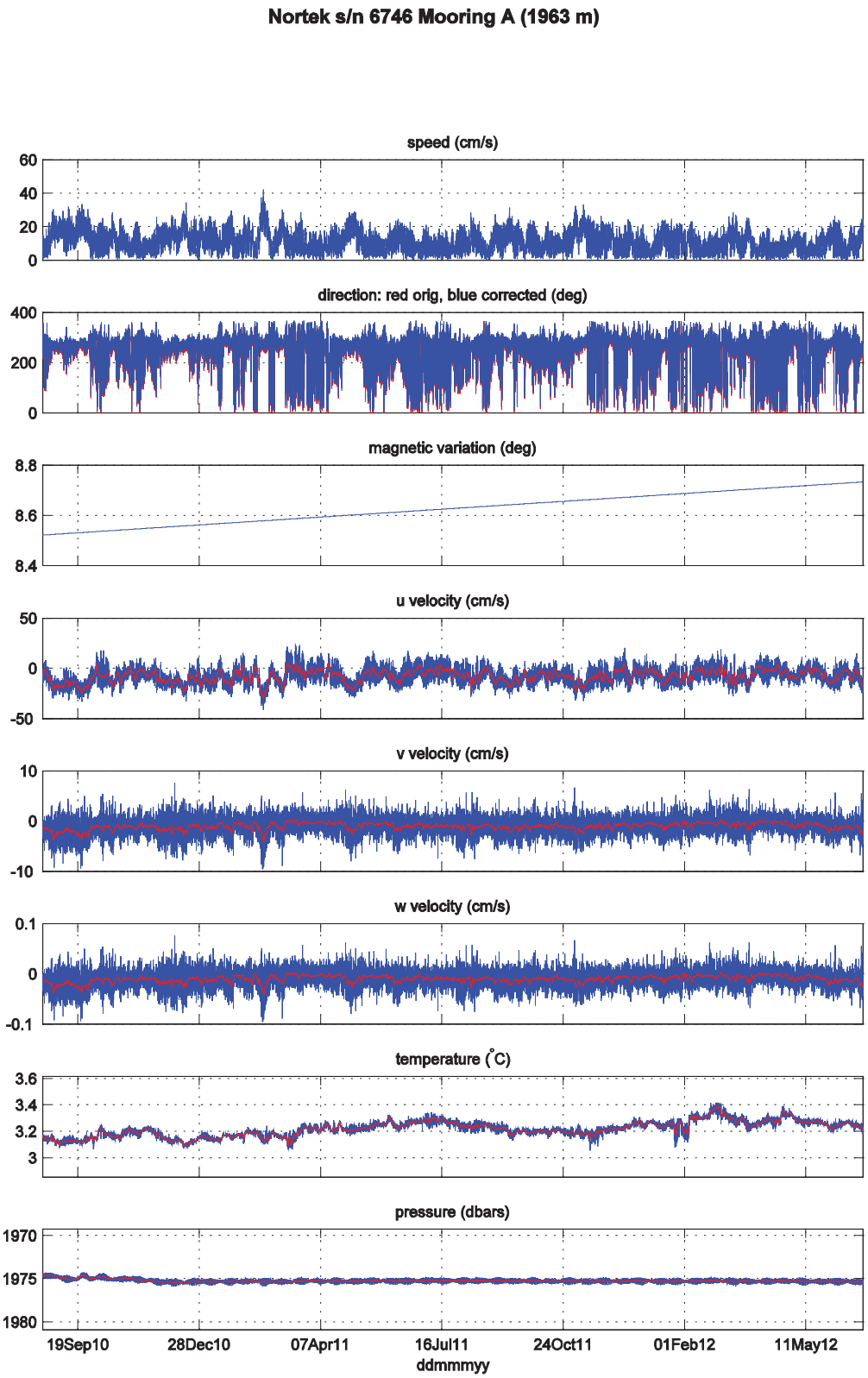

Figure D4. Nortek s/n 6746, Mooring A, 1963 m depth (bottom). Subplots are from top to bottom: speed, direction, magnetic variation, u-velocity, v-velocity, w-velocity, *in situ* temperature, and pressure.

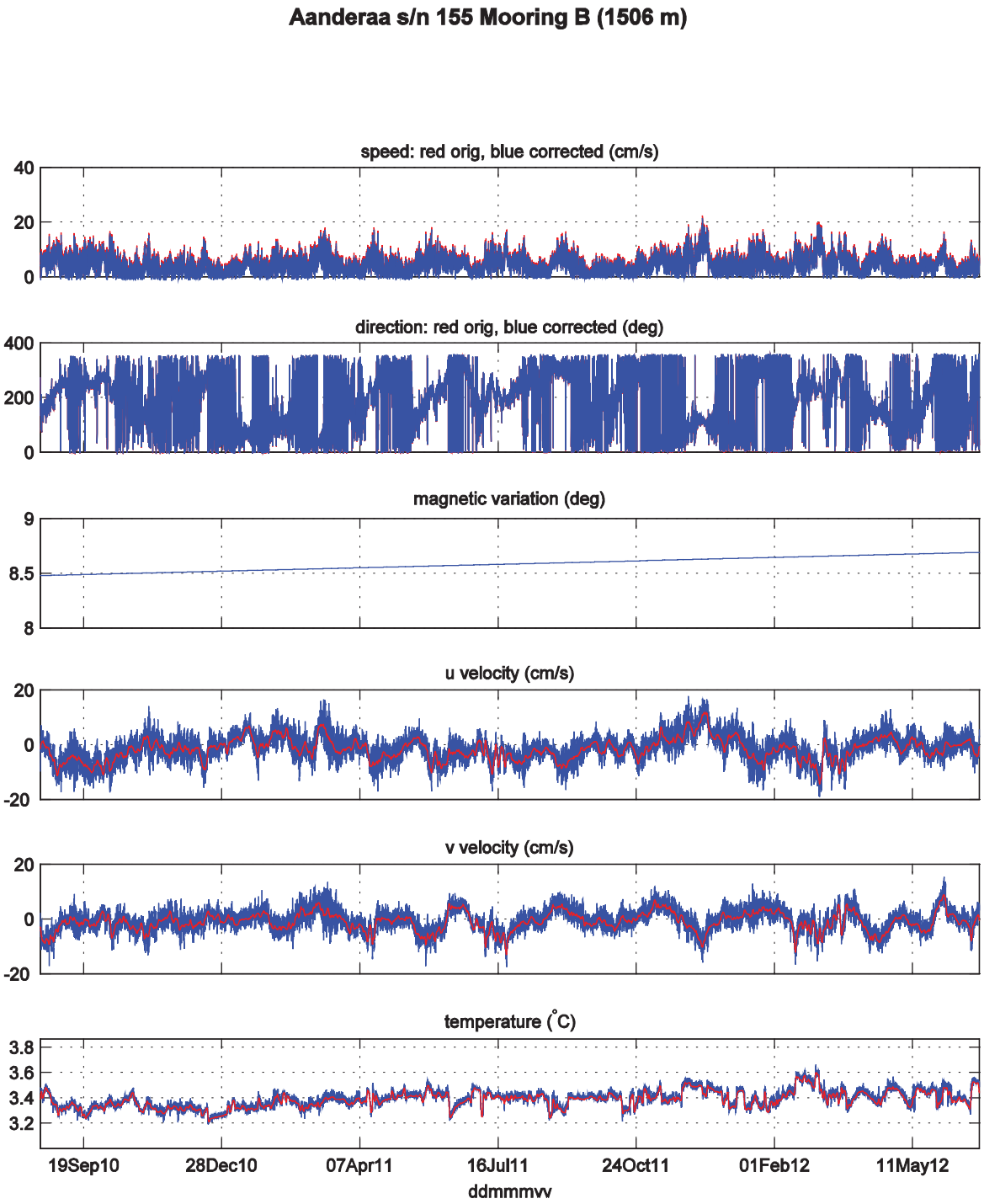

Figure D5. Aanderaa RCM-11 s/n 155, Mooring B, 1500 m nominal depth. Subplots are from top to bottom: speed, direction, magnetic variation, u-velocity, v-velocity, and *in situ* temperature.

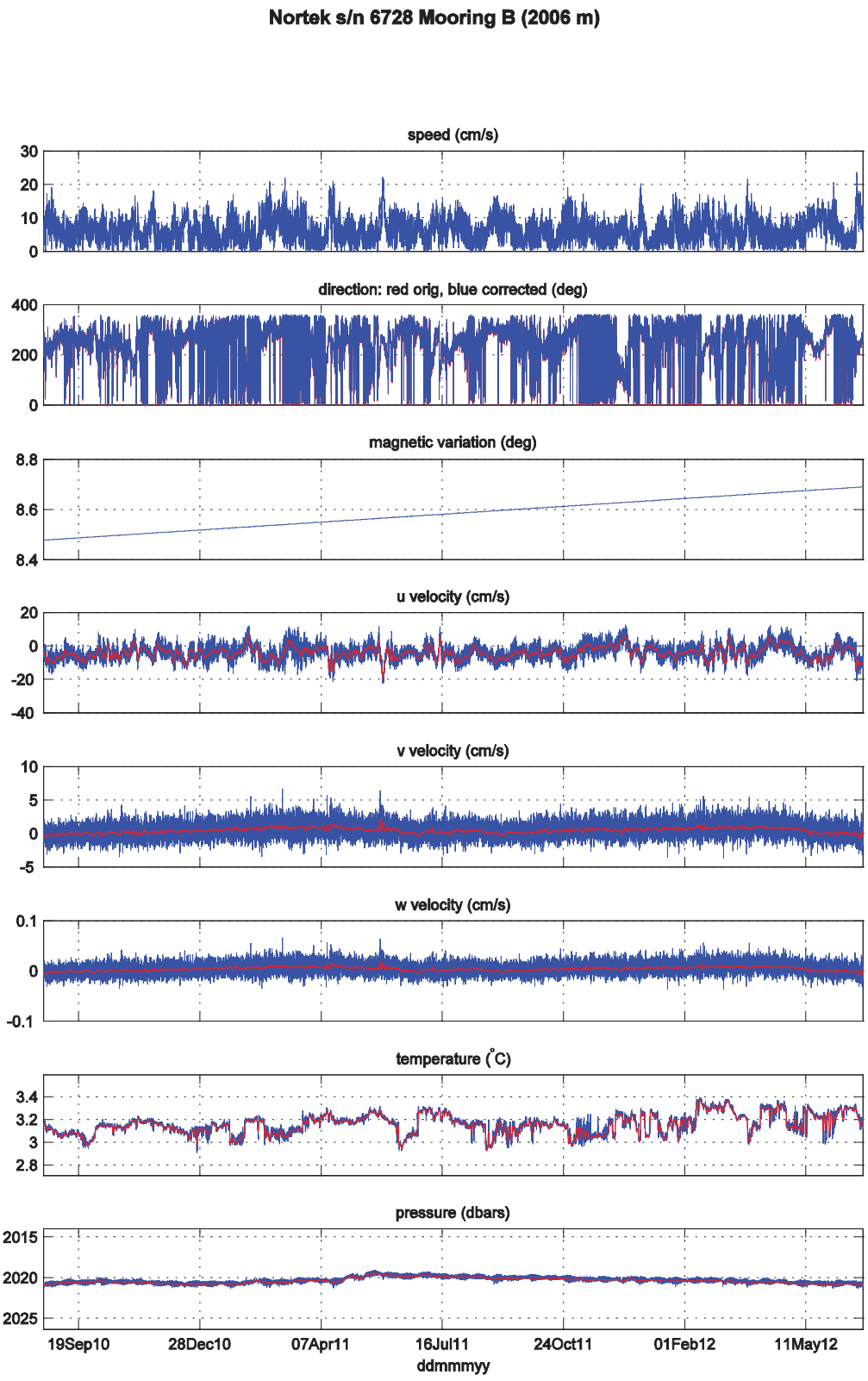

Figure D6. Nortek s/n 6728, Mooring B, 2000 m nominal depth. Subplots are from top to bottom: speed, direction, magnetic variation, u-velocity, v-velocity, w-velocity, *in situ* temperature, and pressure.

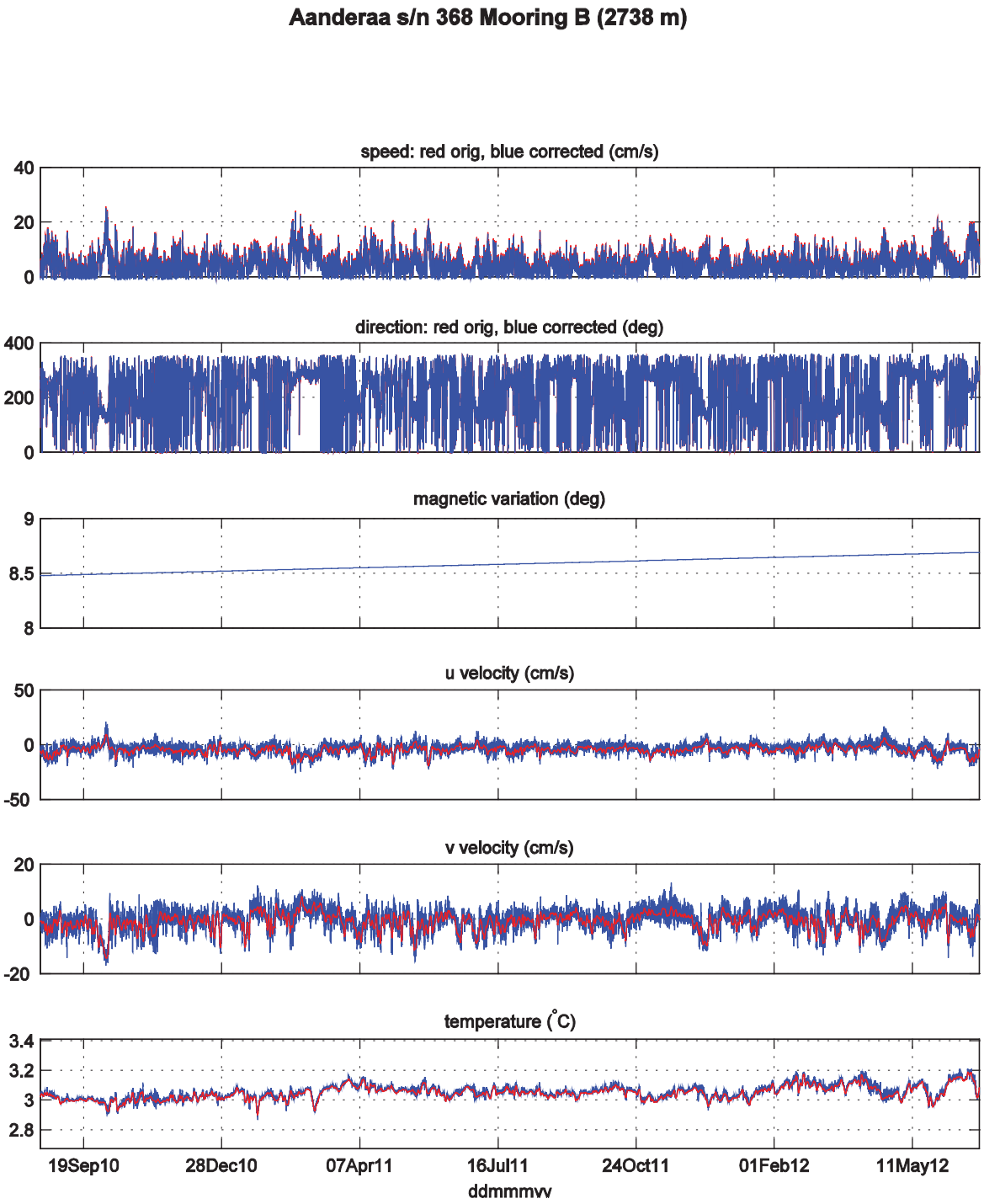

Figure D7. Aanderaa RCM-11 s/n 368, Mooring B, 2738 m depth (bottom). Subplots are from top to bottom: speed, direction, magnetic variation, u-velocity, v-velocity, *and in situ* temperature.

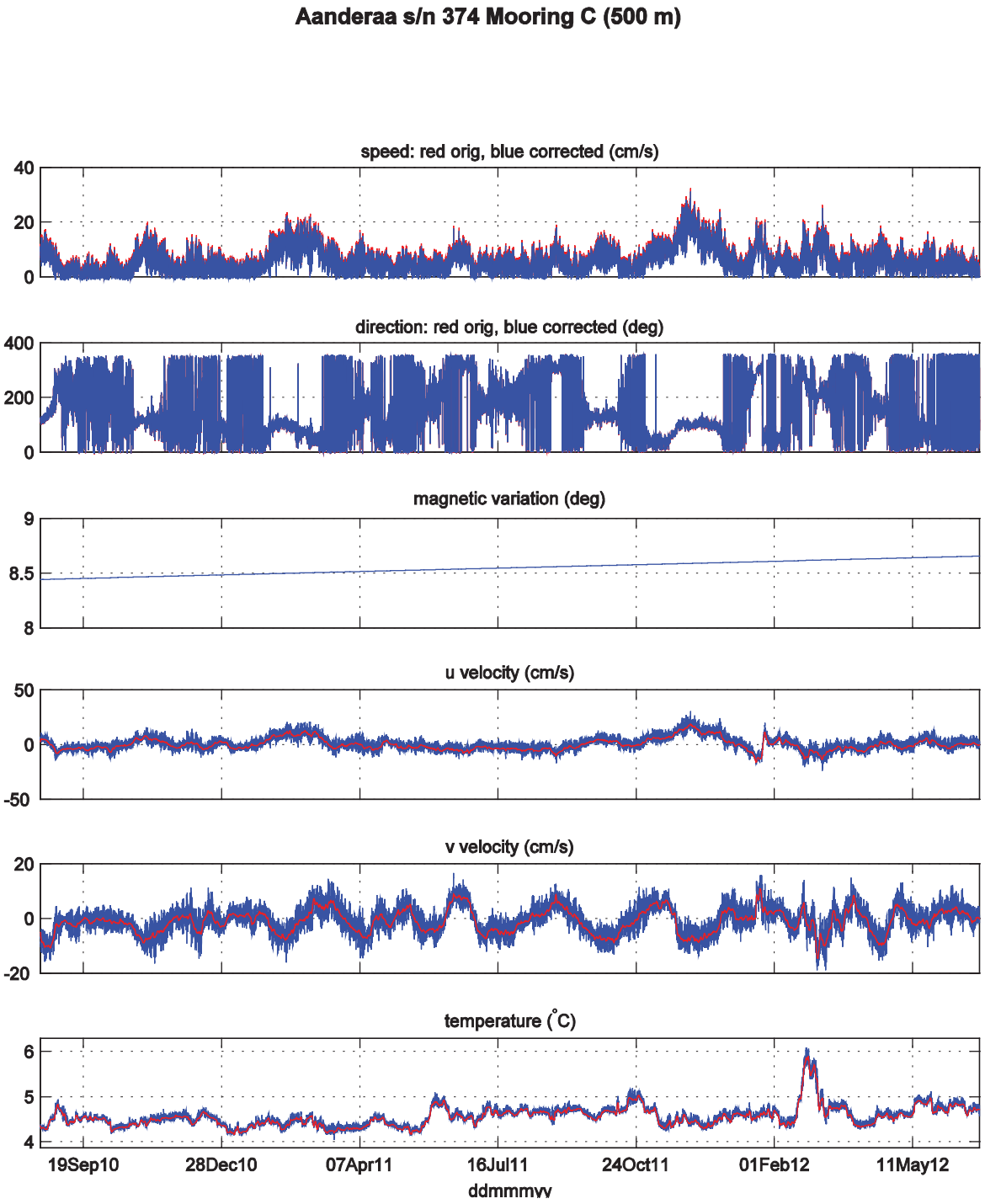

Figure D8. Aanderaa RCM-11 s/n 374, Mooring C, 500 m nominal depth. Subplots are from top to bottom: speed, direction, magnetic variation, u-velocity, v-velocity, and *in situ* temperature.

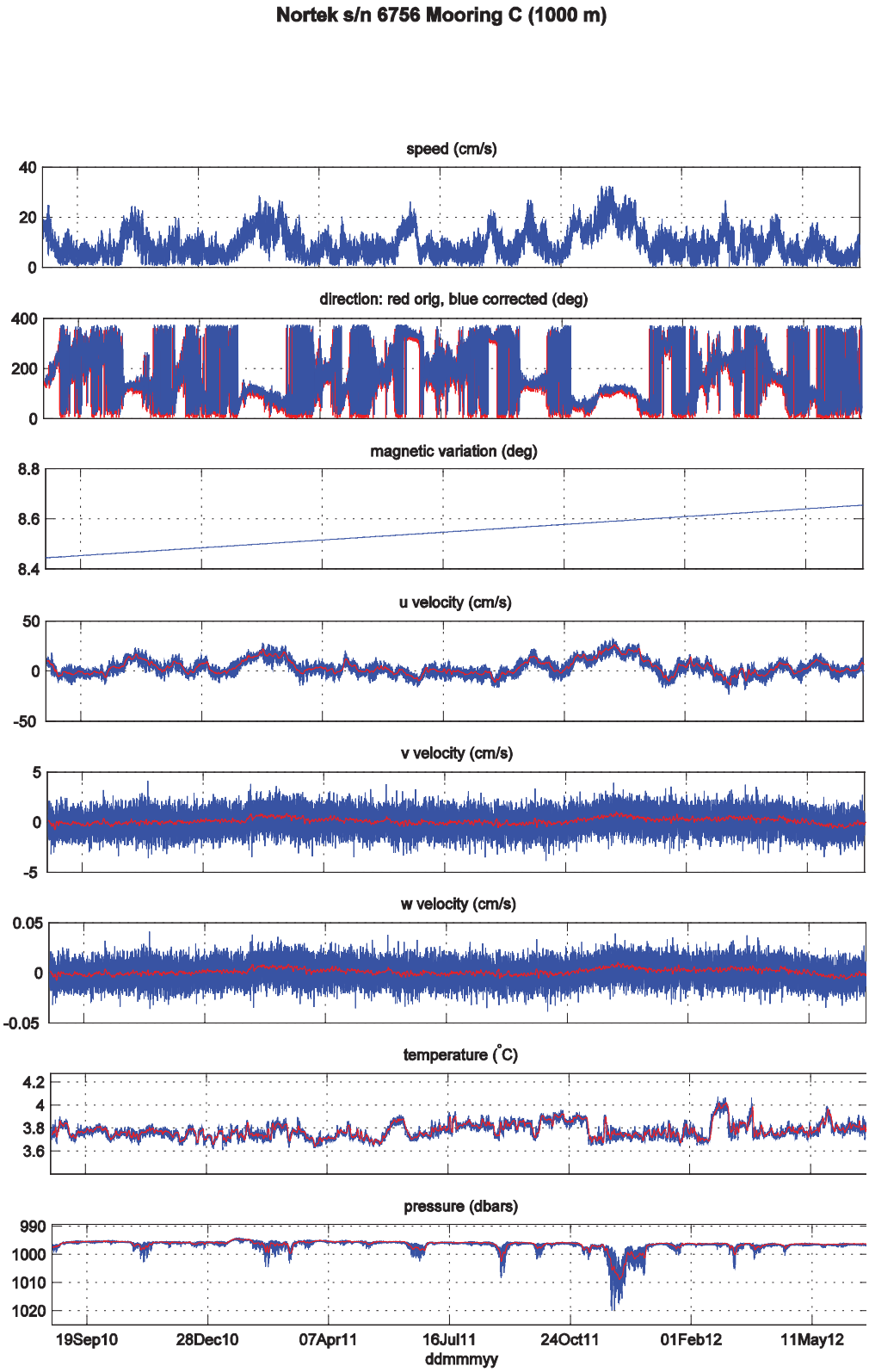

Figure D9. Nortek s/n 6756, Mooring C, 1000 m nominal depth. Subplots are from top to bottom: speed, direction, magnetic variation, u-velocity, v-velocity, w-velocity, *in situ* temperature and pressure.

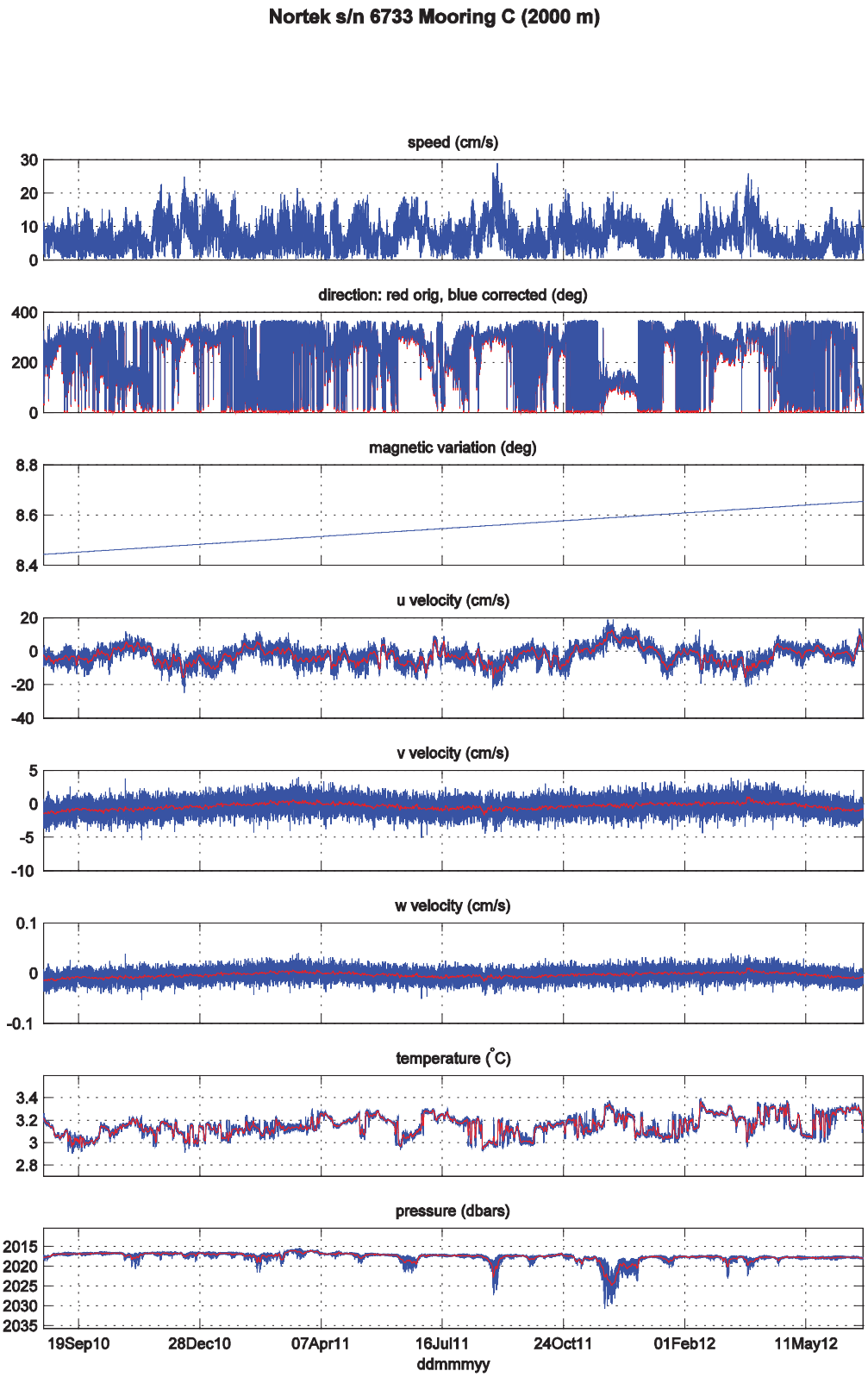

Figure D10. Nortek s/n 6733, Mooring C, 2000 m nominal depth. Subplots are from top to bottom: speed, direction, magnetic variation, u-velocity, v-velocity, w-velocity, *in situ* temperature and pressure.

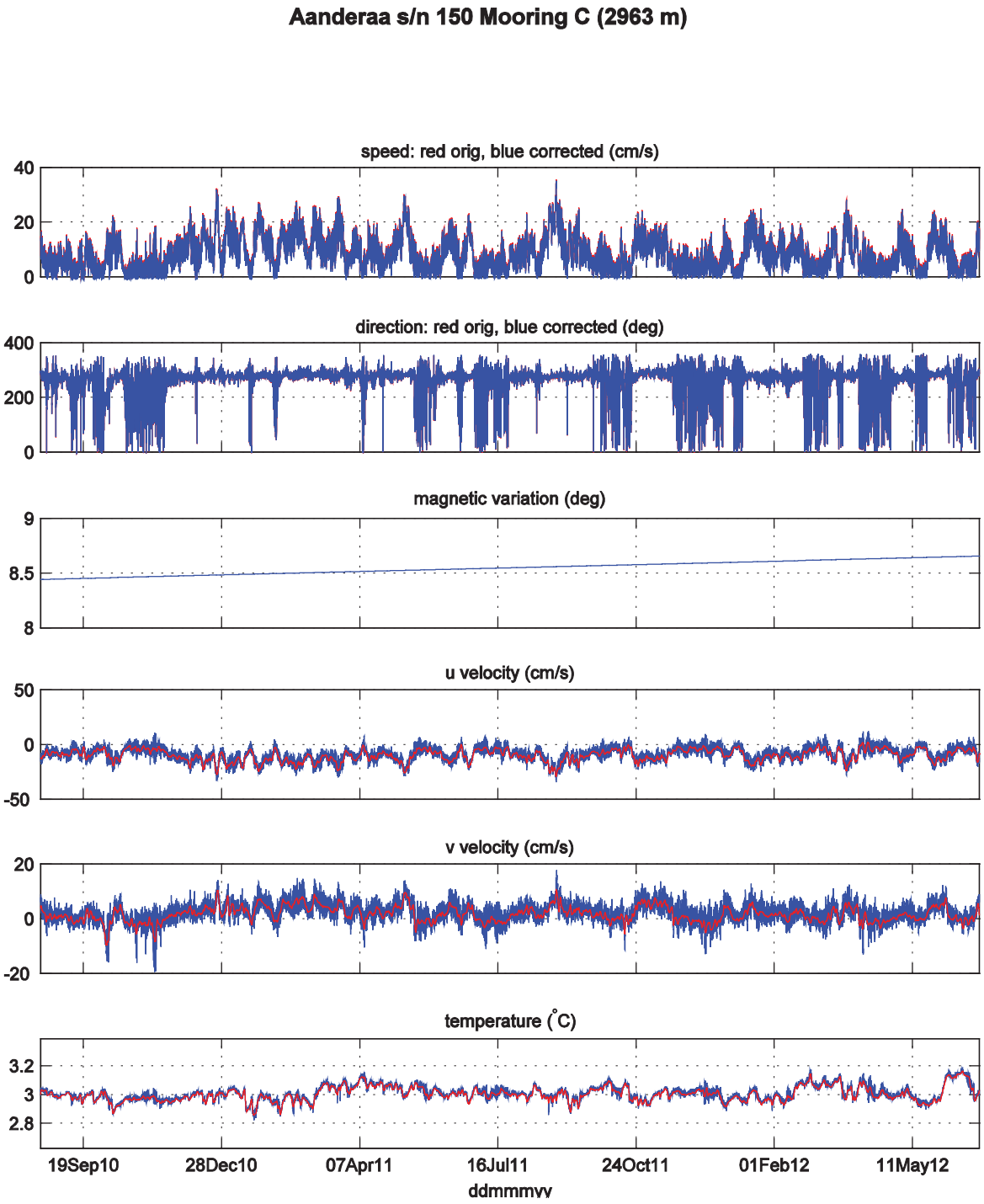

Figure D11. Aanderaa RCM-11 s/n 150, Mooring C, 2963 m depth (bottom). Subplots are from top to bottom: speed, direction, magnetic variation, u-velocity, v-velocity, and *in situ* temperature.

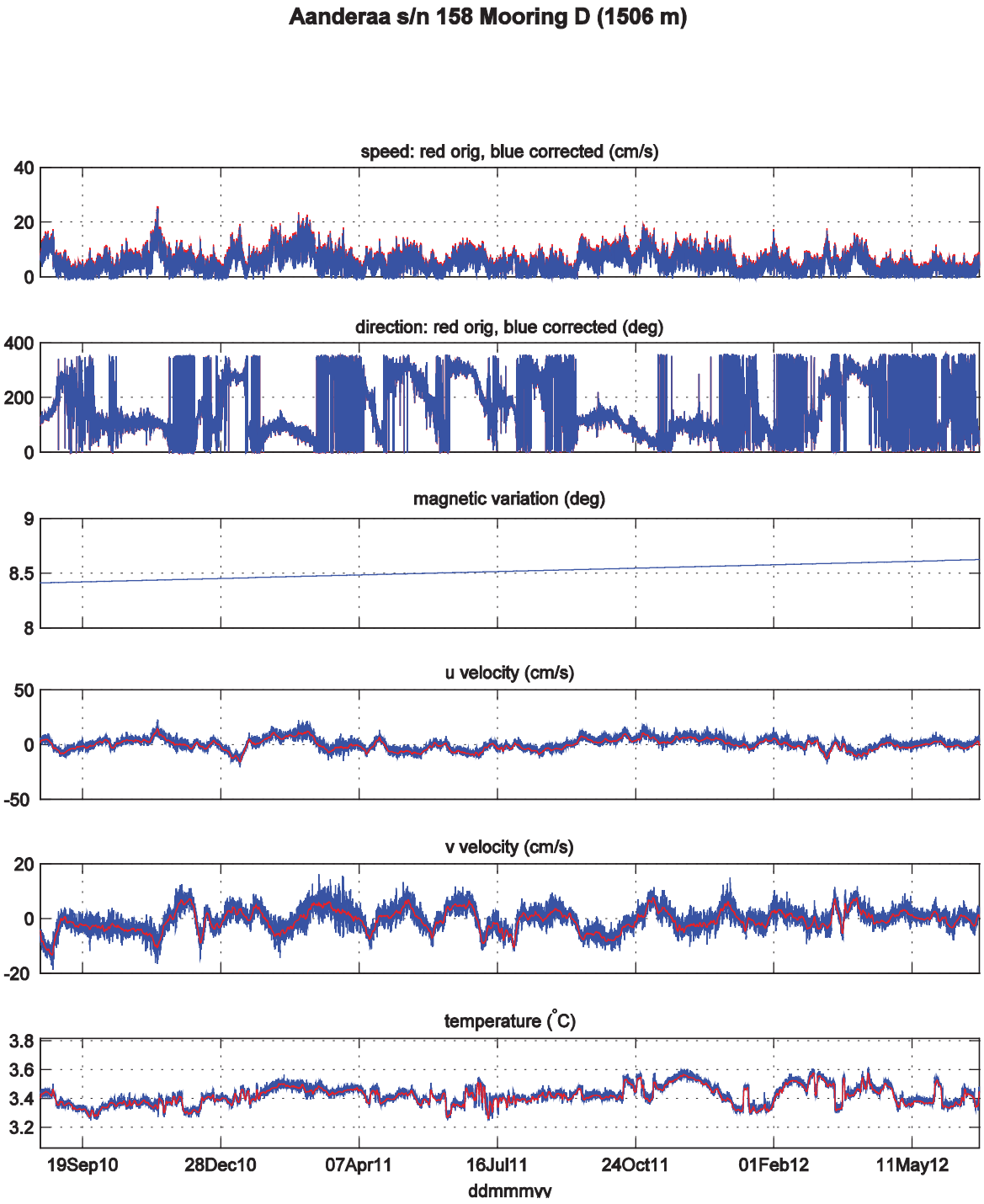

Figure D12. Aanderaa RCM-11 s/n 158, Mooring D, 1500 m nominal depth. Subplots are from top to bottom: speed, direction, magnetic variation, u-velocity, v-velocity, and *in situ* temperature.

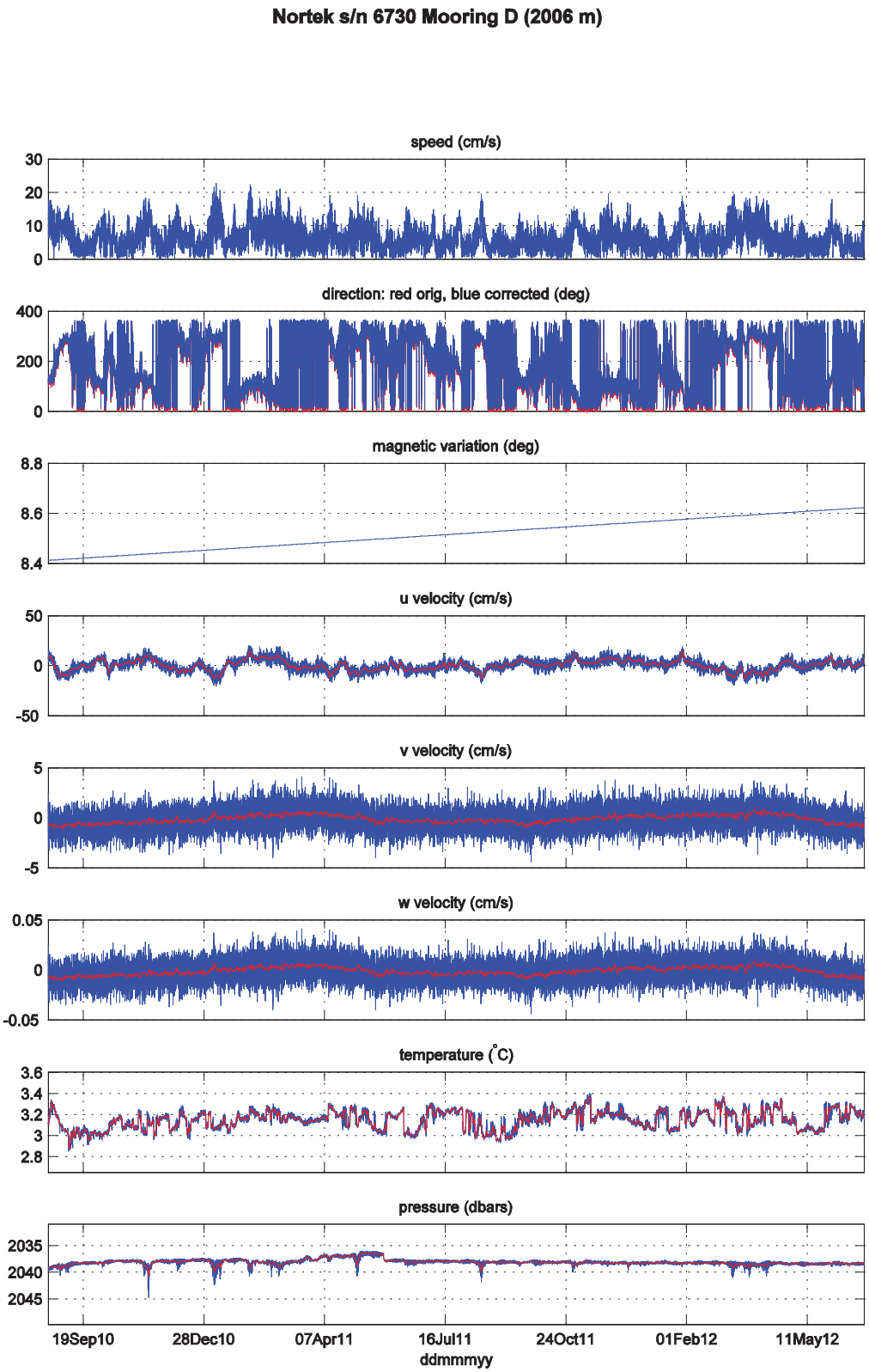

Figure D13. Nortek s/n 6730, Mooring D, 2000 m nominal depth. Subplots are from top to bottom: speed, direction, magnetic variation, u-velocity, v-velocity, w-velocity, *in situ* temperature, and pressure.

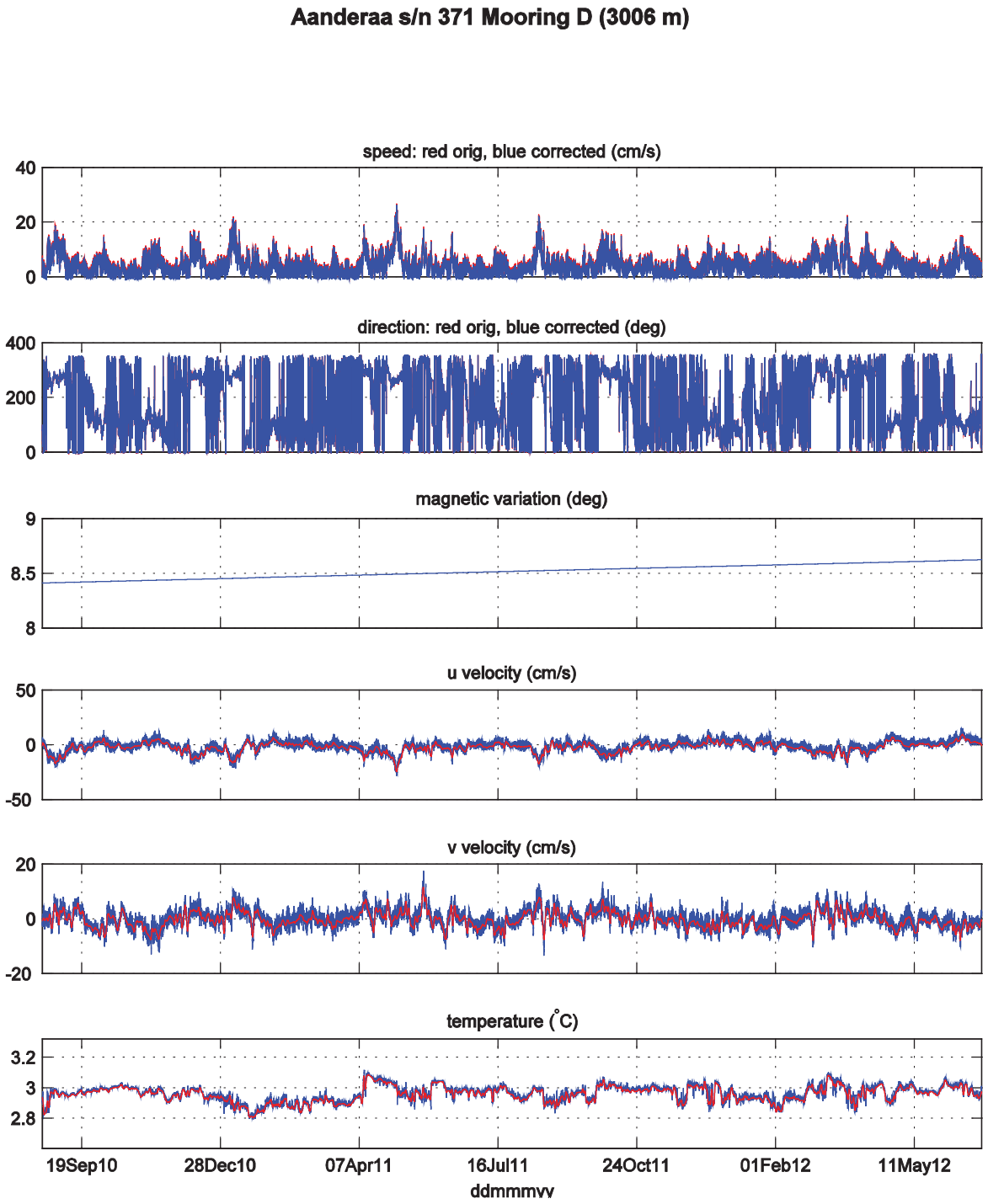

Figure D14. Aanderaa RCM-11 s/n 371, Mooring D, 3000 m nominal depth. Subplots are from top to bottom: speed, direction, magnetic variation, u-velocity, v-velocity, and *in situ* temperature.

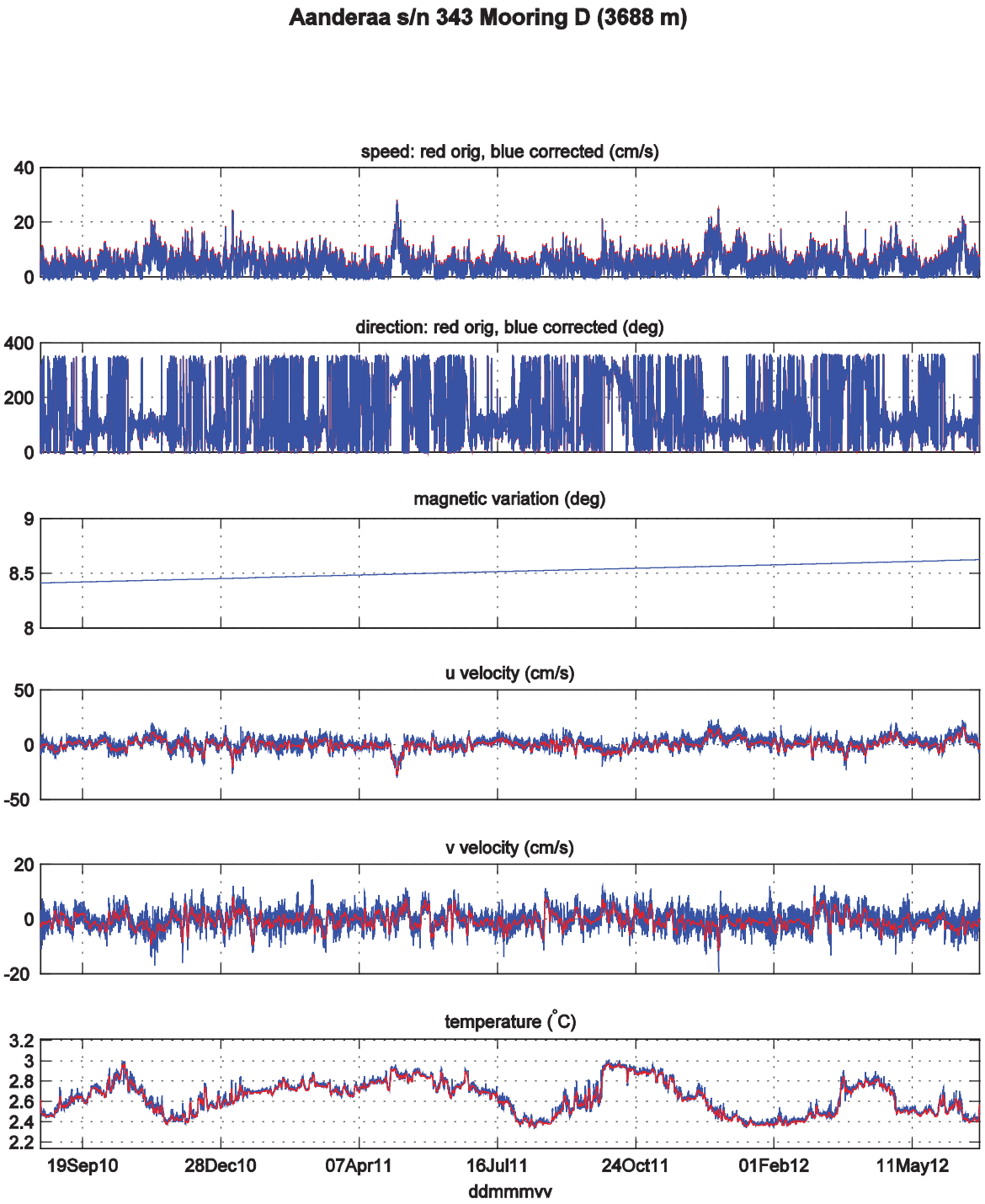

Figure D15. Aanderaa RCM-11 s/n 343, Mooring D, 3688 m depth (bottom). Subplots are from top to bottom: speed, direction, magnetic variation, u-velocity, v-velocity, and *in situ* temperature.

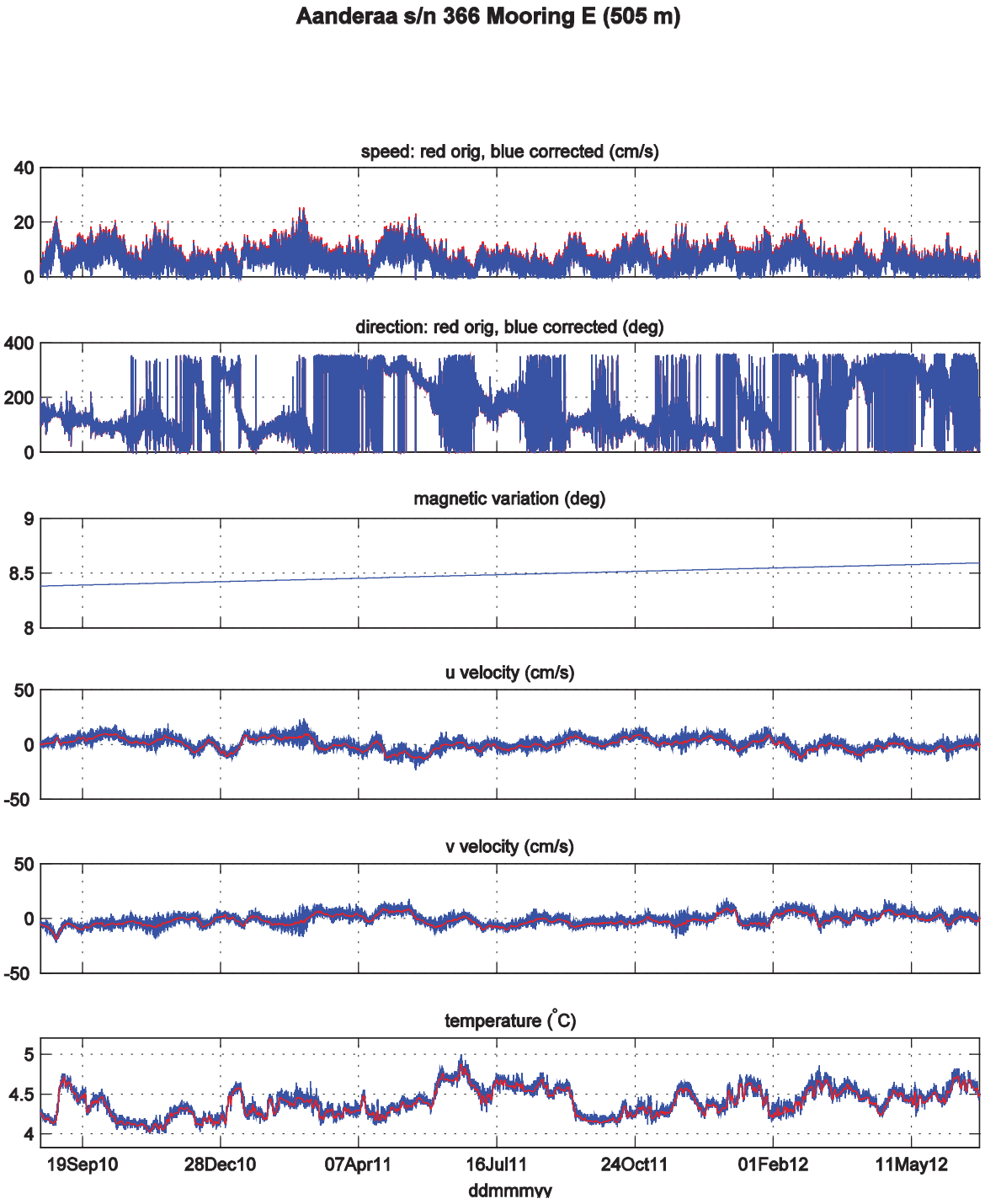

Figure D16. Aanderaa RCM-11 s/n 366, Mooring E, 500 m nominal depth. Subplots are from top to bottom: speed, direction, magnetic variation, u-velocity, v-velocity, and *in situ* temperature.

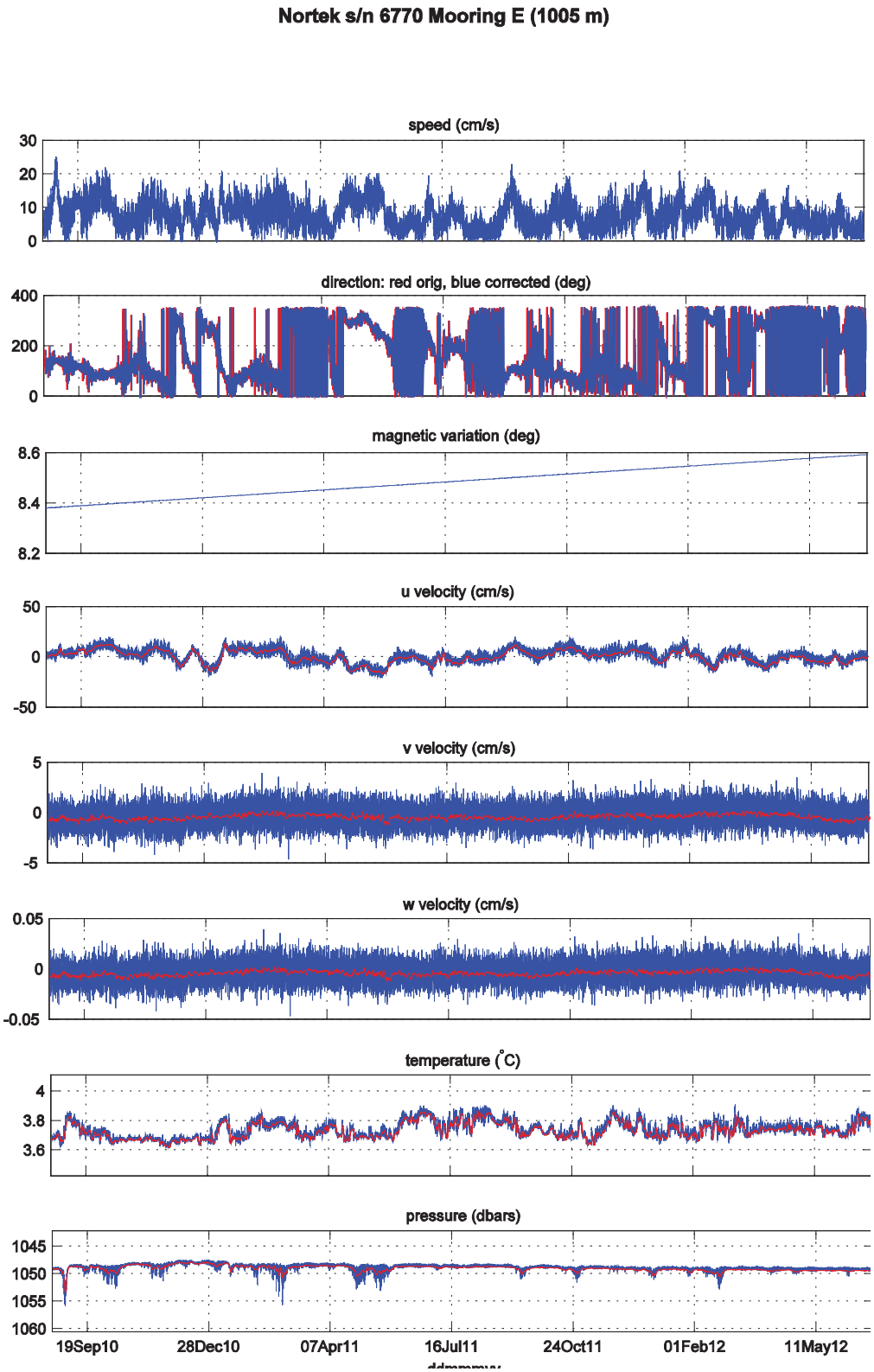

Figure D17. Nortek s/n 6770, Mooring E, 1000 m nominal depth. Subplots are from top to bottom: speed, direction, magnetic variation, u-velocity, v-velocity, w-velocity, *in situ* temperature, and pressure.

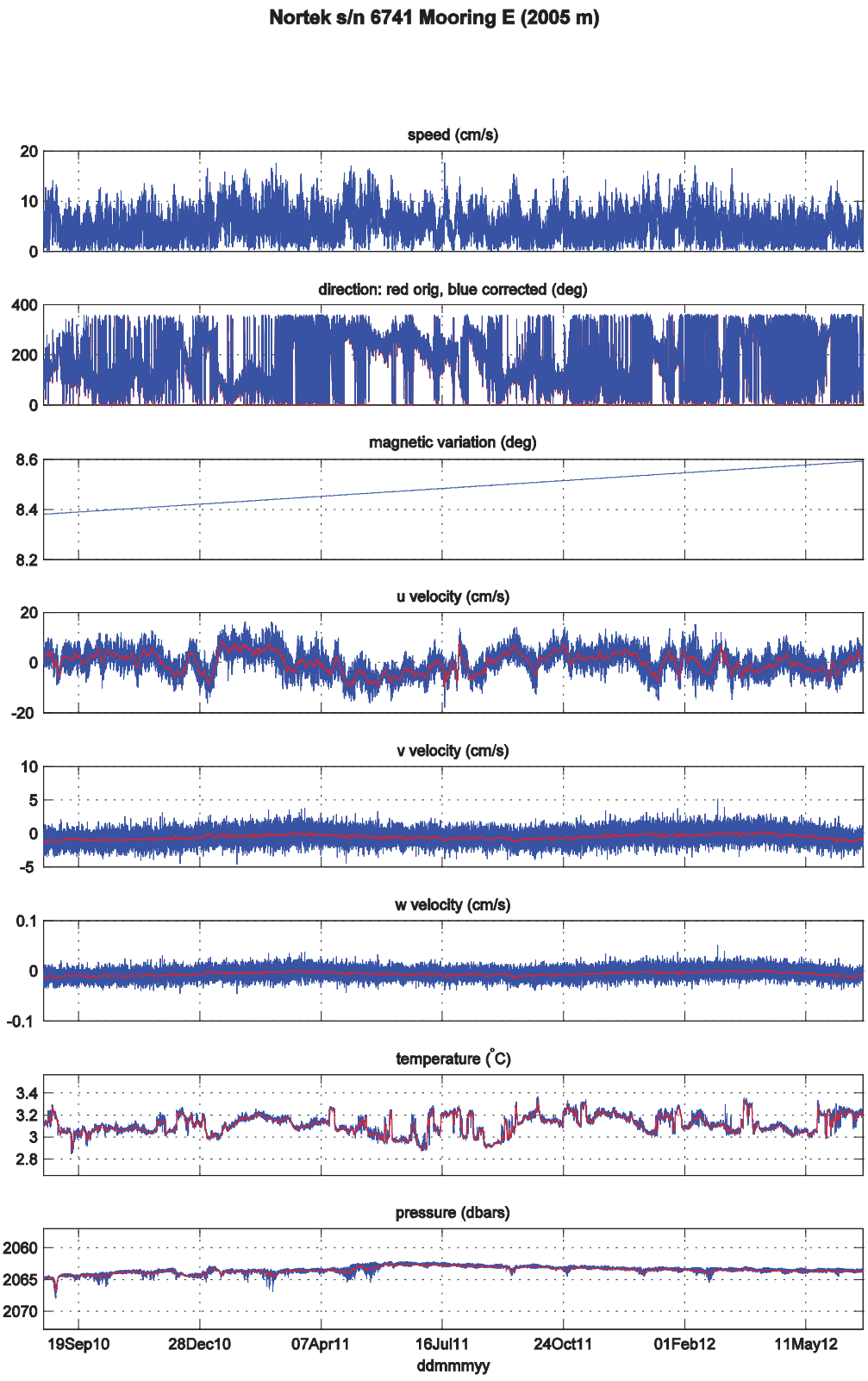

Figure D18. Nortek s/n 6741, Mooring E, 2000 m nominal depth. Subplots are from top to bottom: speed, direction, magnetic variation, u-velocity, v-velocity, w-velocity, *in situ* temperature, and pressure.

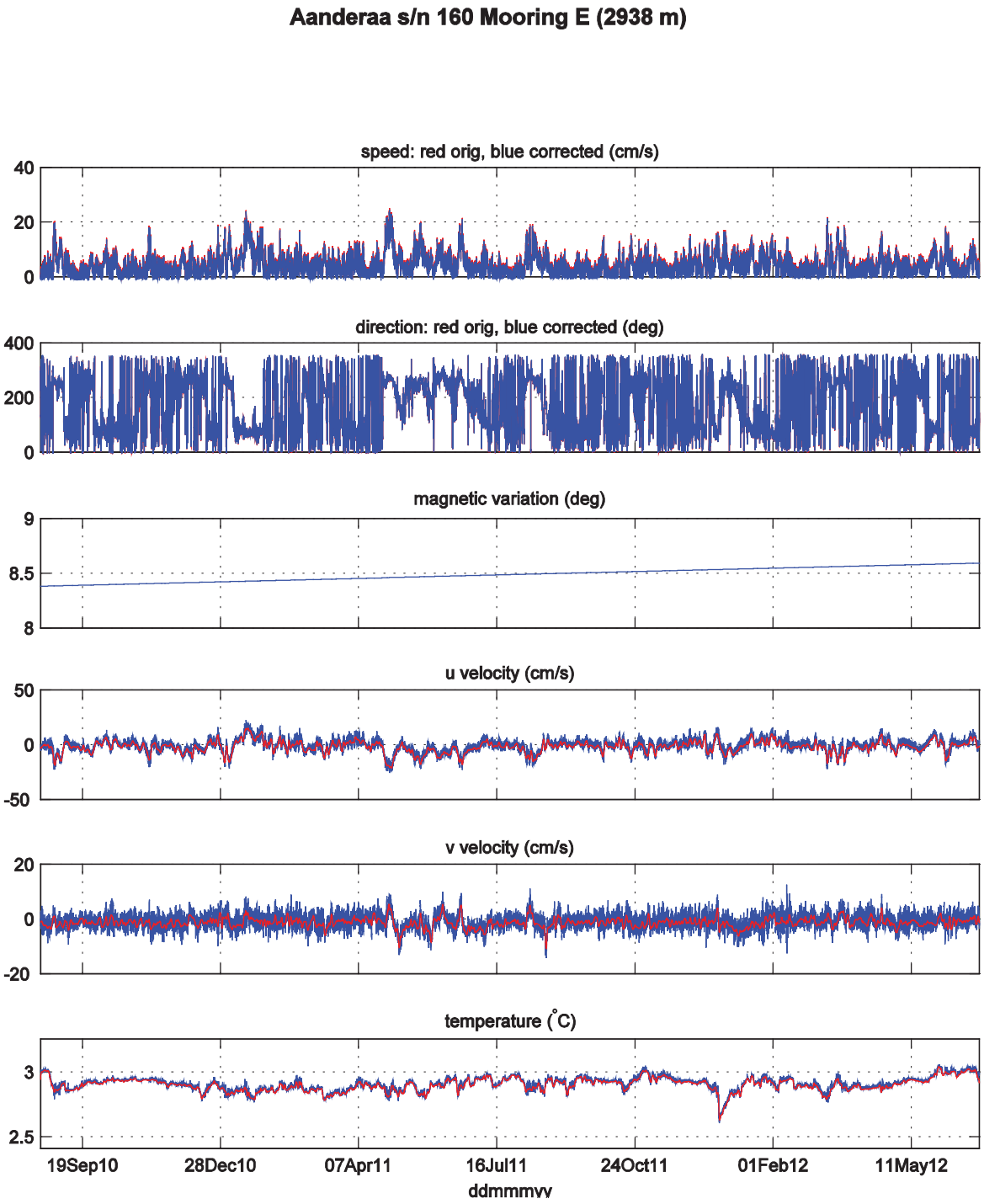

Figure D19. Aanderaa RCM-11 s/n 160, Mooring E, 2938 m depth (bottom). Subplots are from top to bottom: speed, direction, magnetic variation, u-velocity, v-velocity, and *in situ* temperature.

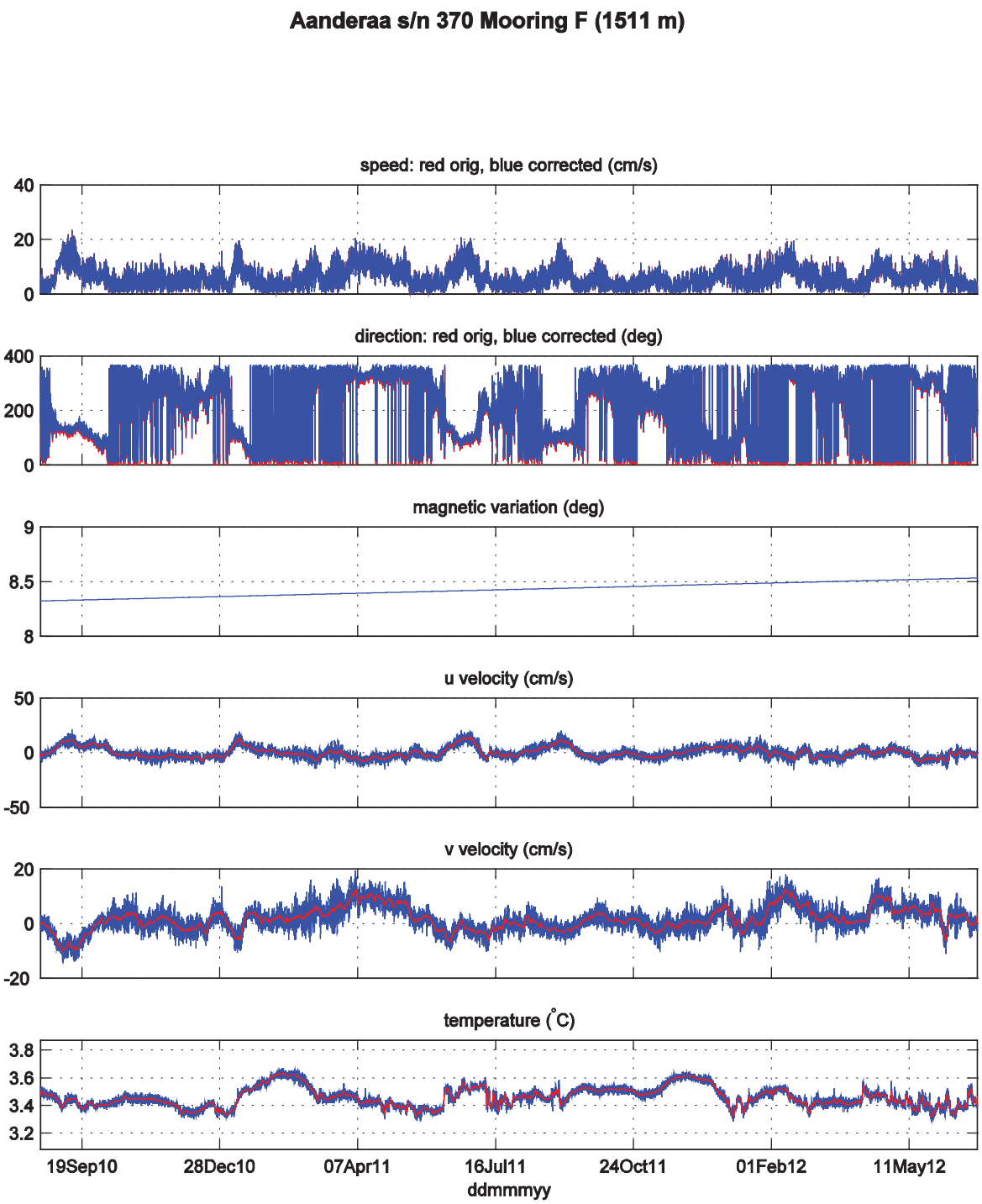

Figure D20. Aanderaa RCM-11 s/n 370, Mooring F, 1500 m nominal depth. Subplots are from top to bottom: speed, direction, magnetic variation, u-velocity, v-velocity, and *in situ* temperature.

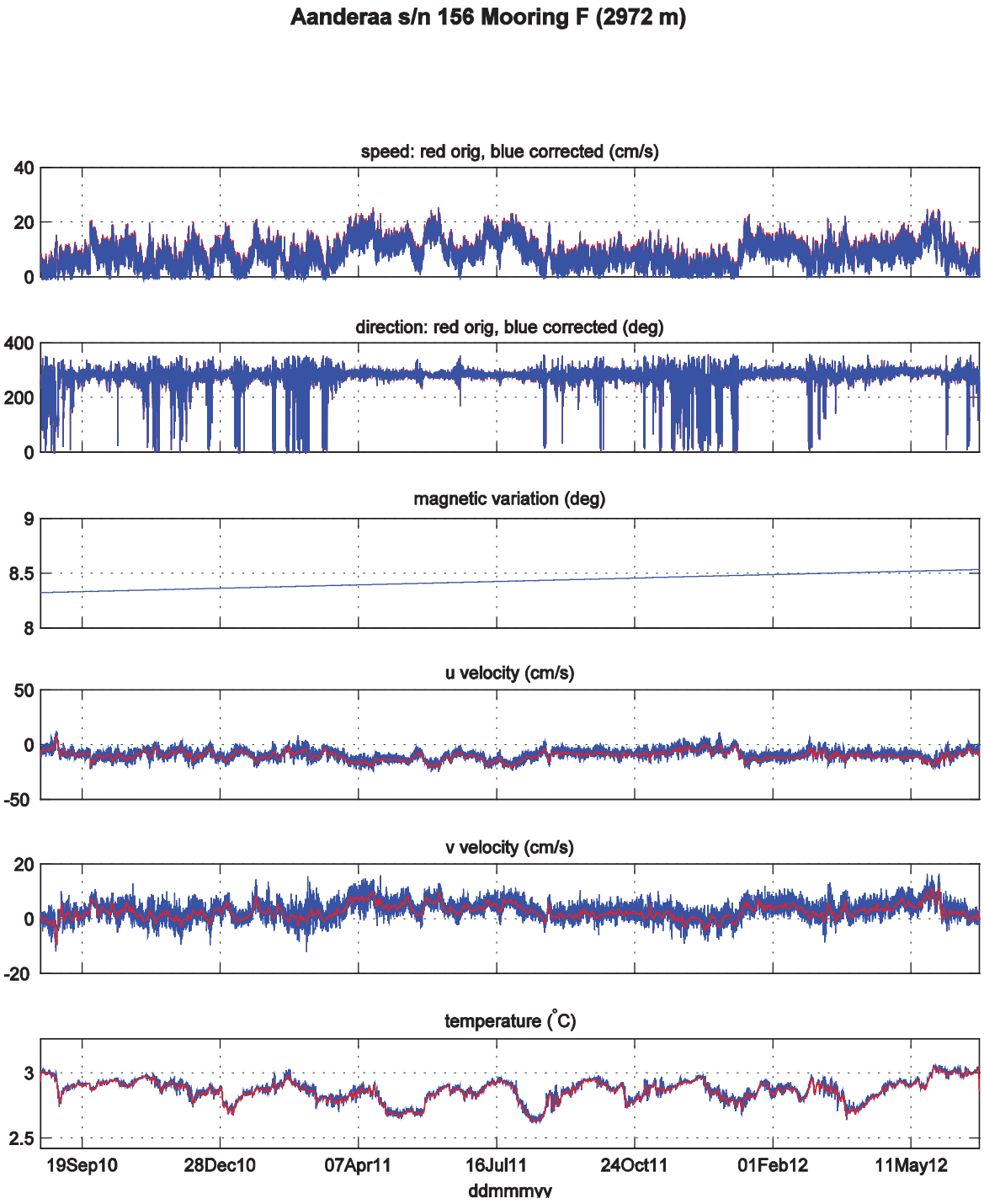

Figure D21. Aanderaa RCM-11 s/n 156, Mooring F, 2972 m depth (bottom). Subplots are from top to bottom: speed, direction, magnetic variation, u-velocity, v-velocity, and *in situ* temperature.

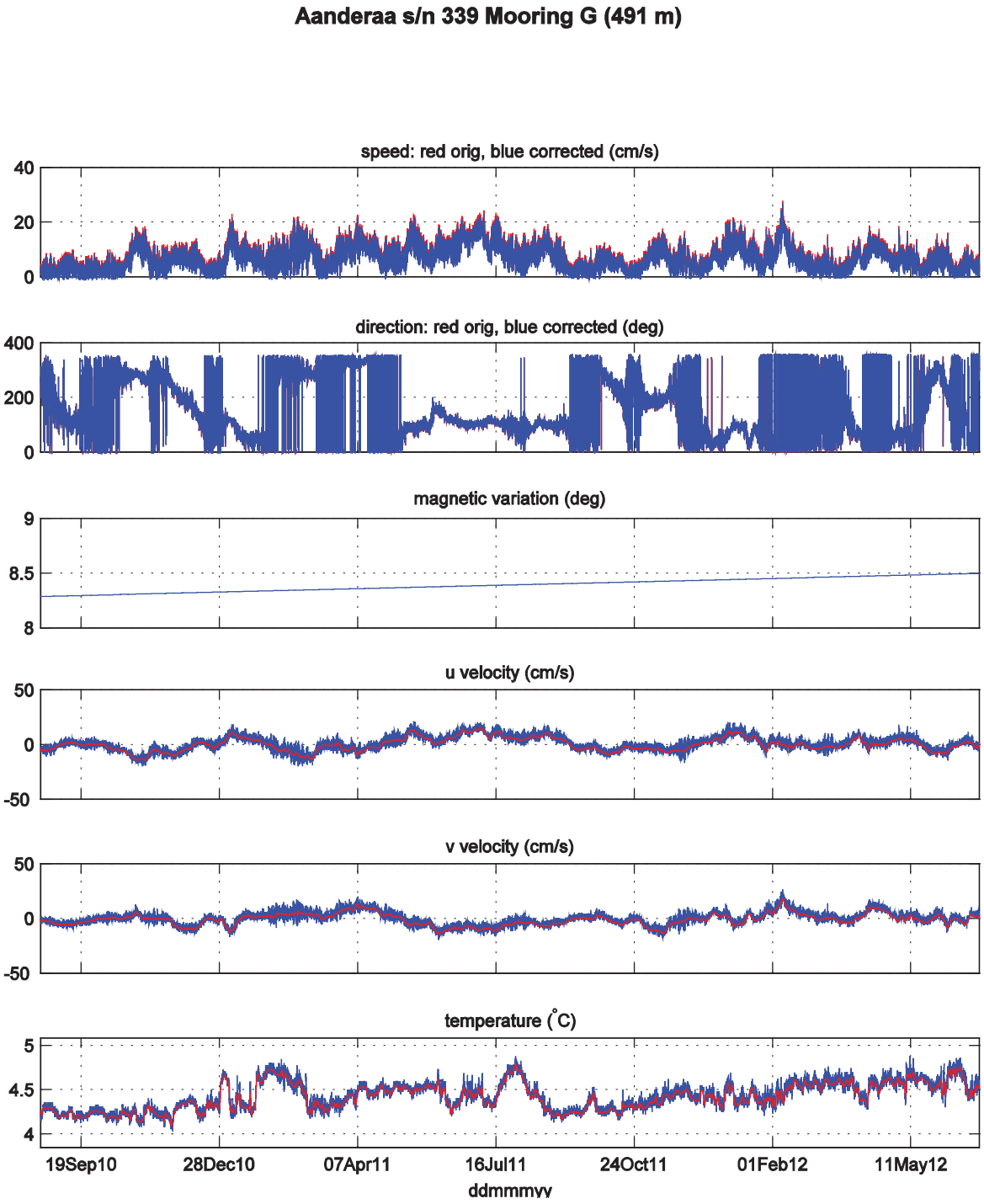

Figure D22. Aanderaa RCM-11 s/n 339, Mooring G, 500 m nominal depth. Subplots are from top to bottom: speed, direction, magnetic variation, u-velocity, v-velocity, and *in situ* temperature.

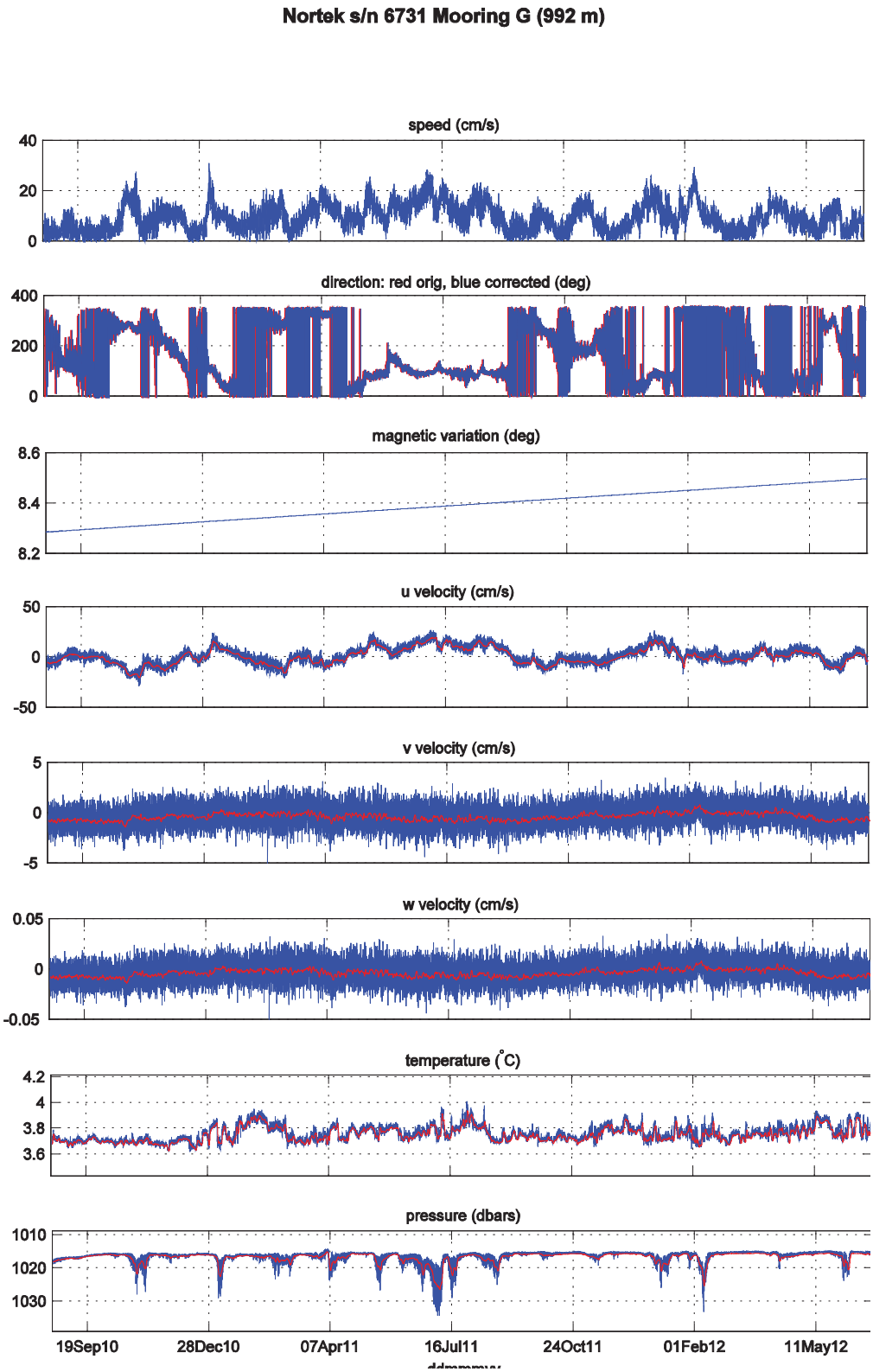

Figure D23. Nortek s/n 6731, Mooring G, 1000 m nominal depth. Subplots are from top to bottom: speed, direction, magnetic variation, u-velocity, v-velocity, w-velocity, *in situ* temperature, and pressure.

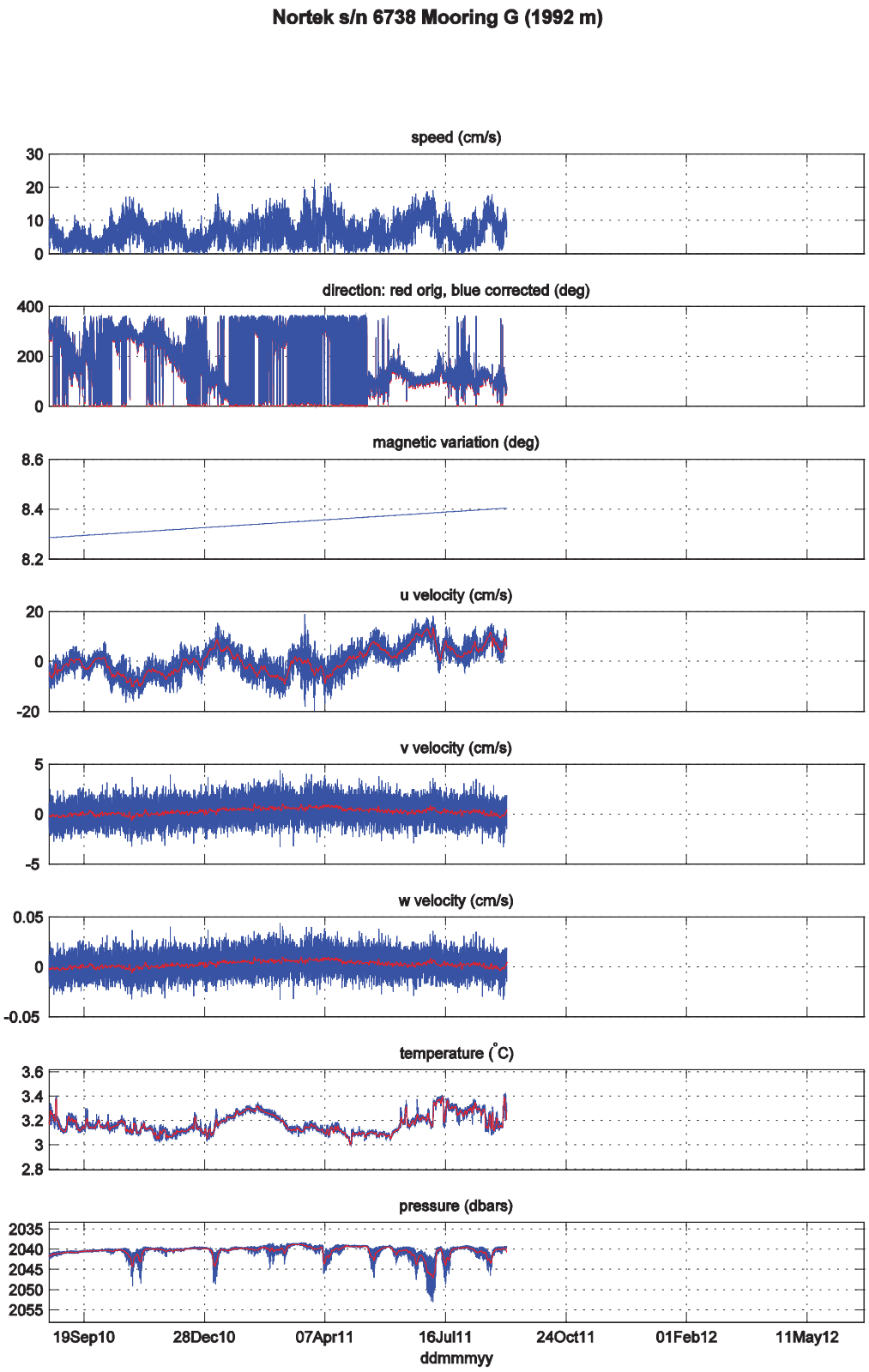

Figure D24. Nortek s/n 6738, Mooring G, 2000 m nominal depth. Subplots are from top to bottom: speed, direction, magnetic variation, u-velocity, v-velocity, w-velocity, *in situ* temperature, and pressure.

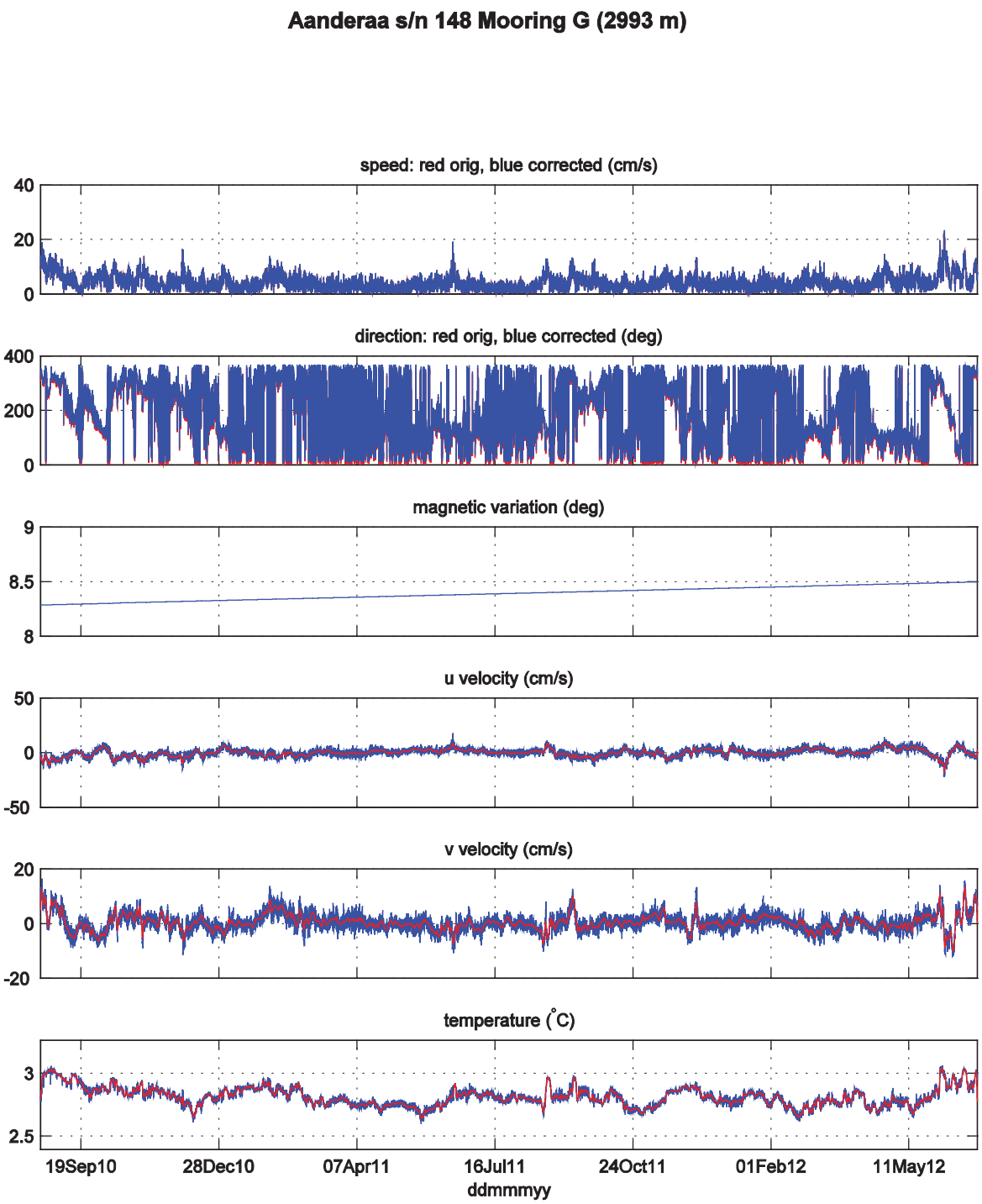

Figure D25. Aanderaa RCM-11 s/n 148, Mooring G, 3000 m nominal depth. Subplots are from top to bottom: speed, direction, magnetic variation, u-velocity, v-velocity, and *in situ* temperature.

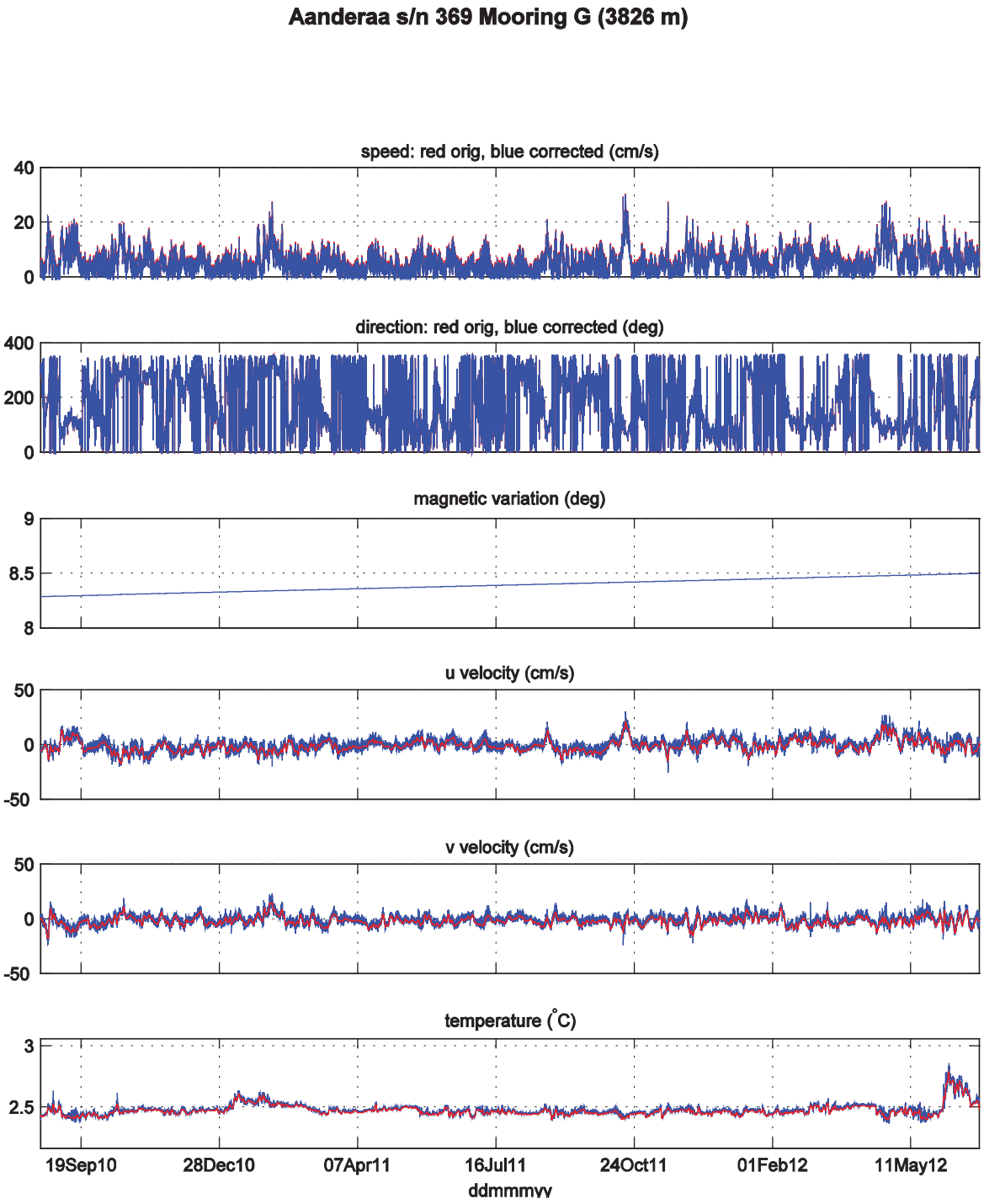

Figure D26. Aanderaa RCM-11 s/n 369, Mooring G, 3826 m depth (bottom). Subplots are from top to bottom: speed, direction, magnetic variation, u-velocity, v-velocity, and *in situ* temperature.

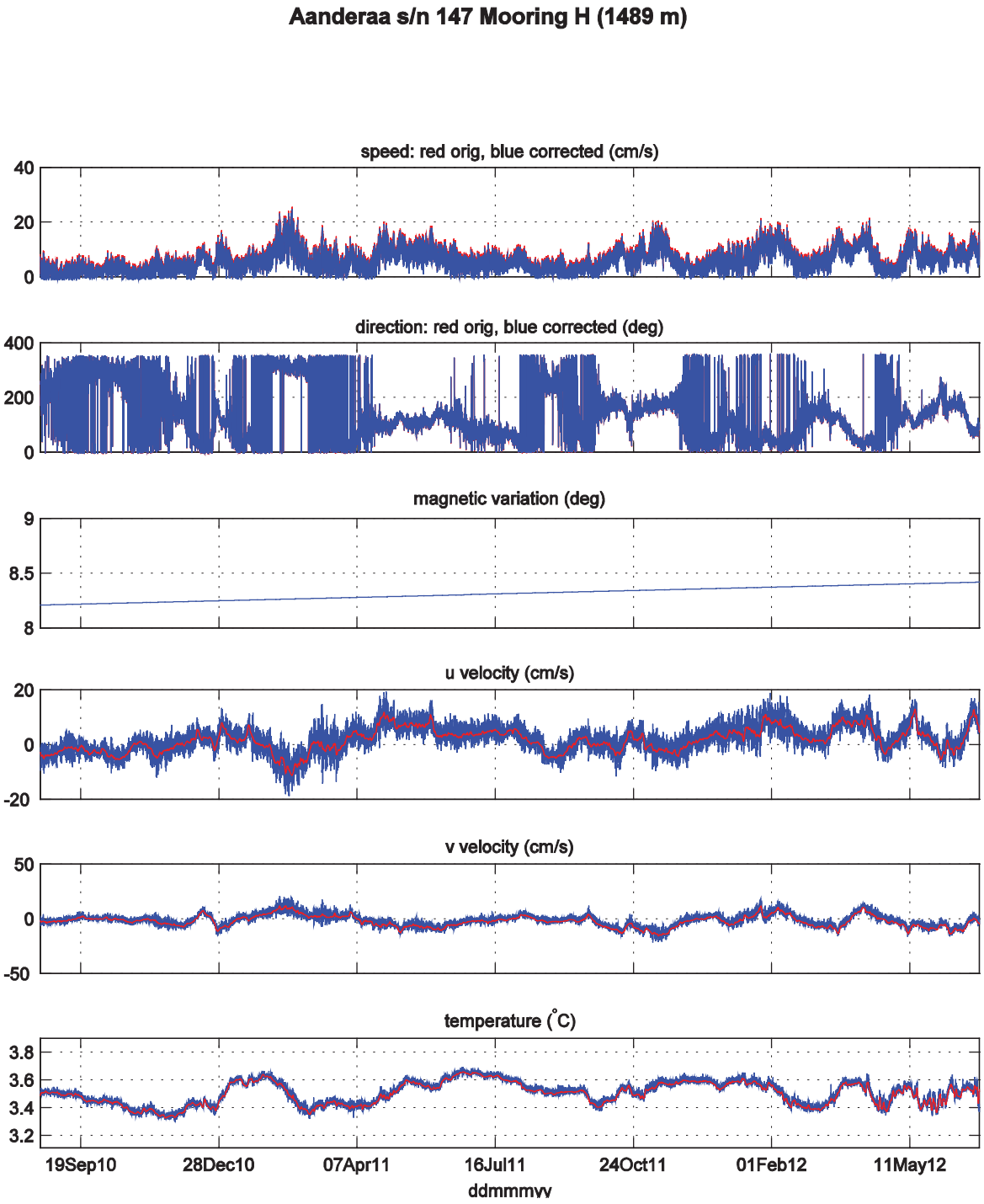

Figure D27. Aanderaa RCM-11 s/n 147, Mooring H, 1500 m nominal depth. Subplots are from top to bottom: speed, direction, magnetic variation, u-velocity, v-velocity, and *in situ* temperature.

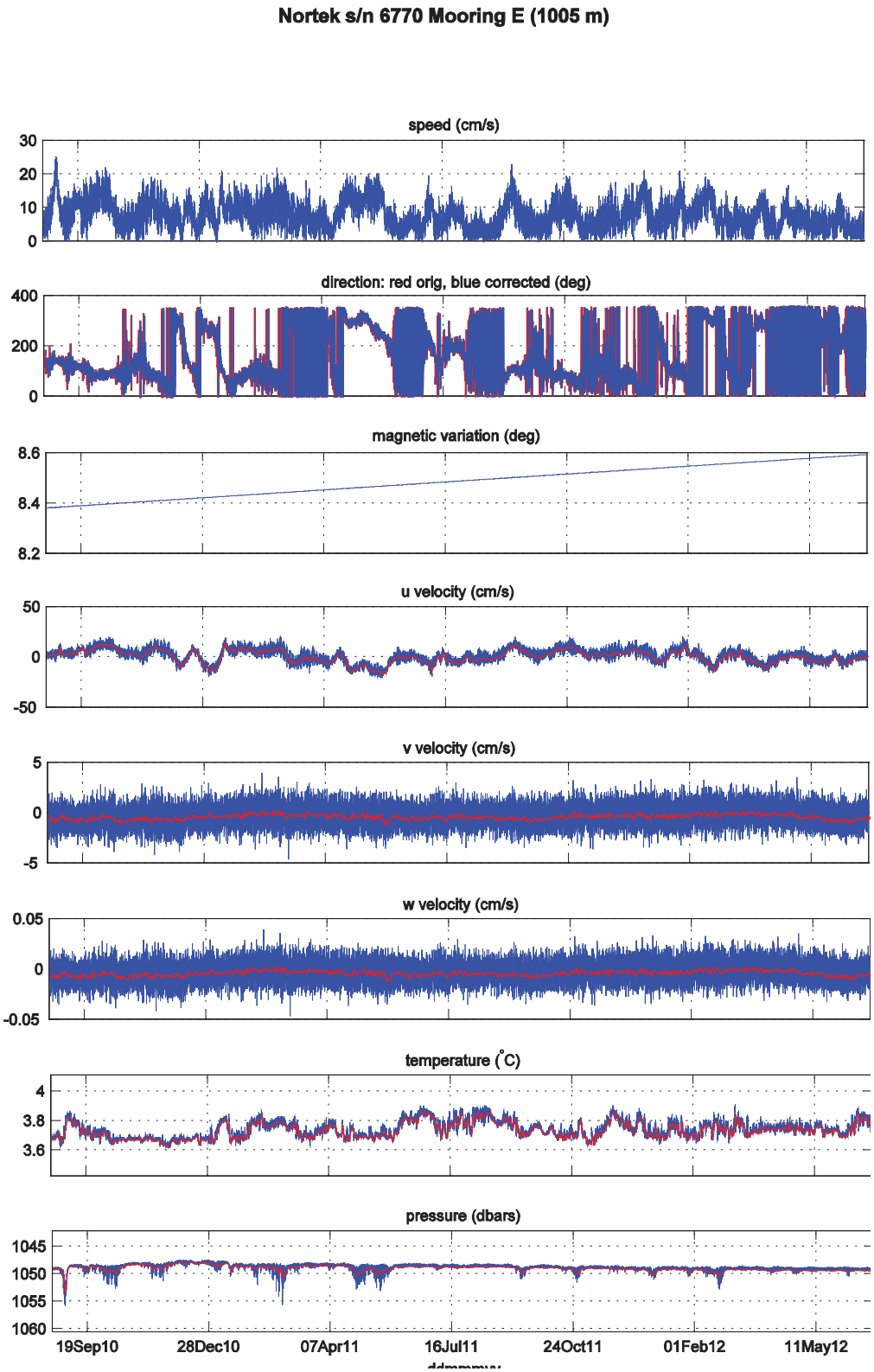

Figure D28. Nortek s/n 6770, Mooring H, 2000 m nominal depth. Subplots are from top to bottom: speed, direction, magnetic variation, u-velocity, v-velocity, w-velocity, *in situ* temperature, and pressure.

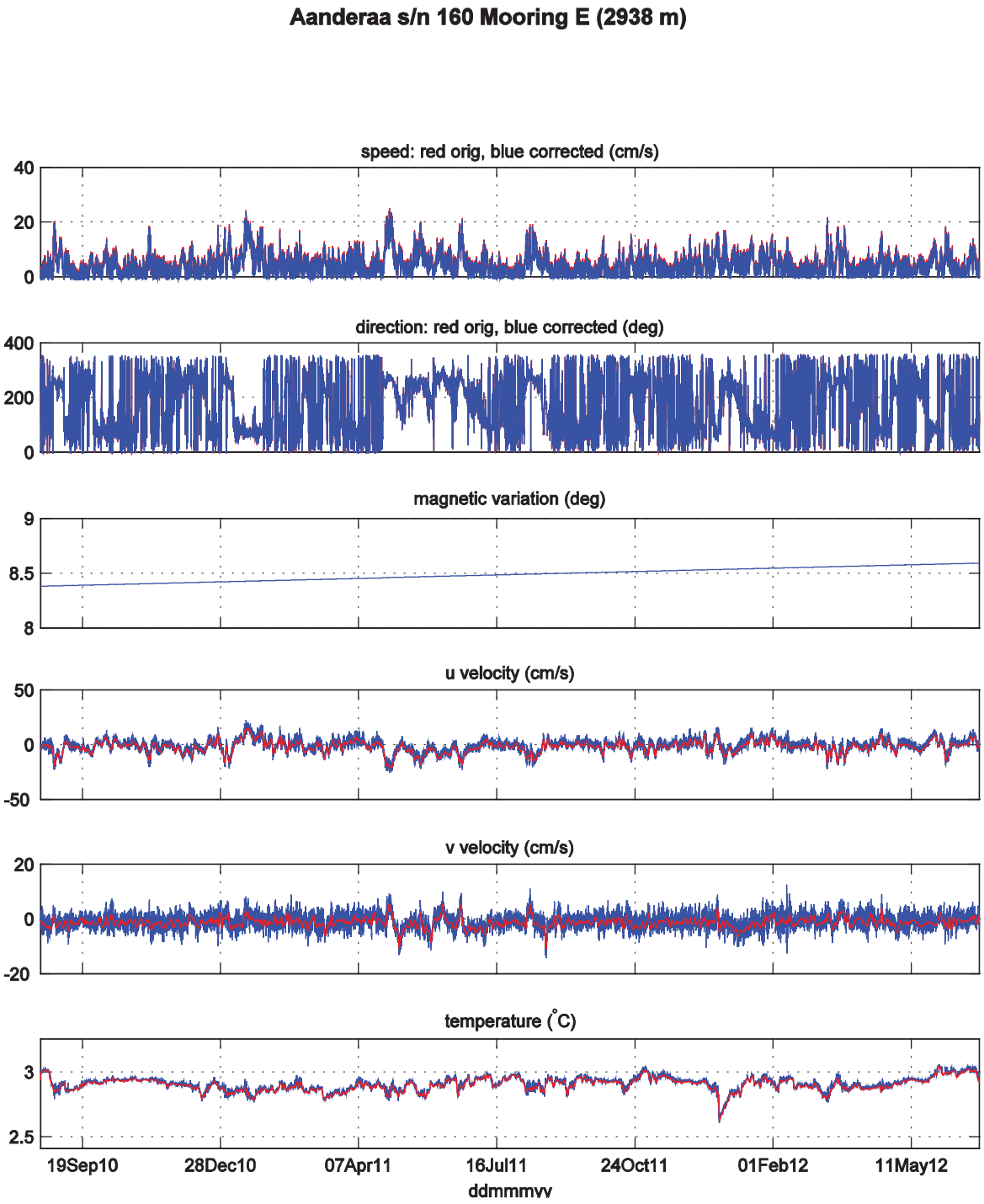

Figure D29. Aanderaa RCM-11 s/n 160, Mooring H, 3161 m depth (bottom). Subplots are from top to bottom: speed, direction, magnetic variation, u-velocity, v-velocity, and *in situ* temperature.

This page left intentionally blank.

Appendix E: Sea-Bird SBE37 MicroCAT data, presented by mooring letter, north to south (A to H), and then depth, shallow to deep. Y-axis scales on all plots are not uniform so as to show the most variability possible. On top panel, red line depicts quality controlled, but un-calibrated data, and blue line depicts same data after calibration. Bottom three panels are drawn with a blue line for quality controlled and calibrated data and red line for the same data with a 40-hour low pass 2nd order Butterworth filter applied. MicroCATs with serial numbers in the 1000s or 2000s have no pressure gauge, and pressure data has been synthesized using methods described in report.

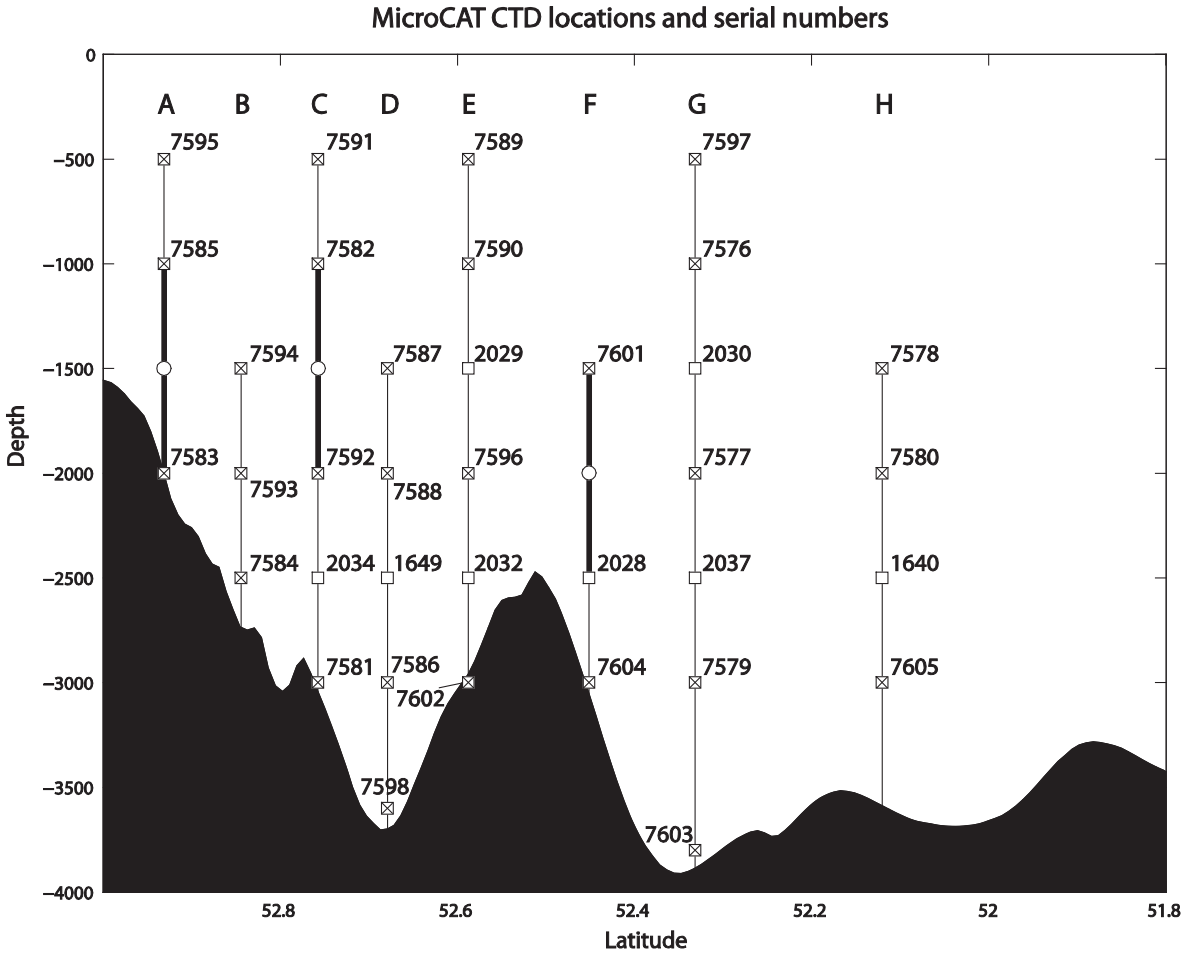

Figure E1. Locations of MicroCAT instruments in array. Serial numbers identify specific instruments and may be used for reference for the upcoming appendix plots.

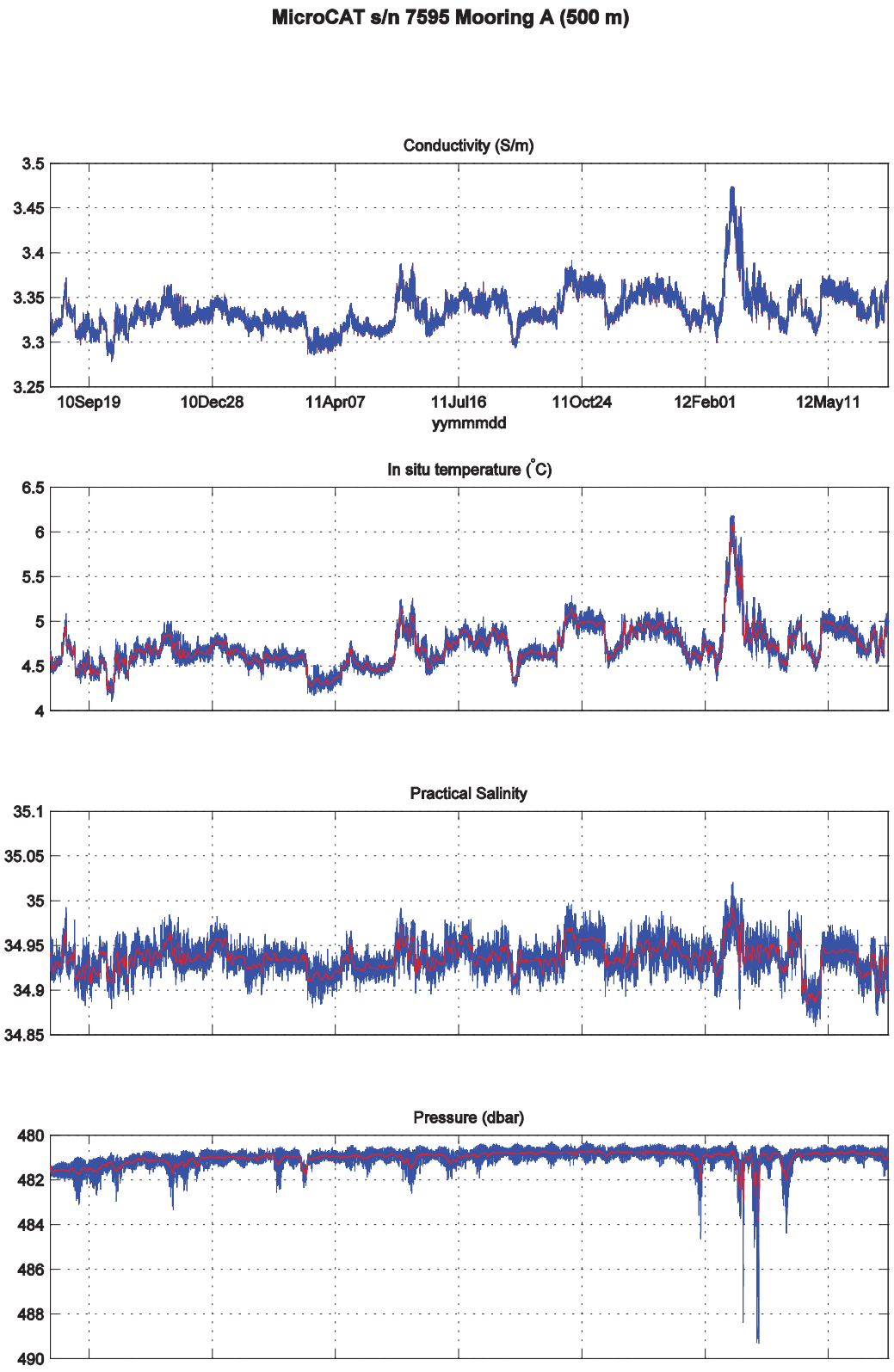

Figure E2. Sea-Bird MicroCAT SBE-37 s/n 7595, Mooring A, 500 m nominal depth. Subplots are from top to bottom: conductivity, *in situ* temperature, practical salinity, and pressure.

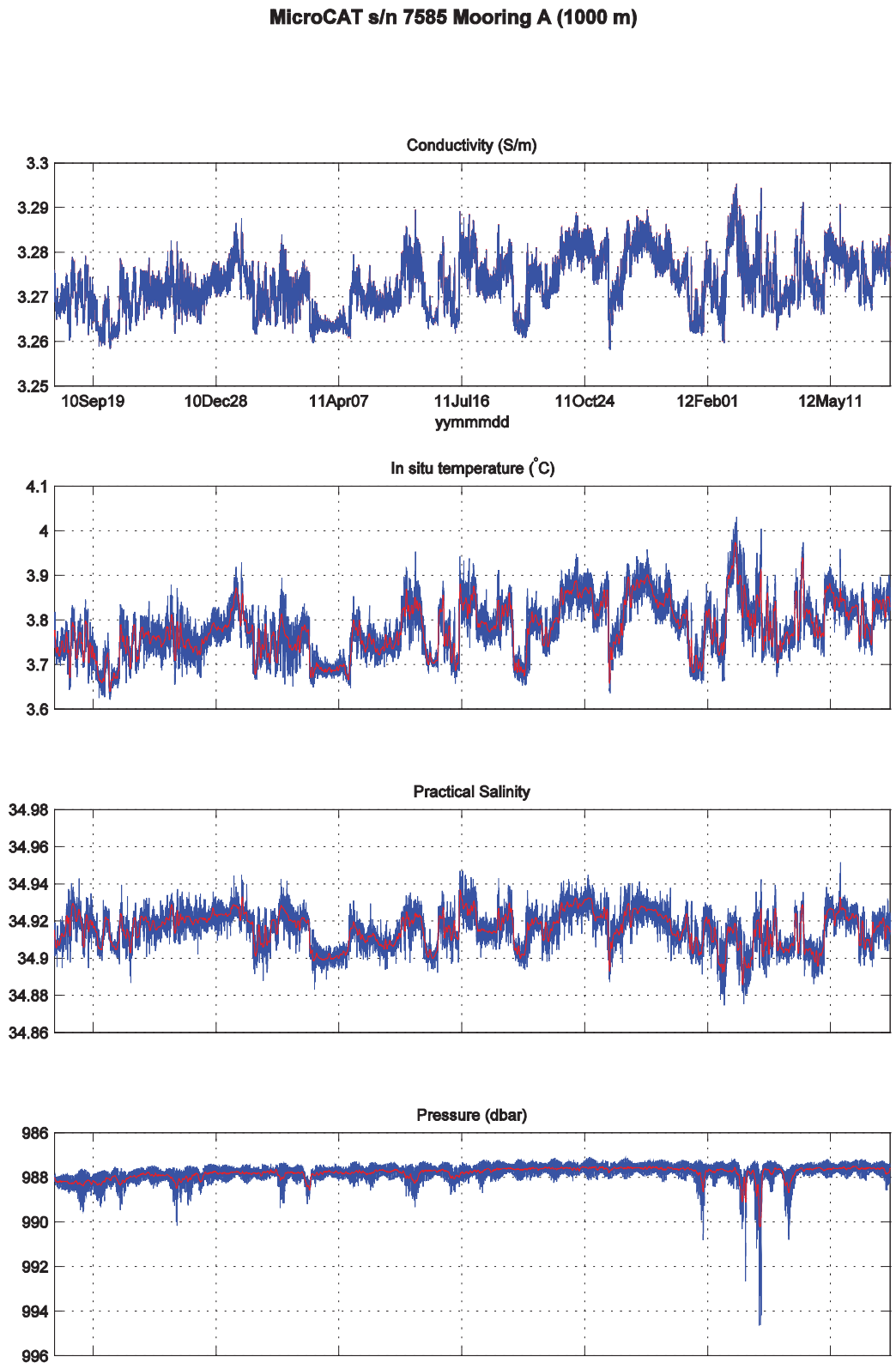

Figure E3. Sea-Bird MicroCAT SBE-37 s/n 7585, Mooring A, 1000 m nominal depth. Subplots are from top to bottom: conductivity, *in situ* temperature, practical salinity, and pressure.

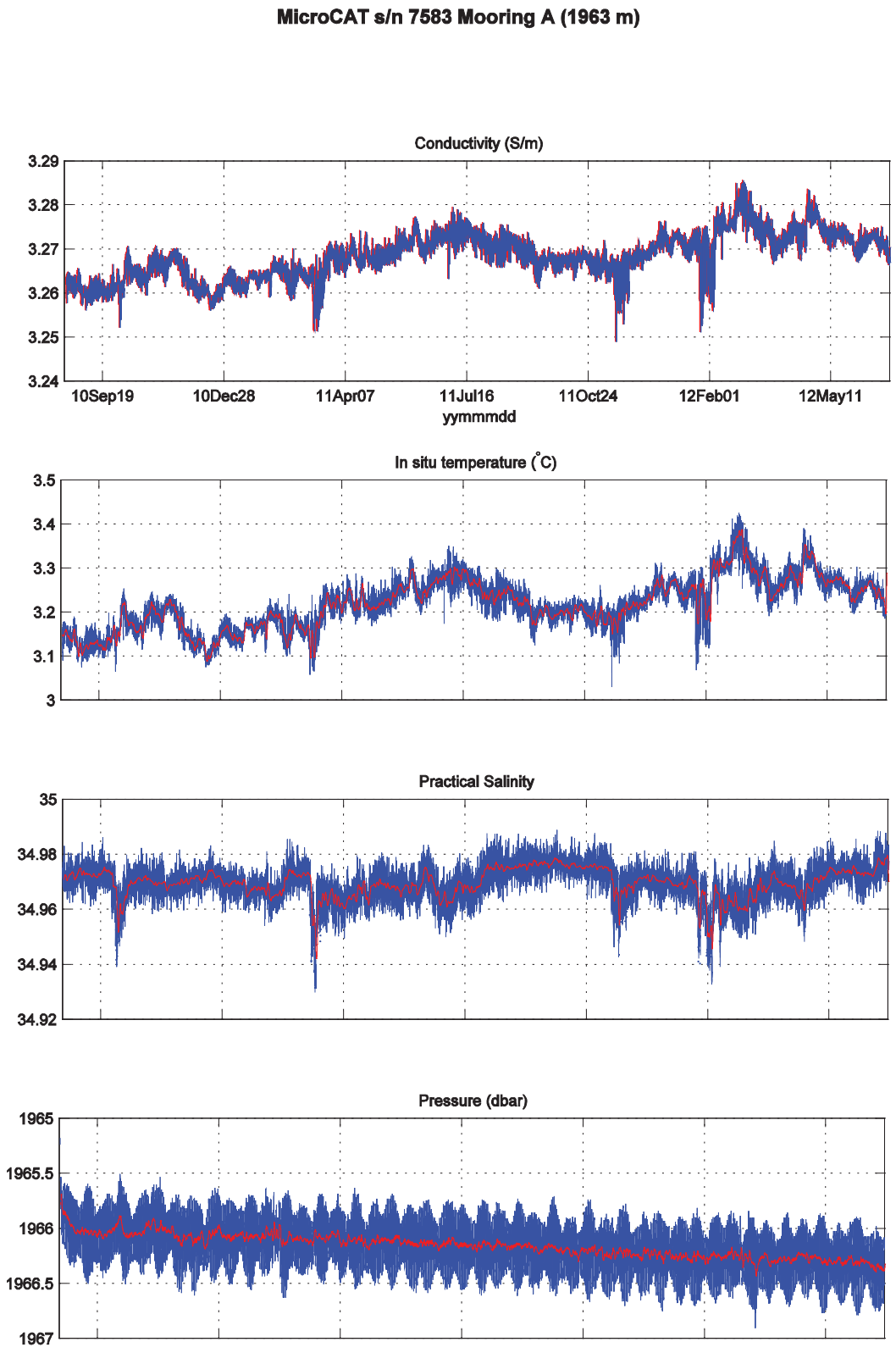

Figure E4. Sea-Bird MicroCAT SBE-37 s/n 7583, Mooring A, 1963 m nominal depth (bottom). Subplots are from top to bottom: conductivity, *in situ* temperature, practical salinity, and pressure.

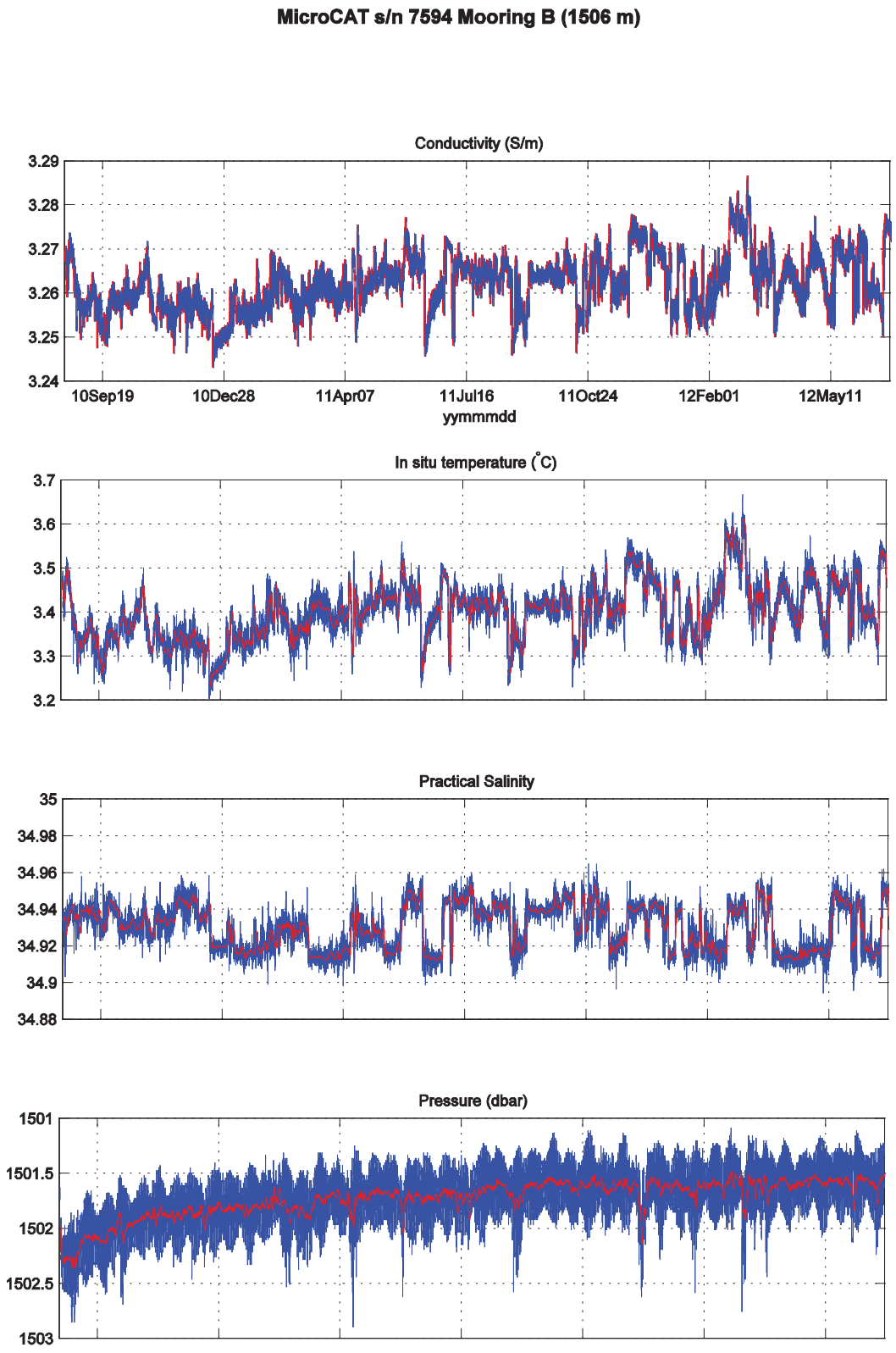

Figure E5. Sea-Bird MicroCAT SBE-37 s/n 7594, Mooring B, 1506 m nominal depth. Subplots are from top to bottom: conductivity, *in situ* temperature, practical salinity, and pressure.

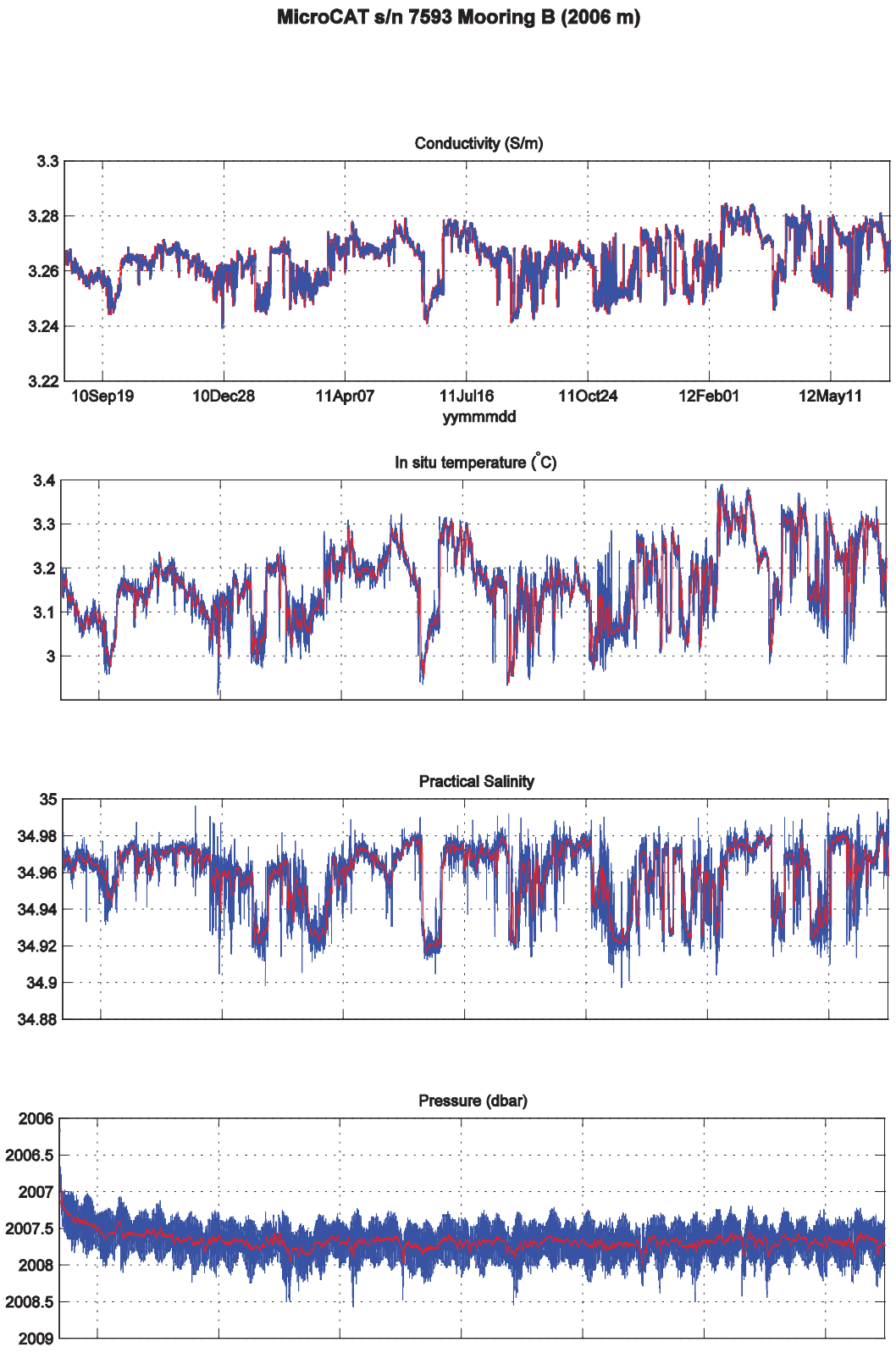

Figure E6. Sea-Bird MicroCAT SBE-37 s/n 7593, Mooring B, 2006 m nominal depth. Subplots are from top to bottom: conductivity, *in situ* temperature, practical salinity, and pressure.

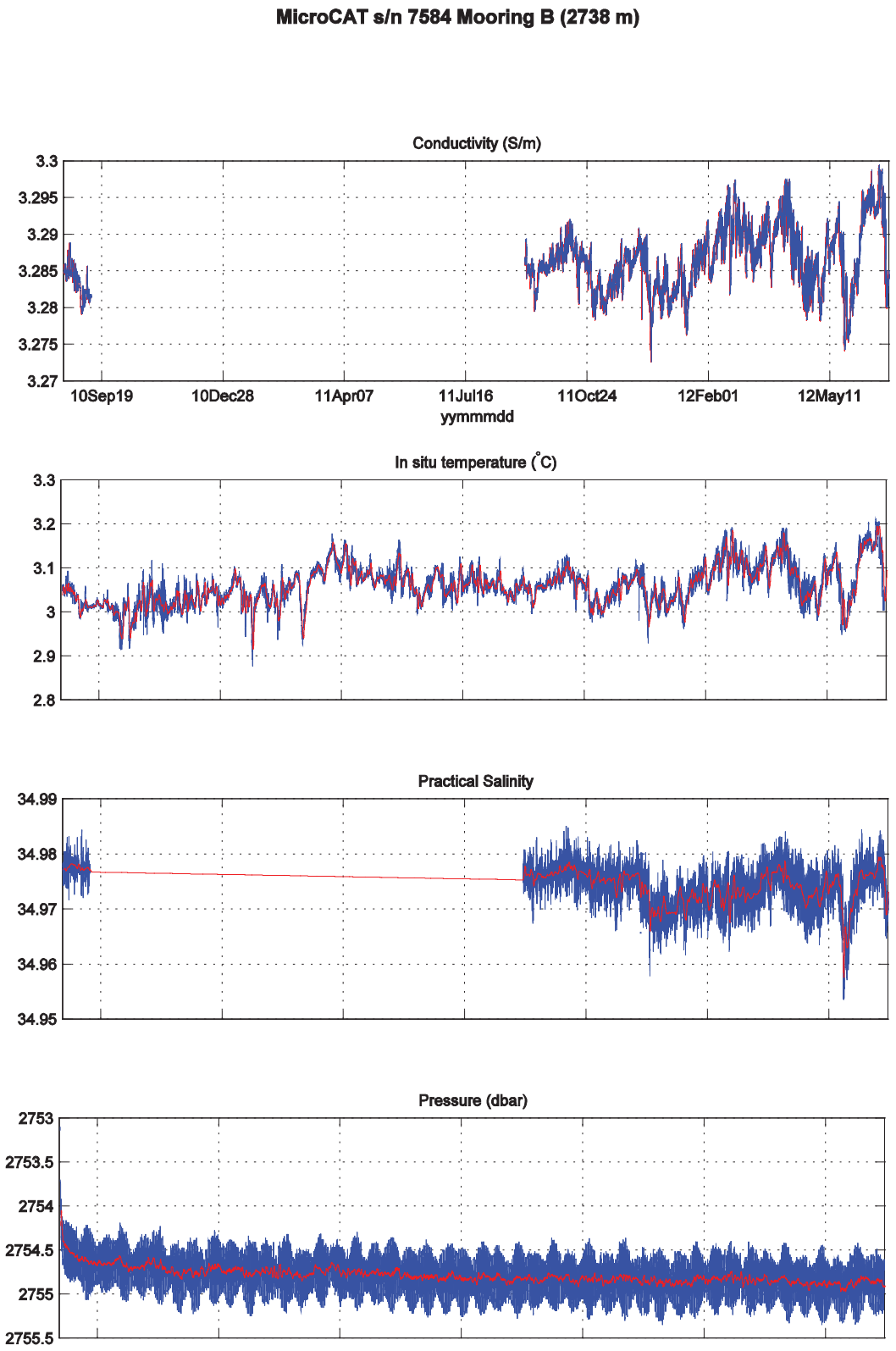

Figure E7. Sea-Bird MicroCAT SBE-37 s/n 7584, Mooring B, 2738 m nominal depth (bottom). Subplots are from top to bottom: conductivity, *in situ* temperature, practical salinity, and pressure.

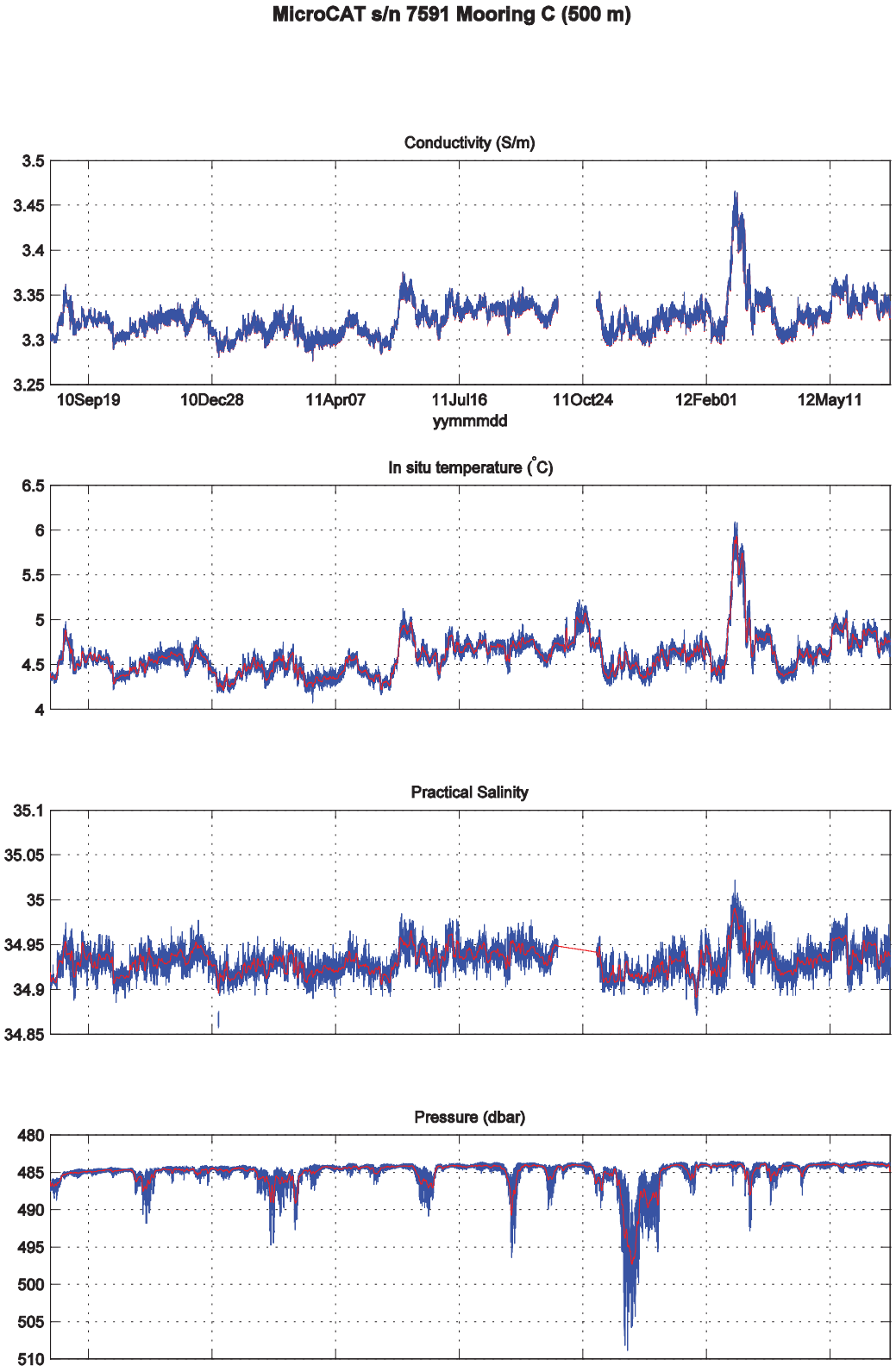

Figure E8. Sea-Bird MicroCAT SBE-37 s/n 7591, Mooring C, 500 m nominal depth. Subplots are from top to bottom: conductivity, *in situ* temperature, practical salinity, and pressure.

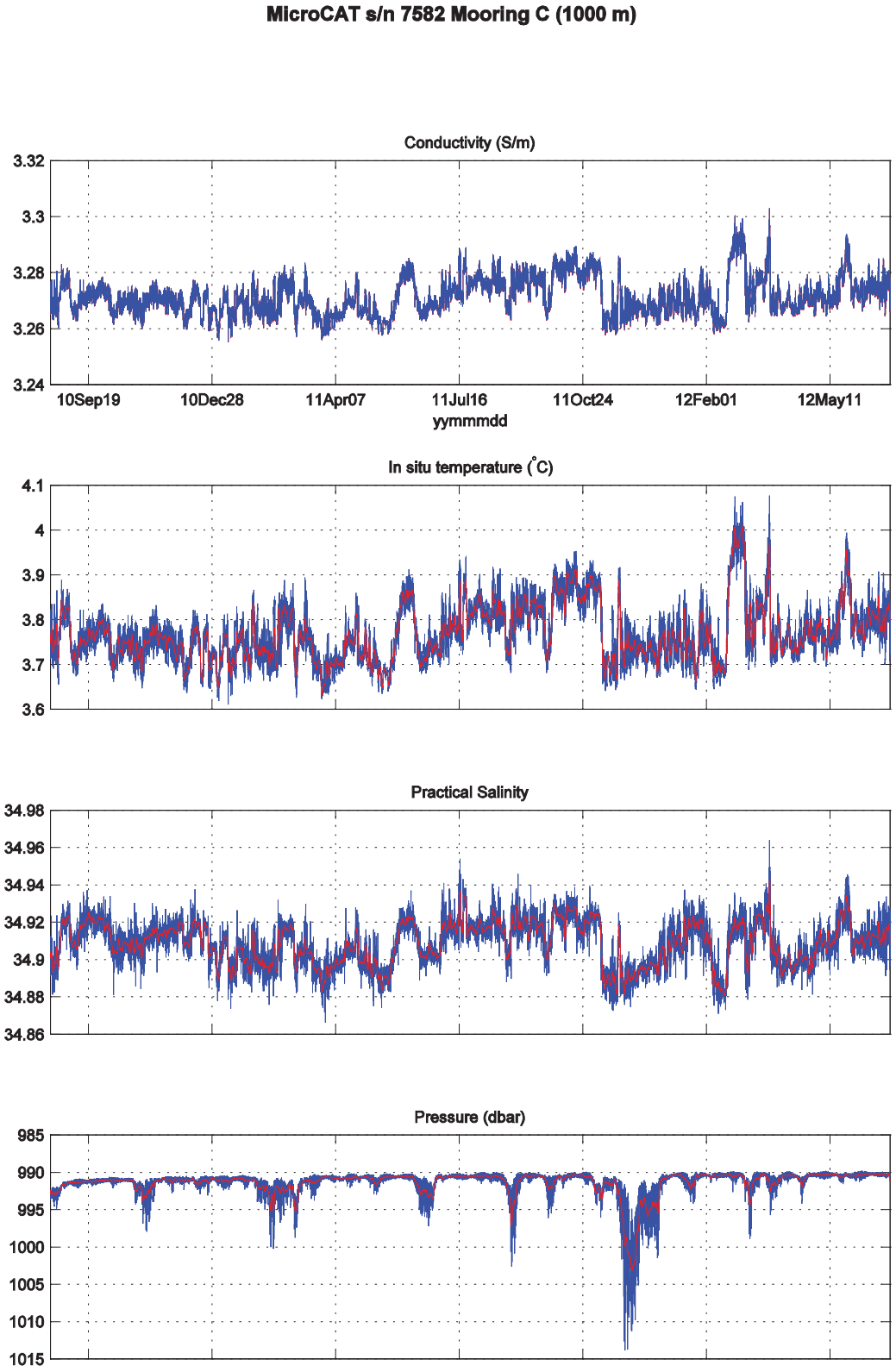

Figure E9. Sea-Bird MicroCAT SBE-37 s/n 7582, Mooring C, 1000 m nominal depth. Subplots are from top to bottom: conductivity, *in situ* temperature, practical salinity, and pressure.

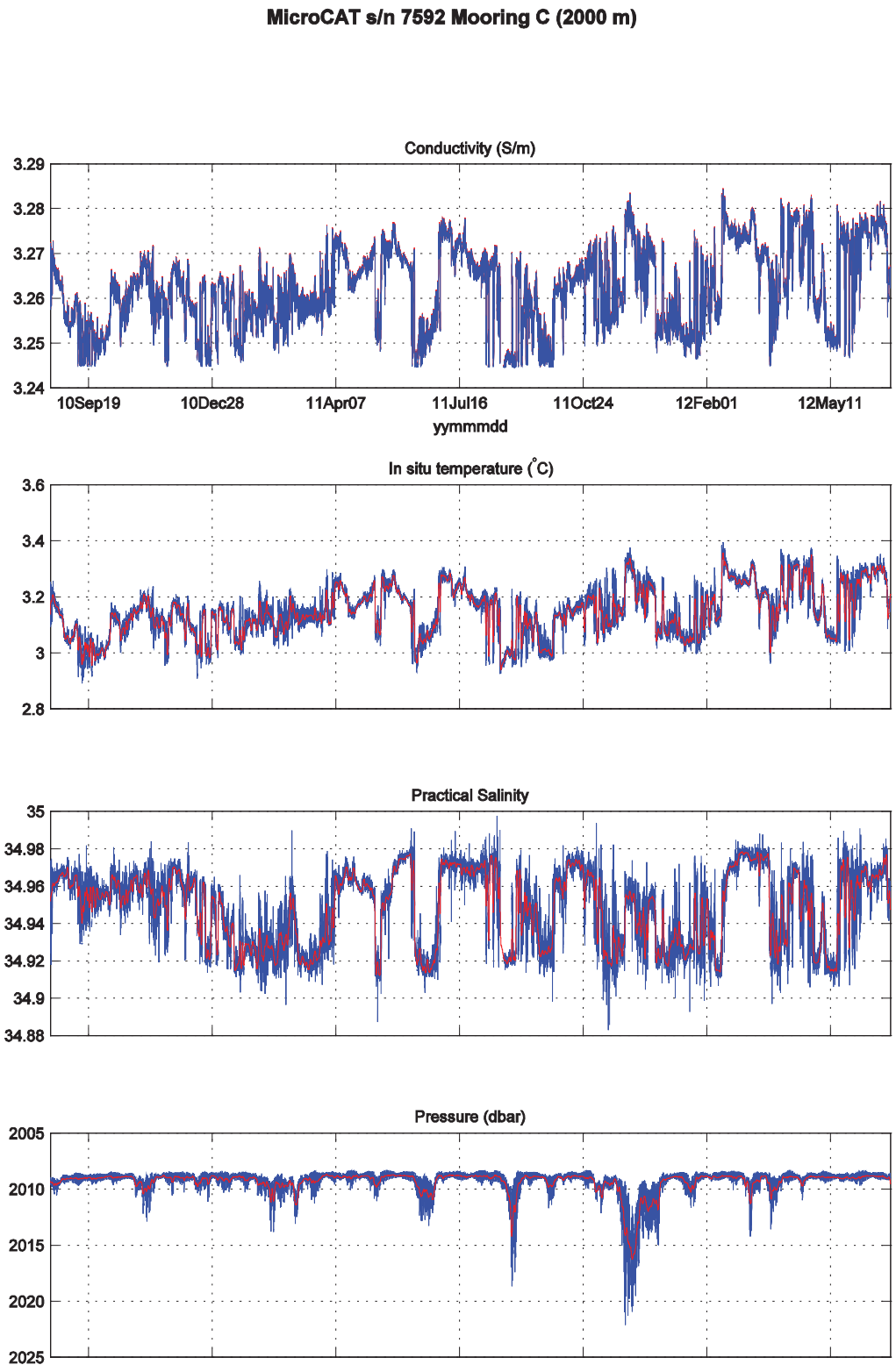

Figure E10. Sea-Bird MicroCAT SBE-37 s/n 7592, Mooring C, 2000 m nominal depth. Subplots are from top to bottom: conductivity, *in situ* temperature, practical salinity, and pressure.

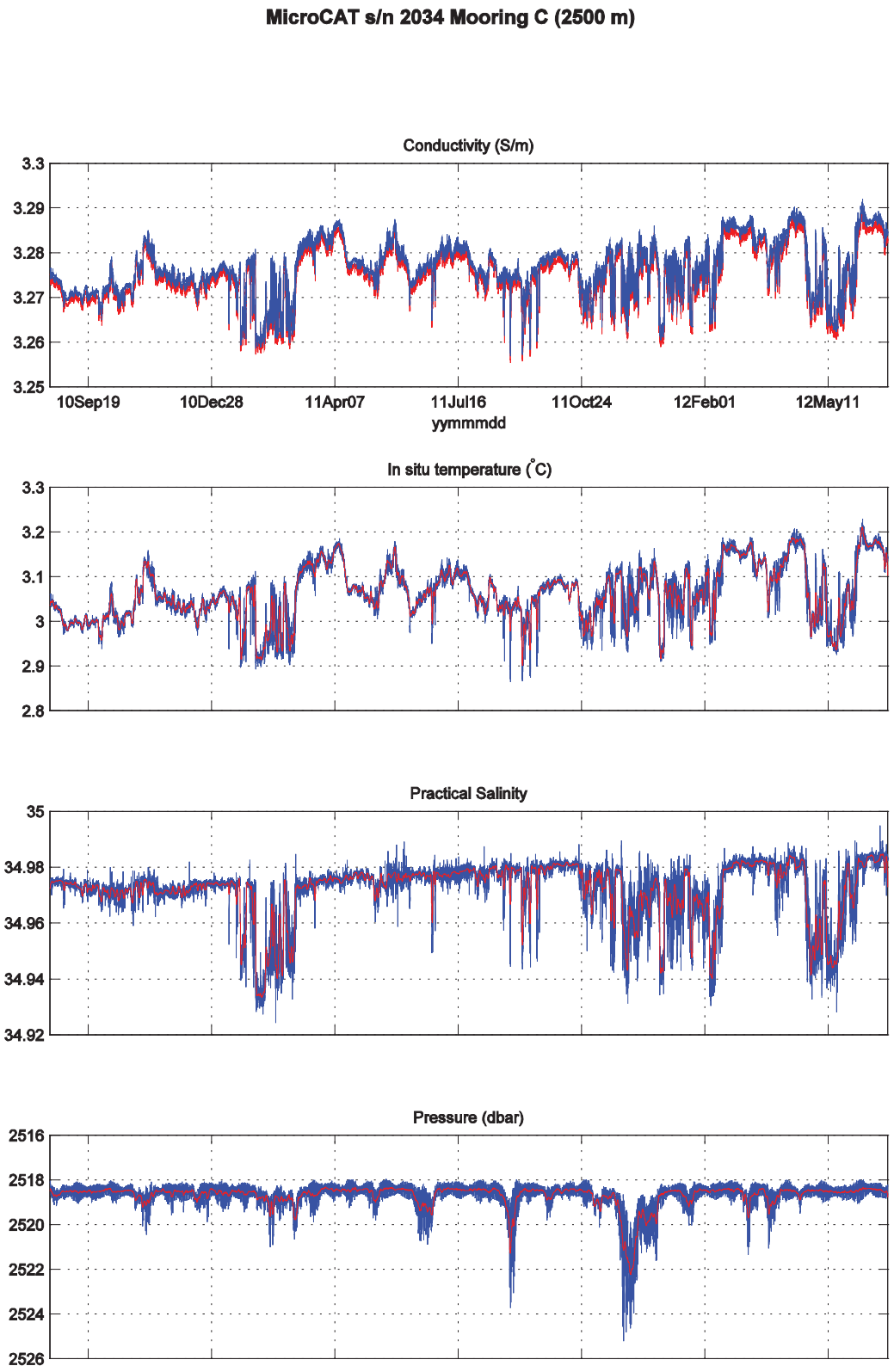

Figure E11. Sea-Bird MicroCAT SBE-37 s/n 2034, Mooring C, 2500 m nominal depth. Subplots are from top to bottom: conductivity, *in situ* temperature, practical salinity, and synthetic pressure.

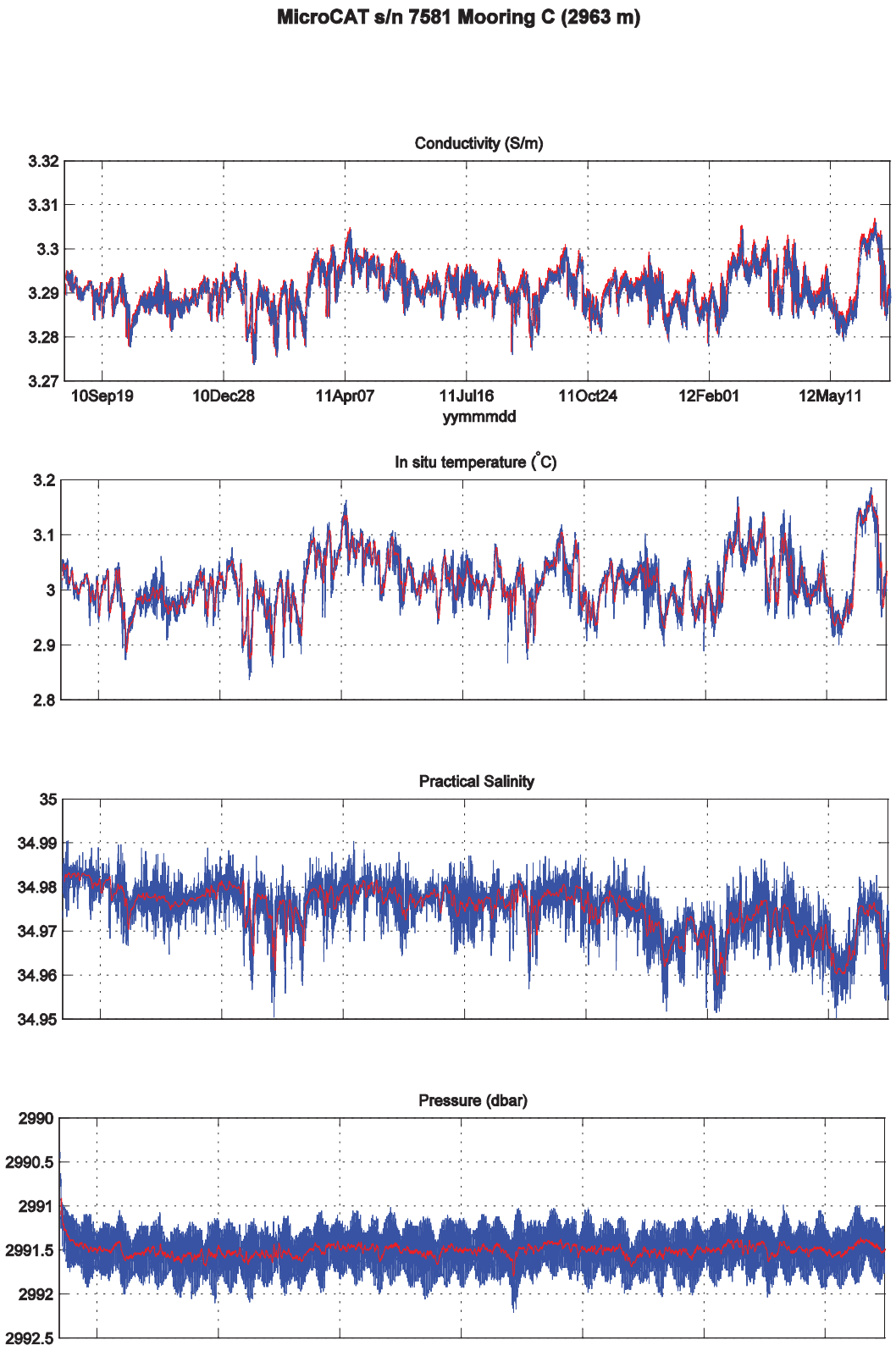

Figure E12. Sea-Bird MicroCAT SBE-37 s/n 7581, Mooring C, 2963 m nominal depth (bottom). Subplots are from top to bottom: conductivity, *in situ* temperature, practical salinity, and pressure.

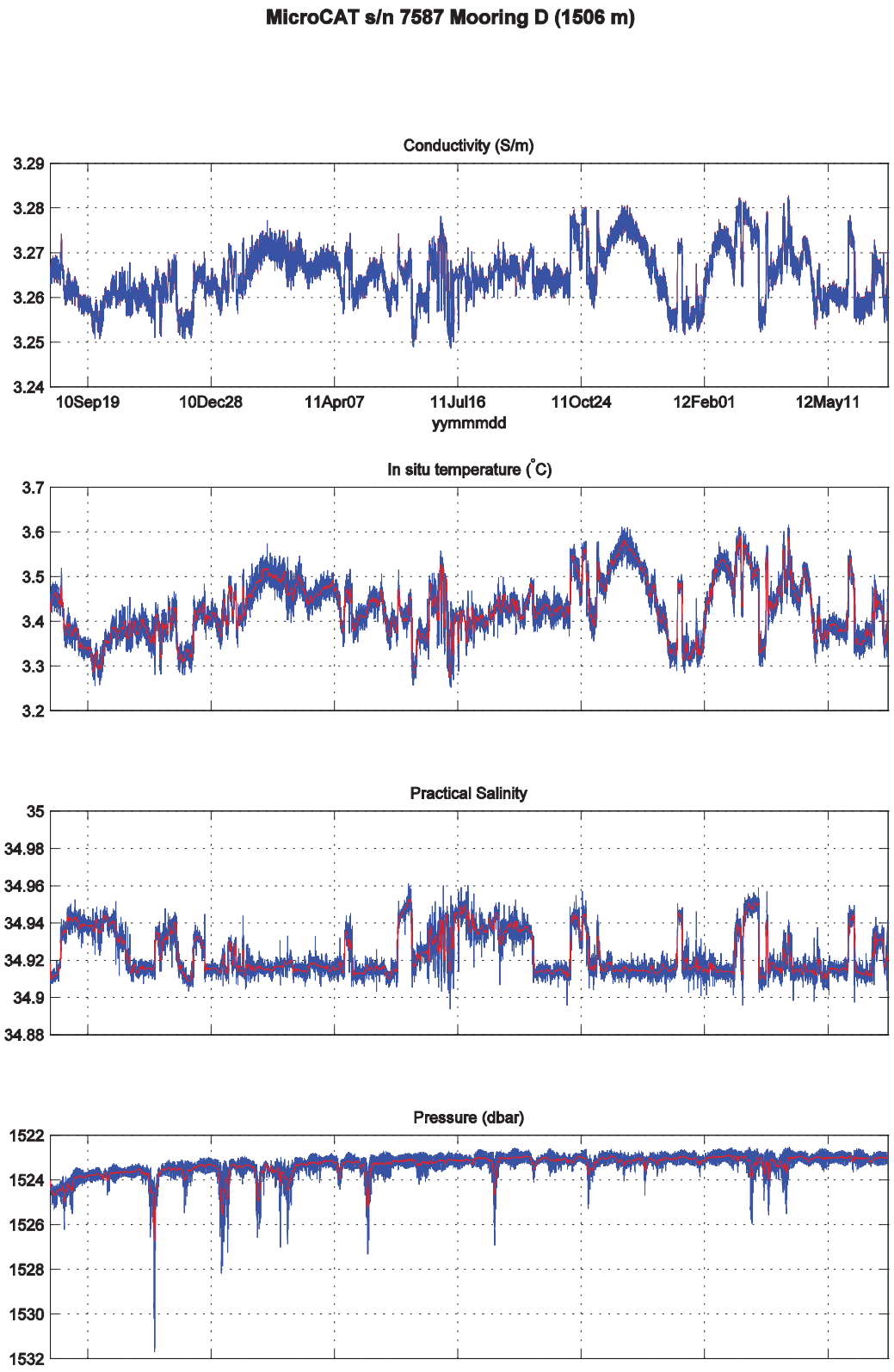

Figure E13. Sea-Bird MicroCAT SBE-37 s/n 7587, Mooring D, 1506 m nominal depth. Subplots are from top to bottom: conductivity, *in situ* temperature, practical salinity, and pressure.

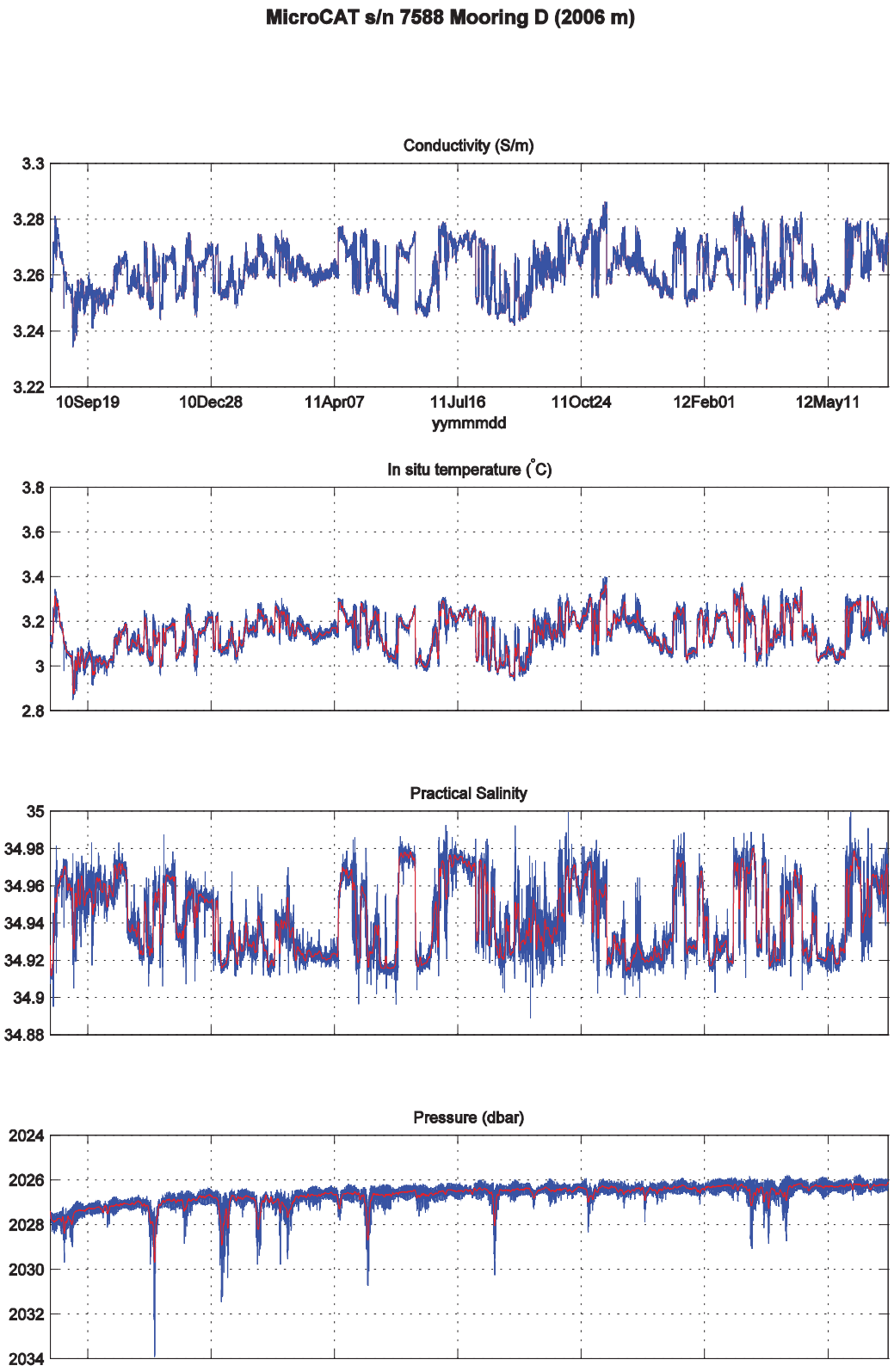

Figure E14. Sea-Bird MicroCAT SBE-37 s/n 7588, Mooring D, 2006 m nominal depth. Subplots are from top to bottom: conductivity, *in situ* temperature, practical salinity, and pressure.

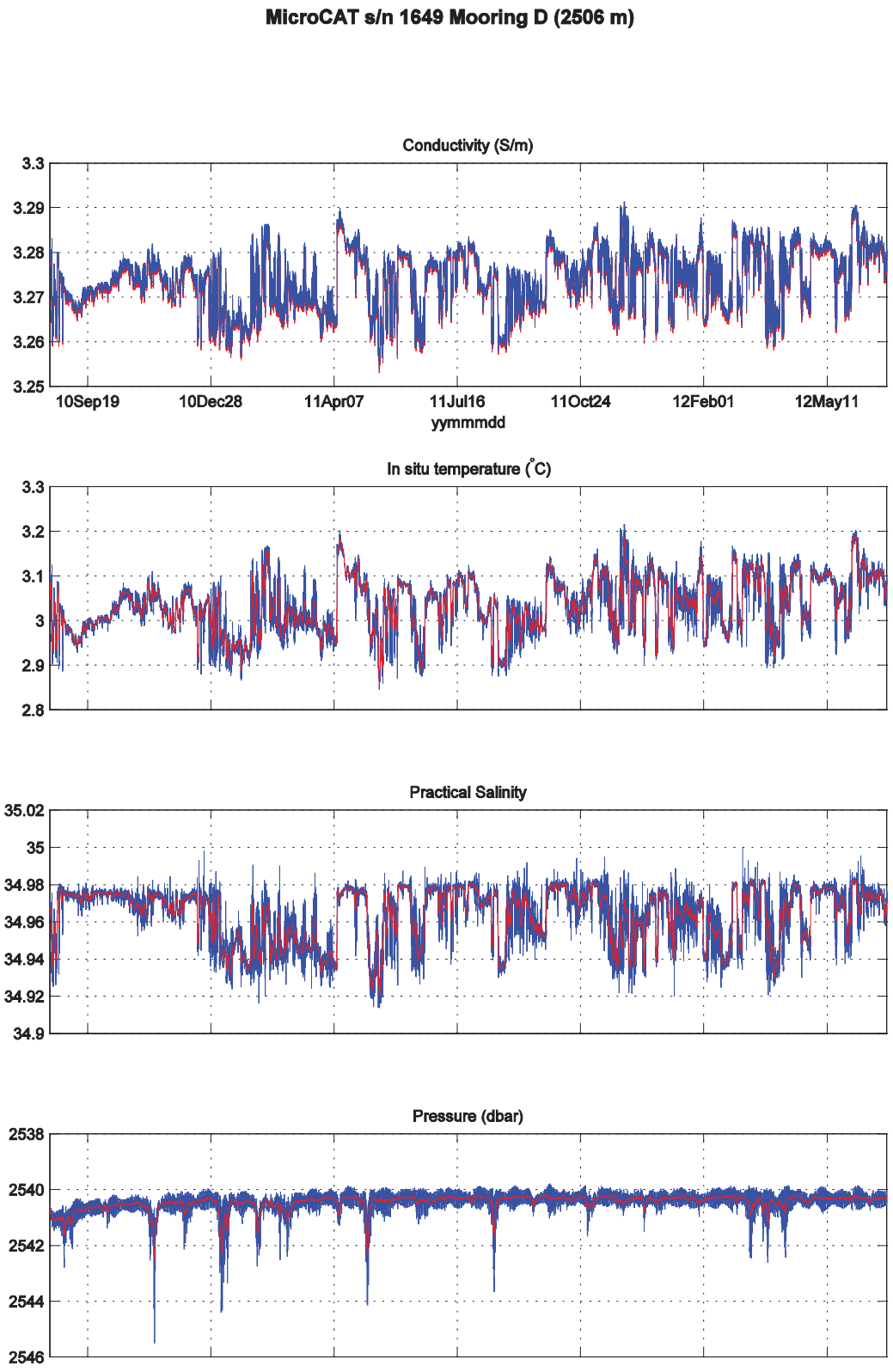

Figure E15. Sea-Bird MicroCAT SBE-37 s/n 1649, Mooring D, 2506 m nominal depth. Subplots are from top to bottom: conductivity, *in situ* temperature, practical salinity, and synthetic pressure.

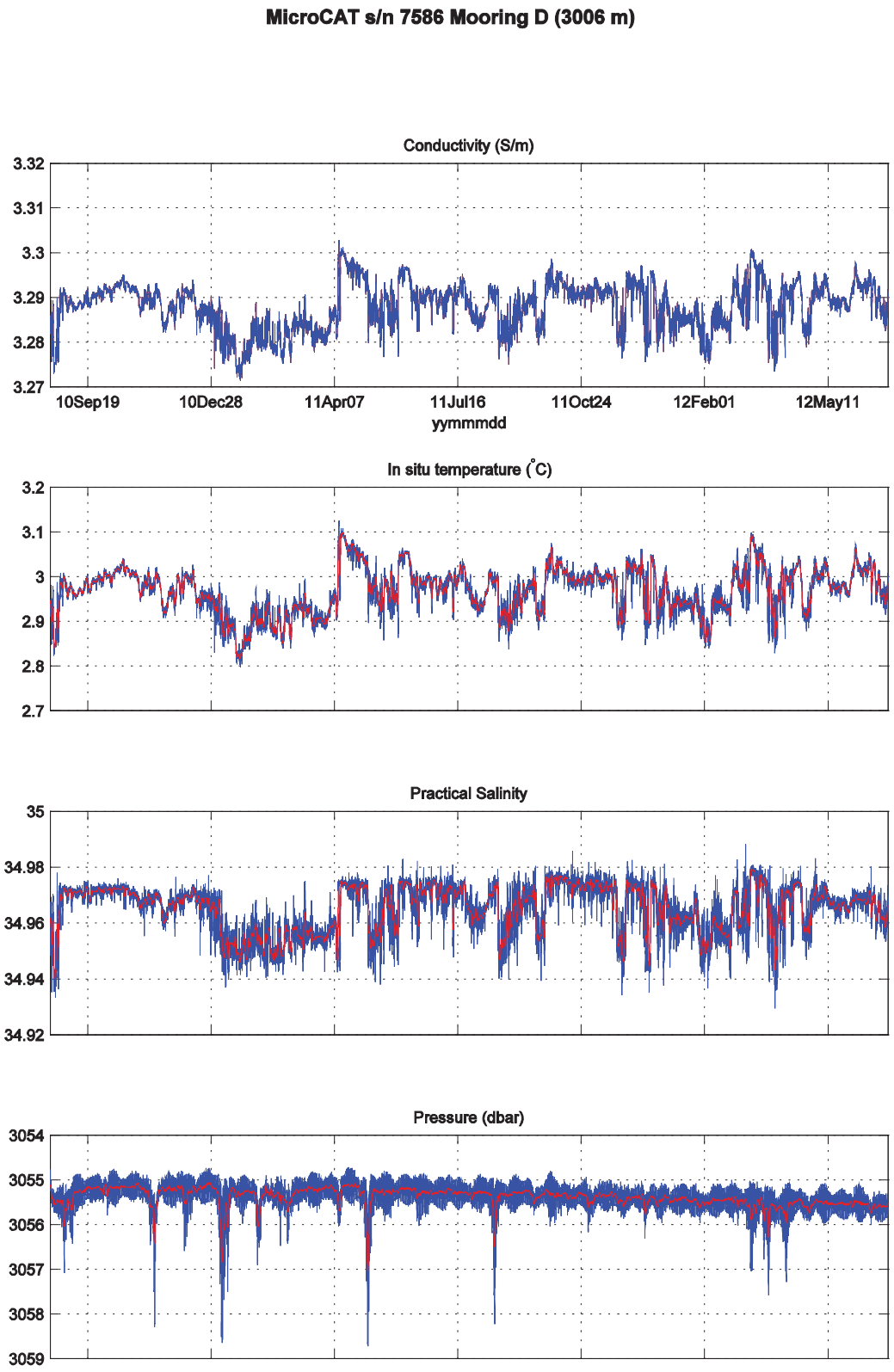

Figure E16. Sea-Bird MicroCAT SBE-37 s/n 7586, Mooring D, 3006 m nominal depth. Subplots are from top to bottom: conductivity, *in situ* temperature, practical salinity, and pressure.

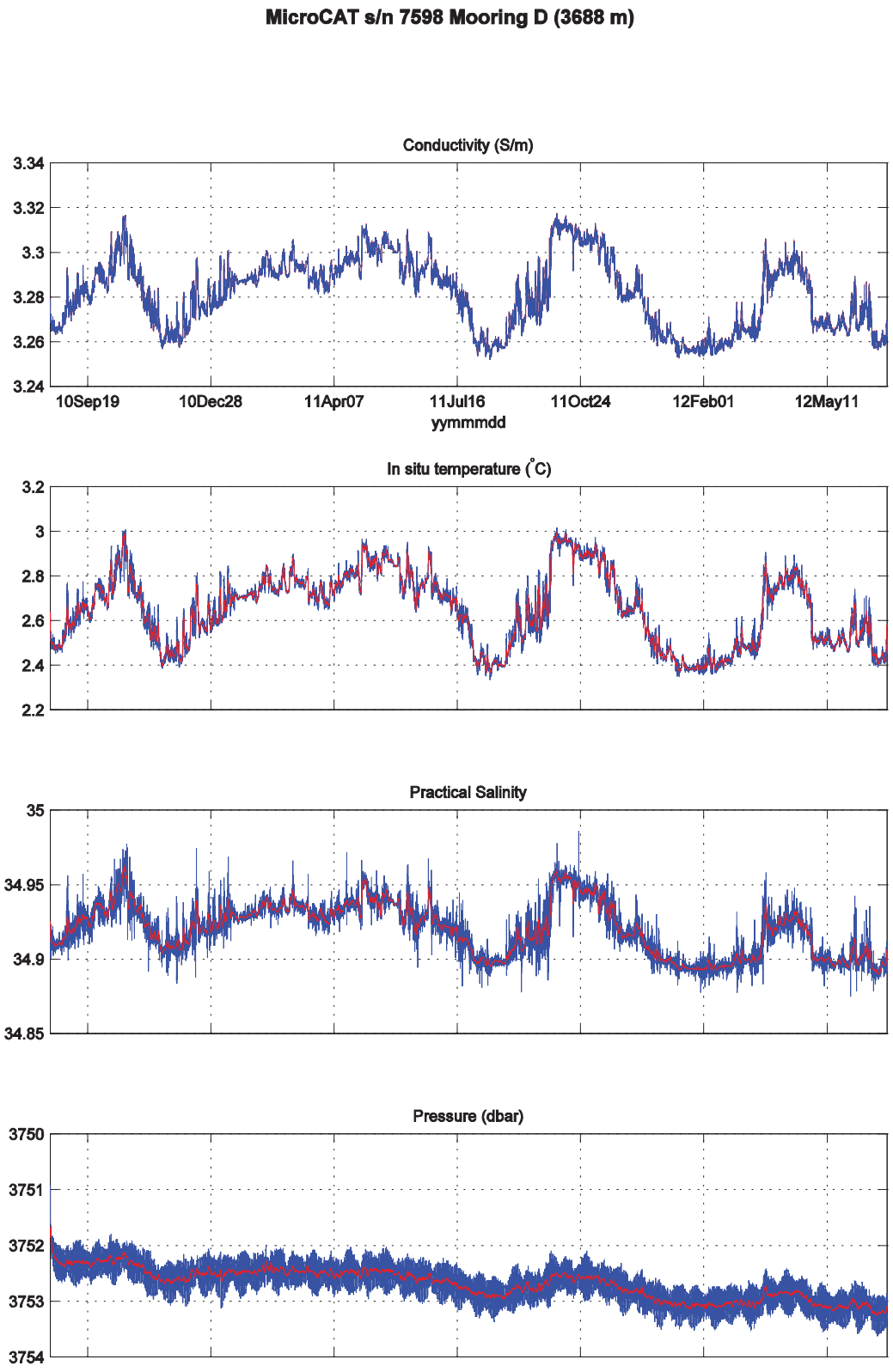

Figure E17. Sea-Bird MicroCAT SBE-37 s/n 7598, Mooring D, 3688 m nominal depth (bottom). Subplots are from top to bottom: conductivity, *in situ* temperature, practical salinity, and pressure.

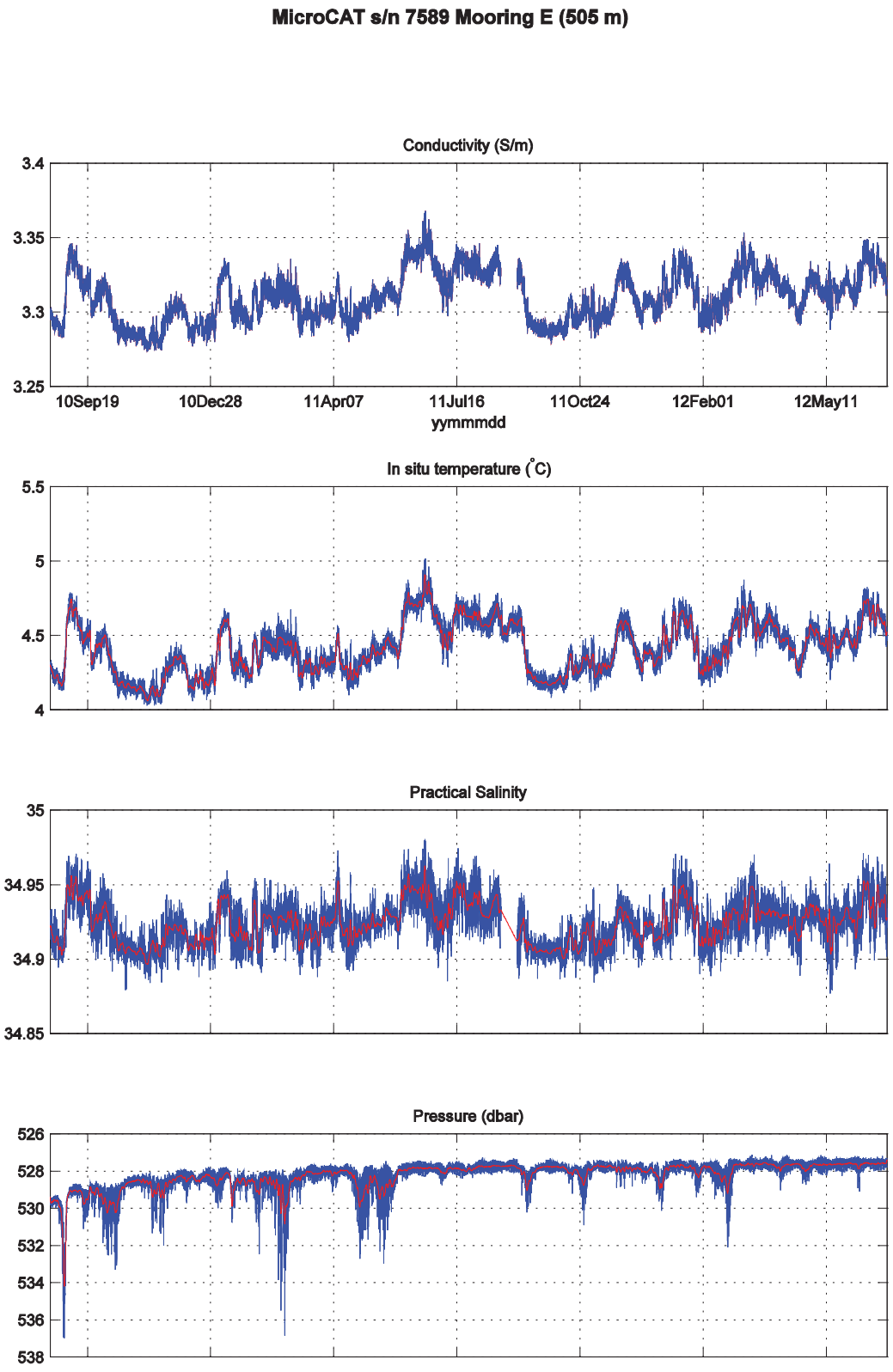

Figure E18. Sea-Bird MicroCAT SBE-37 s/n 7589, Mooring E, 505 m nominal depth. Subplots are from top to bottom: conductivity, *in situ* temperature, practical salinity, and pressure.

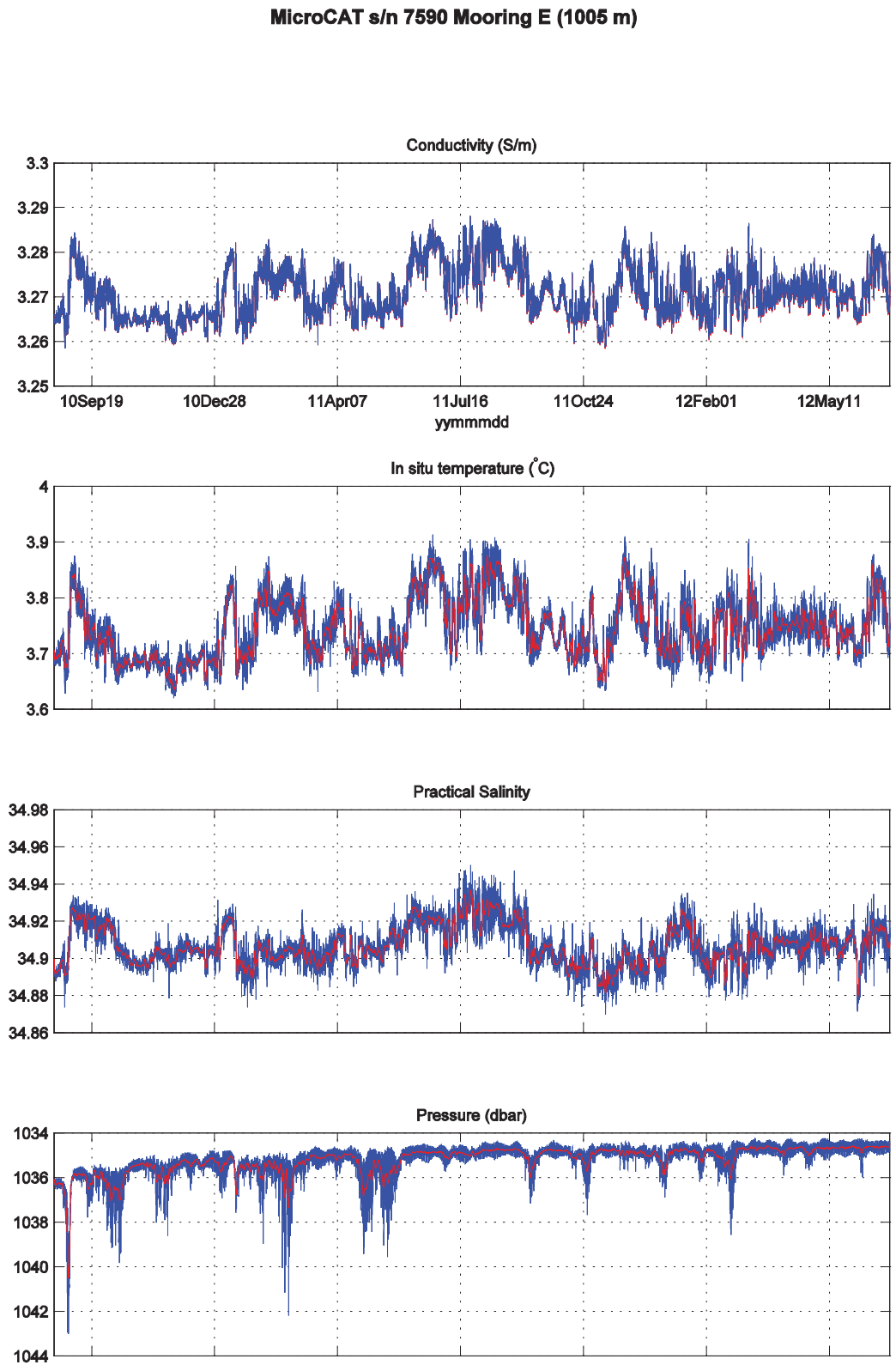

Figure E19. Sea-Bird MicroCAT SBE-37 s/n 7590, Mooring E, 1005 m nominal depth. Subplots are from top to bottom: conductivity, *in situ* temperature, practical salinity, and pressure.

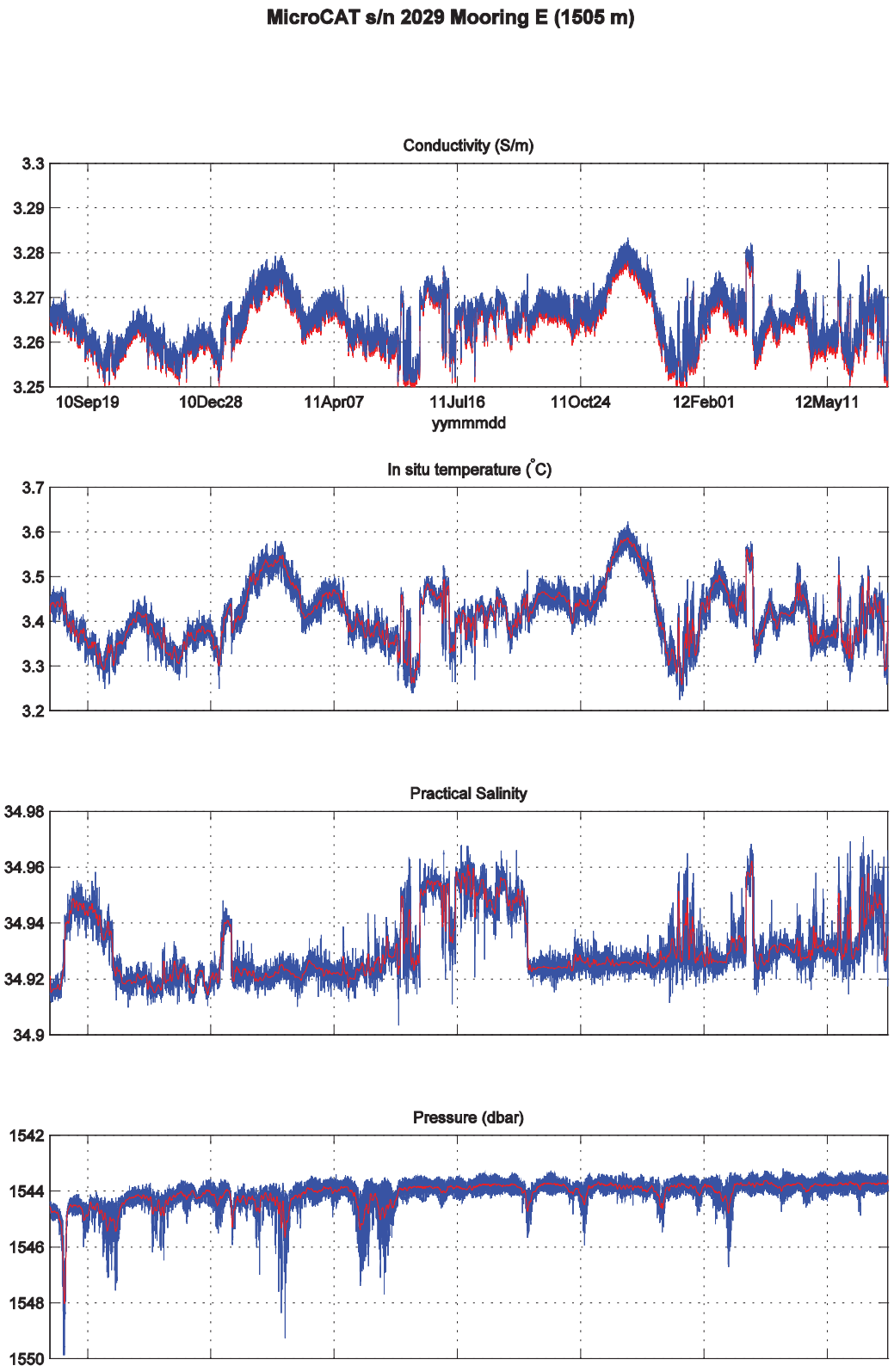

Figure E20. Sea-Bird MicroCAT SBE-37 s/n 2029, Mooring E, 1505 m nominal depth. Subplots are from top to bottom: conductivity, *in situ* temperature, practical salinity, and synthetic pressure.

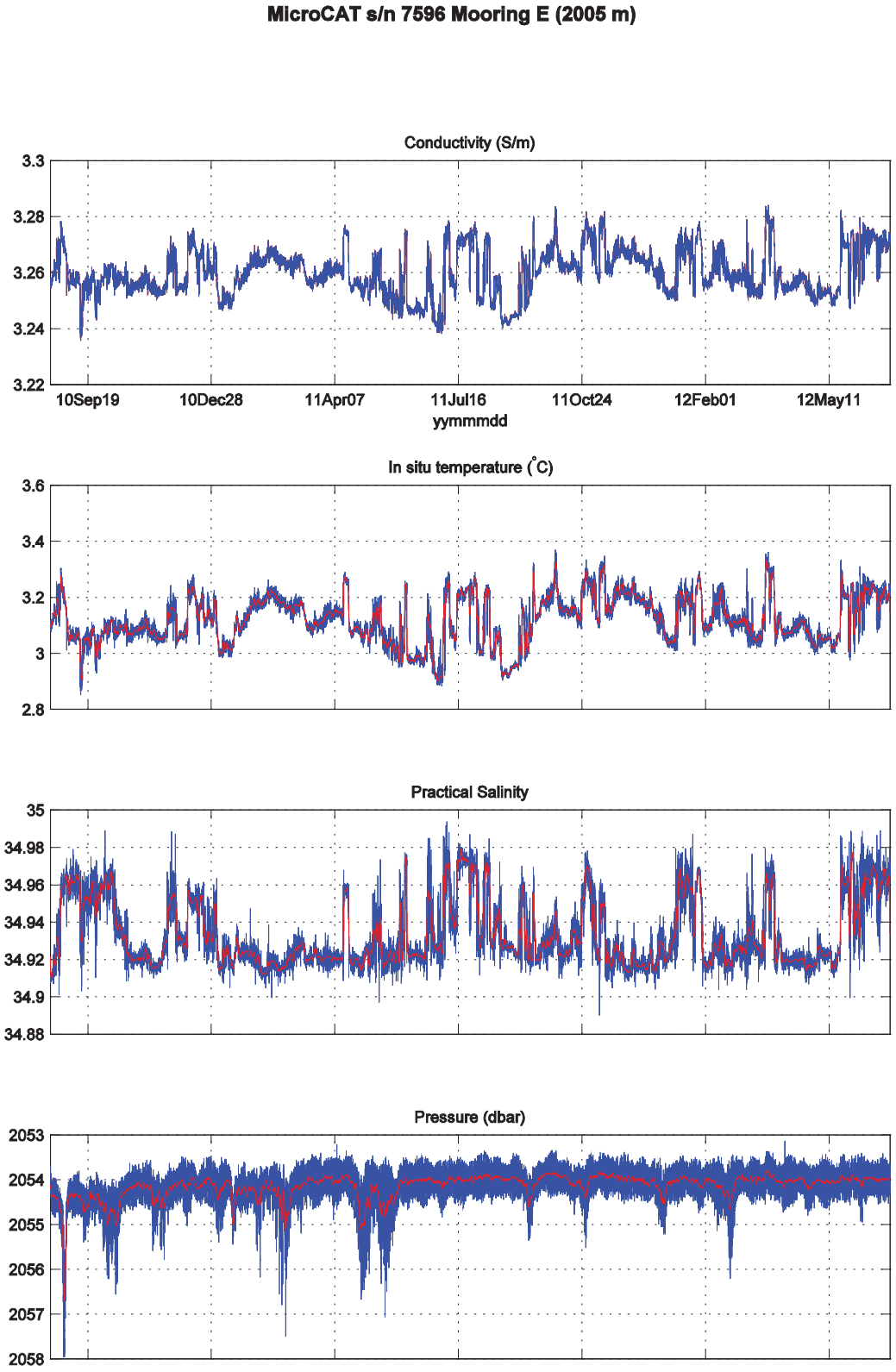

Figure E21. Sea-Bird MicroCAT SBE-37 s/n 7596, Mooring E, 2005 m nominal depth. Subplots are from top to bottom: conductivity, *in situ* temperature, practical salinity, and pressure.

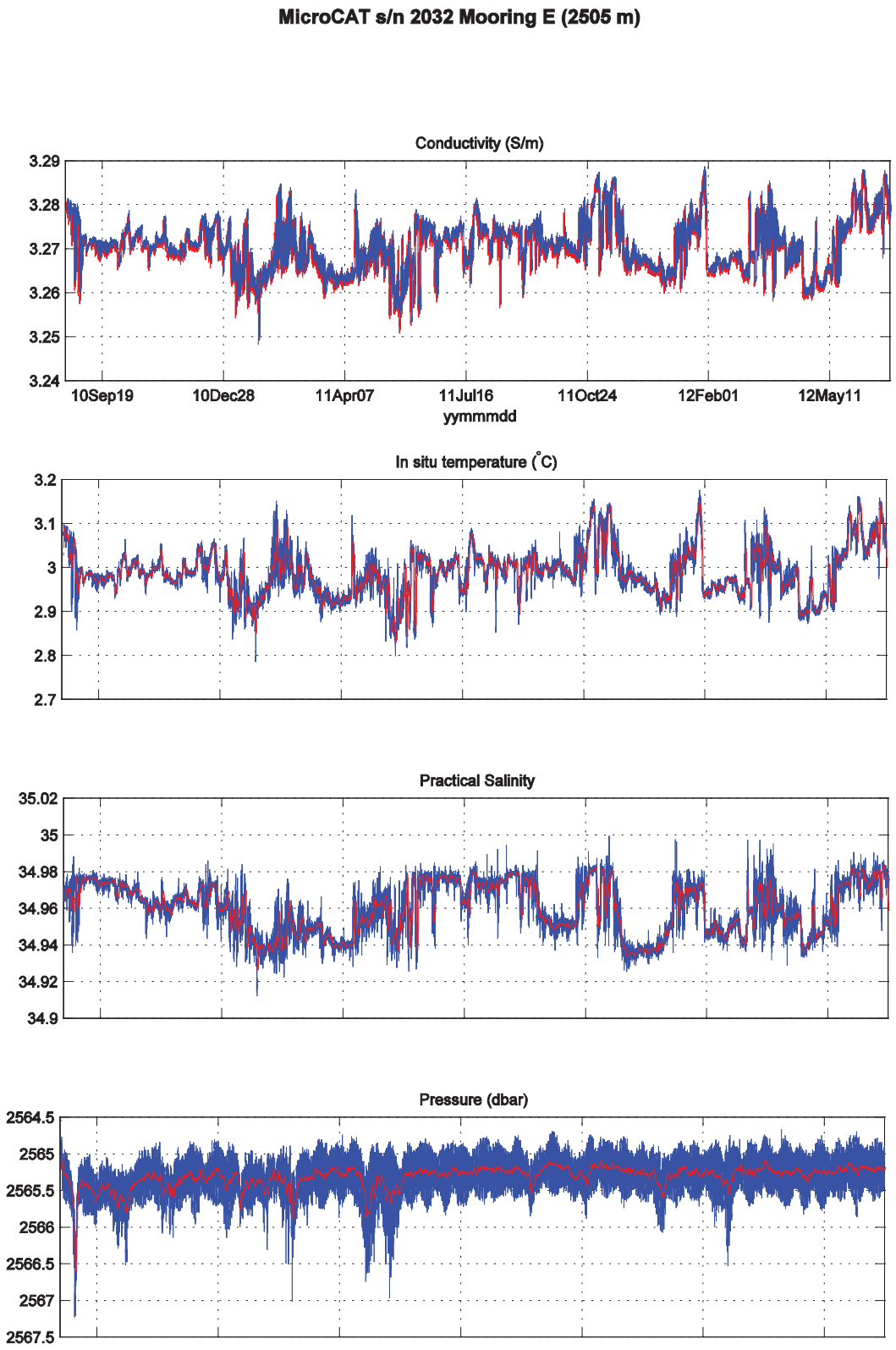

Figure E22. Sea-Bird MicroCAT SBE-37 s/n 2032, Mooring E, 2505 m nominal depth. Subplots are from top to bottom: conductivity, *in situ* temperature, practical salinity, and synthetic pressure.

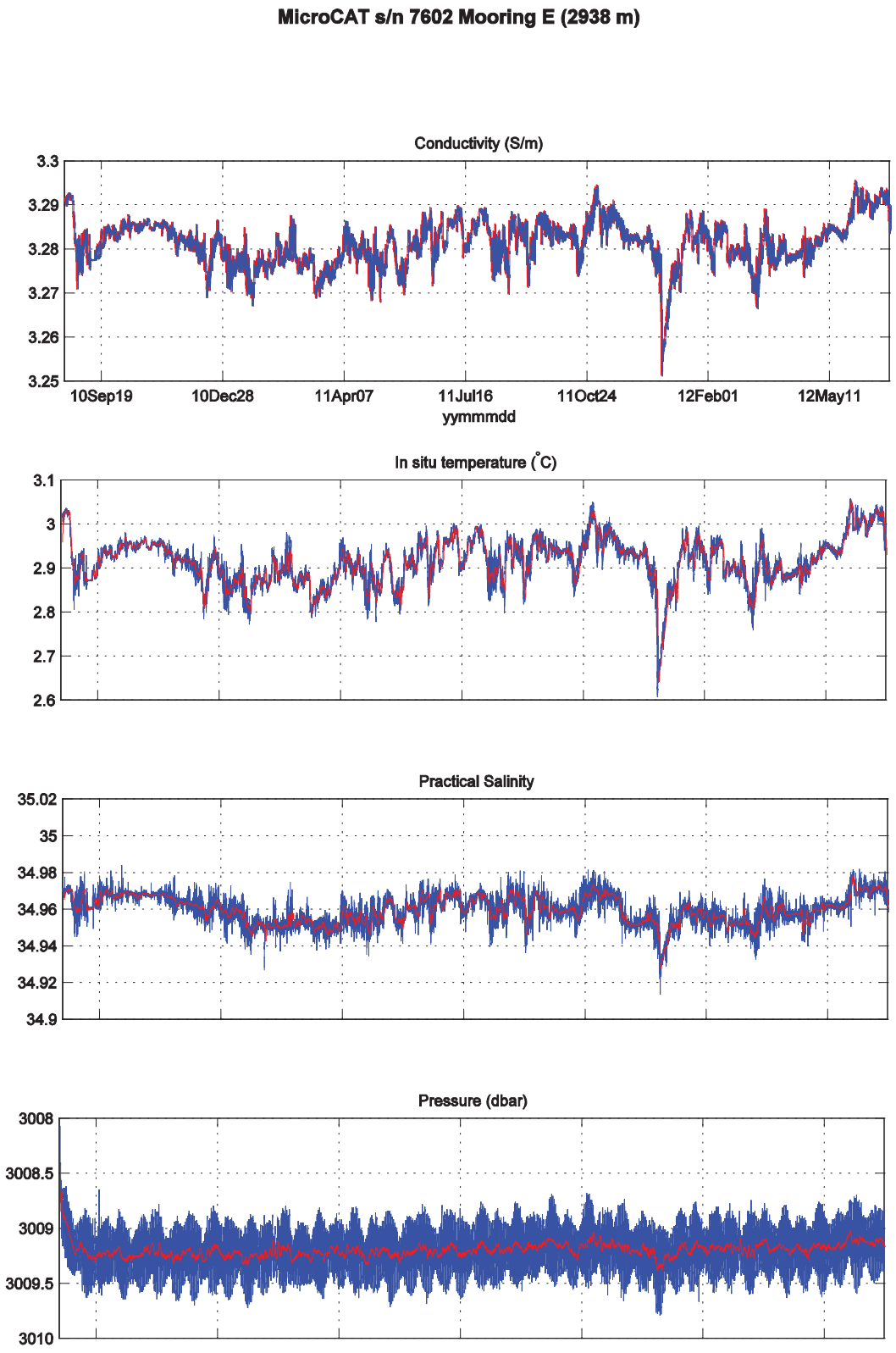

Figure E23. Sea-Bird MicroCAT SBE-37 s/n 7602, Mooring E, 2938 m nominal depth (bottom). Subplots are from top to bottom: conductivity, *in situ* temperature, practical salinity, and pressure.

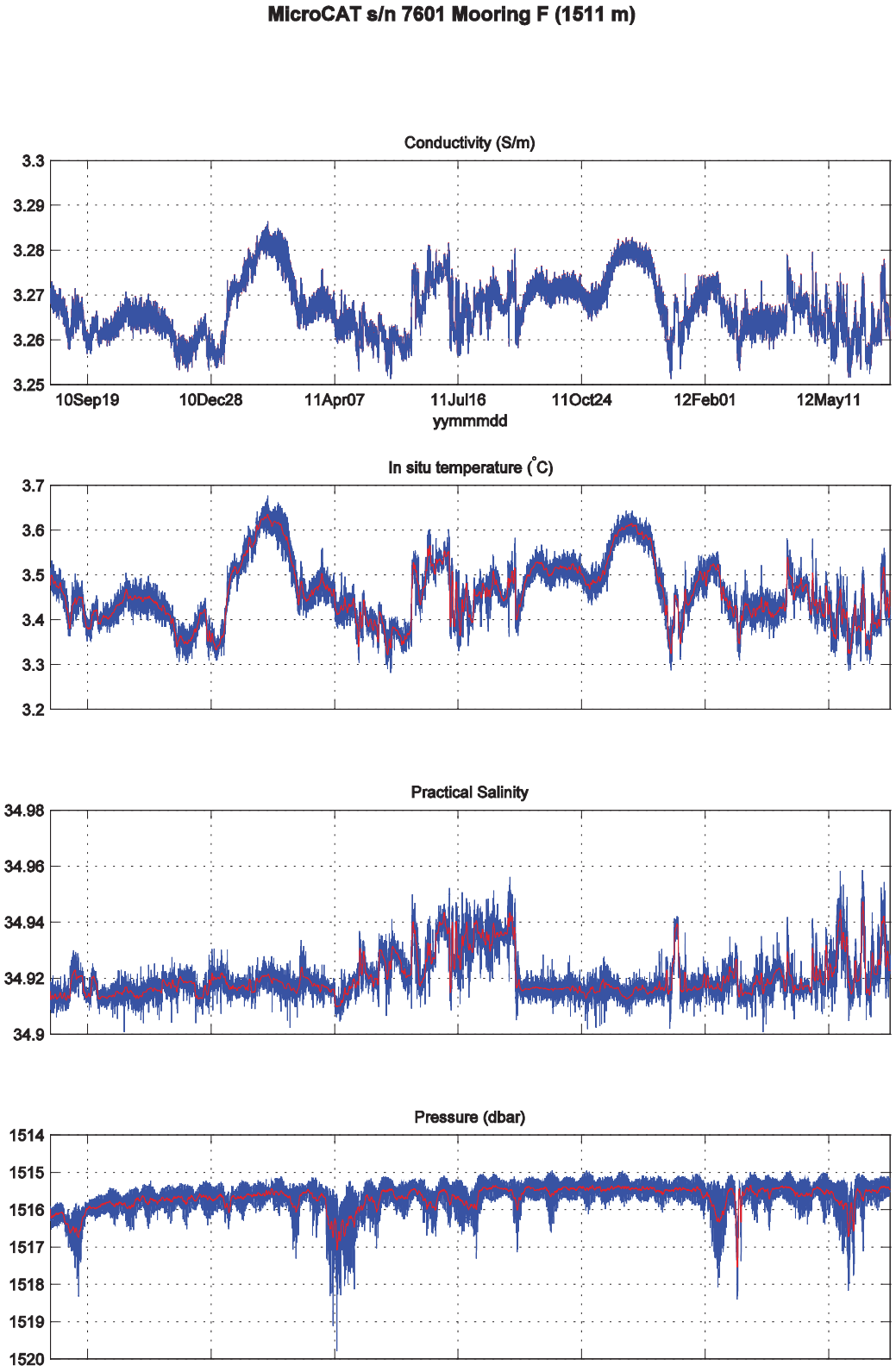

Figure E24. Sea-Bird MicroCAT SBE-37 s/n 7601, Mooring F, 1511 m nominal depth. Subplots are from top to bottom: conductivity, *in situ* temperature, practical salinity, and pressure.

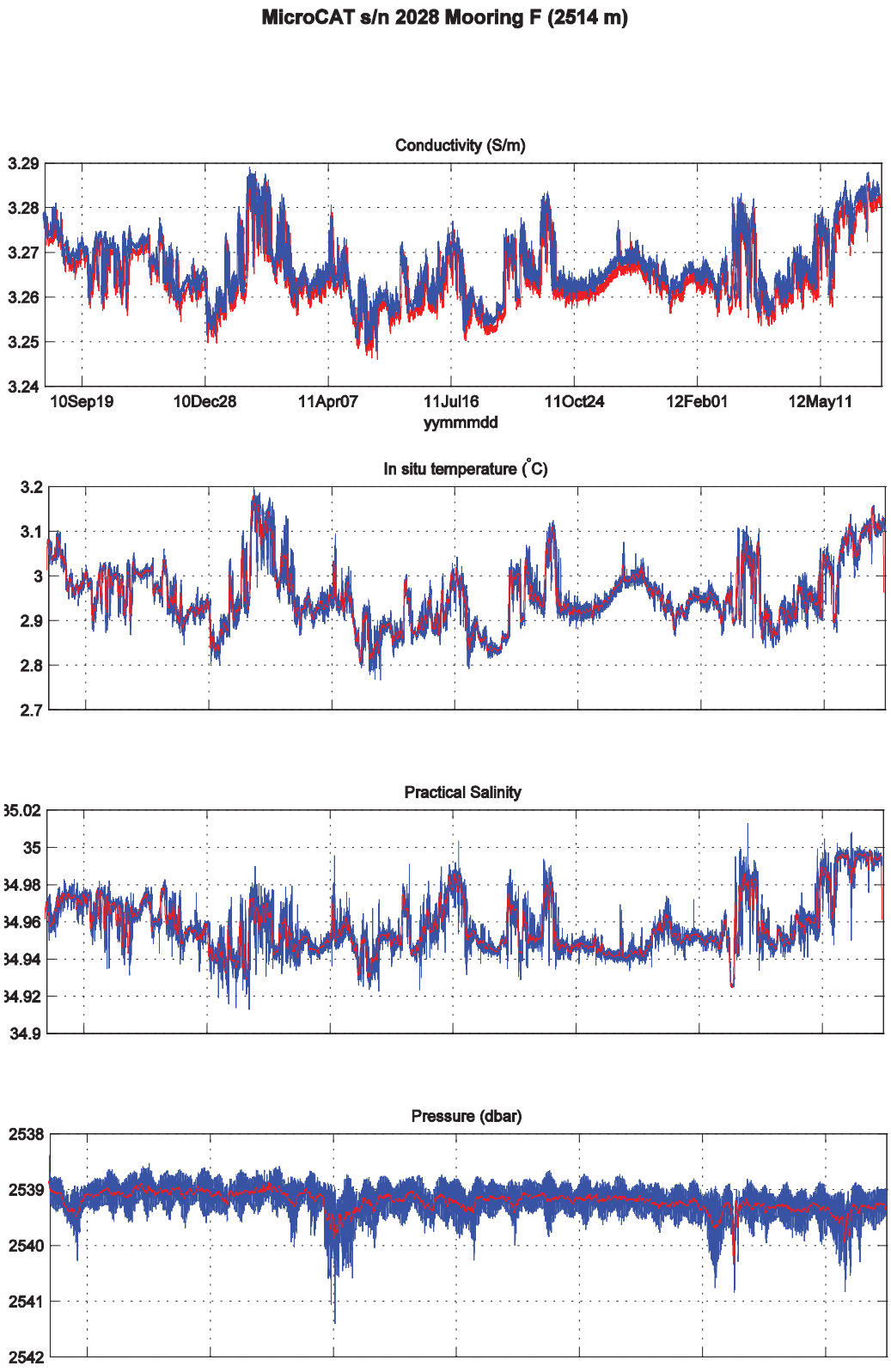

Figure E25. Sea-Bird MicroCAT SBE-37 s/n 2028, Mooring F, 2514 m nominal depth. Subplots are from top to bottom: conductivity, *in situ* temperature, practical salinity, and synthetic pressure.

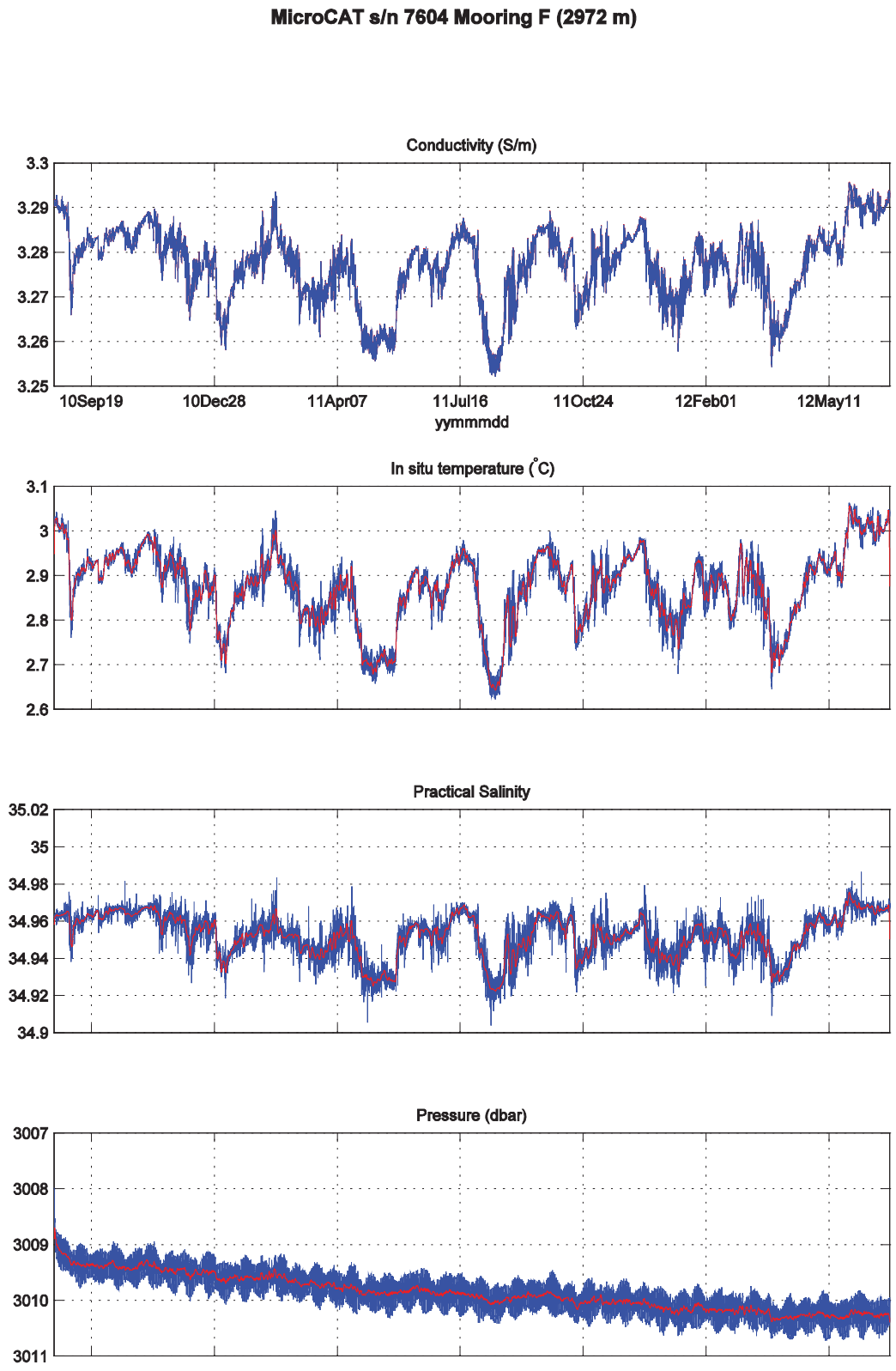

Figure E26. Sea-Bird MicroCAT SBE-37 s/n 7604, Mooring F, 2972 m nominal depth (bottom). Subplots are from top to bottom: conductivity, *in situ* temperature, practical salinity, and pressure.

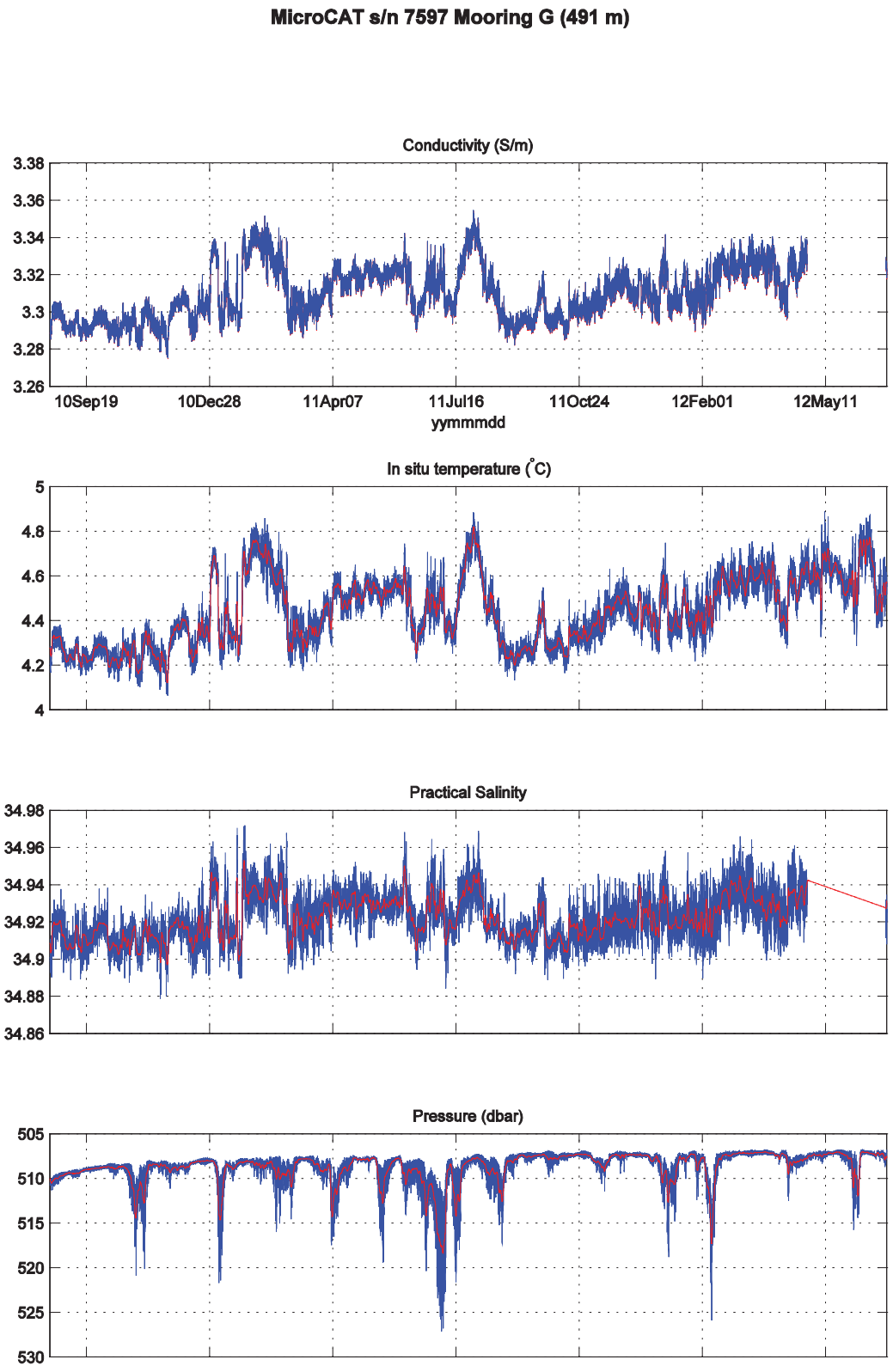

Figure E27. Sea-Bird MicroCAT SBE-37 s/n 7597, Mooring G, 491 m nominal depth. Subplots are from top to bottom: conductivity, *in situ* temperature, practical salinity, and pressure.

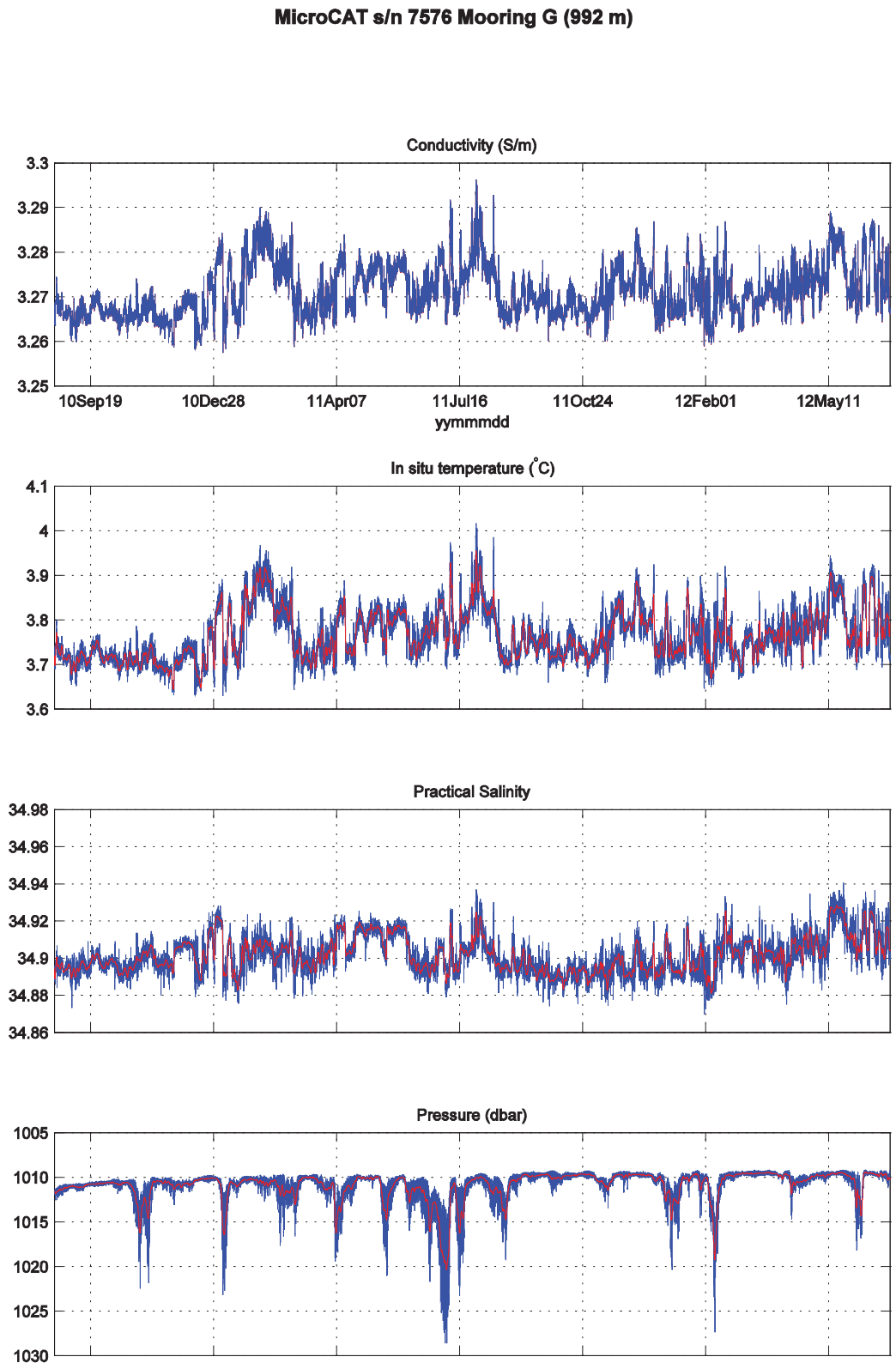

Figure E28. Sea-Bird MicroCAT SBE-37 s/n 7576, Mooring G, 992 m nominal depth. Subplots are from top to bottom: conductivity, *in situ* temperature, practical salinity, and pressure.

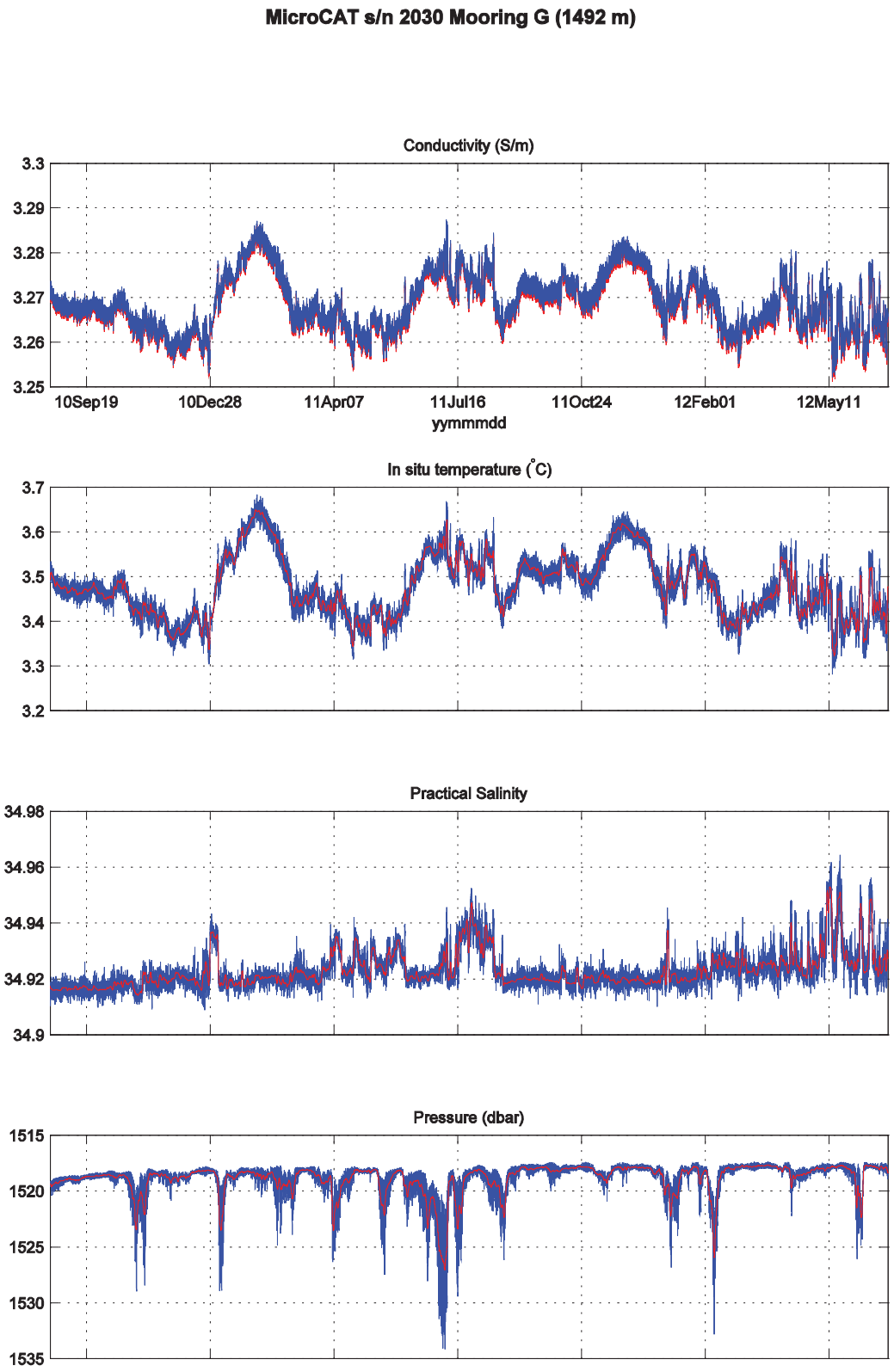

Figure E29. Sea-Bird MicroCAT SBE-37 s/n 2030, Mooring G, 1492 m nominal depth. Subplots are from top to bottom: conductivity, *in situ* temperature, practical salinity, and synthetic pressure.

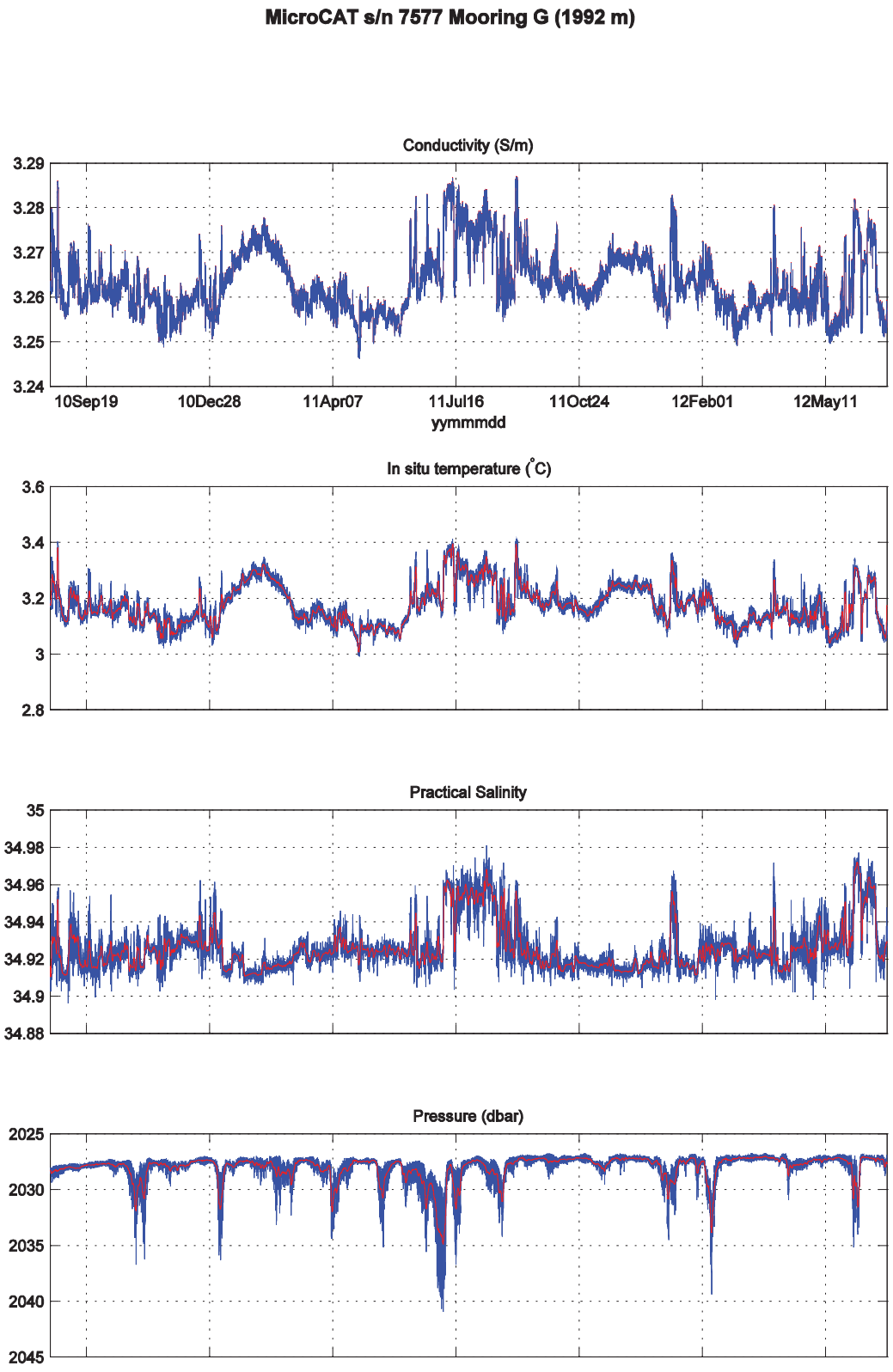

Figure E30. Sea-Bird MicroCAT SBE-37 s/n 7577, Mooring G, 1992 m nominal depth. Subplots are from top to bottom: conductivity, *in situ* temperature, practical salinity, and pressure.

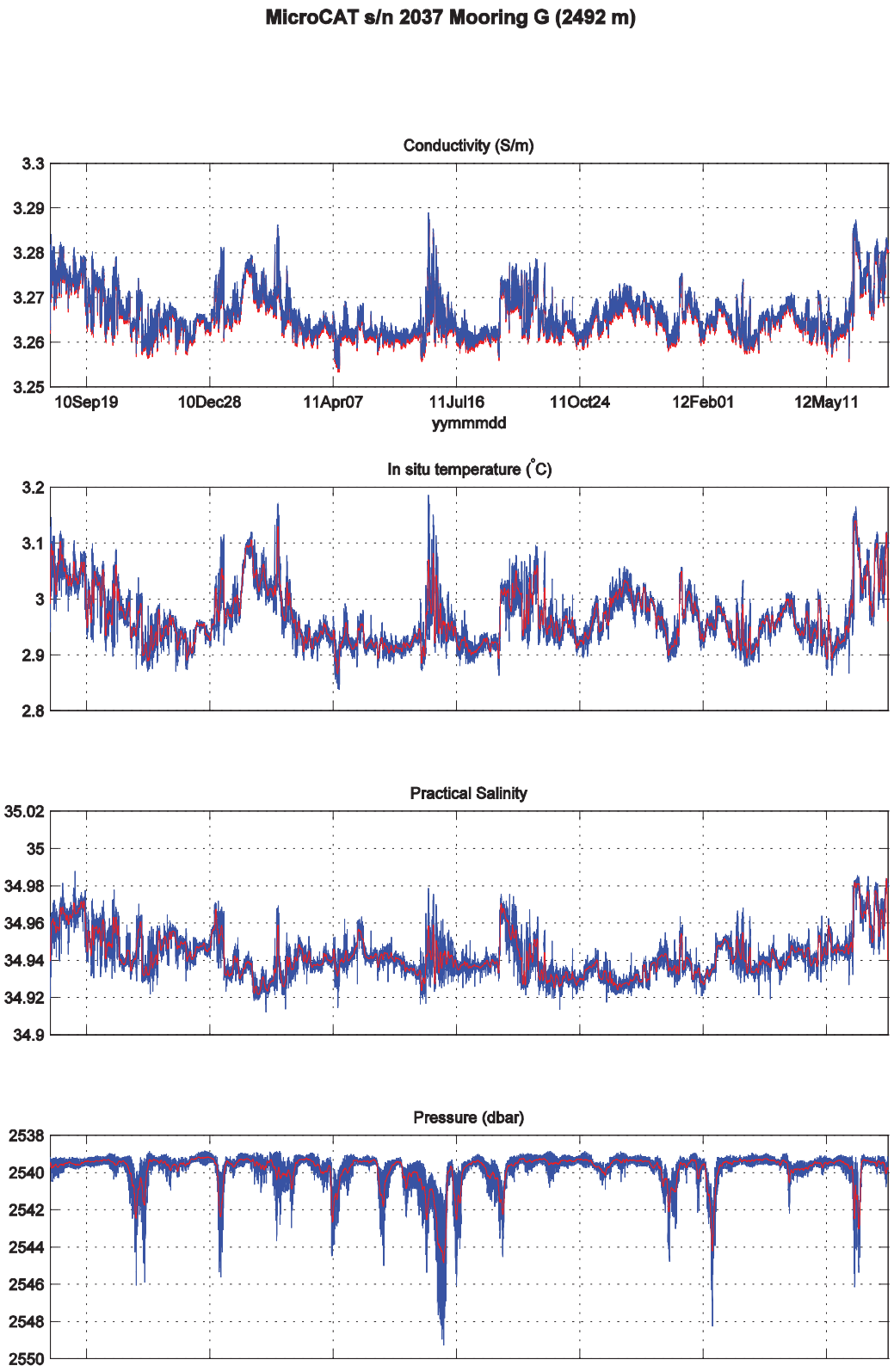

Figure E31. Sea-Bird MicroCAT SBE-37 s/n 2037, Mooring G, 2492 m nominal depth. Subplots are from top to bottom: conductivity, *in situ* temperature, practical salinity, and synthetic pressure.

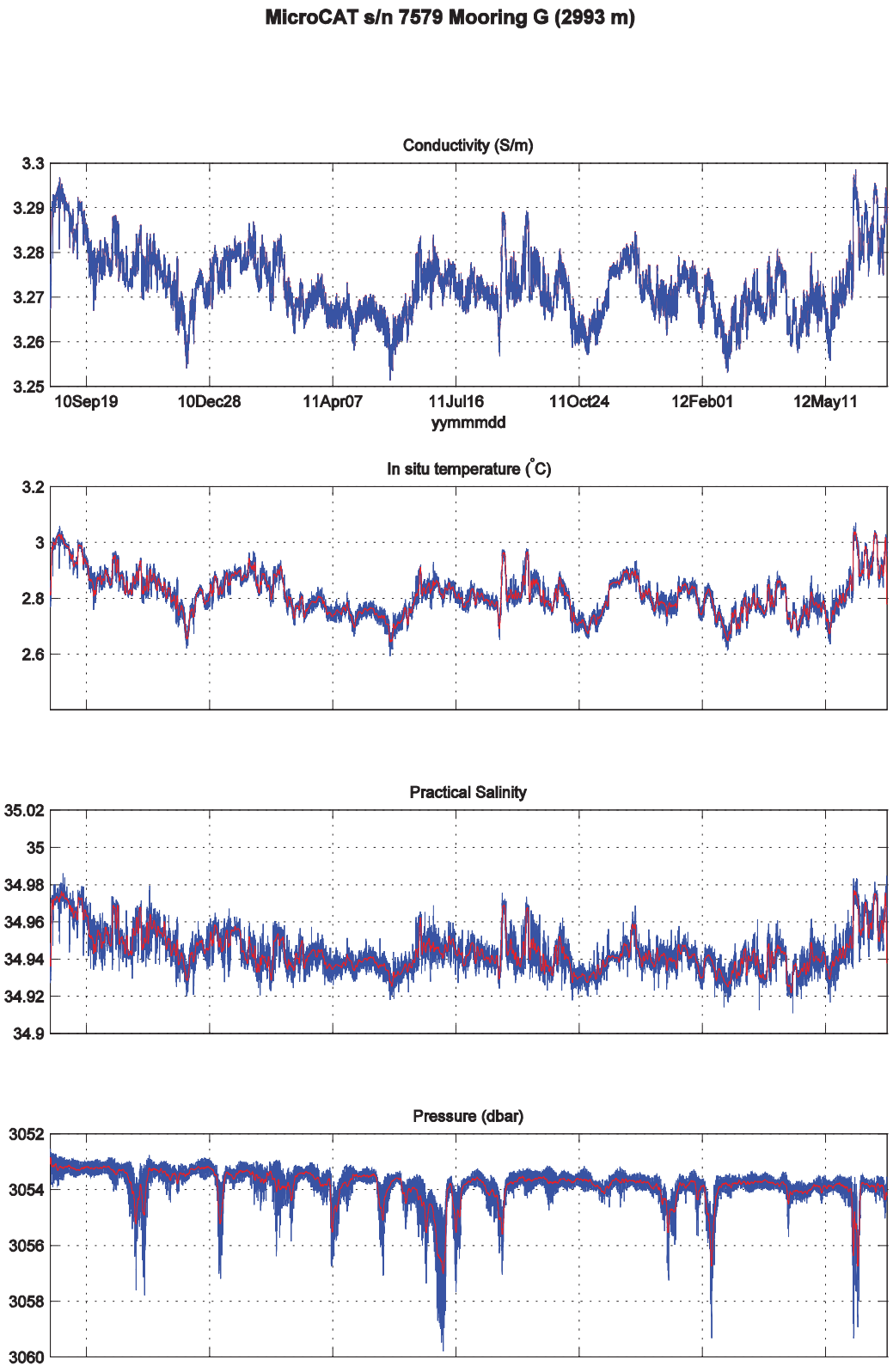

Figure E32. Sea-Bird MicroCAT SBE-37 s/n 7579, Mooring G, 2993 m nominal depth. Subplots are from top to bottom: conductivity, in situ temperature, practical salinity, and pressure.

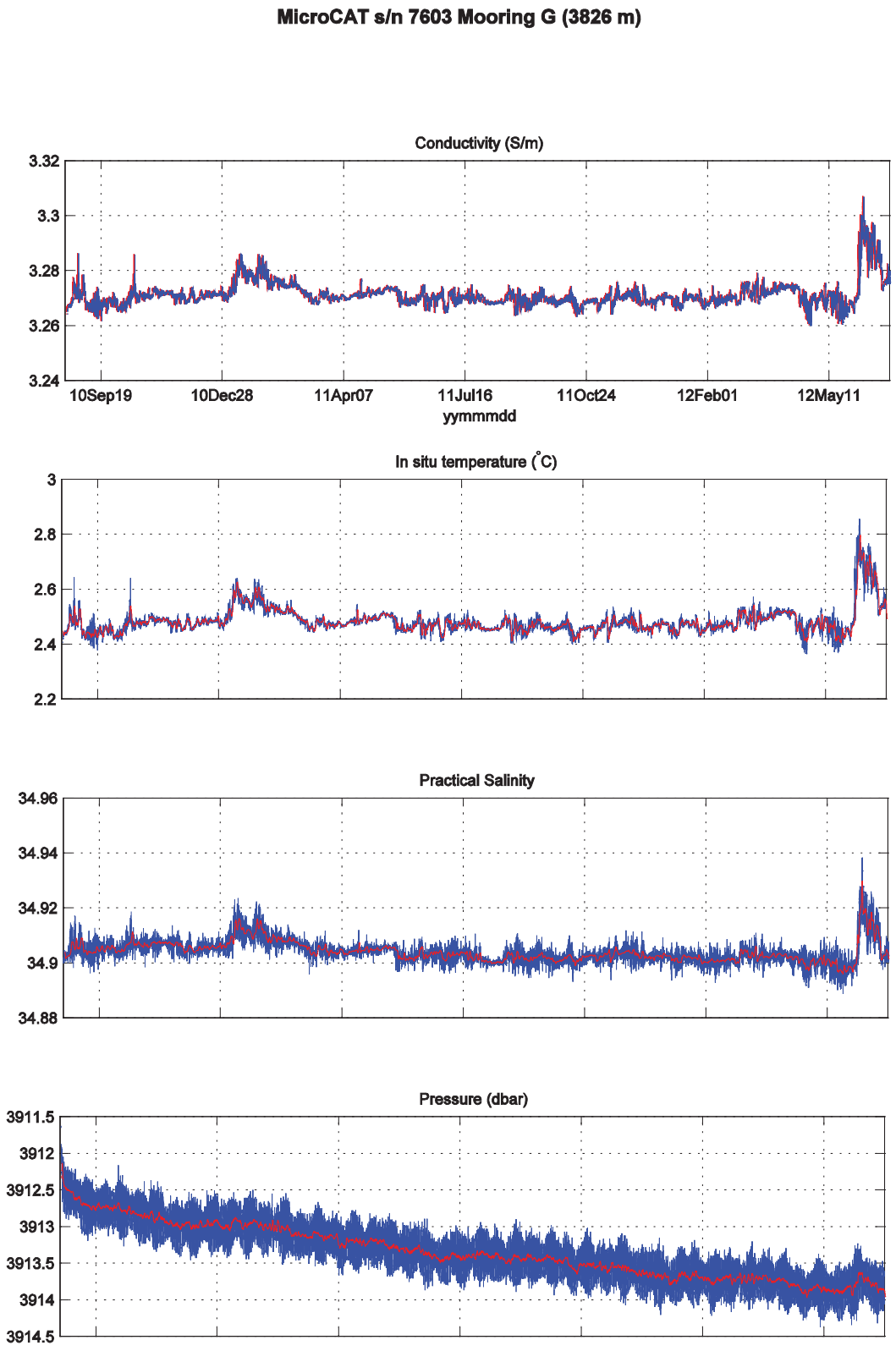

Figure E33. Sea-Bird MicroCAT SBE-37 s/n 7603, Mooring G, 3826 m nominal depth (bottom). Subplots are from top to bottom: conductivity, *in situ* temperature, practical salinity, and pressure.

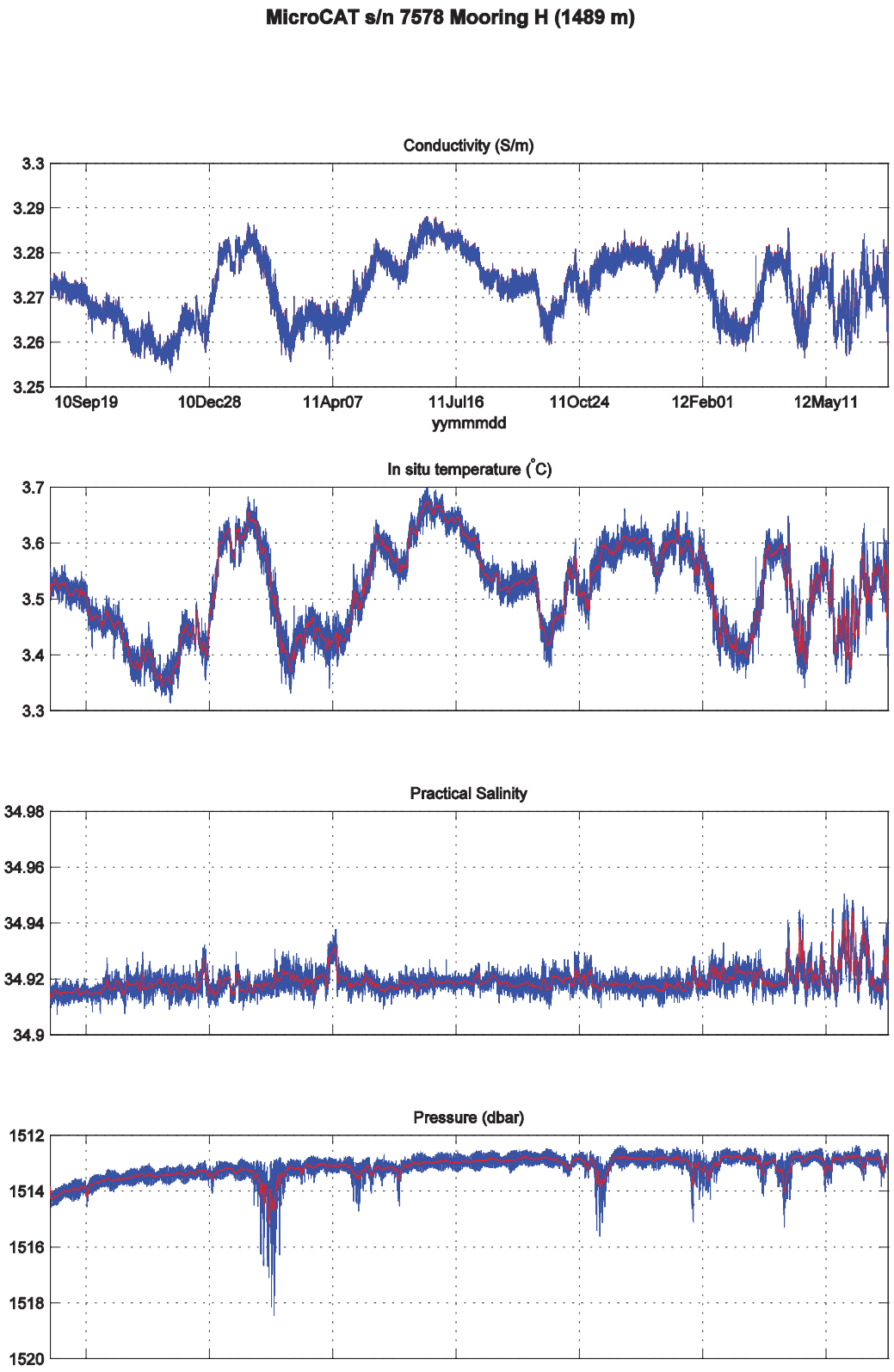

Figure E34. Sea-Bird MicroCAT SBE-37 s/n 7578, Mooring H, 1489 m nominal depth. Subplots are from top to bottom: conductivity, *in situ* temperature, practical salinity, and pressure.

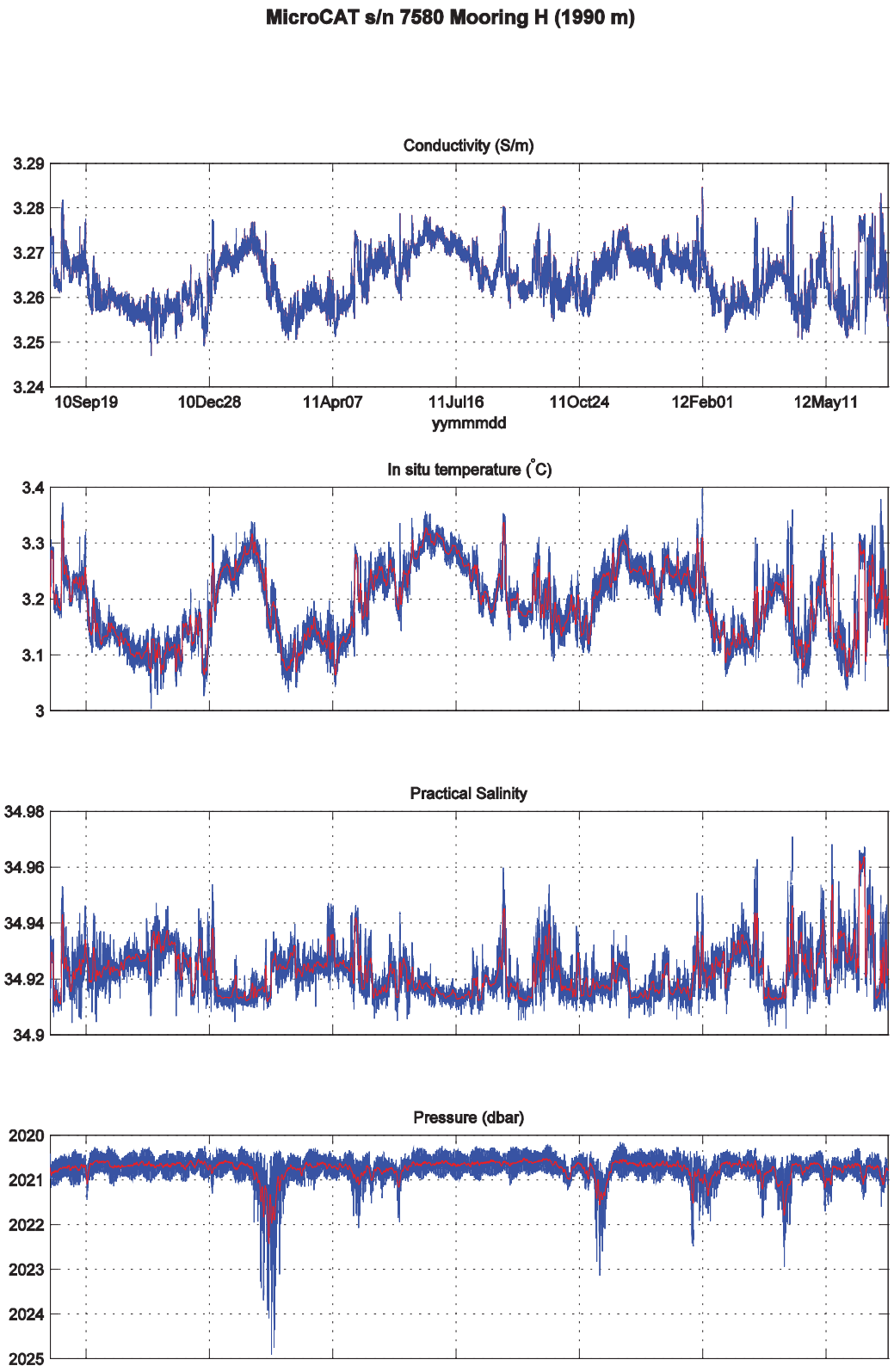

Figure E35. Sea-Bird MicroCAT SBE-37 s/n 7580, Mooring H, 1990 m nominal depth. Subplots are from top to bottom: conductivity, *in situ* temperature, practical salinity, and pressure.

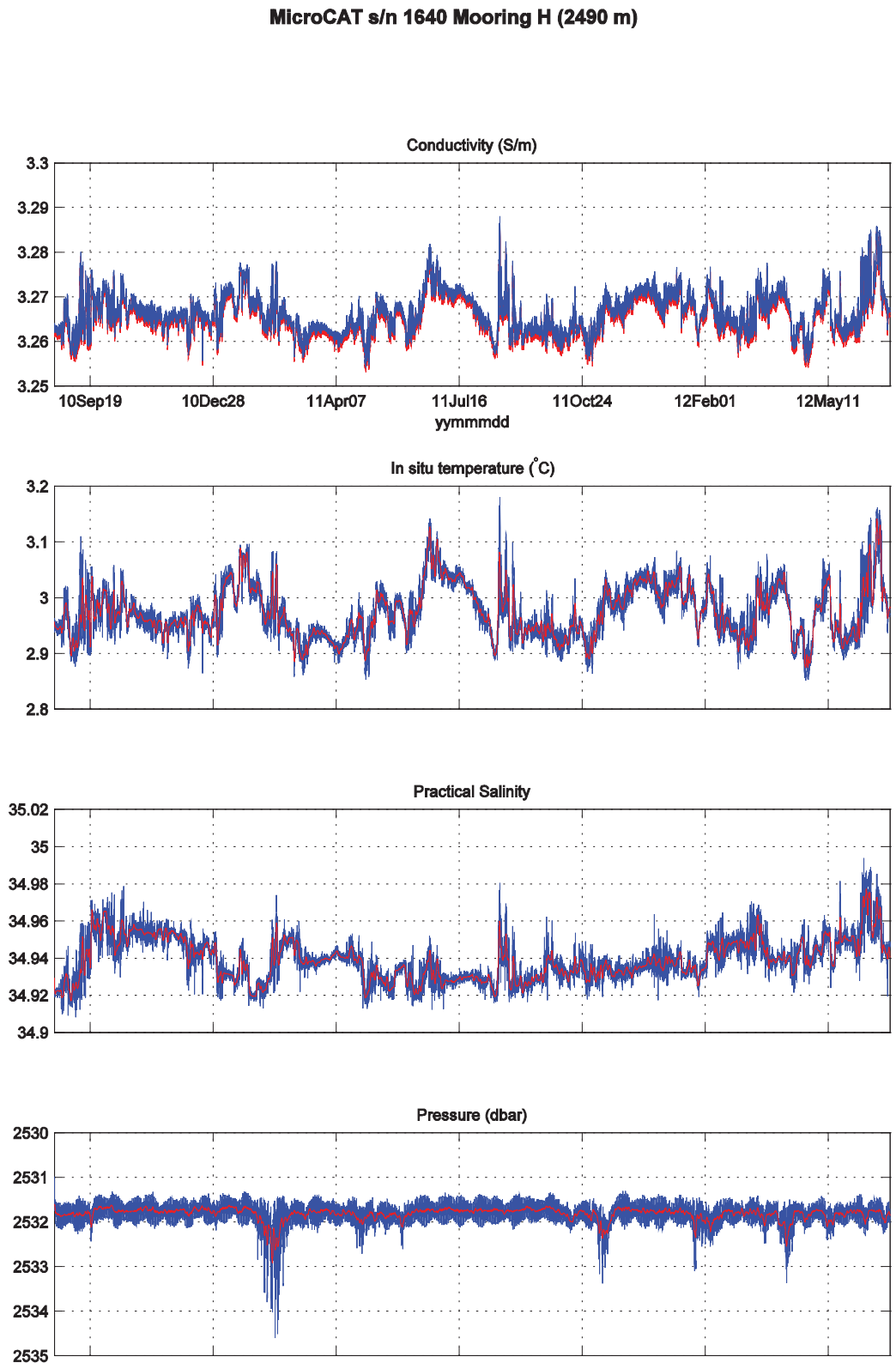

Figure E36. Sea-Bird MicroCAT SBE-37 s/n 1640, Mooring H, 2490 m nominal depth. Subplots are from top to bottom: conductivity, *in situ* temperature, practical salinity, and synthetic pressure.

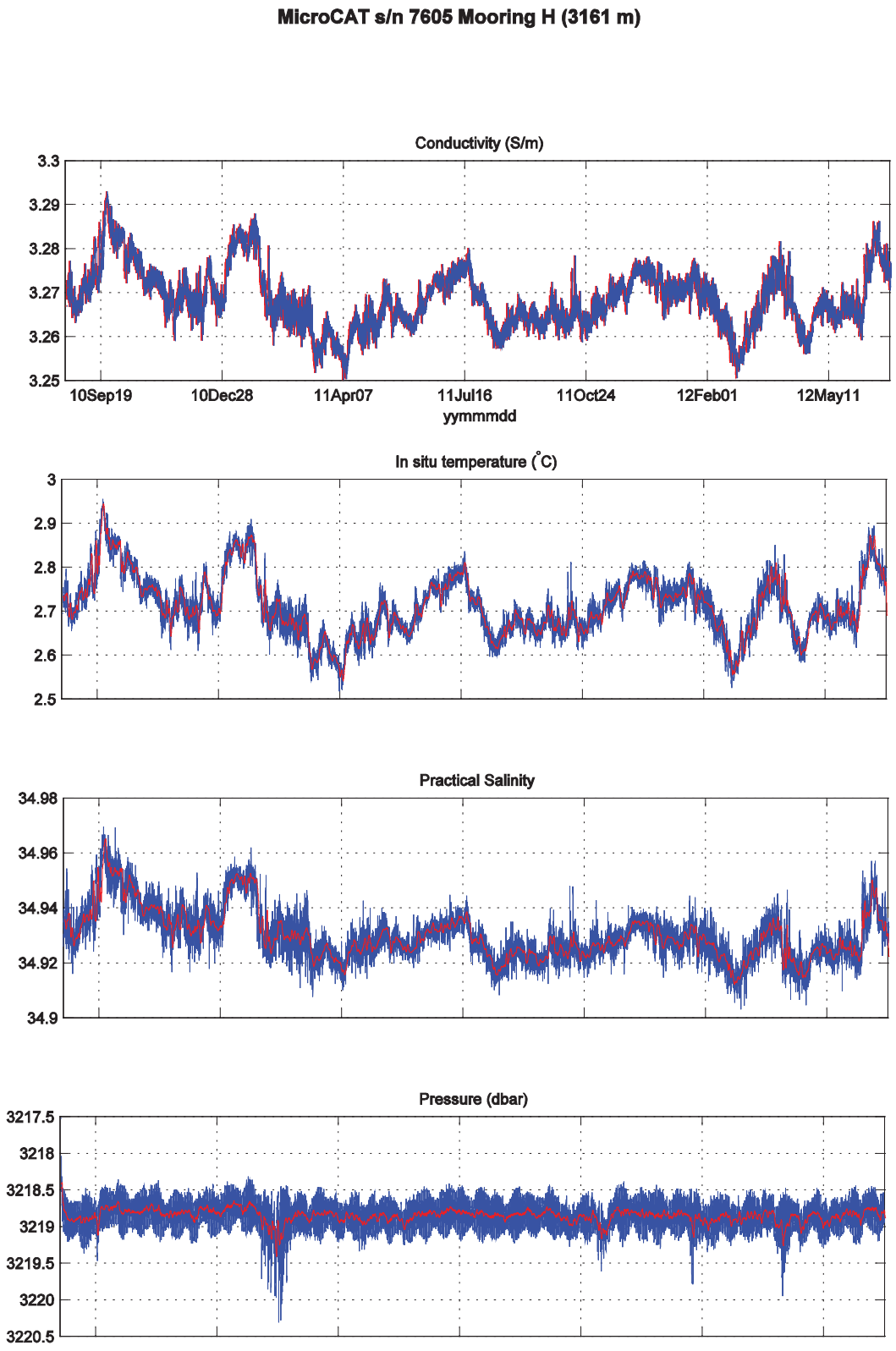

Figure E37. Sea-Bird MicroCAT SBE-37 s/n 7605, Mooring H, 3161 m nominal depth (bottom). Subplots are from top to bottom: conductivity, *in situ* temperature, practical salinity, and pressure.

50272-101

REPORT DOCUMENTATION PAGE	1. REPORT NO. WHOI-2014-04	2.	3. Recipient's Accession No.

4. Title and Subtitle
A Crossroads of the Atlantic Meridional Overturning Circulation: The Charlie-Gibbs Fracture Zone Data Report August 2010 - June 2012

5. Report Date
August 2014

6.

7. Author(s)
Heather Furey, Leah Trafford, and Amy Bower

8. Performing Organization Rept. No.

9. Performing Organization Name and Address
Woods Hole Oceanographic Institution
Woods Hole, Massachusetts 02543

10. Project/Task/Work Unit No.

11. Contract(C) or Grant(G) No.
(C) OCE-0826656
(G)

12. Sponsoring Organization Name and Address
National Science Foundation

13. Type of Report & Period Covered
Technical Report

14.

15. Supplementary Notes
This report should be cited as: Woods Hole Oceanographic Institution Technical Report, WHOI-2014-04.

16. Abstract (Limit: 200 words)

This is the final data report of all mooring data collected by the Woods Hole Oceanographic Institution in 2010-2012 during the experiment A Crossroads of the Atlantic Meridional Overturning Circulation: The Charlie-Gibbs Fracture Zone. The objectives of this experiment were (1) to obtain an improved direct estimate of the mean and low-frequency variability of the deep westward transport of the Iceland-Scotland Overflow Water through the Charlie-Gibbs Fracture Zone (CGFZ), and (2) to gain a better understanding of the causes of the low-frequency variability in the transport of overflow waters through the CGFZ, especially of the role of the North Atlantic Current in generating this variability. A set of eight moorings were set up across the CGFZ to measure the intermediate and deep water variability for a two-year period, from a depth of 500 m to the ocean floor. The moorings held a total of three McClane Moored Profilers (MMPs), 10 Nortek and 18 Aanderaa current meters, and 36 Seabird MicroCATs, deployed from 18-20 August 2010 through 28-30 June 2012. This yielded a nearly two-year record of velocity, temperature, salinity and pressure data across the interface between the generally eastward flowing Labrador Sea Water carried underneath the North Atlantic Current, and the westward flowing deep Iceland-Scotland Overflow Water.

17. Document Analysis **a. Descriptors**

Charlie-Gibbs Fracture Zone
mooring array
Iceland-Scotland Overflow Water transport

b. Identifiers/Open-Ended Terms

c. COSATI Field/Group

18. Availability Statement
Approved for public release; distribution unlimited.

19. Security Class (This Report)

21. No. of Pages
142

20. Security Class (This Page)

22. Price

(See ANSI-Z39.18) *See Instructions on Reverse* **OPTIONAL FORM 272 (4-77)**
(Formerly NTIS-35)
Department of Commerce